The University Of Sheffield.

A Study Into The Feasibility of Local Renewable Energy Systems With Storage, Using Security and Sustainability Metrics for Optimisation and Evaluation

Huw Birch

A thesis submitted in partial fulfilment of the requirements for the degree
of
Doctor of Philosophy

The University of Sheffield
Faculty of Science
Department of Physics

5th October 2015

Contents

List of Figures

List of Tables

Acknowledgements

The work for this thesis was made possible with the assistance of my supervisor Alastair Buckley and the Doctoral Training Centre E-Futures at the University of Sheffield. Collaboration with the research groups Sheffield Solar and Solar Energy in Future Societies was also helpful in providing assistance via access to data and feedback on my work. Finally, many thanks to my friends and family, whose support helped me get this far.

Abstract

The aim of this thesis was to develop tools for evaluating the potential sustainability and security of renewable energy systems in the UK, with a long-term view of maximising the potential renewable energy penetration of wind and solar by deployment of electrical energy storage. Using computer modelled renewable energy systems, a number of system variables are considered such as system size, energy sources (solar and/or wind), type of demand load, and capacity and type of storage technology. The results allow for a broad comparison of different types of renewable energy systems, and their optimisation. The optimisation methodology is also critically evaluated with consideration of its robustness and applicability, using two alternative metrics to measure system energy security and two different measurements of energy return on investment (EROI) to measure sustainability.

When comparing renewable energy systems, results found that large systems that predominately got their power from wind sources were the most sustainable and secure, using optimisation methods that penalised both their overproduction and underproduction. Nearly all systems benefit from the use of electrical energy storage, without impacting too much on sustainability levels, but larger wind systems used less storage, suffering lower energy security as a result. System performance can best be improved by developing solar power technologies with lower embodied energy costs, followed by a reduction in embodied energy of storage technology. The former will enable more effective use of storage methods, while the latter allows for larger storage capacities with less environmental impact.

Sustainability and energy security were given equal priority in the optimisation, however it was found that more sustainable generation technologies were preferable to more secure technologies, as there is more scope to improve energy return on investment than security. Therefore there is a limit, generally around 45-85% (depending on size of system and choice of technology) to the proportion of time that renewable energy systems using variable energy sources can be autonomous, meaning that energy backup from the grid and/or dispatchable sources is still required.

Glossary

BOS Balance of system, the components such as inverter, frame, cables etc, that are necessary parts to an energy system.

CAES Compressed air energy storage, a form of electrical energy storage.

CCGT Closed cycle gas turbines, a modern and more efficient type of gas power station.

DG Distributed Generation, the proposal of decentralised energy systems.

DOD Depth of discharge, the maximum percentage of stored energy that can be used from a battery while ensuring reasonable battery life.

η_G Life cycle energy conversion efficiency of the current electric grid, taken to be currently 0.31 for the EU-27 grid.

E_{in} The measured energy inputs of a technology/system, otherwise known as its embodied energy.

E_{out} A technology's total generated energy over a set period of time, or the net output of energy from a system.

EE Embodied Energy.

$EEIR$ $EROI_{out}$ of a system multiplied by its EIR value. System is able to export energy.

E_uEIR $EROI_{used}$ of a system multiplied by its EIR value. Excess energy is curtailed.

EIR Energy Index of Reliability, measuring the proportion of energy demand not satisfied.

EROI Energy Return On Investment, a metric of energy return used for sources of energy and energy systems. This thesis uses the net energy return (NER) definition.

$ELOLP$ $EROI_{out}$ of a system multipled by its $(1 - LOLP)$ result. System is able to export energy.

E_uLOLP $EROI_{used}$ of a system multipled by its $(1 - LOLP)$ result. Excess energy is curtailed.

EPBT Energy payback time, the amount of time required for a renewable energy technology to produce the amount of energy equal to its embodied energy value.

$EROI_{out}$ Energy Return On Investment using the returned energy value E_{out} that takes into account system inefficiencies.

$EROI_{used}$ Energy Return On Investment using the returned energy value E_{used} that only accounts for energy used locally within the system. Sometimes abbreviated to $EROI_u$.

Li-ion Lithium ion batteries.

LOLP Loss of Load Proportion, proportion of system's lifetime that it spends where demand cannot be met by locally generated demand.

NaS Sodium-sulphur batteries.

NER Net energy return, an EROI metric where energy use/losses within the system is subtracted from the total energy output.

PbA Lead acid batteries (generally referring to deep cycle models in this thesis).

PITS Power integral time scale - a measure of how long a time-series will (on average) keep a positive autocorrelation, i.e. the time-scale over which fluctuations occur. A longer PITS will mean a more predictable time-series.

PHS Pumped hydro storage, a form of electrical energy storage.

PV Photovoltaic solar panels.

RE Renewable energy.

SOC State of charge, how "full" a battery is at given time t. Note minimum SOC$= 100\% - \text{DOD}$.

VPP Virtual Power Plant, an energy system containing points of energy supply and demand, connected to the grid but capable of local energy flow management.

VRB Vanadium-redox batteries, a type of flow battery.

ZnBr Zinc-bromine flow batteries.

Any other abbreviations and symbols in the text are defined where they are used.

Chapter 1

Introduction

1.1 Background

Climate change is one of the most pressing concerns of the world today, where increased greenhouse gas (GHG) emissions in the atmosphere caused by the burning of fossil fuels are triggering changes in the world's climate, leading to potentially catastrophic results [1]. There are many sectors such as industry, transport and agriculture which are creating these emissions, however the ones which receive the most attention are those of electricity generation and other direct use of energy such as space heating and transport. These three sectors are the source of more than 50% of the UK's current GHG emissions, as shown in figure 1.1. Electricity generation in particular has the highest level of emissions and is the one with the largest capacity for transitioning away from fossil fuels to renewable sources such as wind and solar.

Given this attention, and the need for immediate action, countries around the world have set targets for achieving certain percentages of their electricity generation from renewable energy sources, which in principle have zero emissions during their operation. The European Union has the target of achieving a 20% drop in GHG emissions by 2020, in part by increasing its use of renewable energy sources to 20% of all final energy consumption. Each country within the EU has individual targets to contribute to the total of 20%, where the UK has made a legal commitment to sourcing 15% of their energy from renewable sources by 2020. As this 15% target includes all energy, not just electricity, this likely requires the UK's electricity to come from at least 30% renewable energy sources [2]. These targets have been made with the assumption that by 2050 there will have been mass electrification of transport and heating systems, so the shift to renewables will be carried over to those sectors too, leading to reduced carbon emissions across the board. The incentives given for this shift to renewables have primarily focused on individual generation technologies, those being wind, solar and some micro-hydro schemes. The two main policy incentives have been Renewables Obligation Certificates for large installations (mostly wind power) and Feed-in Tariffs for small installations (mostly photovoltaics), however both are now being phased out as of early 2016, despite the UK potentially falling short of the 15% target by 2020. A longer term goal is a reduction of GHG emissions by 80% relative to 1990 levels by 2050, but it has not been fully established how this will be done. However, it can be presumed that renewable energy technologies will be part of this solution. The National Grid predicts an installed capacity of 30-40% renewable energy by 2035, depending on scenario, which translates to 60-100GW capacity. However these scenarios are dependent upon the strength of the UK's economy and the strength of political will to tackle decarbonisation, both of which are unknown [3].

This transition to a higher use of renewable energy sources may be more complex than can

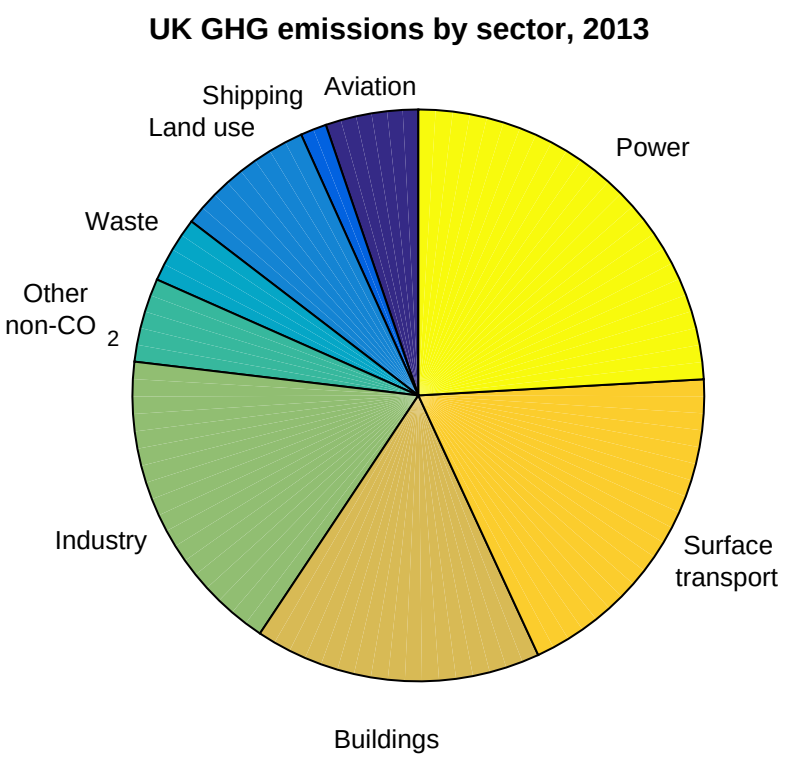

Figure 1.1: GHG emissions of the UK split by sector, normalised to CO_{2e}. "Power" refers to electricity generation, and "surface transport" is all transport except shipping and aviation. Data from the Committee on Climate Change calculations https://www.theccc.org.uk

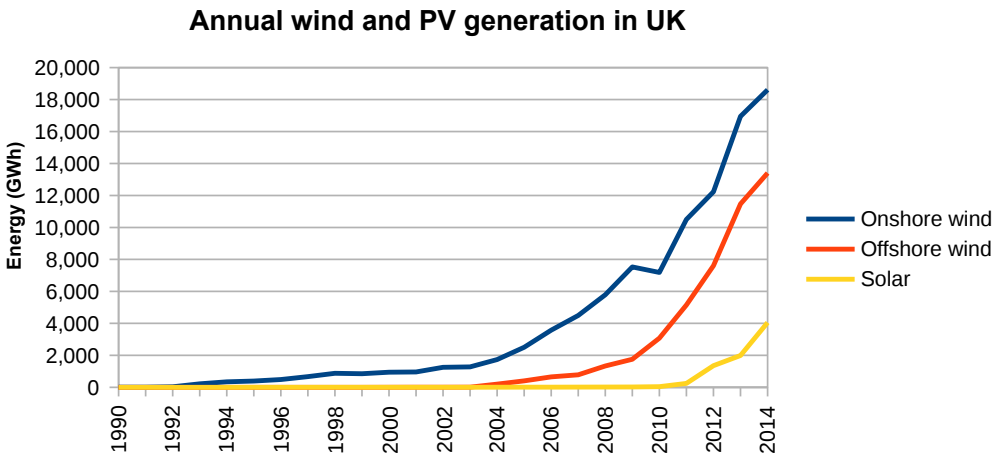

Figure 1.2: Chart showing the annual production of renewable energy sources in the UK, which has followed an exponential trajectory. Data is from the Department of Energy and Climate Change, UK government.

be originally assumed, as the energy system as a whole must also comply with high security requirements. This notion of "security" is somewhat nebulous, however in this context it can be briefly defined as the ability to meet energy demands reliably, ensuring that the "lights stay on". A more considered definition of this concept and security evaluation metrics will be discussed in section 1.1.4. There are concerns that accelerating the transition to renewable energy sources can damage the electricity grid's security, so friction between the two creates a more complex situation, with less straightforward solutions. The third problem of keeping costs low is yet another complexity. The interplay between these three aspects of sustainability, security and cost is known as the *energy trilemma*, where any solution must be a compromise between all three. Furthermore, the three aspects cannot be considered to be independent; for example long-term security is tied to climate change, where political responses may also increase the costs of fossil fuels through carbon taxation or reduction of fuel subsidies.

The increase in power generation from renewable energy sources from 2004 is shown in figure 1.2 using government statistics on electricity generation and supply. Renewable energy provision has increased rapidly over the past 10 years, supplying 19.1% of the UK's electricity over the year of 2014 (including biomass as 35% of the total), however it must be noted that exact annual proportions will be dependent on weather because this is a measure of energy production rather than power capacity. As wind speed is highly variable, certain years may be windier than others, although biomass combustion is not weather dependent. Solar generation made up 6.3% of renewable energy production in 2014, or 1.2% of total electricity production, while wind made up 50% of renewable energy production, 9.5% of the total.

While substantial gains in renewable energy use have been achieved in the past decade, there are concerns about limits to this renewable energy penetration, whereby increasing renewable energy past a certain capacity creates diminishing returns on carbon reductions and increased expense. This is partly because the current structure of the grid requires built-in *capacity reserve* to back up variable sources of power such as wind in order to meet required levels of grid reliability. This is one example of where the energy trilemma comes into play, as this emphasis on sustainability begins to impact on the security and economic costs of grid infrastructure. Increasing wind power capacity on the grid requires a greater capacity reserve for each subsequent unit of renewable generation, where capacity reserves are commonly gas

turbines or even coal generation [4]. Common suggestions for reducing reliance capacity reserves include building greater connections with other countries' electricity networks, installing energy storage on the grid, or managing demand to respond to energy availability (known as demand-side management, DSM). These would all increase the flexibility of the grid, making it more resilient to variability in either supply or demand levels, and providing solutions to the energy trilemma. The more the three problems of sustainability, security and cost are broken apart, the better the compromise can be between them.

However these proposals do not necessarily challenge the fundamental centralised structure of the grid, which was built upon an old system containing large coal and nuclear power stations that, combined with smaller gas or diesel generators, are capable of following demand. If the grid was tailored to fit the needs of renewable energy sources, it would instead use decentralised, or distributed generation (DG), in order to fit the geographically distributed nature of renewable energy sources in general. Well designed DG approaches could also contribute to improved voltage support and improved power quality, in addition to transmission loss reduction and reducing peak power requirements if the systems are well designed [5] [6]. These would not only enable more efficient use of renewably generated energy, but also ensure that energy security remains high while more renewable energy sources come online.

To better understand the potentials for restructuring of the electricity network, we must first understand the current structure, and its positive and negative attributes.

1.1.1 Historical and current structure of the UK's national grid

The electricity network in the UK currently functions in a centralised and demand-led framework, as it is in most Western countries. This means that most of the electricity generated is produced by a small number of large power stations, which respond to the nation's electricity demand in real time. Such a strategy requires a centralised management system; while a certain amount of demand and wind availability can be forecast a day or two in advance, during the day there will be unforeseen fluctuations or hour-ahead predicted changes which need to be matched by immediately turning on or off certain power stations. This leads to three main types of power station [7]: baseload units, which are usually large coal or nuclear power stations that have slow response, cheap fuel, and cannot be turned up or down easily; load-following units, which are smaller quick response plants capable of being turned on or up/down to match load; and peaking units, which are very quick response plants, available for demand peaks and in emergencies. Peaking units have the highest running costs, so are used only when necessary.

Base-load power stations can provide the constant minimum power required to meet electricity demand, load-following plants provide supply to match forecasted fluctuations, and any unpredictable extra demand or losses due to power station failure can be supplemented by peaking units, typically gas, energy storage or spinning reserve (where a rotor is already spinning and can be connected instantly to the grid without needing to start up). Figure 1.3 shows this in action, where nuclear and coal plants supply the baseload, gas combustion in closed cycle gas turbines (CCGT) supplies most of the load-following generation, and pumped hydro storage (PHS) becomes available at peak times. There exists around $1.8GW$ available storage from the PHS plant Dinorwig in Wales, which is the only storage unit of significant size in the UK. PHS plants function by buying power from the grid at times of low electricity cost in order to pump water uphill, and letting this water flow downhill through turbines to generate power at times of high cost, generally when supply is limited due to high demand. Within this framework, wind and solar generation is treated as negative load, and is forecasted alongside the demand load. Therefore as wind and solar electricity generation increases so does the variability of the load, making it more difficult to balance the grid.

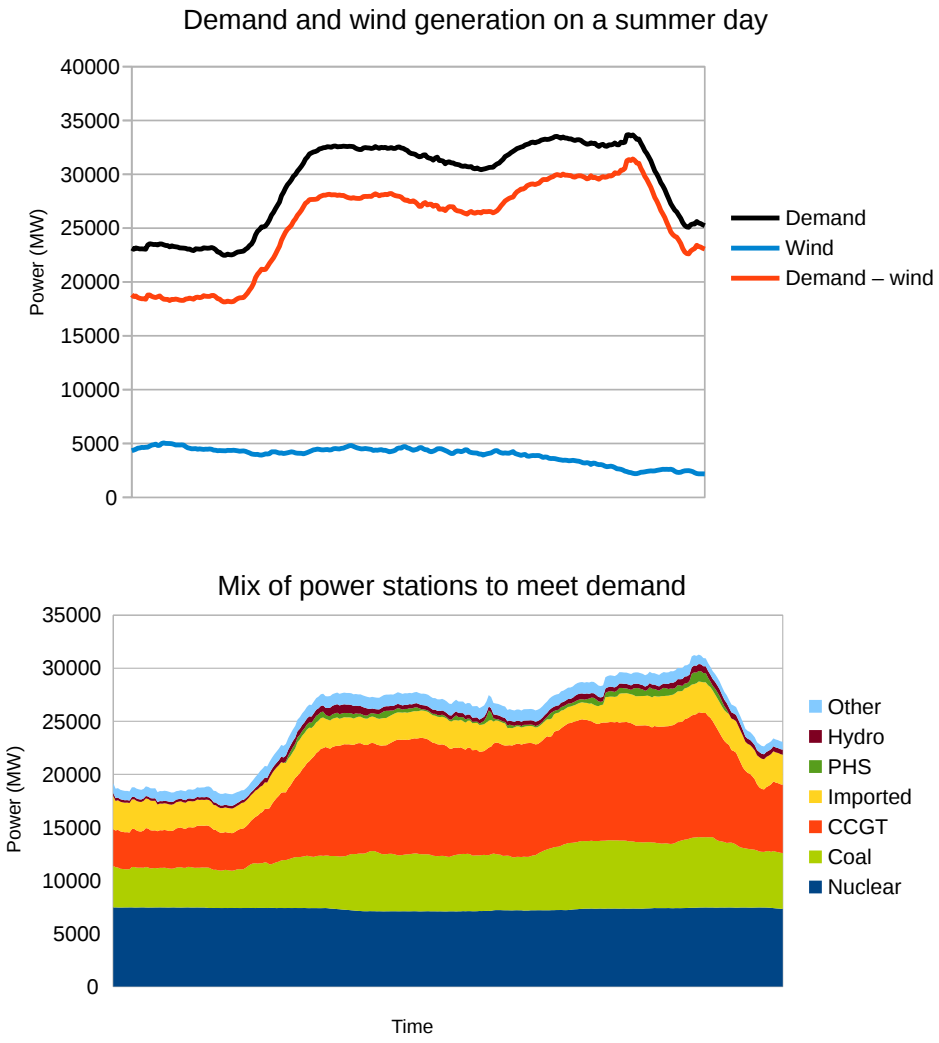

Figure 1.3: Meeting demand (minus wind) with conventional combustion power plants. Baseload is visible as nuclear and coal, while other more flexible sources, mainly CCGT, provide load-following and peak power. Graphs use real power generation data from a day at the end of May.

While this is in principle managed centrally, the market mechanisms that guide the balance of the grid are somewhat deregulated [8]. This is a relatively recent development in the past 25 years, as part of a worldwide movement away from the nationalisation of the energy sector. The hourly or minutely fine-tuning of the grid balance may be conducted centrally using the mechanisms described above, but the basic power capacities available are calculated on the previous day through trade mechanisms on a spot market using forecasted data. To summarise how this market operates, the price of electricity per kWh decreases when demand goes down, which triggers generation to drop as not all suppliers will be able to sell their electricity below certain thresholds. When demand increases, more expensive energy sources such as CCGT or PHS become available on the market to meet this demand, and so the price per kWh will increase. Renewable energy sources are very competitive on the wholesale market, as they are able to sell at very low cost. This trading is conducted on the day-ahead wholesale market by large buyers and sellers, using information on forecasted energy demand and availability. While this does not account for all of the grid, as there are also separate bilateral agreements between some sellers and buyers, the liberalisation of the energy market has opened up the electricity grid to the possibility of a decentralised structure.

This energy management strategy has shown to be very reliable, as the UK's electricity grid is highly secure against the risk of blackouts and brownouts (where a blackout is avoided but voltage drops low enough that power quality is substantially impacted). However, it is limited in its scope. Once renewable energy penetration is high enough, it will impact into the usefulness of base-load power stations because power from renewable sources will outcompete base-load power on the energy markets. If base-load plants are not able to reliably sell their power, they will either run at a loss, creating unnecessary GHG emissions and financial uncertainty, or be forced to ramp production up and down which is less efficient, again creating unnecessary GHG emissions. Variable generation from wind and solar also increases the need for spinning reserves and quick response power stations (which are more expensive) to balance the grid. These are the capacity reserves that were mentioned earlier. Increased use of expensive generation, particularly if power requirements quickly fluctuate, is obviously more costly and can reduce the efficiency of the running of these power stations, thereby undoing some of the gains in sustainability that renewable energy was originally designed to deliver. If renewable generation is particularly high, it may even be necessary to curtail its output. This is why restructuring is necessary, to make the best use of renewable energy sources by ensuring they can increase the entire sustainability of the system and have no negative overall impact on its security.

1.1.2 Distributed generation

The centralised grid described in the previous section has a hierarchical transmission and distribution system as shown in figure 1.4, where the large power stations generate electricity at a high voltage (400kV or 275kV). This voltage is stepped down to 132kV for the subtransmission grid, which then feeds into local distribution networks at voltages of 33kV, 11kV or 6.6kV. The final household consumer then uses the electricity at a voltage of 400-415V (this is three-phase, giving 230-240V per phase). Therefore problems arise when excess electricity is generated at points of low voltage, as local networks are not equipped to export power to the grid in large quantities, and it is a matter of chance whether there will be local capacity for extra generation in a particular location. As the national grid is controlled centrally, and does not monitor small generation installations such as rooftop PV, the imported electricity to a local network will not necessarily be reduced to compensate for any increased local generation, and local power quality (typically voltage/frequency quality) issues may occur as a result.

However, as electricity generation transitions over time to using more renewable energy

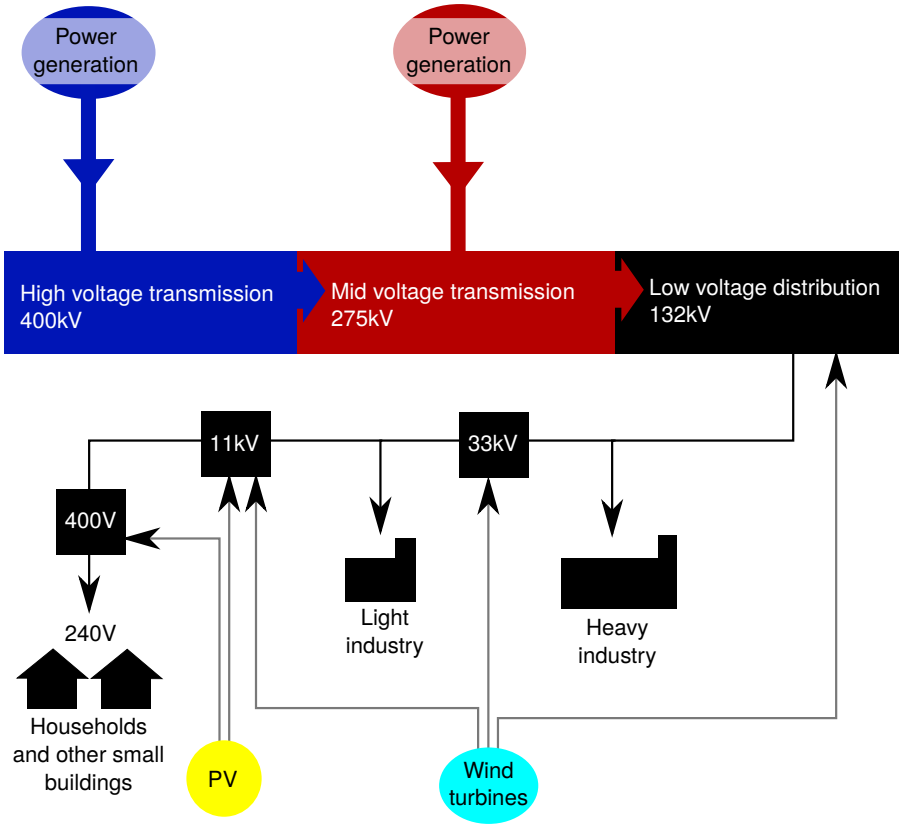

Figure 1.4: Simplified diagram showing the voltage levels of the UK grid. Wind and solar power sources are likely to input to the grid at points of lower voltage than large centralised power stations, which can cause power quality issues.

sources - particularly PV and other forms of microgeneration - distributed generation will likely become more commonplace, where points of generation are close to points of demand and therefore do not feed into the grid at high voltage levels [9]. Distributed generation is not centrally planned by the power utility, has a relatively small power capacity and is connected to the distribution system rather than transmission (black sections in figure 1.4).

This is already happening in the UK; the deregulation of energy markets and adoption of certain policies such as the Feed-in Tariff has facilitated the move to distributed generation, as smaller power generation companies have been able to enter the market more easily, and households have been able to generate their own electricity while remaining connected to the grid. Since 1999 when the market deregulation took place, independent energy suppliers have become more commonplace, increasing from 7 in 2010 to 19 in 2014 and also increasing their collective market-share by over a factor of 6 [10]. Meanwhile distributed generation operating under the Feed-in Tariff (enacted in 2010) increased to an annual total of 4.05GW by the end of 2015, where 99% of these installations are PV, and 2.39GW comes from domestic installations - largely rooftop PV arrays [11]. These installations are too small to connect to the high voltage transmission system, and currently are spread out enough that they have been able to export to the grid without much difficulty, but embracing this decentralisation would require more radical changes to the grid structure as a whole.

Such a decentralised structure would require better communication between network subsystems, and buffering technology to allow for local management of variable levels of wind or solar generation. Electricity subsystems like these are called *smart-grids* [8], where an information system is overlaid on the energy system, allowing for secure and flexible energy management based on real-time demand data. This would enable a more accurate energy spot market functioning similarly to the current day-ahead market, where energy users could shift their energy use to times when prices are lower. A smart meter roll-out is planned for the UK, which would be a crucial step in giving half-hourly demand data for individual households. This is an example of systems based policy.

These smart subsystems could be used to build up a network of distributed virtual power plants (VPPs) that contain points of power generation and also demand, where local renewable energy sources are prioritised and security within the subsystem is maximised using local energy flows as much as is reasonable. A VPP is defined as an aggregation of locally clustered small generation units, generally alongside local points of demand, which is managed within the cluster using smart-grid technology [12]. A VPP will appear to the wider grid as a node on the network that functions much like a single larger power plant, however it may sometimes be a point of demand rather than supply. It differs from a microgrid in that it is always connected to the grid, while microgrids have islanding capabilities, and are designed to function when the larger grid is offline. When it comes to overlaying VPPs on the existing grid, some locations may not allow for two-way electricity flows between the VPP and the distribution network, disallowing the export of electricity to the grid. This is due to technical limitations of the existing infrastructure, as the grid was not originally designed to allow such flows.

In the urban environment VPPs are most likely to use rooftop photovoltaic (PV) powered systems, as these energy resources are by design close to household loads. For local networks with a number of household demand loads, they could also be implemented as community energy schemes, where the ownership of the renewable energy generation would be local, and thus more emphasis is placed on local energy use. Community energy schemes can provide multiple benefits to their local areas and offer bespoke solutions to local energy needs, as there will be better understanding of these needs if solutions are formed within the community [13].

As such systems would be dependent on variable renewable energy sources, local energy balancing methods tend to rely on energy storage and/or demand-side management where

demand is directly managed and/or diversified by connecting to other energy networks such as heating or transport. In particularly, electrical energy storage (e.g. battery storage) has been at the forefront of research and development recently, being seen as the missing link that will enable wider implementation of renewable energy technology [14]. Recent announcements of energy storage projects include a 640kWh capacity battery system alongside a 1.5MW solar park in Somerset [15], where the batteries would actively manage the connection between the PV and the grid, the increase in capacity to 99.9MW of the approved PHS scheme at Glyn Rhonwy in Wales [16], on-grid battery storage with capacity 6MW/10MWh at Leighton Buzzard [17], or the microgrid at the Isle of Eigg where renewables supply nearly 100% of energy demand, backed up by battery storage [18]. In particular, the Somerset installation will form part of an investigation into the feasibility of battery energy storage combined with distributed generation. These real projects are being studied to see if it is realistic to propose distributed generation and electrical energy storage as a future energy system, and the existence of such projects at the commercial stage is encouraging.

These storage units would effectively be run as alternative capacity reserve for variable renewable energy sources [19], so the need for spinning reserves and other plants would be decreased, further reducing coal and gas use by the grid. In an ideal system, wind power would be able to meet baseload demand, facilitated with flexible balancing interventions, and reserve capacity only needed for emergency situations a few days/weeks a year. Such a system would be nearly 100% renewably sourced. It is however unlikely that storage and DSM alone can facilitate a fully renewable electric grid, and connections to neighbouring countries may not have energy available at the right times, so we may still rely on some non-variable energy sources to keep demand met all year round [20].

1.1.3 Integrating heating and transport sectors

Distributed generation can also lend itself to other more creative solutions. As was mentioned earlier, there is a general assumption made in much of energy policy that the future heating and transport energy systems will be gradually electrified, making it possible to run them off renewably sourced electricity rather than the combustion of gas, biomass or liquid fuels. Currently the majority of households in the UK use gas heating, while nearly all vehicles use petrol or diesel fuel, however there are many technologies such as ground/air-source heat pumps, electric storage heaters, battery electric vehicles or hydrogen powered fuel cell vehicles that could facilitate a rapid change towards electrification. This shift will not only allow for decarbonisation of these energy sectors, but also have a large impact on the nature of electricity demand.

Firstly, the demand for electricity would significantly increase to encompass the demand for heat and powering vehicles. While these increases can be mitigated by improved house insulation, improved vehicle efficiency, or shifts to public transport and walking or cycling, they will still have a noticable impact on the grid, demanding more power capacity when resources are already tight. Secondly, changes in type of electricity demand will change the shape of the demand profile; i.e. the daily/weekly/yearly fluctuations in demand. Currently national electricity demand follows a fairly well known pattern, governed by household, commercial and industry loads that are well understood by the grid regulators. However the patterns of vehicle use are less well understood, especially if users of battery electric vehicles use them differently to current internal combustion engine models. While heating demand patterns are better known, as we have figures of gas usage, the need for heating in the winter (in the UK and other high-latitude countries) means that much more power capacity would be necessary in the winter than the summer. This power capacity brings in extra cost, and relative disuse in the summer - unless major demand-side management is brought in - means that the return on that capacity investment would be lower.

Not all this change in demand is necessarily bad, as it may improve energy security; adding points of heat storage, vehicle batteries or hydrogen generation can allow for more flexible demand, the current grid being limited by having to satisfy most of its demand directly in real-time. For example, the grid currently has much higher demand during the day and evening than the night, and turning off wind turbines overnight is a waste of the cheap energy they would produce. However, if this electricity production could be stored during that time in heat storage or vehicle batteries then the production could be utilised, reducing demand later on during the day when there is less capacity to spare. Heat pumps could also allow for some storage as they are generally equipped with a hot water storage tank, but their load profile is generally more constant throughout the day, so has relatively limited flexibility in comparison to storage heaters or even electric boilers [21]. Such approaches work well within the VPP framework, as they allow for further local management of energy system security. Managing such a complex mixture of energy systems would undoubtedly be impractical at the national level, and unnecessary given the amount of built-in flexibility and resilience of the system.

Therefore the diversification of energy demand into heating and transport will likely have a diverse range of effects on the grid, both in terms of its security and sustainability. In fact, it could have both positive and negative effects on either aspect, depending on how well the transition is managed. Given the constraints on how much renewable capacity can be built in the UK, based upon its demand for land area [22], there will likely be a real need to reduce overall demand to have a realistic change in these sectors. This could also have positive effects on health, if improved insulation brings warmer homes and more active transport such as walking and cycling benefits people's physical health. However it makes the potential demand modelling and future extrapolations difficult to predict accurately.

1.1.4 Calculating energy security

While the energy trilemma lists security as a single entity, the reality is far more complex. Energy security is commonly thought of as fuel supply security, most commonly related to oil and gas supplies, which is further linked to geopolitical security. However, in the event of a transition to renewable energy sources, fuel supply ceases to be as relevant, and the reliability of the electricity network becomes more important. The notion of energy system reliability can be divided into two definitions: *adequacy* and *security*, as shown in figure 1.5.

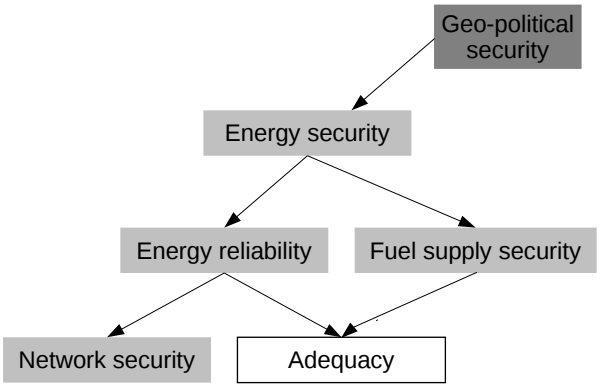

Figure 1.5: Showing the different dimensions of energy security. In the context of a transition away from fossil fuel use, fuel supply security becomes less relevant, but concerns about unreliability of variable energy sources (such as wind) become more important. This type of security can be evaluated using adequacy evaluation, where adequacy describes how well the energy system can satisfy demand.

In this context, the energy system's adequacy refers to whether there are sufficient resources to satisfy energy demand, and the system's security is its ability to respond to dynamic disturbances within the system [23] [24]. Reliability evaluation usually refers to simply adequacy evaluation, which makes use of a number of probabilistic indices, the most common being loss of load indices and loss of energy indices. Loss of load indices estimate the expected length of time (within a given timeframe) that the system cannot supply enough energy to meet demand, while loss of energy indices give the total amount of energy demand that cannot be supplied during those loss of load events. Their probabilistic metrics Loss of Load Probability (LOLP) and Energy Index of Reliability (EIR) can be calculated simply for a total time period of length H hours. The most commonly used metric is LOLP:

$$LOLP = \frac{LOLH}{H} \tag{1.1}$$

where LOLH is the loss of load hours, or the number of hours that generation will not be high enough to meet demand. This is sometimes also called LOLE, or loss of load expectation. The industry accepted standard in the USA for a reliable system is to have LOLE less than 0.1 days per year [25].

The equivalent index EIR gives the proportion of energy demand (the cumulative energy demand over time H being E) that is met, and is defined as

$$EIR = 1 - \frac{EENS}{E} \tag{1.2}$$

where $EENS$ is the expected energy not supplied (or loss of energy expectation), measuring the cumulative energy demand that is not met when the system suffers from loss of load.

For demand-following power plants these indices can be calculated by a simple comparison of peak load versus grid capacity, taking into account probabilities of power plant outage. However, when applied to variable sources of energy such as wind or solar, the analysis is somewhat more complex and requires consideration of the time-dependent nature of both demand and supply variability. This generally requires a sequential simulation using time-series to demonstrate fluctuation of supply and demand, as the correlation between the two is of vital importance, although non-sequential models are also possible and have a lower computational cost [25].

Concerns about meeting demand can therefore be reduced to a simple application of one of these adequacy metrics. However focusing entirely on security could bring in some unwanted costs, whether those be financial or environmental, so cost analysis is required as part of any security evaluation in order to find natural limitations to a given system's security. These costs could come from any kind of additional infrastructure, such as storage units, IT networks, or connections to external electricity grids, thermal systems or transport systems. To establish a purely physical evaluation of these energy systems, the costs brought into this study were environmental rather than financial, investigating the idea of a "sustainability metric".

1.1.5 Calculating energy sustainability

In order to sufficiently measure sustainability of our energy systems, sustainability must be defined in a quantifiable and accountable way. The most commonly used definition from the Brundtland Report [26] is "Sustainable development is development that meets the needs of the present without compromising the ability of future generations to meet their own needs". However, this is not a quantifiable statement, as the needs of the present and future generations are undefined. It is also unclear whether "sustainability" is intrinsically separate from "sustainable development", but in the context of this research they can be assumed to be the same, the focus being on new energy systems that are being proposed and analysed.

The main motivation behind a transition to renewable energy is to reduce GHG emissions, particularly carbon dioxide, and for that reason, analyses of renewable energy sustainability are often focused on the potential for GHG emissions reductions only. These must take into account the emissions from any (fossil fuel powered) capacity reserve mentioned earlier, and the embodied emissions created in the lifecycle of the renewable energy technology. However, in a potential future with 100% renewable energy sources, this approach is lacking rigour, as renewable energy technology could be built using energy entirely from renewable sources, and the capacity reserve could be replaced by flexible energy management or have net zero emissions by using renewable sources of fuel such as responsibly sourced biomass/biogas. However we do not want to create systems that are unsustainable in terms of energy production despite having low GHG emissions. Measuring the energy return on investment (EROI) as a ratio of energy output against lifecycle energy costs, can evaluate energy systems with regard to this greater level of sustainability, and gives an good indication of carbon dioxide emissions when considering renewable energy technology built using fossil fuel sources [27]. This analysis has already been used on biomass and biofuels to argue that biomass's low EROI levels contradict the claim that it is a long term sustainable solution for electricity generation [28]. This analysis also points out that a transition to energy systems with lower EROI will result in a less efficient economy, as more resources would be diverted simply to energy generation.

Returning to the definition at the beginning of this section, EROI values can give a realistic idea of how our energy needs of the present compare with the ability of future generations to meet their energy needs. If EROI values are high enough then the energy system becomes self-sustaining, creating available energy for our current needs and the needs of future generations. However quantifying a threshold is incredibly difficult in practice, as the entire economy would need to be analysed and compared to our levels of natural resources [29] and in practice neither of these are fully documented.

Sustainability measurement is tackled further in the literature review, as different approaches to the question of sustainability are examined with respect to their practicality and accuracy. While there has been a significant amount of life cycle analysis done on individual components of renewable energy systems, there is less awareness of it at a system level, especially when also considering system energy security. The metric EROI has become a popular method of sustainability measurement, however there is some inconsistency in how it is applied, so it is important to be aware of what energy flows are being managed, and to carefully evaluate the values of embodied energy used in analysis. This evaluation is done through a review of existing life cycle analyses, and includes uncertainty analysis of the model results to test how sensitive they are to the uncertainty of embodied energy values.

1.1.6 Considering economic sustainability

Economic metrics largely fail to consider environmental costs such as carbon emissions, and the economics of renewable energy technologies in the UK are constantly in flux due to rapidly changing markets and unpredictable government incentives. The fluctuating nature of markets makes them a less reliable predictor of long-term energy issues than physical or ecological approaches [29]. Furthermore the influence of Chinese PV production and the subsequent drop in the Feed-in Tariff in the UK, not to mention the potential removal of many renewables incentives or conversely the introduction of carbon taxation, show that renewable energy costs are still heavily influenced by political positions. Current economic analyses of sustainable technology such as marginal abatement cost (MAC) curves also suffer from not considering interdependencies between different technologies [30]. Ignoring these interdependencies leads to too much focus being placed on individual components such as PV, to the potential disruption of energy security or overall sustainability.

There are two potential solutions to tackling this economic unpredictability; to either bring environmental costs into the economic sphere, such as by estimating potential future carbon taxation levels, or to address strictly the physical ramifications of energy systems. Taking the physical analysis approach would determine general costs in relation to resource use and energy intensity. This particular study took the latter approach, where physical parameters can be measured using life cycle analyses of the technology involved. Some notion of financial cost would be imbued in this energy cost, however additional costs would be unaccounted for.

1.2 Overview, aims and objectives

This thesis brings together a number of studies centred around local renewable energy systems. The aim is to establish to what extent localised renewable energy systems and storage can provide values of sustainability and security. This is done at multiple sizes of demand networks, from single households building up to a community energy system with different types of energy inputs.

Most of the studies are chosen to only include mature technologies, however when considering the future energy system we should consider more radical changes such as widespread electrification of heating systems, and hydrogen storage/utilisation. Therefore there is also an analysis of a household system with a heat pump to supply space heating demand, and a household system with hydrogen used for energy storage. The potential for these investigations is limited at this stage, given lack of data associated with future thermal demand and life-cycle assessments of space heating technology/infrastructure or hydrogen systems. However these preliminary assessments can create the space for further work, and signal potential avenues of research and development.

The underlying hypothesis is that combining different types of energy sources and implementing energy storage will improve energy security, with a diminishing return and increasing cost as their sizes increase. Modelling the systems will allow for an understanding of how much the returns diminish, and therefore at what point the energy costs override the gains.

The theoretical framework of this thesis builds on the premise of distributed generation as a new pathway for energy generation, and applies the use of simple metrics to form a straightforward yet comprehensive optimisation/evaluation of these distributed renewable energy systems. The systems are assumed to be connected to the larger electricity grid, and capable of local energy quality management but limited in terms of how much they can export/import energy to and from the grid (this can be due to high renewable energy penetration or not allowing two-way energy flows). They are also mostly assumed to not be connected to other forms of energy systems such as heating or transport, and the limitations of this assumption are explored, as such connections would be useful for managing demand in a more flexible way.

Such a framework is compatible with the current political goals of GHG emissions reduction, which relies heavily upon reforming the energy sector to shift from fossil fuels to renewable energy sources. While the UK is not currently committed to a 100% renewable energy goal, the recent increase in renewable energy sources has prompted some pilot schemes into distributed energy systems and battery storage, listed in more detail in section 1.1.2. Assisting this distributed approach is the smart meter roll-out in the UK, planned to be completed by 2020; a smart meter infrastructure supports the building of smart grids, essential for distributed networks to manage themselves locally. Real pilot installations are important for finding the technical and commercial feasibility of distributed renewable energy systems, however a theoretical approach is also useful to evaluate long-term outcomes, and to

generalise results for comparing the wide range of different system types across different locations. This kind of analysis is also capable of pinpointing potential avenues for improvement, and comparing technologies in a fair way.

Using the fundamental attributes of sustainability and security, both major parts of the energy trilemma, this thesis explores the performance of renewable energy systems through the lens of five major questions:

1. Is there an optimal mix of wind and solar technologies in the UK's climate, and what are the implications from any such optimum, now and in the future?
2. How effective is electrical energy storage at providing security services to local renewable energy systems, and can this be done in a sustainable way?
3. What limits exist regarding the sustainability and security of distributed energy systems?
4. How can the technology be improved most effectively to surpass such limits?
5. When the method is applied to a real case study, how do real world limitations affect these results and conclusions?

These questions are posed for systems of varying size and application, and also for different types of electrical energy storage technologies. By comparing system results with respect to these variables, we obtain a fuller understanding of the optimal results, leading to a more considered evaluation. Therefore this is not simply an optimisation study, many of which already exist in the literature. Instead it is a broad study of the strengths and weaknesses of renewable energy systems, evaluating how they can best be purposed. The study seeks to find the strengths and limitations of energy storage being used to balance renewable power generation, as well as finding its optimal use. The application of these techniques to a case study is an important part of the process, where social, geographical and political aspects have to be brought into consideration.

This study therefore draws together research from multiple areas, covering new ground by considering system optimisation and evaluation from an objective physical view of the systems. While the financial aspect of the energy trilemma is not directly tackled, using EROI as a sustainability metric addresses some economic concerns and refocuses the question on how economic policy can be used to incentivise the best performing energy systems, rather than simply individual technologies.

1.3 Research design

The research approach uses probabilistic methods, modelling large samples of potential renewable energy systems in the UK and generalising these results to find typical outcomes. Several types of modelled energy systems are analysed using metrics that emphasise the importance of sustainability and energy security. These are modelled at multiple sizes: from the scale of a single household system or non-domestic building, to several networked households, to a community energy case study where the energy system contains an entire small town. The systems are shown in figure 1.6.

By modelling systems at a variety of sizes it will be possible to advise the best solution for a system of given size, rather than using a one-size-fits-all approach. This is particularly crucial considering the current debate around community owned renewable energy systems, which will usually be smaller than a privately owned wind farm and also contain demand loads next to the point of generation, therefore could also be considered a virtual power plant (VPP) if combined

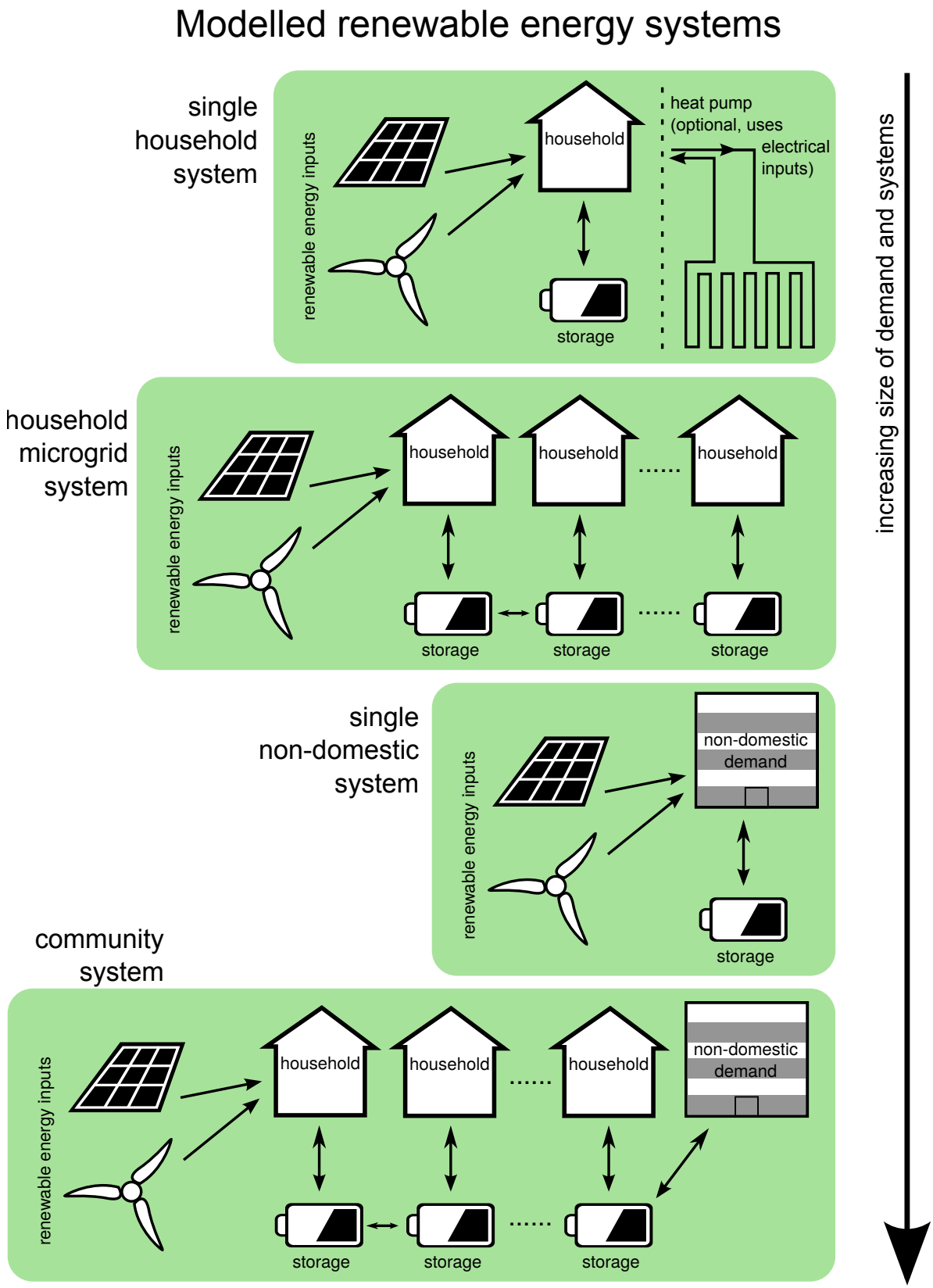

Figure 1.6: Different energy systems to be modelled, all with PV and wind input, modelled either able to export to the grid or with curtailed excess generation.

with local network management. By including demand loads from domestic households and non-domestic buildings, the types of system can also be evaluated and compared. For example, it is often commented that household energy use is anti-correlated with solar production at high latitudes, but the effect this has when storage is used to match supply to demand has not been thoroughly investigated.

A number of different storage technologies are also analysed and compared in terms of their performance for renewable energy systems. As lead-acid batteries are the most mature battery technology, they are often the only battery used in this kind of analysis; however new storage technologies are being developed or repurposed for utility scale storage, responding to the need for new methods of balancing the increasing renewable energy deployment worldwide. In particular, lithium-ion batteries are efficient, long-lived and have a certain level of technical maturity, and new flow batteries such as vanadium-redox batteries [31] are being suggested as suitable for large scale storage. Additional technology relating to heating and transport systems is also considered in relation to the simulation results, where these solutions offer added flexibility and alternative methods of energy storage.

As was mentioned earlier, the approach to energy security measurement has been to use adequacy evaluation metrics, which address underproduction. However, it is recognised in the literature that unmanaged overproduction can also be considered as an energy network security threat. As the energy systems concerned are managed locally, it was assumed that any overproduction is either exported to the grid or curtailed, depending on the resilience of the local network and the renewables penetration in the wider grid, as high penetration may make it difficult to use exported energy. This choice of scenario led to the development of an alternative EROI value: $EROI_{used}$ where any energy production unused in the local system is removed from the recorded energy output. To better distinguish these metrics, the standard EROI is given as $EROI_{out}$ to make it clear that all energy system output is considered in the EROI calculation.

To evaluate energy system performance, composite indicators were created using sustainability metrics $EROI_{out}$ and $EROI_{used}$, multiplied by energy security metrics $LOLP$ and EIR. These composite indicators were used as objective functions to undertake optimisation of the systems, and are shown in figure 1.7. Rather than using a single composite indicator, using these four variants allowed for consideration of different scenarios, and also to compare $LOLP$ and EIR in terms of their accuracy and applicability.

While most of the results rely upon generalisation of a "typical" energy system in the UK, it has been recognised that geography is still an important factor, for both physical and social reasons. Firstly, the wind and solar availability are incredibly dependent upon location, where wind depends upon the local micro-climate, and solar more on general latitude (although cloud cover must also be considered). This will have an effect on the potential best energy source, even within the UK. The social aspect can end up being even more important than the physical geography, particularly regarding wind power where social unacceptability in certain places have prevented it from even being an option within the local energy system. Aside from matters of social acceptability, local support for certain technologies, or traditions that lead towards the use of certain energy sources, means that results must be viewed with practicality in mind. This is why the largest model was based upon a case study in Stocksbridge, Sheffield, an area with abundant natural energy resources but some local opposition to wind turbines. This allows us to examine how the generic systems relate to a theoretical energy system with a particular locality.

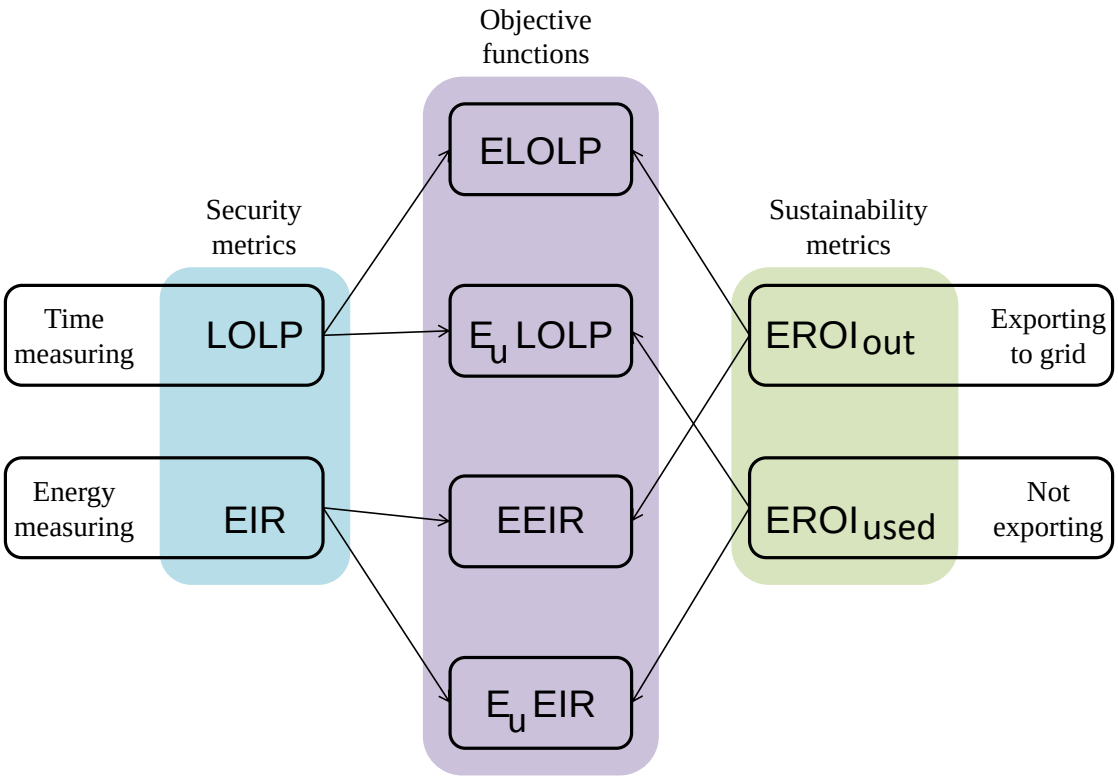

Figure 1.7: The four simple objective functions used for performance evaluation, each created by multiplying a security and sustainability metric together.

1.4 Thesis outline

This introduction has outlined the proposal of a physical evaluation of small renewable energy systems with inbuilt storage. These energy systems are designed to be the building blocks of distributed generation network with a guiding principle of maximising energy from renewable sources in a sustainable and secure way.

The next chapter is a thorough literature review of the subjects touched in this introduction. It begins with a look into appropriate methods of energy system modelling and optimisation, followed by a more detailed investigation into defining and measuring energy security and sustainability. The technology used in the various studies is also examined in more detail, to guarantee appropriate selection of technology and more accurate simulation in the system models, not to mention greater accuracy of their embodied energy costs.

A reflective interrogation of the literature has led to greater potential and more meaningful results, as divisions in the literature demanded closer attention to certain assumptions and testing within the studies. Most importantly these related to discrepancies within EROI calculation, which triggered a need for critical evaluation of how alternative methodologies affect the results. The wide variation in recorded embodied energy values also led to a focus on uncertainty and sensitivity analysis, helping us understand future impacts of technology improvement.

The methodology is covered in chapter three, which explains in more detail how the energy system models are designed and generated from random weather data, and explains the construction of the metrics and objective functions (for application in optimisation) with relation to the specific modelled samples. There is also an analysis on the available input data based on recorded weather (solar irradiance and wind speeds) in the UK and building electricity demand.

The next three chapters cover the results. Preliminary results are shown in chapter four, in particular a validation of the model, statistical features of the models' input data, and its limitations which need to be considered within the main results. These results are based on limited data sets or mathematical reasoning.

Chapter five is the main results chapter, which works through optimal results of all the generalised systems: single households, small networks of up to 20 homes, and commercial/industry demand loads. In addition to the optimisation studies is evaluation of the metrics, uncertainty and sensitivity analysis regarding the model's embodied energy values and battery efficiency levels, and short investigations of alternative systems such as hydrogen storage and domestic electric heating. The results from this section primes the discussion before the case study.

Chapter six covers the results from the Stocksbridge case study, which uses the methodology in conjunction with a real location, taking into consideration how this affects the choice of technology available. This study uses only one of the four composite fuctions ($E_u EIR$) after considering metric evaluation in the previous chapter, and assuming that such a large system with a limited size connection would be unable to export excess production.

Chapter seven is the conclusion, which ties together the results from the generalised systems and the case study, and discusses the deeper meaning of these results.

Chapter 2

Literature Review

As governments increasingly talk about decarbonisation goals, the restructuring of our power systems to include more renewable energy sources becomes more of a pressing concern. Is it possible to have a fully renewables based energy system? How do we ensure that the lights stay on as we switch from mature fossil-based sources to renewable ones? Does the use of renewable resources actually result in a sustainable energy system once all the extra requirements are accounted for? Given the size of this task, and its impact on the lives of many people, there is unsurprisingly a wealth of research already being done to find the answers to these questions. Research of interest includes optimisation studies to determine the performance and cost of renewable energy systems, development and analysis of technology designed to balance supply and demand of electricity, and sustainability assessments of renewable energy technologies.

In order to fully understand the implications of renewable systems optimisation, a literature review was done on the modelling and optimisations of such systems, in addition to the definition and measurement of security and sustainability. This chapter is divided into four main sections in addition to a final conclusion as follows:

1. Energy system simulation and optimisation - examining how past research has devised and optimised hybrid renewable energy systems.
2. Energy security - definitions and ways to measure energy security.
3. Energy storage - methods for modelling battery storage, and the technology options available.
4. Sustainability - definitions and ways to measure sustainability.
5. Identifying further work to be done.

2.1 Energy system simulation and optimisation

2.1.1 Hybrid renewable energy systems modelling

The majority of systems studied in this thesis were entirely electrical, and it was necessary to initially conduct a literature review to see the most realistic types of system to study. Bernal-Agustin & Dufo-Lopez [32] review a number of stand-alone hybrid renewable energy system optimisations with different components, where the most common systems are PV-Wind-Battery and PV-Diesel-Battery. Alternative configurations include PV-battery, PV-diesel, wind-battery, wind-diesel, or PV-wind-diesel-battery [33], and some models examine more unusual components such as fuel cells and ultracapacitors [34]. Control systems

for the hybrid systems are dependent on the complexity of the system; hybrid systems with diesel generators and batteries require a complex control strategy to work out the priorities of these components, whereas using batteries only alongside renewable energy sources is much simpler. It can generally be assumed that batteries will discharge when the load (demand) exceeds renewable energy (supply), and charge when the supply exceeds demand. Some optimisation/simulation software already exists, the most popular being HOMER (Hybrid Optimisation Model for Electric Renewables) developed by NREL (National Renewable Energy Laboratory in the USA), which can use time-series from a number of different types of renewable energy sources as input [32].

Choice of load and geographic location are important for contextualising an energy system model, as these can determine the scale and best possible combination of renewable energy inputs. Loads in existing models vary across single households [35] [36], large buildings [37], microgrids [38] and community-scale grids [39] [40]. Accurate power generation time-series are often not available due to dependence on geographic location, so models can take a probabilistic approach, where energy inputs are represented by probability distributions to estimate availability [41] [42], typically using Rayleigh or Weibull distributions to simulate wind speed distribution [43] [44] [45]. An alternative approach is to simulate the power time-series using wind and solar weather data, where wind power can be estimated using wind speed data and wind turbine power curves [33] [46], and photovoltaic (PV) generation estimated from irradiance levels [33] [47] [37]. Wind turbine power curves can be obtained from power specifications of the proposed wind turbine types, but this is not necessarily completely accurate for wind turbines in practice, as manufacturers can over- or under-predict power output [48] [49]. Levels of PV production are also affected by their performance ratio which has a wide range of values within the literature [50] [51], many considerably higher than the reference value of 75% in the Methodology Guidelines by Fthenakis et al. [52] as technology improves over generations [53].

2.1.2 Incorporating other energy systems

Energy systems quickly become more complex when the types of demand loads diversify to include heat and/or transport. The energy sector as a whole only contributes to around 1/4 of the UK's national carbon emissions, while heat and transport each contribute to 1/6, making them also fairly important. These sectors are currently dependent on gas and oil for most of their energy needs, so the UK's renewable energy targets have been made with the assumption that there will be mass electrification of heat and transport sectors [54], since otherwise their decarbonisation would be very difficult. This can take the form of electric heating through storage heaters or heat pumps, and electric/hydrogen private vehicles or electric public vehicles (including permanently connected systems such as rail). Combining these energy systems may also assist in increasing security, as demand can be made more flexible with the use of hot water storage, vehicle battery charging or hydrogen production, the final being effectively a form of energy storage. Vehicle batteries also increases the value of battery technology, being dependent upon batteries for power.

There is support in many countries [55] for using combined heat and power (CHP) generation alongside renewable energy to supply electricity and heat demand, however it has been observed in Denmark that this imposes a limit to how much demand can be fulfilled by distributed generation, while increased renewable generation ends up being exported to neighbouring grids. This is explored by Blarke [56] where they found that the proportion of electricity demand met by distributed sources peaked in 2005, while wind penetration has continued to grow. This has caused some operators retire CHP units or move to simply heat production. Blarke suggests that a better approach would be to improve flexibility of the

system by introducing alternative thermal technology, such as electric boilers or heat pumps to use any excess electricity production to supply heat demands. They found that while electric boilers can provide better flexibility to the system, heat pumps are more cost-effective, particularly when using waste flue gas from CHP units as a heat source [21]. This suggests that both technologies are potential candidates for analysis using EROI, if reliable sources of their embodied energy data is available. A major benefit of heat pumps is their high operating efficiency, typically stated as 300% or coefficient of performance (COP) 3 [57], made possible by their utilisation of underground ambient heat. In practice the COP will vary throughout the year [58], being highest in summer, however most simulations assume a static COP. Also important to note is that the UK's Renewable Heat Incentive offers the greatest incentive to ground source heat pumps and solar thermal, giving 19.33pkWh and 19.74p/kWh respectively, in contrast to 7.51p/kWh for air-source heat pumps and 5.2p/kWh for biomass boilers/stoves (numbers correct for April - June 2016). Solar thermal systems do not count as an electrification of the heating systems, so have been considered out of scope for this study.

The effectiveness of heat pumps is reinforced by a number of other studies [59] [57] [60], showing that the combination of wind power and CHP units brings limitations to the flexibility of the system, and that heat pumps are likely the most economically sound [61] and resource-efficient way of utilising excess wind production to meet existing energy demand, especially in high-density housing [62]. They are also effective at reducing GHG emissions when combined with low carbon electricity, and show only minor environmental impacts (mainly related to limited pipe leakage) over their entire lifecycle [63]. The main alternative candidates for electric heating are electric boilers, which are more expensive [64], or heat accumulation tanks for heat storage. Heat pumps can also be used in conjunction with thermal storage, either using storage tanks or passive heat storage with specially designed thermal materials in housing infrastructure. Comparisons suggest that passive heat storage is more efficient [59]. However, the feasibility of heat pumps is dependent upon their performance, the most widely used metric being coefficient of performance (COP) [60] which can be measured at local or system level. Therefore the installation of heat pumps must be well considered, using best practice operation methods. There are a number of heat pump technology available, but ground source compression heat pumps show better COP on average than air source heat pumps, whether in theory or in practice [65]. More unusual heat pumps include absorption heat pumps (using waste heat flows) and solar assisted heat pumps, which use either solar thermal or hybrid PV/thermal panels to increase the heating potential of the heat pump [66] [67], but ground-source heat pumps are less complex as they not depend upon additional technologies such as solar heat accumulators or waste heat from CHP units. Field studies of 83 sites suggested that ground or air source heat pumps often perform at COP lower than 3, due to poor operational management or unsuitably designed systems [65], however growth of the industry should improve these practices as companies gain experience in manufacturing and installation, and customers become more used to the technology. Notably, a small percentage (13%) actually performed with COP above 3. The heat pump's performance is also affected by the wider system: for example new-build homes are able to use under-floor heating, which requires lower water temperatures than radiators and thus enables more efficient running of the heat pump, as heat pumps run less efficiently when heating above $40°C$. However it is always necessary to heat above $60°C$ occasionally to stop any Legionella bacteria growing in hot water tanks, whether using the heat pump directly or an additional immersion heater [65].

There are a number of studies measuring the carbon savings of different heating technologies, and heat pumps are shown to deliver the highest savings while also increasing system flexibility, allowing for a higher penetration of variable renewable energy sources [68] [69]. However, nearly all these studies only measure the GHG emissions during operation, and do not include embodied

emissions or energy use across the entire life cycle. The limited sources of embodied energy data are reviewed in section 2.4.6 and used to estimate embodied energy of a typical household pump.

The transport sector was considered to be out of scope for this study, as fully electric cars are highly complex in terms of components and still not widely deployed, and thus we are lacking in embodied energy data for such technology required. However linking to thermal systems using electric heat storage or heat pumps may bring more flexibility than using plug-in vehicles, as heat pumps bring benefits to base load power while battery electric vehicles facilitate the management of variable power demand instead, and hydrogen vehicles may offer the most flexibility but are not currently cost competitive [70].

2.1.3 Methods of energy system optimisation

System optimisation is concerned with finding the best performing combination of inputs to a system, evaluated by minimising or maximising a function constructed from those inputs. Existing optimisations of renewable energy systems range in complexity from simply finding the most appropriate size of PV systems [71] to more complex systems with multiple energy sources and battery storage where optimal sizing of different components is required [32] [33]. There are many optimisation methods available, most of which can be divided into two main types: single-objective optimisation and multi-objective optimisation. Single-objective optimisation focuses on one output variable, minimising or maximising this subject to constraints, while multi-objective optimisation is concerned with multiple variables that might correlate or conflict with each other, in addition to system constraints [72]. Some studies optimise control strategy in addition to sizing or type of components [32].

When a single-objective optimisation is carried out, this is usually done to minimise net present cost or levelised cost of energy [32], i.e. it is generally an economic optimisation. Some consideration of system performance must be included to act as constraints in the optimisation, the simplest being a measure of energy balance over the year, showing whether enough power is generated overall to meet demand [34]. This kind of optimisation can be done with system reliability in mind too, giving a minimum level of system reliability as one of the optimisation constraints [42] [35], or a range of constraints on reliability [73]. However when the energy system is grid connected the local limit on reliability is less well defined, so it is more useful to evaluate reliability as part of a general performance analysis. This can be done as part of a multi-objective optimisation of cost and system reliability to find the optimal size of storage [74] [75], alongside the sizing of generation capacities. Where storage is not applied, multi-objective optimisation has been used to optimise a mix of energy sources and the practice of strategies such as demand-side management [76]. Multi-objective optimisation does not generally give a single optimal result, but a set of equally optimal results known as the Pareto front [77] [78], from which the most suitable result can be chosen by a decision maker.

Environmental impacts of hybrid renewable energy systems are rarely included in an optimisation process, despite some recommendations in the literature that these need to be addressed alongside reliability [32]. Exceptions include evaluations where costs of reducing CO_2 emissions are calculated but not optimised [79] [38], one study that carries out a multi-objective optimisation process combining life cycle cost, embodied energy and reliability analysis [78], and a couple of multi-objective optimisations of levelised cost of energy against CO_2 emissions [80] [81].

When these optimisation studies are carried out, they usually give a broad recommendation of different paths rather than absolute optimal results. This is more practical and realistic because of uncertainties and the multitude of variables and indicators. For example, the most common optimisation method is to minimise cost - whether this is the levelised cost of energy, initial costs or some other cost function - for a range of different reliability thresholds, typically

95-99% system reliability measured using LOLP or similar metrics. Results from all these studies generally agreed that while renewable systems could not meet reliability thresholds when only wind power was available [39], hybrid systems such as PV-wind-battery and PV-wind-hydro-battery were capable of meeting requirements within acceptable cost limits [74] [76] [82] [42]. In hot countries such as Greece, PV-battery systems were also capable of meeting these requirements [73] [71].

Some optimisation studies include greenhouse gas emissions or embodied energy as an optimisation variable; their objective is generally to evaluate the cost of CO_2 reductions or to evaluate efficient values of financial incentives to encourage reduction in emissions [83]. In the case of the latter type of studies, plotting the Pareto front (optimal combinations of cost and emissions) shows that initial reduction in emissions costs very little, but the system eventually reaches diminishing returns where an additional large investment can only reduce emissions slightly [84] [46]. Optimising only with respect to cost gave more specific costs of CO_2 emissions reduction using only wind and pumped hydro storage plants, ranging $41-56$ per tonne of CO_2 depending on the scenario [79]. This study suggested that wind generation and pumped hydro storage were a good combination, however traditional fossil fuel plants were included in the optimisation as backup, which would have a impact on the system's security.

One study optimising with respect to cost and environmental impact suggested that using diesel generators as backup in addition to batteries can actually reduce emissions overall, by avoiding oversizing of the other components, and again showed that in hot countries PV is less in need of wind generation backup [81]. Optimising with respect to cost, reliability and embodied energy gave a specific result for 95% energy index of reliability (EIR) chosen from a Pareto front with many levels of reliability with $2.16kW_p$ PV, $900W_p$ wind turbine and $180Ah$ battery storage for a household in Colorado [78]. This combination of system components is specific to this region and the single monitored household, but the method can be expanded to further case studies. A similar multiobjective optimisation - measuring CO_2 emissions rather than embodied energy - had 35 results in its Pareto front, with an example optimal system at 95.5% reliability with $8kW_p$ PV, $6.5kW_p$ wind turbine, $88.7kWh$ battery, and $1.9kVA$ diesel generator [80]. This was for a much larger load, however results showed that despite the high cost of batteries, optimal results rarely used the hydrogen storage component that was given as an option, due to its high cost and low efficiency.

In summary, these optimisation studies showed that a combination of renewable energy inputs gives realistic systems in terms of their cost, security and environmental impact. However it appears unlikely that an electricity grid could function securely with only variable renewable energy inputs, as the oversizing of storage would be unsustainable. Their optimisation approaches generally assumed a fixed lower limit of energy security, around 95-99%, however this is lower than the usually accepted limits in the UK or USA, while simultaneously imposing very strict limits on these small systems.

2.2 Energy security

2.2.1 Defining energy security

Energy security is commonly thought of as regarding fossil fuels only, in relation to political or geographical security. However it can be regarded in a wider sense to mean the general availability of energy: whether the supply of energy is enough to meet our needs now and in the future [85]. Using this definition, it becomes possible to relate the issues of energy security to renewable electricity as well as fossil fuels, as the entire system and supply chain of energy generation are taken into consideration. This is particularly important if the goals

of decarbonising our energy systems are met, as this entails a move away from oil if transport and heating systems become electrified [3]. There are concerns that efforts to broaden the definition of energy security are in fact diluting its purpose, as some definitions overlap with sustainability [86] and a too broad definition can make measurement difficult [87]. Attempts to classify energy security into separate elements or dimensions are not yet fully cohesive, but generally include availability, affordability, sustainability and accessibility [88] [87]. Metrics or indicators pertaining to these aspects are generally applied at the wider system level, such as a country or international grid.

As electricity is our main concern, it therefore makes sense to follow the established theory of electrical power system reliability evaluation, which is divided into system adequacy or security as mentioned in section 1.1.4 [23]. This asserts that the most relevant application of energy security for this study is that of "adequacy" - how well supply is able to meet demand.

2.2.2 Risks to energy security posed by renewable energy sources

The transition from fossil fuels to renewable energy sources can improve energy security in some aspects, as their non-reliance on fuel supply removes many of the geopolitical insecurities that previously defined energy security, but instead there are issues with supply variability according to weather patterns. It has to be noted that renewable energy sources are not intermittent, but variable: the variation in renewable power production across a country like the UK will be fairly smooth, a consequence of having hundreds of smaller generation units summed together. It has been found in practice that as connected wind farms become more dispersed across a larger area, their wind speed correlation drops and total power production tends towards a steady output [89] [90]. There will still be occassional drop-offs in production [76], but this geographical spread means that the drop will be more gradual as the weather will not change suddenly in all places simultaneously. This is very different to when a large coal or nuclear power station shuts down due to failure; wind and solar fluctuations are more predictable and failure of individual small units are less of a shock to the overall system [91]. When renewable sources only make up a small percentage of the energy sources across the entire grid (i.e. there is a low penetration of renewables) these fluctuations are a small fraction of the overall supply, and can be managed in the same way as variable demand - changing the output from traditional power stations to balance supply. However, as renewables penetration increases, fluctuations in supply become large enough that new approaches must be taken to balance the system [92]. Some literature refers to "limits to penetration", however there is dispute about whether these limits are absolute, or simply temporary barriers that can be overcome by reorganisation of the energy system in order to use renewable energy sources flexibly and effectively [93]. It may be possible that even with all the possible changes made to accommodate variable renewable energy sources, a system based primarily on wind and solar power will require conventional fossil fuel power stations for backup in dark windless periods [20]. There are also economic and environmental limits to how much the system can be changed [94], as adding on new technology to manage and balance the electricity network requires significant investment in money and resources.

The effects of high renewables penetration on energy quality have been documented thoroughly, particularly with respect to PV. Solar power production is generally anti-correlated with household power demand in colder countries (i.e. without air conditioning), which is significant because much of PV deployment is on domestic rooftops [95]. Photovoltaics also have the disadvantage of frequently being deployed in areas that were designed for electricity consumption only, not production, where the local network is ill-equipped to export large loads of locally generated power to the electrical grid [96]. Wind power installations are often larger and connected to the high-voltage grid, so can be more

easily managed by the operators of the grid using wind forecasting techniques, but still the current techniques are not sufficient to manage future projected levels of wind penetration [97].

Concerns about the impact of variable power supply on the grid are deeper than simply not being able to match demand to supply, as the cost of an imbalanced electricity network affects the grid stability, voltage regulation and power quality [96]. Large-scale implementation of PV in small areas can result in large loads that follow the same variable pattern in supply (as cloud cover will affect all installations similarly) that would be difficult to manage, and vulnerable to large disturbances [98]. Overproduction can result in too high a voltage and decreased efficiency in grid transmission, to the extent where it is sometimes suggested to orient panels east and west rather than south [99]. This may give a slightly decreased production, but the improved matching to demand load makes the reduction worthwhile. Close together PV deployment also risks causing harmonics on the grid which can distort voltage, but this can be managed by carefully designing inverters as part of each PV array [100]. However spreading out the deployment of PV systems geographically can actually increase the power quality of the system [101] [102], and performance ratio of PV modules was found to be higher in grid-connected systems [100], so it is still worth connecting renewables to the grid.

2.2.3 Improving energy security for renewable systems

Inserting flexibility into energy systems with high renewable penetration is therefore necessary to minimise risk to the grid, where flexibility refers to ability of the grid to ramp power up and down with differing magnitude, frequency and speed [103]. This can be achieved in multiple ways: increased interconnections between electricity grids, energy storage, and demand-side management [94] [103]. Such approaches will not only improve grid stability, but also use renewable energy sources to their fullest potential, as the needs for generation curtailment and over-sizing of power capacity will be reduced. Flexibility can also be achieved by choosing a mix of renewable sources spread out to utilise different weather conditions, so the power quality effects of large PV arrays mentioned in the previous section can be avoided with careful planning [90] [76].

Implementing a smart grid, where electricity consumers can plan their energy use according to the amount available that day, is seen as a necessary step for encouraging demand-side management, and many countries have or are planning to start introducing smart meters for the starting of such a grid [97], including the UK from 2014 onwards [54]. Smart meters are also seen as a method for improving energy efficiency, and reducing energy use in general due to consumers realising where they can save money on their energy bills. However, they are not a complete solution, as it is unrealistic to expect people to simply use no energy if the sun is down and the wind isn't blowing. Increased interconnections across Europe would take advantage of the variable weather patterns across the continent [104]. This works with the simple theory that the majority of the time, if the wind is not blowing in one area of Europe, it will be elsewhere. International connections would require the building of new HVDC cables to reduce transmission losses, and the built capacity for electricity generation would by necessity be much larger than the peak energy use, which brings extra costs. There would also still be no guarantee that there wouldn't be occasional times when the generated energy would still be too low, which is where energy storage shows itself to be a key component [14] [105] [43]. Storage and demand side management are the only interventions that are capable of *time-shifting* loads [76], i.e. delivering power when demand exceeds available supply at that moment, and storage has an advantage of being more directly controllable, although demand side management can be considered more efficient because no energy conversion occurs [19]. This evaluation does not consider the energy use by additional technology such as smart meters that may be necessary

for effective demand side management, so in reality there will be some energy losses involved in their life-cycle energy costs.

It is generally considered that all approaches to improve system flexibility must be used together, so a future secure renewable system will require a diverse mix of renewables, improved connections to other systems, some energy storage and demand-side management facilitated with methods such as pricing mechanisms or smart grids [106] [93] [92]. However, significant changes would need to be made to the design and structure of the UK's electricity network, which is currently very centralised regarding both energy management strategy through the National Grid, and how the majority of supply comes from a small number of large coal or nuclear power stations. The rapid deployment of wind and solar production across the country has challenged this dynamic, giving a distributed structure more in line with the distributed nature of wind and solar supply.

In particular, smart grids may work more effectively in a decentralised/distributed structure where management of energy becomes more flexible, allowing coordination between hierarchical energy subsystems [107]. These subsystems, known as *virtual power plants* (VPPs), would contain distributed energy resources and multiple demand loads alongside some kind of management structure that balances supply and demand locally as much as possible, before exporting to or importing from the larger network [12] as illustrated in figure 2.1. This security management could utilise energy storage or demand side management, and its local positioning makes it more capable of reacting to fluctuating loads in real time [12]. VPPs are particularly relevant to rooftop PV generation, where the energy resources are necessarily near to household loads, and excess solar production can result in reduced energy quality on the local network, as explained in section 2.2.2.

Furthermore, VPPs can be applied as part of a Supergrid with increased interconnections between different countries, enhancing energy security while enabling higher penetration of renewables [108] [109]. Such a structure would apply all the flexibility approaches outlined above, combining the seemingly contradictory locally managed subsystems (thought necessary for smart grid infrastructure) with international interconnections. The aging of current infrastructure across much of Europe, in addition to the forecasted increase in electricity demand from electrification of heat and transport, gives an incentive to redesign the electricity network soon to avoid wastage of components [110]. However there are competing theories of how best to organise such a network, with some advocating the already mentioned electrification of heat and transport networks, and others arguing that combining district heating (generally gas or biomass/waste combustion, occasionally geothermal where available [111]) with electricity from renewable sources is more efficient [112]. This is the current procedure in Denmark, which already has a very high penetration of wind power on the grid. Both approaches include interconnections between energy grids, but they differ greatly in application and the choice of direction may often be political or geographically dependent. It was noted in section 2.1.2 that CHP in fact limits the flexibility of the system, so it is unlikely that a future 100% renewable system would only use wind and CHP components to supply energy and balance the grid.

2.2.4 Energy security metrics

Methods used for measuring energy security depend on the location in the system that it is being measured at. If it is the broader system, e.g. over an entire nation, then metrics are very complex, consisting of a number of indicators measuring different security impacts [87] [88]. Section 1.1.4 showed how the conventional methods for measuring security of electric networks use metrics of system adequacy such as $LOLP$ or EIR [23]. However, there is some inconsistency of nomenclature in the literature when exploring optimisation studies: suggested metrics include

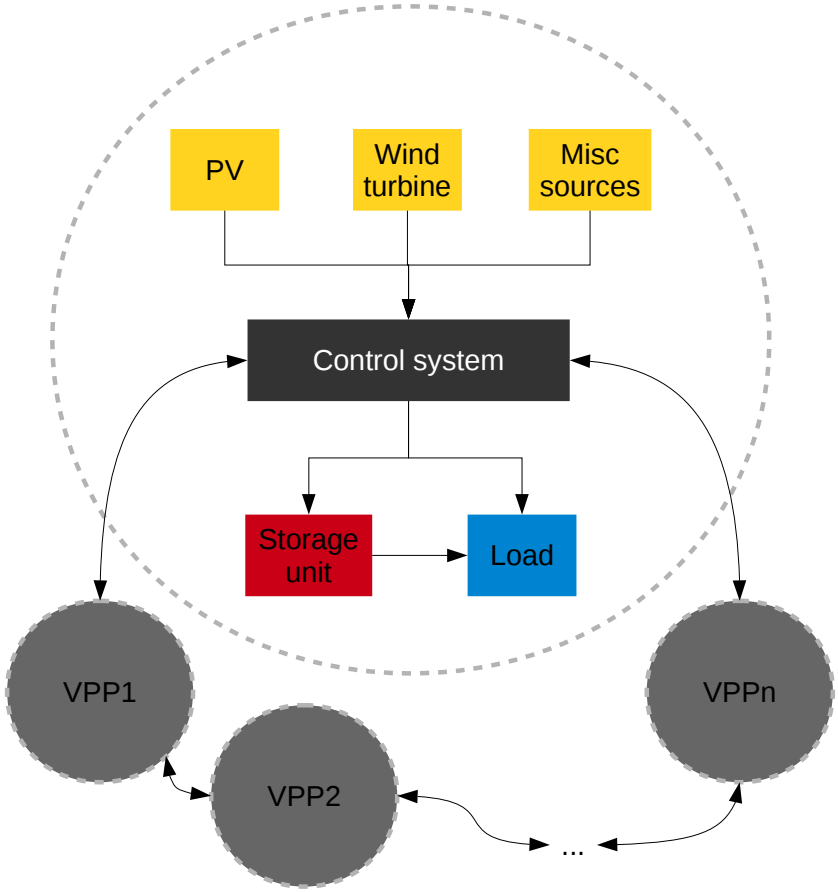

Figure 2.1: Simplified diagram of a virtual power plant within a smart grid, surrounded by n other VPPs (VPP1, VPP2,...,VPPn) that share information and energy flows. The control system allows for efficient communication between the VPPs, where each one is aggregated into a single node on the network.

Loss of Load Hours or LOLP [6] (sometimes referred to as loss of load expectation [45]), Loss of Energy Expectation, Frequency of Loss of Load, Duration per interruption, Load Not Supplied per Interruption, Energy Not Supplied per Interruption [45], Loss of Power Supply Probability [78] [34], Unmet Load [32], and Energy Expected Not Supplied (EENS) [44], the last two which can be normalised to give the energy index of reliability $EIR = 1 - EENS/\text{load} = 1 - UL$ [23].

These metrics can be divided into three categories: time-dimensional, energy-dimensional, and event-descriptors. The first type include Loss of Load Hours (LOLH) and its derivatives Loss of Load Probability (LOLP) and Loss of Power Supply Probability (LPSP). Loss of Load Hours is the number of hours during the year where the system fails due to not being able to satisfy required demand, and the other two metrics are proportions using LOLH. LOLP is the proportion of time (generally over a year) that the system undergoes power failure, while LPSP gives the probability that the system will fail when it is underproducing. LPSP is only applicable to subsystems that are supported by external connections, or when implementing storage/demand-side management, where the denominator is the same as the LOLH value of the system without any balancing intervention. Note inconsistent use of security metrics within the literature means that LPSP is defined in [82] similarly to EENS, and in [34] a metric named LOLP is again defined similar to EENS.

Energy based security metrics are less common in the literature, but Loss of Energy Expectation or Energy Expected Not Supplied are both defined as the sum of demand energy that is not met over a year, while UL is normalised to be this sum of unmet demand energy divided by the total demand over the year, therefore is the inverse of the EIR metric.

Finally, the third type of security metric is the least commonly used, where the Loss of Load periods are quantified individually rather than summed over time or energy. Frequency of Loss of Load describes how frequent these periods are over the year, Duration per interruption measures their average length in time, and Load Not Supplied per interruption measures their average unmet load.

LOLP is the most commonly used security metric, as it is applicable to most electricity networks and easy to measure and define. It is unclear whether using one of the energy-dimensional metrics such as EIR might be better, as they would have the advantage of quantifying the energy shortfall more accurately. It is generally not expected to measure overproduction as part of system security, even though overproduction has severe consequences for power quality, which is an important part of energy security [19] [7]. The only example is the occasional calculation of excess energy generation [82] [71], but this is not used as one of the optimisation constraints in the cited studies, simply calculated for deeper understanding of energy flows within the systems. However, the likely reason for the lack of overproduction metrics is that in reality, if production is higher than demand within a smart managed system, production will be either curtailed or exported to the grid. Therefore overproduction can be better accounted for in the sustainability metric, discussed further in section 3.4.2. This is because when the overproduction is managed through curtailment, the impact is to reduce energy output, rather than reducing system reliability.

2.3 Energy storage

It is becoming clear that storage is expected to have a large part to play in improving the security of energy from renewable sources [31]. Storage units are capable of replacing generating units within the grid to supply energy at times of peak demand load, and are more flexible than demand-side management strategies in balancing the grid, possibly more reliable than existing thermal power stations of equal power capacity [113]. However, the type of technology employed has a large impact on its effectiveness, and must be chosen carefully with respect to the type

and size of energy demand. The modelling of energy flows in and out of storage must also be accurate enough to differentiate between each type of technology so the systems can be compared authentically.

2.3.1 Energy storage technology options

While batteries are often touted as the main option for storage, the main storage technology used currently is actually pumped hydro storage, at $127,00MW$ storage capacity worldwide [114]. However, the trend towards renewables is matched by a trend towards distributed generation [19] where localised energy storage is required to buffer grid imbalances [115] and allow for bi-directional energy flows between areas of high PV deployment and the grid [116], thus avoiding the security problems mentioned in section 2.2.2. As pumped hydro storage is only practical in mountainous areas with significant inclines [117], and only economical for large installations, research into finding cheap and energy dense (capacity per land area use or volume) energy storage technologies has been increasing in importance [118], which would be more applicable to VPPs. Most of this innovation has been into electrochemical storage [119], i.e. batteries.

Currently available storage technologies are summarised in table 2.1, along with their energy and power capacities, and possible applications. There is much variation in available capacities for each type of technology. There are four possible levels where storage can be inserted into the grid: at site of large generation (e.g. wind farm), individually as large storage units to support the transmission grid, dispersed as medium-sized storage units on the distribution network, or at end user points as part of small systems [119]. The last two are directly applicable to VPP networks, being situated close to demand loads. Different types of storage are suitable for different locations, dependent on the services they can provide. The services are generally related to their capacity and speed, where the services required specifically for renewables integration are voltage support (power quality), time-shifting loads - i.e. storing overproduction to supply demand at other times, see figure 2.2 - and rapid demand support [114]. High energy storage capacity is required for time-shifting loads, while high power capacity and response speed (one second response) is required to quickly balance fluctuations in power for demand support, and high response speed (less than 5 seconds) is required for supporting power quality on the grid, such as correcting voltage sag or frequency problems [116]. However when it comes to small energy systems, choosing only one type of storage technology is preferable to reduce the complexity of the system, particularly with regards to the power control strategy [32]. This chosen technology will preferably be capable of addressing most of these energy security issues, so needs to have high energy and power capacity (with respect to the size of the local system), and quick response times. Obviously such a flexible technology will be more expensive, so costs also have to be taken into consideration. The energy capacity and response time are graphed in figure 2.3, with values taken from table 2.1.

Pumped hydro storage

Pumped hydro storage refers to systems where water is pumped uphill during periods of energy surplus and allowed to flow downhill to provide power when it is needed. The conventional placing of these systems is on steep hillsides, but some use underground reservoirs to maximise drop and thereby their storage capacity, resulting in more flexible systems at higher cost [122]. The UK only has limited areas where PHS is suitable, as mountainous regions are limited, and often protected or remote from any grid connections. One major advantage of PHS is its lower embodied energy cost [123] and technological maturity, however placement in unsuitable areas could negate those benefits.

Storage technology	Power capacity range	Energy capacity range	Speed of response	Possible applications
Pumped hydro	$280 - 4000MW$	$1,680 - 100,000MWh$ [118] [114]	Slow (minutes) [116]	Time-shifting loads.
Compressed air energy storage (CAES)	$5 - 400MW$ [120]	$> 5,500MWh$ [118]	Slow (minutes) [120]	Time-shifting loads.
Lead-acid deep discharge batteries	$10 - 100MW$ [117] [114]	$40 - 400MWh$ [121] [114]	Fast (ms) [120]	Power balancing.
Lithium-ion batteries	$1 - 2MW$ [117]	$301 - 521Ah$ [117]	Fast (ms) [120]	Power balancing and/or electric vehicles.
Other electrochemical batteries (NiCd, NiMH, NaS)	$50MW$ [114]	$300MWh$ [114]	Fast (ms) [120]	Power balancing and/or electric vehicles.
Flow batteries (VRB, PSB, ZnBr)	$1 - 1.5MW$ [121]	$1.5 - 4MWh$ [121]	In development.	Time-shifting loads.
Supercapacitors	$0.1 - 0.3MW$ [120]	$0.48Ah$ [117]	Very fast $(< 3ms)$ [120]	Power quality management.

Table 2.1: Available storage technologies, their applications and characteristics.

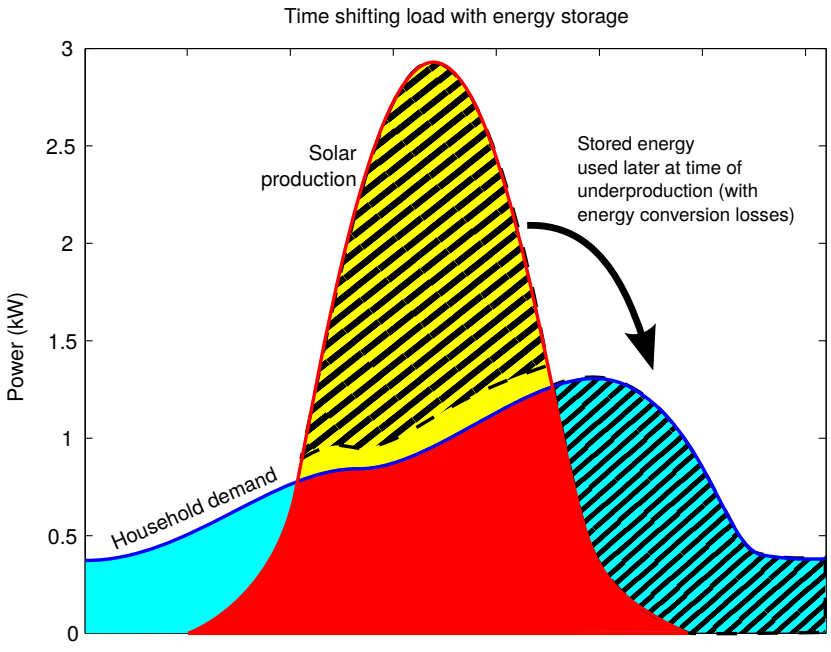

Figure 2.2: Illustration showing the shifting of solar production from peak supply to evening household demand, using energy storage.

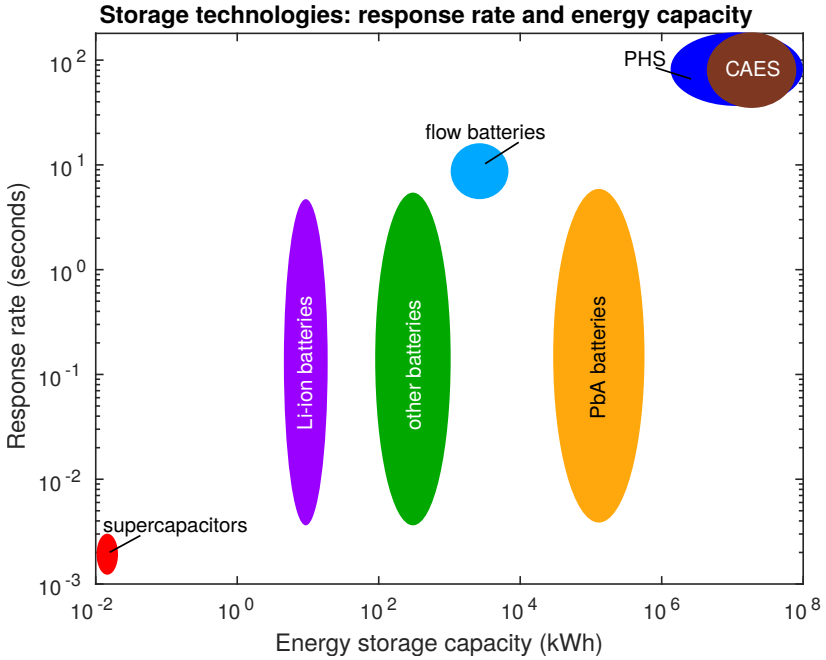

Figure 2.3: Plot of possible ranges for energy capacity vs response rate for all reviewed storage technologies, assuming voltage of 24V for conversion from Ah to kWh. Values are taken from table 2.1. PHS is pumped hydro storage, CAES is compressed air energy storage.

Compressed air energy storage and cryogenic storage

Large-scale compressed air energy storage (CAES) is a relatively mature technology [118] but used much less than pumped hydro storage. CAES systems use excess energy to compress air in underground caverns, which is then heated through expansion and used to drive natural gas through conventional turbines to produce electricity, essentially resulting in a more efficient gas turbine [114]. While CAES potentially has low embodied energy costs, its reliance on gas distracts from a renewably powered electricity network, and would only be applicable in larger systems. The case study would provide a large enough system but PHS was seen as more viable given the available geography.

Other, less mature technologies using compressed air are adiabatic CAES, which uses only compressed air to drive the turbine, and cryogenic storage, which liquifies air or nitrogen at very low temperatures and again uses this air to drive a turbine. Cryogenic storage is not particularly well developed; it currently has low cycle efficiency [117] and little available data on embodied energy. Adiabatic CAES is even less developed, being noted as at the "idea" in 2010 [114].

Electrochemical batteries

Traditional rechargeable batteries are currently used for many types of small storage applications, having high power densities and good response speeds, but large storage capacity systems are currently very expensive because of the need for high energy density batteries [121] [14]. There are also problems with self-discharge over long time periods, particularly for nickel-cadmium (NiCd), sodium-sulphur (NaS) and lead-acid (PbA) batteries [121].

Lead-acid batteries are the most commercially mature rechargeable batteries available, and there are a number of different types, but deep-cycle stationary batteries are the most suitable

for utility purposes [124]. They are very heavy and their maintenance requirements in addition to short lifetimes make them relatively unreliable [114] so there are a number of other types of battery technologies that have been developed to fix these problems. There is some disagreement in the literature as to whether PbA batteries are realistic to be used in a utility scale storage system, as some cite the issues with the environmental impact caused by their material requirement [118] [125], but their technological maturity makes them a common front-runner for use at this scale [114] [14] [126]. Their maturity means that recycling is easier than less mature battery technologies, which reduces some of the environmental risk [127].

Lithium-ion batteries have a much higher energy density, low rate of self-discharge [120] and greater capability for deep cycling than PbA batteries, although serious damage is risked if they are discharged to too low a level. Their current cost inhibits their potential to be used for large-scale storage, but their lower weight makes them an option for electric vehicles, which could be used to balance the grid by opening up a new use for electricity capacity at times of overproduction [121]. Additionally it is hoped that the scaling up of manufacturing will make lithium-ion batteries an option for utility storage at the user end, such as in households or community powergrids [114].

NiCd and nickel-metal hydride (NiMH) batteries are more mature than lithium-ion, but suffer from problems such as low energy density, memory effect, and a similarly limited discharge to PbA batteries. Another type of rechargeable battery is NaS, which have similar lifetimes and deep discharge as lithium-ion batteries [128], but suffer from high self-discharge and require high temperatures for operation [120]. Therefore three types of traditional rechargeable batteries were chosen for further investigation: PbA, Li-ion and NaS. These represent diversity of efficiencies, maturity and lifetimes, and are all currently available for energy storage on a small scale. While it may be true that PbA are less suitable for utility storage than other more modern batteries, their widespread use alongside PV [129] makes their analysis necessary.

Parameters used for modelling all battery technologies are summarised in the methodology in table 3.6.

Flow batteries

Flow batteries use electrochemical reactions similar to traditional batteries, but their electrolytes are in liquid or gaseous form and stored in separated storage tanks. This gives them two major advantages: capability to being discharged to their full capacity (allowing for more flexible operation), and well designed for utility-scale operation [117]. They are likely to also have a lower cost, however flow batteries are relatively new technologies, and have not been tested extensively at a utility scale [130]. Such large scale testing is required to improve their safety and refine how they are operated [31], this being more complex than conventional batteries due to the use of pumps and other moving parts. Vanadium-redox (VRB), zinc-bromine (ZnBr) and polysulphide bromide (PSB) batteries are the most mature examples, where VRB has already been installed in a number of text sites, at up to 5MW/10MWh capacity [131]. Therefore VRB and ZnBr batteries were chosen to be taken forward in this study: VRB judged to be the most mature and ZnBr with the most data available for analysis.

Supercapacitors and other short-term storage

Capacitors store energy electrically by charging one of a pair of metal plates, separated by an insulator. Supercapacitors (also known as ultracapacitors) use highly porous carbon materials rather than metal plates to give a much larger surface area, increasing storage capacity. They have a very high power density, fast charging/discharging capability [120] and long lifetimes,

but cannot be used for long term storage due to high self-discharge rates [117] and lower energy density than batteries. Possible applications are to use them in conjunction with batteries to manage short duration grid insecurities, such as frequency or voltage disturbances, but this would be on the order of seconds or minutes rather than hours [31].

Similarly, flywheels (which store kinetic energy) and superconducting magnetic energy storage (which stores energy within an induced magnetic field) have very quick response times; this in combination with their long lifetimes make them applicable for continuous use and regular cycling (charging and discharging) [132]. This is useful for maintaining voltage/frequency regulation as with supercapacitors, but these benefits are less noticable at the half-hourly resolution.

Hydrogen production and storage

Excess electricity production can be used to produce hydrogen using electrolysis of water; this hydrogen can be stored and then used to generate electrical energy using polymer electrolyte membrane (PEM) fuel cells, or burned for heat. Hydrogen's main advantage is its versatility, as it can be transported more easily than the other storage mediums, and used as a fuel in hydrogen cars. Its cycle efficiency of electrolysis and then fuel cell production is considerably low at around 25-35% [32], but its reported low embodied energy costs may offset this to compare more favourably with batteries, as long as the number of required storage steel cyclinders remains low [133]. However it must be noted that the EROI analysis conducted here was lacking in specific embodied energy figures for many components, and relied upon data for the raw materials such as steel for the electrolyser frame, compressor and storage cylinders, when in reality the precision required for manufacturing such high-quality components would entail further energy costs. The fuel cell is the most inefficient component at 47-50%, while electrolysis has an efficiency of 70% [134] and hydrogen compression for storage adds another conversion efficiency of 89% [133]. The difficulty of hydrogen storage is one of the main barriers to implementation, particularly in transport as the weight and size of compression cylinders is much greater than that of fuel tanks supplying the same quantity of energy, even if it is more convenient than most batteries. However hydrogen's application to transport is considered its most important attribute [135], being less mature than other stationary storage technologies and there being few other options for electric personal vehicles.

2.3.2 Additional impacts of storage technologies

Adding storage into renewable energy systems can bring advantages and disadvantages: they can be necessary to ensure the reliability/security of these systems, but their added cost and environmental impact may have negative effects if not managed correctly. Sustainability being the main focus of this research, it is necessary to ensure that any environmental issues they bring with them do not undermine the goals of transitioning to renewable energy in the first place.

Choice of storage technology and type of system is paramount to economic feasibility, lead-acid batteries possibly adding costs of up to £1000 to an individual renewable energy system [125], while pumped hydro storage at $1GW$ power capacity could actually reduce wider system costs associated with increasing wind power penetration (up to $2GW$ power capacity depending on the scenario) on the grid, by reducing the need for gas power stations [79]. Further analysis exists to compare different types of storage technologies, suggesting for example that 10-minute flywheel storage is economically worthwhile, and that hydrogen production in combination with redox flow cells are the most economic form of daily energy storage, but still not economically justified (pumped hydro storage was not included in the

analysis) [43]. When considering large-scale storage for time-shifting loads, compressed air energy storage and possibly hydrogen production were suggested as possible candidates, pumped hydro being rejected for its dependence on suitable sites, and batteries for their cost [118]. However others consider that lithium-ion or NiMH batteries will be useful if their cost and reliability are significantly improved [114], and/or if their deployment is combined with electric vehicles [121].

Further comparisons can be made of their environmental impacts. Net energy analysis accounting for embodied energy shows that including storage in energy systems still results in net energy production, despite the increased embodied energy resulting from including additional technology [136], and that pumped hydro storage and compressed air energy storage give the best energy return [137]. Regarding other environmental impacts, the toxic components of lead-acid batteries are well known to be an issue, despite measures to increase environmental regulations and recycling of the lead [127]. In comparison, vanadium-redox flow batteries (VRB) are a good candidate for large-scale storage, having better efficiency and lower environmental impact, although there are still some toxic by-products [132]. NiCd batteries' use of toxic cadmium is also an issue [120], this being one of the reasons that they were not explored further in this thesis. While lithium-ion batteries are low in toxicity, the limitation of lithium reserves raises some concerns for how much we can use them in the future [138], especially as net energy analysis does not account for limits to raw materials.

2.3.3 Simulating storage units as part of an energy system

In order to analyse the effectiveness of different storage technologies, their modelling as part of the energy system must correctly express the different characteristics outlined in the previous section. The study will compare a total of six different storage technologies: three different rechargeable batteries, two flow battery technologies, and pumped hydro storage. It is likely that a future energy system would likely require multiple types of storage technology to fulfill all of the system balancing requirements such as quick response, large capacity, high efficiency, low cost etc [31], however the precision required for such a comparision would not be available in a half-hourly model. Therefore supercapacitors and the other quick-response storage technologies would be out of scope for this model.

The most commonly modelled type of batteries in the literature are lead-acid, presumably because of their aforementioned maturity and widespread use. The difficulty in battery modelling is estimating state-of-charge, as this is determined as part of a complex dynamic system, depending upon charge and voltage [139]. PbA batteries have been modelled as part of PV systems, taking into consideration dynamic processes affecting the resistance, current and voltage [140], in addition to usable capacity which can decline due to multiple factors [141], and temperature [126]. Degradation and corrosion can also be modelled using a variety of methods, which can lead to PbA battery lifetimes of 5.8 - 15 years (the real lifetime being 6.2 years) or 4.4 - 9 years (the real lifetime being 5.8 years), the most accurate method using weighted Ah throughput of the battery as a variable [142]. An alternative method of modelling the battery state-of-charge can be to treat charging efficiency as the main dynamic component, dependent on state-of-charge [143]. Discharging can be assumed to be 100% efficient [144]. This is a useful approach to take because at a half-hourly time-series resolution, the voltage and charge would have to be averaged which simplifies many of the dynamic processes, making their simulation unnecessary.

Modelling the PHS system is much simpler, as efficiency can be assumed to be constant and power output is linearly dependent on the height of upper reservoir [79].

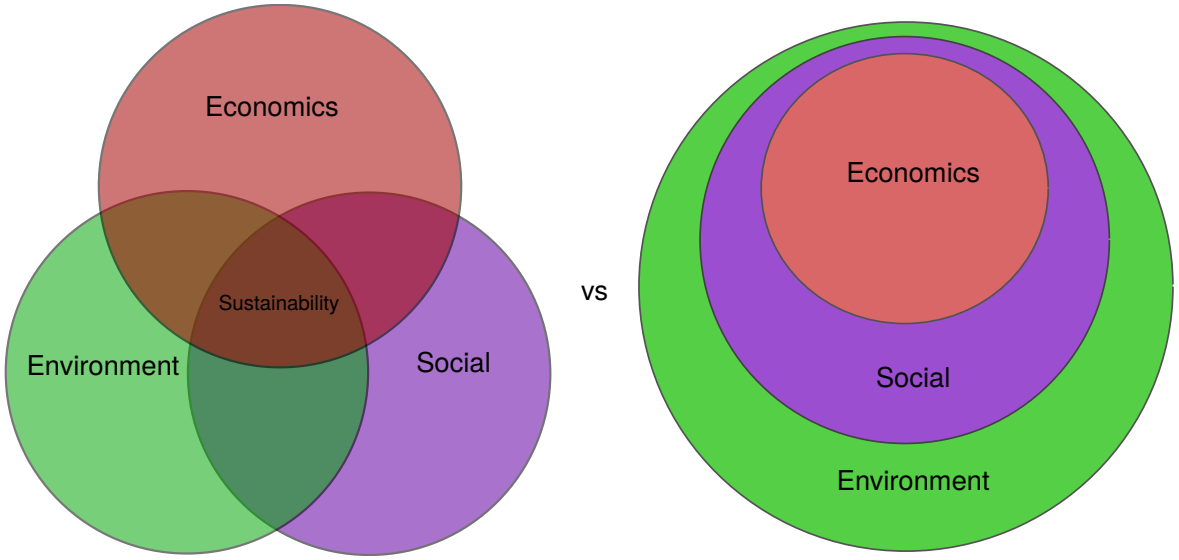

Figure 2.4: Full sustainability includes environmental, economic and social aspects, however economic and social aspects are fundamentally dependent on resources from the environment, so it is questionable whether the "human" spheres of social and economics can be separated from the environment.

2.4 Sustainability

2.4.1 Defining sustainability

While sustainability was summarised in the introduction as a concept of comparing our present day's consumption with how many resources we leave for future generations, it was noted that this is a somewhat nebulous idea, possible to be applied in various different ways. Sustainability is sometimes split into the three overlapping sections of environment, economics and social impacts [26], despite often being thought of as just reflecting environmental concerns. However arguments from ecological economics show that economic and social spheres are in fact dependent upon ecological processes, which gives a different understanding of how these three areas relate (see figure 2.4). This viewpoint does not try to assert that economic cost is correlated with environmental costs, but that the underlying drivers of society and economics come from environmental resources (e.g. economic production requires material goods) and are reliant upon a certain health of ecological processes and systems [145]. Therefore we cannot have economic and social sustainability without a strong foundation of environmental sustainability.

Some argue that sustainability cannot be quantified, but must be qualitatively assessed, particularly when it comes to complex impacts on ecosystem services [146] or social sustainability [147]. This can make analysis of the impacts difficult, so some attempt at quantification is done through aggregating numerous measurements into large composite indicators, but there are doubts about their accuracy and methods of aggregation [148] [149]. Such composite indicators are usually applied to entire countries, whereas in the case of individual technologies an alternative approach is taken of listing the indicators separately, generally including embodied greenhouse gas emissions, embodied energy, multiple pollutants and ecosystem impact [150]. The number of different indicators will depend upon the particular study, but the end result is a multitude of sustainability metrics, with no single definition of sustainability. The separate metrics are usually reviewed qualitatively, as in

practice certain ones are chosen to fit the criteria of the study.

Most attempts to quantify sustainability in a physical way use the notion of thermodynamics and exergy [151]. It is proposed that such an approach is capable of treating sustainability in both qualitative and quantitative terms [152]. One such study in [153] reframes the above quote from the Brundtland Report in terms of ecosystems, as they are concerned with the rate of raw material depletion (i.e. needs of the present) in comparison to raw material production in the ecosphere (i.e. ability of future generation to meet their needs), in addition to how waste production damages its capacity for raw material production. It is asserted that such processes can be expressed in a single quantity of exergy, defined as the maximum work that can be produced in a system that is approaching thermodynamic equilibrium with its surrounding environment [154]. Exergy can be seen as a measure of the quality of energy, e.g. electrical energy is of higher quality than thermal energy. Such analysis is capable of quantifying the depletion of natural resources [155], although some aspects such as the full impact from depletion of non-renewable minerals are missed from such a measurement [156]. Some research has gone even further, suggesting emergy analysis as a measure of energy quality [157], normalised to solar energy inputs. However the robustness of this approach is in dispute [158], and it is unclear whether emergy is a function of exergy [159] [160].

Moving away from a theoretical definition of sustainability, our approach must be guided by the availability of data and practicality of measurement. While measurements such as exergy and emergy may be theoretically more accurate and broader in scope, a lack of data makes their implementation impractical, so it may be beneficial to use more available data even when this does not give the full picture of sustainability. With this in mind, this research is primarily concerned with environmental sustainability, as it can be more quantitatively defined than social sustainability, and deals more directly with the physical processes than economic sustainability, which is not necessarily as important when finding the most sustainable approach to GHG emission reduction [161]. Energy analysis rather than exergy or greenhouse gas emissions was chosen as the most practical option, being a cost-effective assessment of environmental impact [162]. Energy use continues to be correlated strongly with greenhouse gas emissions [27] despite expansion of renewable energy sources in the electricity grid, and the energy theory of value [163] [164] suggests that economic sustainability can be linked to energy measurements of environmental sustainability (namely embodied energy or exergy). There is some evidence that energy can be displayed as a function of economic factors [165] but the theory as a whole is contentious with little research done so far [163]. While there may be some correlations between embodied energy and economic costs, these do not appear accurate enough to support the claim that energy analysis can replace economic evaluation. When addressing the issues of energy quality measurement missed by not using exergy, some compensation can be made by scaling all energy to primary energy, i.e. the energy required from fossil fuel combustion in order to give work of equivalent quality [52]. This improves comparability of energy measurements between technologies, so renewable energy technologies can be compared fairly to fossil fuel powered technologies [166].

Finally, social sustainability should not be completely ignored. Theoretical links between energy analysis and social impacts can be made through economic connections, such as the previously mentioned energy theory of value, as GDP is often used to show societal well-being. Additionally, if energy is affordable then the better access to home heating and electricity will naturally improve social well-being, this being dependent upon physical health. Links can also be made through environmental sustainability, as a safer climate and low pollution levels have a positive effect on social wellbeing. It is accepted that development of human society has been often very strongly linked to our use of energy [167] because a greater energy return gives value to society, as people can use that energy to create jobs, services and produce technology that

improves their quality of life. However there are so many indicators of society sustainability [168] [147] such as equity, health, education etc. that finding a quantitative measure, let alone finding a strong correlation, is unlikely. It may be noted that it is common for social aspects to be largely ignored by sustainability analysis [168] and while this is regrettable, it makes sense due to the mentioned difficulties. However, it could also be argued that energy security has a social element, as one aspect of social sustainability is social acceptance of new technology [169] and the more reliable the technology, the more accepted it will be by its users and therefore society. Energy security is also broadly linked to feelings of safety [86], which is a necessary part of social sustainability [169]. Thus if energy security is included in the analysis separate from sustainability, social sustainability will be partially addressed.

2.4.2 Measuring sustainability

In order to find the environmental impacts mentioned in the previous section, a life cycle assessment is usually performed on the technology in question. A life cycle assessment is a methodological framework for assessing the environmental impacts over the life cycle of a product, typically including the component manufacture, transportation and on-site construction, operation and maintenance, and end-of-life/decommissioning stages of a device [170]. There are multiple frameworks available, but the most commonly used are input/output analysis and process analysis [171]. Results from a life cycle assessment are only useful if they can be compared to other results, so consistency in accounting and system boundaries are of utmost importance. Typically the initial stage of technology design is unaccounted for in life cycle assessments [170] but more sophisticated assessments have included the impacts of advertising, insurance and financial services, capital investment and the business system as a whole [171] [172].

There are two distinct types of life cycle assessment, differentiated by their goals of either describing a device and its environmental impacts (attributional), or describing how the choice of actions taken will affect future environmental impacts (consequential) [170]. This research is only concerned with the former type, thus uses results from attributional rather than consequential or dynamic life cycle assessments. Consequential life cycle assessment not only assesses the localised impacts, but also considers how the implementation of certain technologies will affect the wider system in the future using economic modelling approaches [173]. Similarly, dynamic assessments consider future energy mixes and projected manufacturing methods [174]. Life cycle assessment is still a young discipline, with no absolute consensus in the best methods to be used [170].

To perform an attributional life cycle assessment, first a life cycle inventory must be formed [170]. This is a preliminary analysis of all environmental flows in and out of the system being analysed, from "cradle to grave" over the stages mentioned earlier. These flows include raw material extraction, energy acquisition, materials production, manufacturing, use, recycling and disposal. The inventory is a methodology for quantifying these flows, and defines the system boundaries for assessment. Next, the actual flows must be measured. As we are only concerned with the energy flows, only the measurement of energy acquisition will be explained. The input/output method of energy accounting does not actually measure energy use directly, but records the cost of each activity, and combines these costs with the activity's known energy densities to find the total energy use. Alternatively, process chain analysis measures energy more directly, summing up energy use for each process within the device's life cycle by recording fuel use (this is also useful for finding accurate greenhouse gas emission rates) [175]. The methodology guidelines for PV lifecycle assessment [52] recommends using only process-based LCA results, as input-output and hybrid methods have not been fully tested. Energy use can be expressed in units per kg, power rating (applicable only for power generation technologies),

size, or per "functional unit" which can be defined however the authors choose.

2.4.3 Energy metrics

Once embodied energy values are available, there are multiple methods of assembling them to create a sustainability metric. This usually requires comparing the embodied energy to the energy output from the resulting energy system. The most commonly used metric for PV modules is Energy Payback Time (EPBT) [176], which is a prediction for the length of time required for the system to run in order to generate the same total energy required for its existence. A number of energy return ratios have also been defined in the literature concerning net energy analysis, and while these were originally used for analysis of fuels, they can be applied to renewable resources such as wind and solar with some changes to the methodology. The term Energy Return on Investment (EROI) is frequently used, but there are four possible formulations of this ratio, all applicable for different goals or systems [177]. These are the Net Energy Return (NER), Gross Energy Return (GER), Net External Energy Return (NEER) and Gross External Energy Return (GEER). Net returns use the net production of energy, subtracting the energy use within the system, while gross returns include all generation. External energy return metrics will only consider the external inputs when calculating the embodied energy value, while NER and GER include all energy inputs to the process. From henceforth in this thesis, the term EROI will be used to only refer to the Net Energy Return, as this is the most applicable to renewable energy systems designed to supply energy to an external demand. A sixth energy ratio is the energy intensity ε, which is the inverse of EROI, calculating the amount of energy required per system energy unit output [178]. This is therefore equivalent to EROI, but is more useful when expressing the energy efficiency of a nation, for example.

2.4.4 Formulation of metrics

If all energy is normalised to primary energy (PE) - i.e. the amount of energy currently required to generate the equivalent quantity of electrical energy - using the coefficient $\eta_G = 0.31$ to represent the average efficiency of the EU25 grid, [166] then a system with lifetime L, net energy generation without curtailment E_{out} over entire lifetime L and lifecycle embodied energy costs E_{in}, has an $EROI_{PE}$ calculated as follows [52] [177]:

$$EROI_{PE} = \frac{E_{out}}{E_{in} \cdot \eta_G} \tag{2.1}$$

The coefficient η_G is important to preserve energy quality in the analysis; while most of the energy input for technology manufacturing is thermal, mostly derived from fossil fuels, the energy output is in the form of electricity, a high quality form of energy. Raugei [166] states that "by expressing E_{out} in terms of its Primary Energy equivalent and calculating $EROI_{PE}$ accordingly, one is in fact calculating how much Primary Energy is virtually returned to society (i.e. preserved for alternative uses) per unit of Primary Energy invested in PV, given the composition of the current electric grid." Such EROI values would be comparable to "mine-to-mouth" fossil fuel EROI, rather than the EROI of fossil fuel powered electricity, and would naturally be significantly higher than standard EROI.

Energy intensity and energy payback time are calculated with similar inputs, but expressing the result in different units. So energy intensity is the inverse of EROI:

$$\varepsilon = \frac{1}{EROI_{PE}} = \frac{E_{in} \cdot \eta_G}{E_{out}} \tag{2.2}$$

and energy payback time is defined on the yearly system output $E_{out,yr}$:

$$EPBT = \frac{E_{in} \cdot \eta_G}{E_{out,yr}} \tag{2.3}$$

Energy intensity and EROI are unitless ratios, while energy payback time is measured in years. Choosing which metric to use can be down to personal preference, but the the unitless property of EROI and energy intensity make them more flexible with regards to combination with other metrics, and EROI is widely used for energy analysis of all kinds of systems and fuels, so using it allows for easier comparison with other systems [179].

A benefit to using EROI is that it can be used to give a simple description of sustainability; a system with EROI value less than 1 is by definition unsustainable in isolation, as this cannot be sustained without overuse of resources, and is likely to be unprofitable. However this does not imply that a system is automatically sustainable if it has EROI$>$ 1. Any cut-off point is likely to be higher; for example liquid biofuels have been calculated to require a minimum EROI of 3:1 in order to be feasible [29], but a minimum threshold for any specific technology, let alone energy systems, is difficult to define given the variables and error margins involved. Past calculations of EROI (excluding conversion to primary energy) for PV and wind turbines have given 3-10:1 for PV, depending on latitude of operation, and average 18:1 for operational wind [180], but this will vary because, as discussed earlier, larger turbines tend to have a higher EROI due to increases in efficiency and the non-modular nature of wind-turbine embodied energy [181]. The higher EROI an energy system possesses, the better it can replicate itself and provide energy to society.

There are concerns in the literature that EROI lacks a consistent framework [182] [177], whether this comes from inconsistency or non-transparency around LCA boundaries, conflation of different EROI metrics, use/disuse of different grid efficiency coefficients etc. Therefore a concerted effort has been made in this study to set out exactly which energy flows are being measured in the analysis, and how the system boundaries are being defined.

2.4.5 Primary energy

Primary energy is defined as energy from the original sources such as fossil fuel combustion, solar, wind, water etc [176]; although some sources will only include fossil fuel combustion as a primary energy, here these are all included. Typically when bringing together different energy sources for embodied energy calculations, these will be converted (normalised) to primary energy, to prevent the summing of energies with wholly different energy quality. For example, if one component was manufactured using 100kWh electricity from entirely renewable energy sources, and another using electricity from 100kWh of coal combustion at 30% efficiency, the renewable energy input would have to be scaled to account for the fact that its transference into the grid is much more efficient, and that if both components were manufactured using coal then the former one would actually require much more energy inputs.

There is some dispute in the literature as to whether energy output should be normalised to primary energy at all. In the Methodology Guidelines on Life Cycle Assessment of Photovoltaic Electricity, Fthenakis et al. [52] note that while EPBT always converts generated electricity into primary energy, it being a specific measure of how well renewable energy can replace traditional fossil fuel power plants, EROI is not always formulated to include such a conversion. This results in much lower EROI results (by a factor of the grid efficiency η_G), so when presenting these results it is necessary to make it clear whether primary energy normalisation was used.

In fact some argue that the conversion of electricity output to primary energy is deceiving, resulting in unrealistically high EROI values for renewable energy [183]. Their methodology gives the advantage to fossil fuel powered systems, whereas using primary energy scaling gives better EROI values for renewable energy systems. Raugei also argues in [176] that the use of

primary energy scaling in EPBT calculations makes it difficult to apply to long-term planning, as the increased deployment of more grid-efficient renewable energy technology would increase the coefficient η_G, giving worse values of EPBT if the technology stays the same, or not reflecting the full advantages if technology improves in lifecycle efficiency. He estimates a future grid efficiency to be $\eta_G = 0.42$, 11 percentage points higher than the current 0.31, which is based upon a projection of 20% PV penetration in 2050. EROI is suggested to be a more useful objective energy performance indicator, but he argues in other papers [166] and [184] that EROI should also be scaled by η_G, giving it the same comparative nature.

A third argument is levelled against the conventional use of fossil fuels as the primary type of energy use, although this has already been addressed by widening the concept of primary energy to include renewable sources. An alternative approach would be to choose solar energy as the "primary" energy, as this is the source of most forms of energy on Earth, and normalise energy with respect to that [185]. King admits that it is subjective whether fossil fuels are the energy vectors from a renewable primary energy, or if renewables are an energy vector from fossil primary energy sources. Advocates for the former would argue that coal, oil and gas are stored solar energy from organic matter, while the latter would argue that in this point of energy transition, renewable energy technology is being manufactured using mostly fossil fuels, so their power generation is a way of using fossil fuels more effectively. However if we truly wish to have an entire (or majority) transition to a renewably sourced energy system, then the latter argument will lose relevance as more manufacturing will be using renewable energy sources, for example the steel industry switching to arc welding so electricity can be used in in more industries.

Such a transition would have complex impacts that are not fully reflected in any kind of simplistic coefficient scaling methodology, or even in exergy analysis. The energy losses and inefficiencies involved in electrification of multiple industries and energy systems are incredibly difficult to calculate, being dependent on variables that are largely unknown or social in nature, e.g. whether vehicles will be battery or hydrogen powered. As an interim measure, energy inputs such as thermal energy, embodied energy in materials, transport etc could be considered separately if their use is radically different, but embodied energy data is not necessarily split easily into those categories. This split is however applied by Pacca et al. [186] when they attempt to find a theoretical net energy ratio of second generation PV - modules manufactured using electricity generated by PV. This is a simplifed way of considering how renewable energy technology could be used as "breeders" to create more of themselves, when in reality PV production would be available for all sorts of applications.

Using η_G as a catch-all coefficient of primary energy efficiency essentially assumes that all the renewable energy technology being manufactured today will use electricity from "primary" energy sources, and that they will be implemented into a world which only uses electricity, without any energy losses resulting from this transition. While this is unrealistic, it is also unrealistic to not apply any conversion factors to account for the higher efficiencies of PV and wind turbines in comparison to fossil fuel combustion. A middle-ground approach would be to assume that we are not attempting to replace all of society's energy sources with wind and solar, but that they are replacing units of capacity on the electric grid, and here it would be fully appropriate to use grid efficiency as a primary energy conversion.

Calculation of the grid efficiency η_G is somewhat inconsistent, some sources defining it as the average efficiency of primary energy to electricity conversion [52], and others as the life cycle efficiency of the grid [166] using life cycle data of the grid in addition to conversion efficiency. The former definition specifies that it only includes the efficiency of fossil fuel and other combustion power plants, while the latter includes renewable energy inputs within the sphere of primary energy, and considers the full life-cycle of all these technologies. This is essentially an extension

of the first definition; it finds the efficiency of all primary energy inputs into the grid, whether those inputs are embodied in the materials and construction, from renewable sources, or simply the fuel inputs of combustion power plants. It is a more robust definition; it notes that while the denominator uses a primary energy scaling (as all embodied energy is converted to primary energy), the energy output E_{out} will likely not just be replacing fossil fuels, but fitting into a system that also includes some renewable energy sources.

Therefore to calculate the grid efficiency of a grid with different sources of energy (or types of power station), we use the formula:

$$\eta_G = \sum_i \omega_i \cdot \eta_{i,LC} \tag{2.4}$$

where each generation technology i has weighting ω_i and its life-cycle efficiency $\eta_{i,LC}$ is defined as:

$$\eta_{i,LC} = \frac{E_{out}}{E_{in} + {}^{E_{out}}/_{\eta_{conv}}} \tag{2.5}$$

Using this definition can therefore lead to a better understanding of how useful the electrical energy output is from a renewable energy system. If the electrical energy output is n times greater than the primary energy inputs (i.e. has unscaled EROI of n), then not only has the technology effectively multiplied energy availability by n, but if that primary energy E_{in} had instead been spent on the grid, then it would have produced $\eta_G \cdot E_{in}$ electrical energy output. Therefore the full benefit to using the renewable energy system is not an n multiplier, but an n/η_G multiplier. Furthermore, as renewable capacity on the grid increases, the coefficient η_G will also increase. Therefore this definition is used with values of $\eta_G = 0.31$ and higher to encompass potential renewable energy penetration levels.

2.4.6 Embodied energy values

The values of embodied energy to be used in the analysis are extremely important, as EROI results are highly sensitive to embodied energy levels, particularly of PV technologies [187]. Choosing these values is difficult, as the range in the literature is very high even within specific technologies for multiple reasons. Chosen manufacturing techniques are very important, and may depend on country of manufacture [188], maturity of technology (as efficiency tends to increase over time due to improved methods and scaling up of operations [186]), or simply the resources available. Country of manufacture is also relevant to transportation costs, as shipping adds to energy use, although this is considered a small fraction of the overall embodied energy for onshore projects [189]. As discussed earlier in section 2.4.2 the boundaries of the life cycle analysis have a significant impact on the recorded embodied energy; for this reason, the embodied energy values were picked from studies with similar boundary conditions. Thus the studies were based on input/output analysis or process analysis done over the four stages of component manufacture, transportation and on-site construction, operation and maintenance, and end-of-life/decommissioning. Finally, the variety of technology available means that not all life cycle analyses will have been done for devices of the same efficiency, size or power capacity. For example, a decrease in silicon thickness of PV panels can result in a much lower embodied energy value overall [190]. Most notably in the case of wind turbines, the materials used to manufacture the components may not be consistent between models of turbine, and different materials will have different levels of embodied energy. To maintain some consistency, results for PV panels have been categorised by broad type of technology (mono-Si versus multi-Si) and their efficiencies have been noted, while wind turbines have been analysed with respect to rated

Technology type	Embodied energy level (kWh/m^2)	Comments	Ref
Multi crystalline Si, energy efficiency 12-13%	1,500	Includes module, frame, array support and converter only	[191]
Single crystalline Si, energy efficiency 10%	1,334	Full balance of system evaluation (battery input has been removed from original calculation)	[192]
Single crystalline Si, energy efficiency 14%	905	Also used in [166]	[190]
Multi crystalline Si, energy efficiency 13.2%	1,194	Calculated using their EPBT values	[193]
Single crystalline Si, energy efficiency 14%	1,555	Calculated using their EPBT values	[193]
Poly crystalline Si, average efficiency 12.3%	1,087 (mean)	Standard deviation $614kWh/m^2$, all done with cradle to gate system boundary (16 samples)	[187]
Mono crystalline Si, average efficiency 13%	1,729 (mean)	Standard deviation $801kWh/m^2$, all done with cradle to gate system boundary (16 samples)	[187]
Multi crystalline Si, efficiencies 10.7-13.2%	1,064 (mean)	Standard deviation $226kWh/m^2$ (8 samples)	[194]
Mono crystalline Si, efficiencies 12.2-14%	1,628 (mean)	Standard deviation $796kWh/m^2$ (8 samples)	[194]

Table 2.2: Photovoltaic embodied energy values from the literature.

power, as this correlates with size and choice of materials. Such categorisation was not possible for storage technologies, due to a shortage of available data.

While there are databases available such as ecoinvent that have embodied energy values for specific technologies, it was decided that the best way of representing an average energy system was to use average embodied energy values from the literature. This way, it is not just one specific manufacturing process or brand that is being used, but an average representation of the technology. However errors in this data are still recognised, and evaluated in an uncertainty analysis.

Embodied energy of PV modules

A literature survey was done to collect possible embodied energy levels of PV panels, the results of which are shown in table 2.2 and summarised in fig 2.5. These values include the full balance of system: panels, frame and support structure, cabling and inverter. Here the inverter is included, but it is removed from the final PV embodied energy in the methodology to account for its non-modular scaling properties - larger inverters will have a lower embodied energy per kW rating.

Taking average values of all results in the papers reviewed, the typical embodied energy of mono crystalline Si modules is $1650kWh/m^2$, while the typical embodied energy of multi crystalline Si modules is $1099kWh/m^2$. The slightly higher efficiencies of mono crystalline panels are not enough to offset the increased embodied energy levels; for an average annual

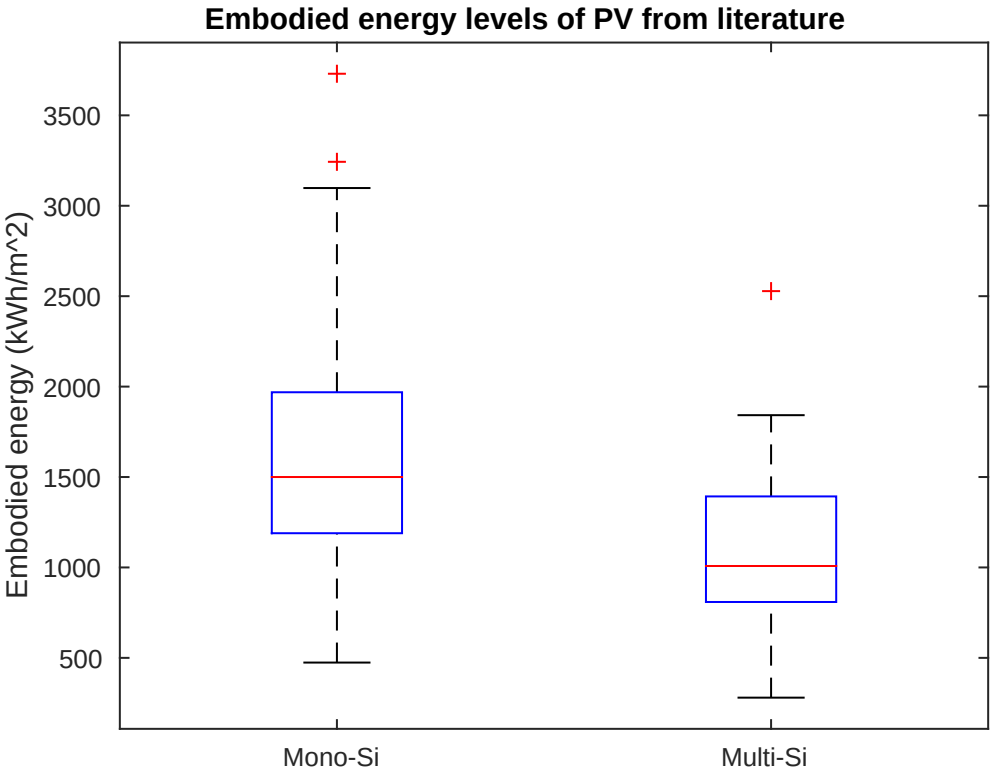

Figure 2.5: Box plots showing range of embodied energy of PV modules in the literature, from 54 samples. These include the inverter's embodied energy.

insolation of $1700kWh/m^2$, performance ratio 75% and lifetime of 30 years, multi crystalline panels with energy efficiency 13.2% would have an EROI of 14.8 (4.6 not scaling for primary energy) while mono crystalline panels under the same conditions with energy efficiency 14% would have an EROI of 10.5 (3.2 not scaling for primary energy), which is significantly less. Note that this method of calculating power production is simplistic in comparison to the actual methods explained later in section 3.2.1 but the rough comparison between technologies remains the same.

Embodied energy of wind turbines

Measuring the embodied energy of wind turbines is slightly different to that of PV, as wind turbines benefit from economy of scale: the larger the wind turbine power capacity, the lower the embodied energy value per kW_p. This is partly driven by the fact that power capacity is correlated with the cube of the turbine blade length, so wind turbines become more efficient as their size increases, but also that larger wind turbines operate at higher altitudes where wind is stronger, and tend to be newer and thus more efficient than smaller ones [180] [181]. With this in mind, finding the embodied energy of wind turbines in general required embodied energy data of turbines with varying power capacities. Different construction materials are also important to acknowledge. A micro wind turbine typically consists of a steel tower and aluminium/fibreglass blades, while a larger wind turbine may have a concrete tower and fibreglass/epoxy resin blades [195]. The different manufacturing processes required for these materials result in very different embodied energy levels. Finally, wind turbines require more maintenance than PV modules, having moving parts that are more likely to break or degrade, and the work and transport involved in maintenance contributes towards their lifetime embodied energy.

Embodied energy for a wide range of onshore wind turbine capacities was collected from a literature survey in the same way as for PV, results shown in figure 2.6 from 12 articles and the ecoinvent database [78] [196] [197] [198] [150] [199] [200] [188] [201] [202] [203] [204] [195]. Studies were a mixture of process analysis and input/output analysis, only including wind turbines with a horizontal axis and maximum power rating of 2MW . Results from [171] for $850kW$ and $3MW$ turbines were considered for inclusion, but the alternative use of hybrid process analysis, while it may give more accurate results with wider boundary conditions, was so different to the other studies that they were eventually excluded to retain consistency. Further investigation using more exhaustive methods of life cycle analysis may be necessary to fully understand the energy costs of wind turbines.

Plotting power rating against embodied energy per unit of capacity in figure 2.6 shows that the measure of embodied energy depends on the power rating of the wind turbine in question, thus a linear fit of $y = -0.825P + 3081$ (orange curve) can determine embodied energy of a generic wind turbine of any power rating up to the maximum needed in this study at $1.2MW$. The resulting embodied energy range is shown in figure 2.7 alongside embodied energy levels of PV modules for comparison. Note that this fit will give a negative embodied energy value for wind turbines of capacity above $3.7MW$; this is due to a nonlinear relationship once power capacity becomes higher, but the linear relationship is accurate enough to use for the range of wind turbines in this study.

Embodied energy of storage technology

There were six major different storage technologies considered, and all had to be compared with respect to their embodied energy. Large scale battery storage is still an emerging technology, particularly in combination with renewable energy systems, so rather than taking average embodied energy values from the literature, where only a handful of life cycle

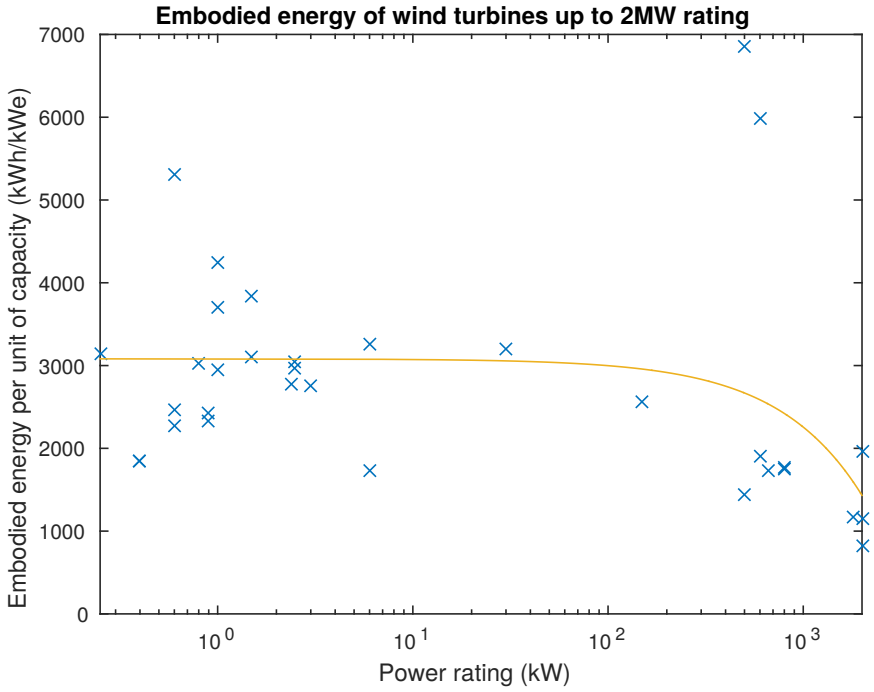

Figure 2.6: Plot of embodied energy per kW power rating for wind turbines up to $2MW$, showing that as turbine size increases, embodied energy becomes more efficient in producing capacity. Anomalous points in top right-hand corner were both obtained from Lenzen 2004. Linear fit is shown in orange (note log scale).

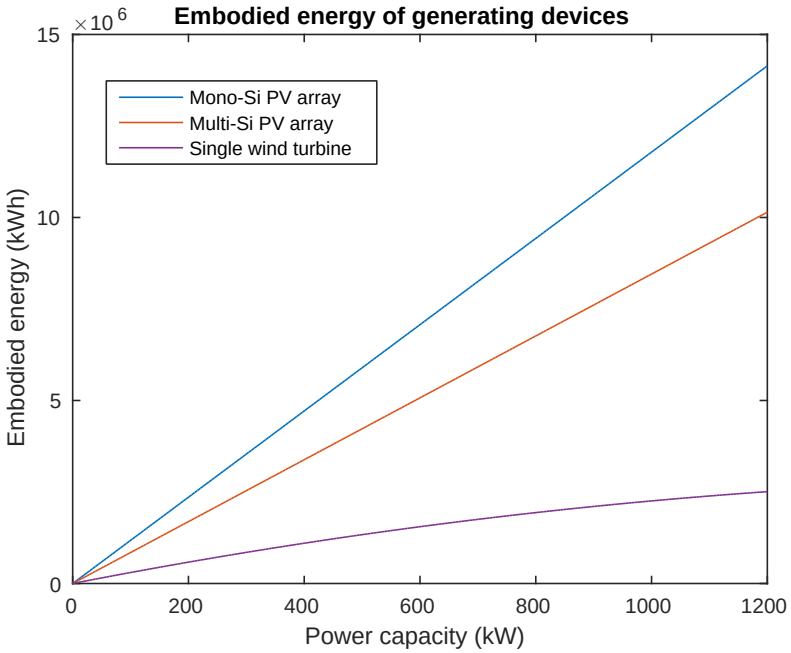

Figure 2.7: Embodied energy of PV and wind turbine devices. Note linear plots for modular PV technology, in contrast with decreasing energy intensity for wind turbines.

assessments exist, the most recent values were taken as standard. Embodied energy values for batteries lead-acid (PbA), lithium-ion (Li-ion) and sodium-sulphur (NaS), and redox flow batteries vanadium-redox (VRB) and zinc-bromine (ZnBr), were taken from [137] over a lifetime of 30 years to fit with typical PV lifetimes, thus accounting for battery replacement during this time. Using EE data from a single study allows for fairer comparison between all types of batteries, as there are not enough studies to allow for averaging, and different studies generally use slightly different methodology and accounting boundaries.

Nickel-cadmium (NiCd), nickel metal-hydroxide (NiMH) and polysulfide-bromide (PSB, also known as Regenesys) batteries were not included in the model, due to unavailability of recent embodied energy calculations and doubts about the practicality of their use in renewable energy systems, as NiCd and NiMH suffer from being older technologies without the advantages of being as widespread as PbA, and PSB is a developing technology with many similarities to ZnBr batteries. The embodied energy for non-remote pumped hydro systems was calculated from [123] to depend on system output in addition to storage capacity, in order to correctly account for energy embodied in operation and maintenance. All embodied energy values are shown in figure 2.8, referenced in table 3.6. Note that while the embodied energy for lead-acid batteries may appear impressively low at $321kWh$ per kWh energy storage capacity, this is thanks to their maturity and increased recyclability of their constituent parts, which is again only made possible by their maturity and widespread use. It must also be pointed out that when depth of discharge is considered, a lead-acid battery with depth of discharge 50% will have embodied energy at $642kWh$ per kWh of usable storage capacity, while a lithium-ion battery with depth of discharge 90% will have embodied energy at $504kWh$ per kWh of usable storage capacity. Additionally, there is more scope for newer battery technologies to reduce their energy costs, so flow batteries could end up with lower embodied energy than lead-acid eventually.

The embodied energy values for a small hydrogen storage and fuel cell unit was also calculated using the paper by Pellow et al. [133], assuming the electrolyser was chosen to reflect the power capacity P of the generators, and the fuel cell sized at 20MW capacity to safely meet the highest recorded domestic demand of 17MW. Therefore using their suggested energy intensities and component lifetimes of an electrolyser, compressor, n steel cylinders for hydrogen storage, and PEM fuel cell gives a total embodied energy of $EE_{H2} = 2260P + 644n + 161160kWh$. Each steel cylinder is sized to store 0.72kg hydrogen, equivalent to 24kWh energy (not accounting for inefficiencies of fuel cell). This must be considered an experimental calculation, as many of the embodied energy values are based only on the materials required, and extrapolated to different sizes. However there is not enough available LCA data to conduct a more thorough review. The results with hydrogen are likely to be fairly different to the battery systems, as the hydrogen system has considerably lower cycle efficiency, embodied energy is less dependent on size of storage due to considerable costs of non-storage components, and the units of storage are much larger.

Compressed air energy storage, while not applied in the models, was estimated to have an embodied energy cost of $75.3kWh/kWh_{cap}$ for an installation lasting 40 years, where the construction costs $73.8kWh/kWh_{cap}$ and the gas fuel costs $1.45kWh/kWh_{cap}$ [123]. This is of a similar order of magnitude to PHS systems. PSB flow batteries were found in [191] to have EE of $1189kWh/kWh_{cap}$ for a system lasting 25 years, a little higher than the value of $1080kWh/kWh_{cap}$ for VRB systems in the same study, and with a lower cycle efficiency at 60-73% [205]. Given their similar mode of operation, it could be assumed that PSB systems, if modelled in this thesis, would give slightly worse performance than VRB systems, and their results can be encompassed within the uncertainty analysis.

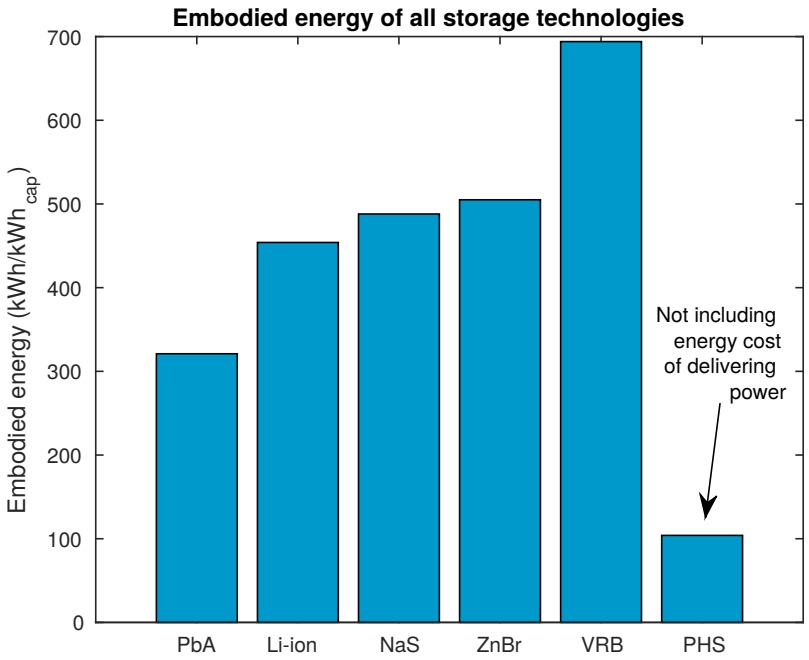

Figure 2.8: Embodied energy of storage technologies. The bar for pumped hydro storage doesn't take into account energy costs of delivering stored energy, but this is a small amount and actual value is dependent on the system.

Embodied energy of further system components

The balance of system for a renewable energy system includes more than simply the solar panels, wind turbine and batteries; also essential is an inverter to convert DC power to AC power for exporting to the grid, and a charge regulator to control the charging of the battery. The embodied energy for both these components was calculated to be $278kWh/kW$ power capacity [206] [191], and these figures have also been used in further publications by different authors [81]. This is based upon a 3kW rated inverter. The power capacity of the inverter and charge regulator (the latter only being included when a battery is present) should be chosen to match the total power capacity of generation. While the embodied energy of the inverter is usually included in the solar panels' embodied energy values alongside its other balance of system components, the wind turbine evaluation does not include this, so the full power rating of the inverter must be accounted for in the embodied energy calculation. This is a different type of inverter, being AC-AC rather than DC-AC, but the lack of data for these specific types of inverter means that we assume that both have the same embodied energy.

However, it cannot be assumed that there will be a linear relationship between the size of inverter and its embodied energy. Much of the embodied energy will be for the metal casing, which does not necessarily scale with power capacity. Data from the ecoinvent database gives lower embodied energy values for higher capacity inverters, which are shown alongside the 278kWh value for a 3kW inverter in figure 2.9. The embodied energy data from these four inverters was then fit to a log curve $y = -36.8\log(P) + 256$ where P is the power rating of a hypothetical inverter, shown in figure 2.10. This fit cannot be said to be absolutely accurate, as it is dependent upon only 4 datapoints, however it gives a rough idea of the expected inverter energy cost at different sizes. Given that the 3kW inverter would typically only contribute to

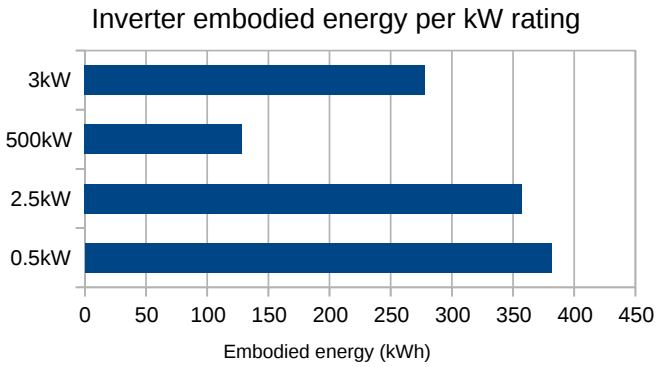

Figure 2.9: Embodied energy of differently sized inverters.

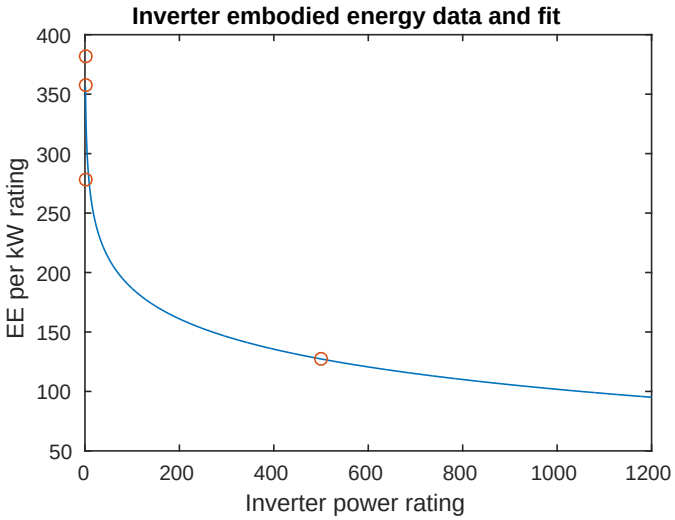

Figure 2.10: Embodied energy of differently sized inverters, plotted with log fit $y = -36.8\log(P) + 256$.

3% of a PV installation's embodied energy, this is a reasonable estimate to make. Wind systems will have a proportionally greater embodied energy contribution from the inverter, and there must be an awareness of this in the results. It was assumed that this relationship between power rating and embodied energy is also followed by the charge regulator component, as they are of similar construction.

Embodied energy for a 3.5kW rated domestic heat pump was estimated to be 2130kWh using embodied energy data from two different heat pumps, both of which were attached to a solar thermal system [207]. This included the following components: storage cylinder, glycol (an anti-freeze used in the circulation system), expansion vessel and copper piping. An additional 20% extra embodied energy was added to the components' embodied energy to account for digging and installation energy costs. Only taking into account these components, the total embodied energy for the two heat pumps was 1850kWh for a heat pump with 300l storage cylinder capacity, or 2403kWh for a heat pump with 400l storage cylinder capacity. The 2130kWh figure was reached by taking an average value.

2.4.7 Gaps in the literature

While there is much discussion of off-grid hybrid renewable systems with lead-acid battery storage, or evaluations of national grid scale storage interventions using pumped hydro storage, these results have limited relevance in future energy scenarios for multiple reasons. Firstly, the suitability of lead-acid batteries for utility storage is questioned, due to their high rate of failure, low depth of discharge levels, high weight and toxicity concerns. The suitability of pumped hydro storage is also a concern, being geographically dependent. In the UK particularly, there is a shortage of locations suitable for pumped hydro stations. Secondly, off-grid renewable systems are likely to always be a niche interest. While their application in developing countries and very large countries with remote communities is important, in countries such as the UK where most areas are reached by the electricity network, off-grid systems have limited benefits. Thirdly, there is increasing interest in restructuring our electricity networks in order to fully exploit the benefits of variable renewable energy sources. These modern structures are rarely considered in the context of the optimisation procedures, despite being designed to hopefully improve performance and integration of renewable energy, which will obviously have an effect on system optimisation. Such structures will likely not have as absolute limits on energy security, as they are subsystems within the larger grid, and can import and export electricity when required. However in order for the entire system to function, their energy security must be increased as much as is practical, entailing an optimisation considering security and some measurement of cost.

While some work has been done to compare different battery technologies in terms of their EROI [208], this has not been done in the context of the wider system, as system sizing of components was not a concern in that study. More work therefore needs to be done to optimise future systems with newer battery technologies such as lithium-ion and flow batteries. Additionally, while many studies include a consideration of energy security in terms of how well demand is met by supply (usually by quantifying loss of load periods in some way), the wider terms of energy security are not fully examined. The limits to renewable penetration do not solely come from the threat of loss of load or cost, but also from overproduction and its negative effects on the infrastructure of the electricity network. Merely curtailing production is not a long-term solution, as it limits the capabilities of renewable energy technologies and ends up being less cost effective [110]. Considering the effects of overproduction must then be a part of any optimisation that takes energy security seriously. There is also little standardisation of security metrics in the literature, despite industry standards of using LOLP and EIR for adequacy analysis so a simple comparison between time-dimensional metrics and energy-dimensional metrics would be useful to clarify which are more useful.

This project therefore addresses these concerns by focusing on grid-connected energy system models using a variety of different storage technologies, and applying a physical performance evaluation of those systems. The methodology in the next chapter explains how the goal of optimising power subsystems with alternative storage technologies, with respect to a full understanding of energy security and energy sustainability, will be approached in this study.

Chapter 3

Methodology

The broad goal of this thesis is to analyse renewable energy systems at different sizes and levels of complexity, to give insight into how local storage solutions interact with variable renewable energy sources, and optimise ideal renewable energy subsystems in terms of their sustainability and security. There are a large number of possible system scenarios that need to be considered, comparing the important variables shown in table 3.1.

The only practical approach for full comparison between these variables was computational modelling of renewable energy systems with electronic energy storage, as building such a large number of energy system experiments would be outside the scope of this project. To ensure accuracy, the model used input energy time-series based on real world data of wind and solar availability, and electricity demand measured in domestic and non-domestic buildings. While probabilistic simulations of all three categories of time-series do exist, the importance of realistic variability in the model necessitated the use of real world data.

This chapter is divided into four major sections as follows.

1. Energy flow simulation - how the energy flows within the networks are modelled, in particular the behaviour of the battery or pumped hydro storage.

2. Construction of energy generation and demand input data.

3. Ensemble building and statistical sampling.

4. Approaches to analysis and interpretation of results.

In section 3.1, the simulation of battery technologies and pumped hydro storage is explained, showing the reasons behind the methods chosen, and the different properties of the available energy storage technologies that affect their behaviour.

In section 3.2, it is shown how energy generation time-series for solar and wind were constructed, based upon UK weather data and limited photovoltaic (PV) generation data. Just as importantly, the choice of household demand time-series, and construction of demand for larger-scale networks, is explained.

Section 3.3 shows how the input data from section 3.2 is fed into the energy flow simulation from section 3.1 in order to produce samples of energy networks for analysis. This must be done according to the variables listed above, so the size of the network varied from a single household, to street-level size (20 households), to a case study of the area of Stocksbridge, encompassing 6000 households and 5.5MWh/year of non-domestic electricity demand. There are also samples of non-domestic electricity demand time-series, 93 generation scenarios of varying total capacity and relative capacity between solar and wind, and eight different battery technologies alongside pumped hydro storage for large networks.

Variable	Range/examples	Comments
Type of electricity demand load	Domestic household, non-domestic building.	Choice of domestic household is also relevant, as domestic electricity use varies widely in terms of total demand.
Size of demand-supply network	Single household/non-domestic building, up to 20 networked loads, case study of small town.	See table 3.5 for full demand ranges of all system scenarios.
Annual energy available to meet demand locally	Scaled to demand: generate up to 260% of annual demand.	While supply is scaled to demand during the modelling stage, systems are optimised with respect to absolute power capacity during the analysis stage.
Ratio of wind to solar generation mix	93 combinations from entirely wind, to hybrid mixes to entirely solar.	Resolution is at every 20% step, see table 3.4 for full range of inputs.
Type of electrical energy storage technology	5 different types of battery and pumped hydro storage for large networks.	See table 3.2 for full list of batteries and their properties.
Storage capacity of energy storage unit	$0 - 50kWh$ energy storage per household, 0-500% daily demand per non-domestic building, $0-180MWh$ energy storage for entire town.	Capacity is normalised to kWh rather than Ah because voltage and current are not modelled. Availability of real storage capacity is determined by depth of discharge.

Table 3.1: Important variables for consideration that might affect the sustainability or security of the system

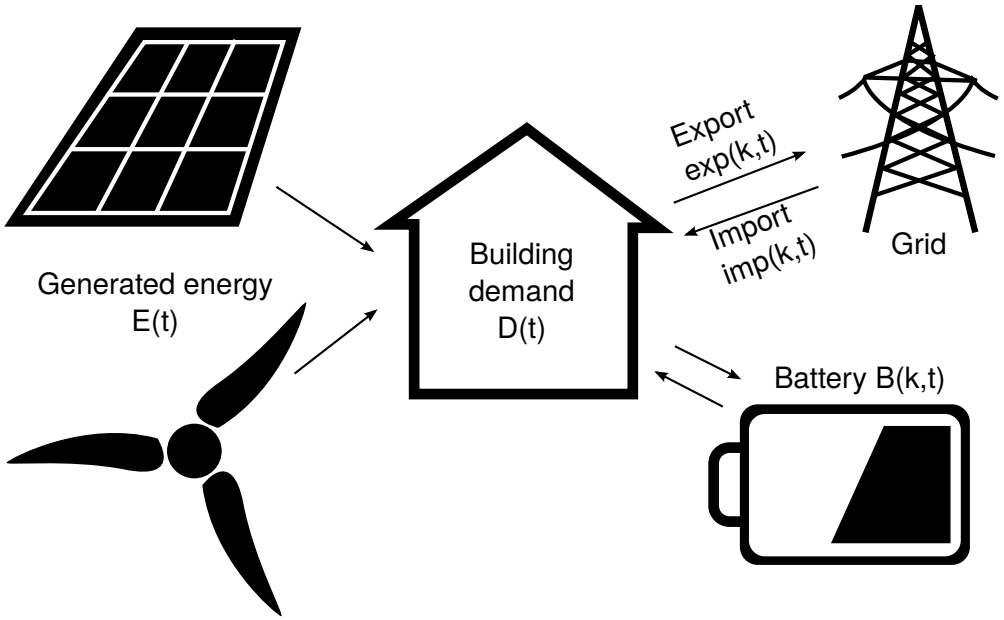

Figure 3.1: Schematic of generic energy system, where t is time and k is battery capacity. The grid is not modelled as part of the simulation, but is depicted here to illustrate energy over- and underproduction in terms of exporting and importing energy

Finally section 3.4 explains how the results from the model are analysed. This encompasses the metrics chosen to measure sustainability and security, the methodology of combining these into some measurement of network performance, and methods of comparing these performance results. Errors in the available data, particularly embodied energy values of the technologies concerned, are considered by performing sensitivity analysis on the results. This is done by varying parameters with the largest error margins to see the effect this has on the calculated performance.

3.1 Energy flow simulation

The energy systems characterised in this study are made up of three main components, illustrated in figure 3.1. These are energy input, storage unit and demand load. Energy input is the electricity generated from a variable renewable source, storage unit can be an electrochemical battery for small systems, or a flow battery/pumped hydro for larger systems, and demand load is the demand from domestic households, non-domestic buildings, or networks of multiple loads. When considering the physical aspects of the systems there are more components to consider: energy input may come from PV panels and wind turbines, these will be connected to an inverter to ensure AC output of electricity, and there may be a number of household loads and storage units.

When modelling the energy system, the time-series $E(t)$ and $D(t)$ - representing generated energy and energy demand respectively - were constructed separately as discussed in section 3.2, so the priority of the system model is to simulate the energy storage technology correctly, which creates the battery time-series $B(k,t)$, in order to find the export and import output time-series. Results are calculated using these output time-series, alongside other results such as battery losses and on-site demand satisfaction.

The energy storage technologies examined were chiefly rechargeable (secondary) batteries, flow batteries and pumped hydro storage (PHS). Different technologies were suitable for different sizes of system, e.g. secondary batteries are more suited to small installations, whereas pumped hydro storage is only possible for large systems.

All energy storage technologies were modelled over time with the same central structure: a black box model with energy input and output. The technologies were differentiated by applying appropriate charging/discharging efficiencies, depth of discharge and capacity degradation. In each half-hour time-frame, a stepwise simulation calculates the state-of-charge of the battery, which stores surplus electricity from a source of energy generation and releases it when the demand load exceeds available generated electricity. The battery is only charged with on-site energy that is unused at the point of generation, and is only discharged when the load requires it.

3.1.1 Energy conversion efficiency

Lead-acid battery charging efficiency at time t was modelled as dependent on state-of-charge while battery charges, and 100% while discharging. As state-of-charge increases, voltage decreases, which reduces efficiency. Thus efficiency was modelled linearly for PbA batteries as

$$\eta = \frac{2(1-\eta_C)SOC + DOD(2\eta_C - 1) - 1}{DOD - 1} \tag{3.1}$$

where DOD = depth of discharge of the battery technology, SOC = state-of-charge of the battery, η_C is average cycle efficiency and η is actual time-variant efficiency. Lack of information in the literature meant that for other battery technologies their charging efficiency was assumed to be constant at η_C while charging, 100% while discharging.

For pumped hydro storage systems, as there are losses in both water pumping (i.e. charging) and hydro generation (i.e. discharging) but only cycle efficiency η_C is known, the efficiency was modelled to be static at $\eta = \sqrt{(\eta_C)}$ for both charging and discharging.

3.1.2 Depth of discharge

The batteries included in the model nearly all have limits on how much they can be discharged by, as part of requirements for safe usage and encouraging optimal battery life; this significantly impacts on usable storage capacity, and thus affects their performance and total embodied energy (as larger batteries are necessary to make up for technology with shallow depth of discharge levels, which obviously would require more embodied energy). While in reality the depth of discharge is slightly variable, and can be changed with an impact on efficiency and battery longevity, the batteries have been modelled as not being capable of discharging below depth of discharge, as effects of discharging below are not yet fully understood. Used depth of discharge values are shown in table 3.2. Pumped hydro storage can also be assumed to have a depth of discharge at 95%, as the top reservoir cannot usually drain completely in practice [128].

3.1.3 Battery degradation

Over time, the batteries degrade in two ways: usable storage capacity decreases, and the batteries eventually reach the end of their lifetime. Once batteries drop to 80% of their original capacity they are removed to be replaced with new batteries at full capacity (this is modelled to only occur at the end of years, rather than during the year, as capacity degradation is calculated at the end of each year). The lifetime of the system was chosen to be

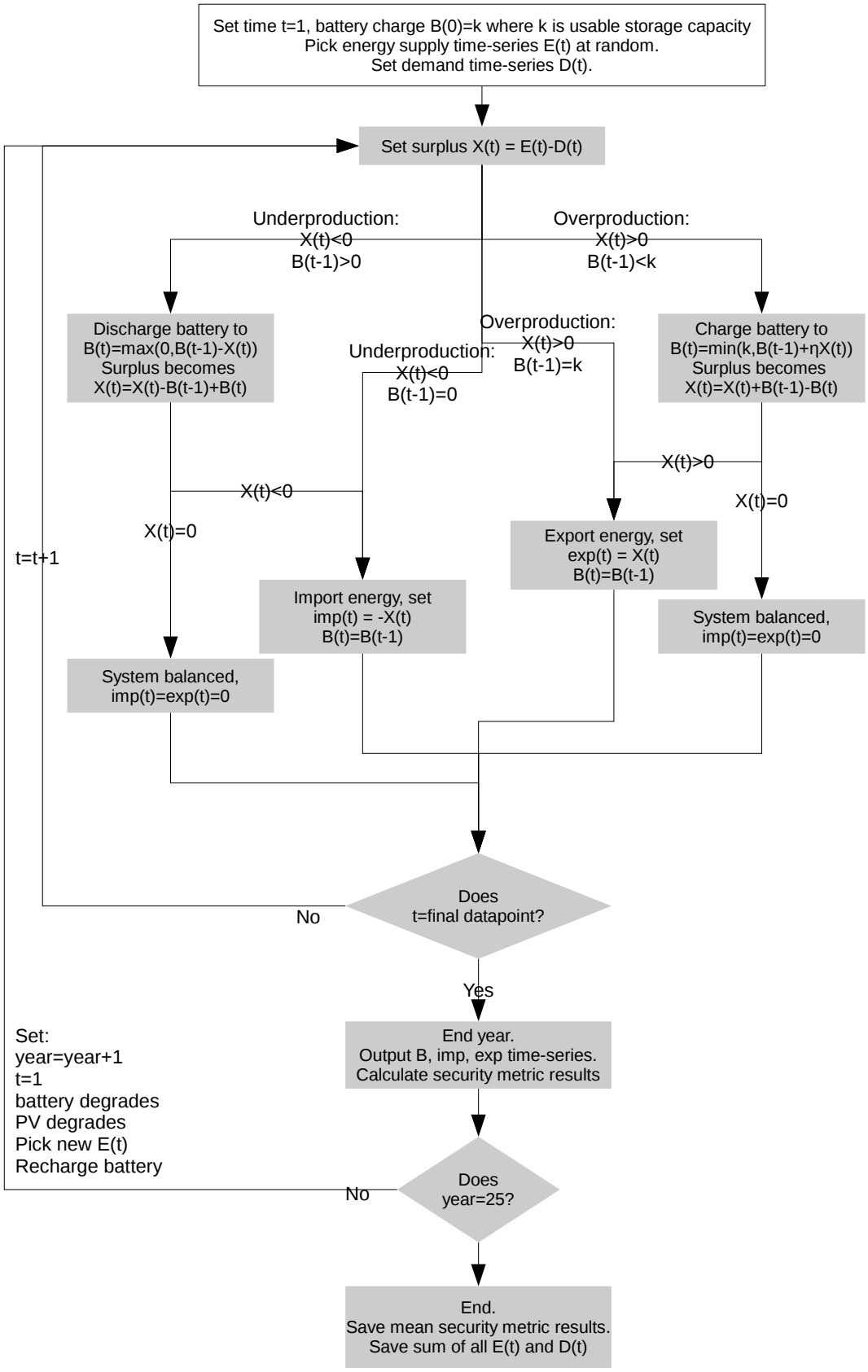

Figure 3.2: Flow chart illustrating energy flows around a generic single-load system, for a single battery with maximum usable capacity k and efficiency η.

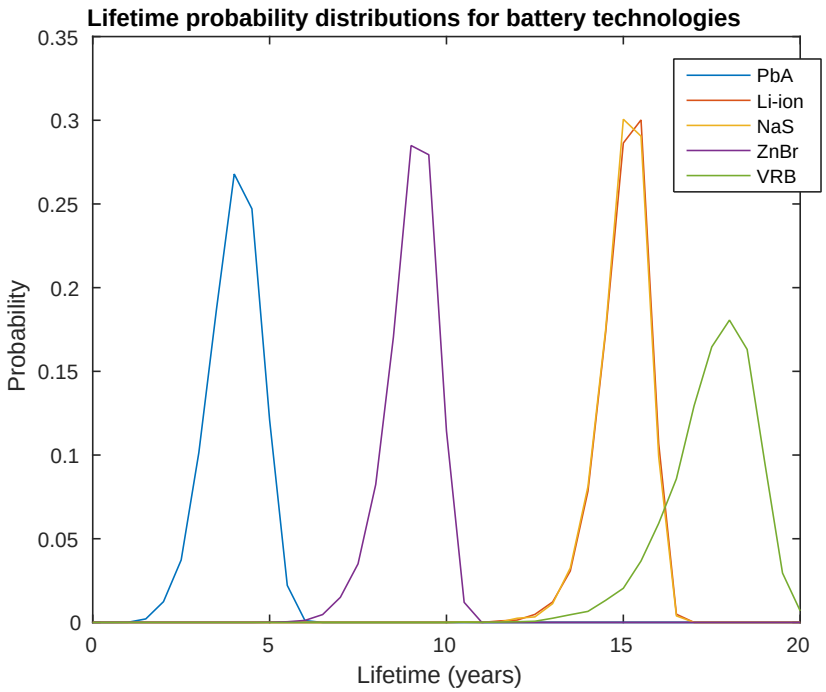

Figure 3.3: Probability distributions for the lifetimes of all modelled battery technologies. Li-ion and NaS batteries share a line.

25 years, as a compromise between the estimated lifetimes of PV modules (20-30 years) and wind turbines (20-30 years, with land often only leased for 25 years).

In calculating battery lifetime, there are two values that can be used: float life (calendar life - i.e. dependent on time used) and cycle life (dependent on number of cycles). The reason for these alternative values is that the mechanics behind battery degradation vary, including electrode corrosion which limits cycle life, and more complex processes that affect float lifetime. These are dependent on frequency and depth of discharge, the float voltage and the ambient temperature. The shorter of the two lifetimes was given for all batteries, assuming 365 cycles per year (realistic for a PV system given its diurnal cycle), and are shown in table 3.2. Battery capacity degradation was taken to be 1.2-1.5% per year for each battery type [209].

In order to model the impact of battery degradation, battery lifetimes were assumed to fit the Weibull distribution with PDF described in equation 3.2, this being the most commonly used probability distribution for failure rate. Figure 3.3 applies these probability distribution functions for each battery technology, based on the lifetimes from [191] (note Li-ion and NaS have identical distribution).

$$f(x;\lambda,k) = \begin{cases} \frac{k}{\lambda}(\frac{x}{\lambda})^{k-1}e^{-(x/\lambda)^k} & x \geq 0 \\ 0 & x < 0 \end{cases} \tag{3.2}$$

Capacity degradation was modelled using the normal distribution $D \sim N(0.0135, 0.0015)$ to estimate usable capacity loss each year for each battery in the system. If battery lifetimes are ignored (as can occur for those technologies with very long lifetimes) this means that all batteries drop to the minimum 80% capacity after an average of 17 years (max 32, minimum 12 years). Capacity degradation rates for all batteries except PbA are based on calendar (float) life rather than number of cycles, as cycles are difficult to track given the varying minimum

Battery type	Efficiency and range (%) [205]	Depth of discharge (%)	Lifetime (years) [191]	λ	k
Lead-acid	75 (70-84)	50 [128]	2.5-5.5 (cycle)	4.29	6.57
Lithium-ion	90 (85-95)	90 [128]	14-16 (float)	15.30	27.59
NaS	79 (75-83)	90 [128]	14-16 (float)	15.30	27.59
ZnBr	66 (60-73)	100 [130]	8-10 (float)	9.30	15.84
VRB	70 (60-80)	100 [130]	15-20 (float)	18.03	17.96

Table 3.2: Battery properties for model, affecting performance and degradation. Note PbA batteries have a short cycle life when operated daily, so this lifetime was chosen rather than their float life. All batteries' lifetimes are modelled using a Weibull distribution with parameters λ and k.

state of charge that the batteries experience. The cycle life of PbA batteries is so low that it has been used instead of float life, with an assumption that the batteries cycle once per day on average over the year.

Table 3.2 shows the battery characteristics used in the model for each battery type, including cycle efficiency, depth of discharge, lifetime range (whether based on cycle or float lifetime) and the Weibull scale and shape parameters (λ and k) used to model this expected lifetime.

To ensure that the model was working correctly, and to provide a baseline demonstration, it was initially run with a small test sample of flat time-series and square waves as data input. The results from this initial test are given in section 4.2 in the next chapter.

3.2 Construction of generation and demand data

In order to simulate a wide variety of systems, a great deal of time-series data was required to represent electricity generation and demand loads. Electricity power generation time-series, being produced from solar or wind sources, were created from PV and wind turbine generation data, or simulated using weather data when the former were not available. Demand time-series were collected from a survey of 22 homes in Loughborough in 2008/9, 15 non-domestic buildings (a mixture of publicly available data and local buildings), and a group of homes fitted with community PV installations. Given the need for accurate security results, high temporal resolution was required, hourly at minimum. Using weather data rather than direct generation data for wind and solar power generation had a number of advantages: nationwide data was available for a number of locations, production could be modelled for wind turbines with different hub heights (using the wind shear equation), and degradation of PV panels could be included in their power simulation. Inaccuracy in the simulated power time-series was minimised by considering a number of aspects of performance.

3.2.1 PV generation

Given the limited availability of nationwide PV generation data, the generalised model made use of global irradiance data from weather observation stations around the UK, available on the MIDAS database. The generalised model used simulated power generation by multi-Si PV panels, chosen for their lower embodied energy levels and wide market availability. All panels were assumed to have a rated energy conversion efficiency of 13%, chosen to match typical efficiencies of multi-Si PV seen in the literature review (section 2.4.6). This ensures that the embodied energy values used in the analysis will correctly match the technology that is being analysed.

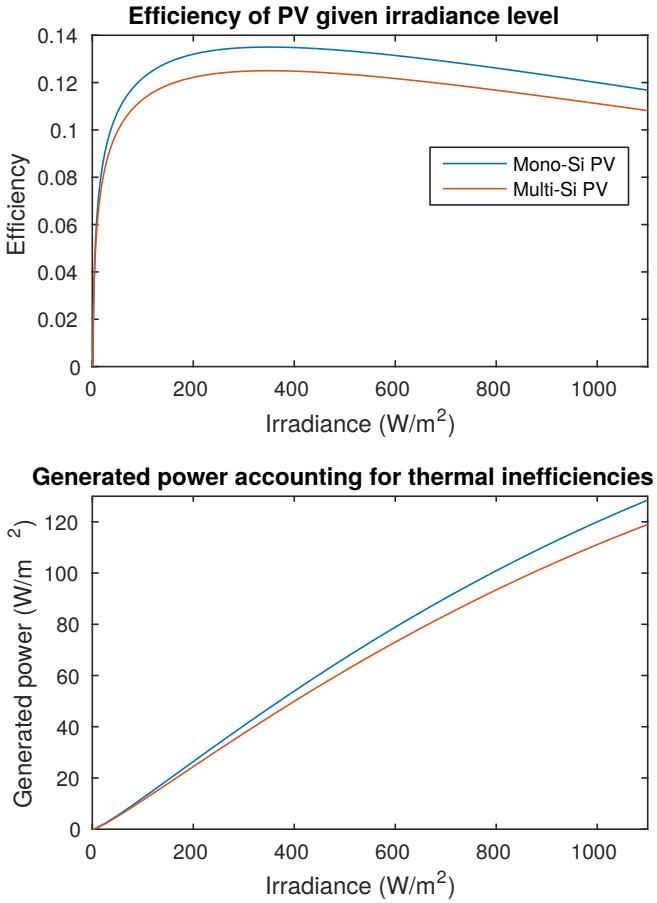

Figure 3.4: Upper: efficiency of multi-Si solar panel accounting for thermal losses, with mono-Si panel for comparison. Lower: Resultant power generation accounting for thermal losses. Peak efficiency is at $400W/m^2$ irradiance, but highest level of generated power is still highest at the top levels of irradiance.

Calculating power generation from global irradiance data required knowledge of panel efficiency and the PV module's performance ratio. Performance ratio was split into two parts: firstly the thermal losses from heating of the panels, and secondly the module losses from inverter and system inefficiencies, which were assumed to increase over time but remain constant within each year. As temperature data was not available for all irradiance data sources, panel efficiency was assumed to depend on irradiance level, using results from [47]. Thus the efficiency η depends on irradiance I according to the equation

$$\eta(I) = (b_1 + b_2 I)log(I) - b_3 I \tag{3.3}$$

where $b_1 = 0.029$, $b_2 = 0.000022$, $b_3 = 0.00023$ for a panel with rated efficiency of 13%. This is graphed in figure 3.4, showing that peak efficiency is at irradiance level of $350W/m^2$. Using the available global irradiance data with this equation gives panels an average efficiency of 10%, with annual energy production being 92.4% of idealised modelled production with a constant 13% efficiency.

To bring the overall performance ratio to 84% [53], further losses of 9.07% were added into the system. This system efficiency of 91% is close to the 93.5% conversion efficiency assumed in

the database ecoinvent [176] and is caused by inverter inefficiencies and general system losses. Furthermore, when modelling solar generation over the full lifetime of the model, performance ratio was further impacted by a panel degradation of 0.5% (percentage points) per year in accordance with recent findings on modern PV modules [210]. Thus after 25 years, the modules would be estimated to have a performance ratio of 73.5%. This linear rate of degradation is recommended by multiple sources [52]. Photovoltaic failure rates were not included in the model, as the simulation is of an ideal and well-maintained system, which is expected to have a lifetime of 25-30 years.

With knowledge of efficiencies and performance ratio, the power generation can then be simulated as follows. If the time-series of global irradiance $I(t)$ measures the direct solar irradiance per metre squared, then to model the power generation $P(t, y)$ (in W) of a poly-Si PV array of age y years with initial performance ratio 84%, area Am^2, variable efficiency $\eta(I)$ using eq 3.3 , and 13% rated efficiency (so that peak power $130W/m^2$ is reached only at test conditions of irradiance $I = 1000W/m^2$), the following formula was used:

$$P(t, y) = 0.9093A(1 - 0.005y) \cdot \eta(I(t)) \cdot I(t) \tag{3.4}$$

The available MIDAS data from 82 weather stations is shown in figure 3.5 using equation 3.4 to estimate annual PV generation potential per metre squared of PV arrays. The linear fits of this data are compared in the lower graph to actual UK PV generation from the Sheffield Solar microgen database at www.microgen-database.org.uk, which contains installations over the period of 2006-2014. With only global solar irradiance data available, it was not possible to construct perfectly accurate PV power generation time-series, as data is gathered from a horizontal receptor with no separation of direct and diffuse irradiance, which are required to model angled PV arrays [33]. However the close match to real UK data shows reliability in this method of power generation estimation, and patterns of variability in solar availability would be preserved so energy security can be calculated accurately. Where gaps existed in the data, these were filled in by copying the solar irradiance measured at the next nearest weather station. If after performing this step there were still gaps in the time-series, data from the previous day at that location were used.

For the non-generalised models, some real PV generation was available from the microgen database at Sheffield Solar at hourly or higher resolution; time-series from 5 locations were used in the Stocksbridge model. This was not possible for the generalised model, as only a small amount of data was available at high enough resolution, all from Sheffield locations, which would give unrealistic results for the whole of the UK. The PV panels used on the test bed as part of the Sheffield Solar project are mono crystalline Si, and thus have a higher energy efficiency of 14%, producing peak power $185W$ per $1.3m^2$ panel. This installation is the source of the high resolution PV generation data mentioned in section 3.3.2, and some of the input solar data for the Stocksbridge case study.

3.2.2 Wind turbine generation

The main data available for wind power generation were time-series of wind speed and direction at half-hourly resolution from the MIDAS database provided by the Met Office, for weather stations across the UK and Ireland. There was also real generation data from a wind turbine located at the Centre for Alternative Technology (latitude 52.6, longitude -3.82), being a $500kW$ Nordtank NTK turbine with hub height $7m$, wind speed and direction measured at a 10-minutely resolution. Where wind power generation data was not available, two calculations were required to convert wind speed measurements to wind power generation: conversion of the recorded wind

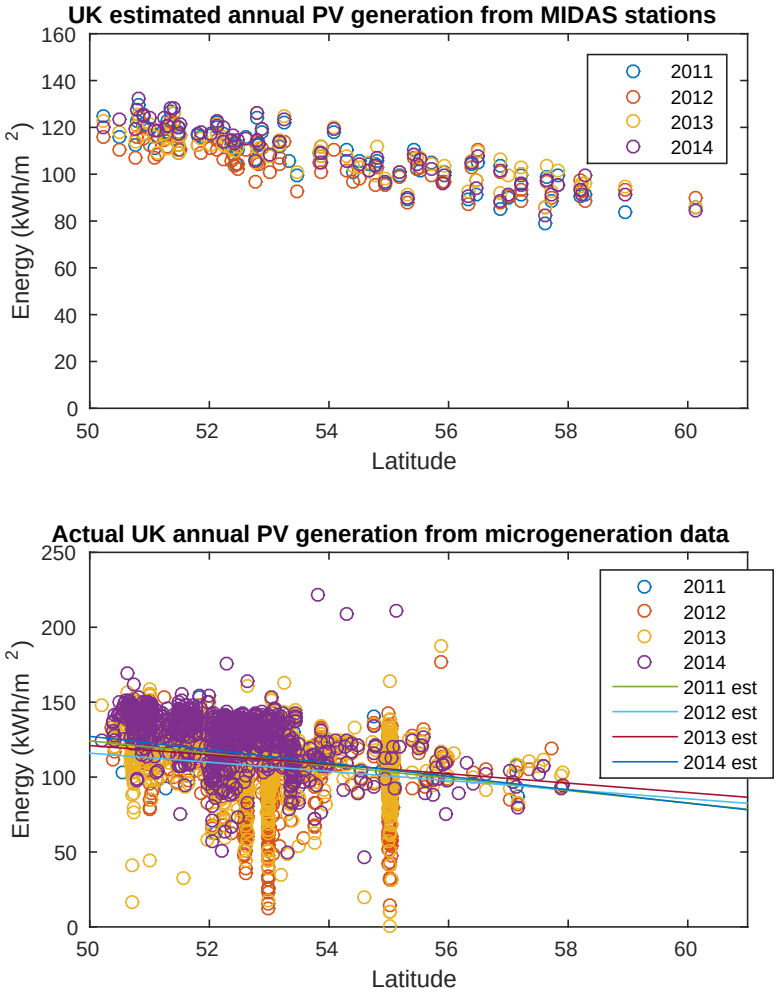

Figure 3.5: Upper: graph of simulated total energy generation for 13% efficiency PV, from years 2011 to 2014. Lower: graph of actual PV generation across the UK (normalised to $130W/m^2$), compared to linear fit of estimated values derived from upper graph. Estimates using irradiance are slightly lower than real PV due to conservative measure of performance ratio and assumption of horizontally inclined panels.

speed to the expected speed at turbine hub height, and use of power curves on wind speed to estimate potential power generation of the wind turbines.

To calculate the wind speed U at height z when wind speed data is available at height z_r, the power law profile can be used with an appropriate value of the wind shear exponent α [211].

$$\frac{U(z)}{U(z_r)} = \left(\frac{z}{z_r}\right)^{\alpha} \tag{3.5}$$

The value of α is often taken to be $1/7$, but this is not an accurate value for real world situations. Higher values are recommended for grass and forested landscapes, and a value of 0.2 is standard for areas suitable for wind turbine location; typically grassy land with minimal shrubs and some low buildings nearby. Where hub height was not immediately available (e.g. when modelling systems with large non-domestic building demand) an approximate formula based on existing wind turbine data was used to estimate the turbine blade length l of wind turbine with capacity CkW, and therefore hub height z:

$$z = 2l = 2\sqrt{0.7028 \cdot C + 36.02} \tag{3.6}$$

Using the resulting wind speed time-series $U(z,t)$, the power generation was calculated using standard power curves, modelled as being a cubic curve up to the maximum power (at rated speed) and flat up to the maximum wind speed when the turbine cuts out. These curves were based on the manufacturers' recommended cut-in speed, rated speed and cut-out speed, with an example power curve shown in figure 3.6. Manufacturers typically give a wind power curve with constant power for wind speeds above the rated speed, and while in practice there is likely to be some decrease in production due to gusty conditions or overstrain on the turbine, it is generally accepted to use this shape of power curve [33]. For most half-hourly wind speed time-series, there are likely to be only few occurrences of sustained wind speed above the rated speed. The generic wind turbine used for the generalised model has cut-in speed at $3.5m/s$, rated speed at $14m/s$, and cut-out speed at $24m/s$. When connecting wind turbines to a grid, it is necessary to include an AC-AC inverter to manage output and keep the network safe. This inverter would typically work at 95% efficiency, slightly reducing the wind turbine's output. To represent this in the model, the final energy output was multiplied by 0.95.

Estimated wind power generation from the 130 suitable weather stations are plotted in figure 3.7, given a power curve with the same shape as figure 3.6 but power capacity $1kW$. There is more variation in the wind power production than PV generation, and this is indicative of the more variable nature of wind. However, some weather stations were situated in areas that would never be chosen for wind power generation, so these locations were removed to give a more realistic sample of wind speeds. The threshold chosen for removal was a mean capacity factor of 10% for $1kWh$ turbines, which is still low but realistic for micro turbines with a low hub height.

The same underproducing locations remained unused for turbines with higher power capacities, however the minimum capacity factor is changed, as resulting capacity factors are affected by modelling taller hub heights with $\alpha = 0.2$ in figure 3.8. This effect on the wind power is non-linear, being subject to the power curve, so minimum capacity factors for wind turbines with power capacity 1.2MW and hub height 60m are on average doubled, rather than simply multiplied by $(60/10)^{0.2} = 1.43$. There is also a more even spread of capacity factor values, rather than the clustering of low capacity factors that is observed for $1kW$ turbines. Further analysis of the wind and solar generation data, in addition to demand data, is covered in section 4.3 in the preliminary results chapter.

Methods differed depending on the system being modelled. For small networks of demand with low demand energy, wind turbines typically had a power capacity between 1 and 10kW,

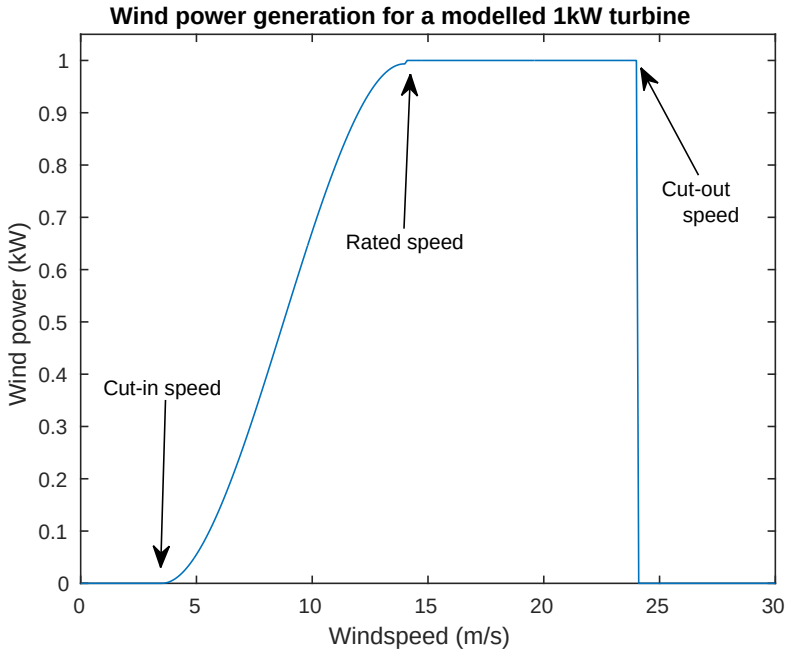

Figure 3.6: Power curve for a $1kWh$ turbine, used to convert wind speed data into wind power generation data. Power generation is highest between its rated speed and cut-out speed. For lower speeds the relationship between wind speed and power is cubic.

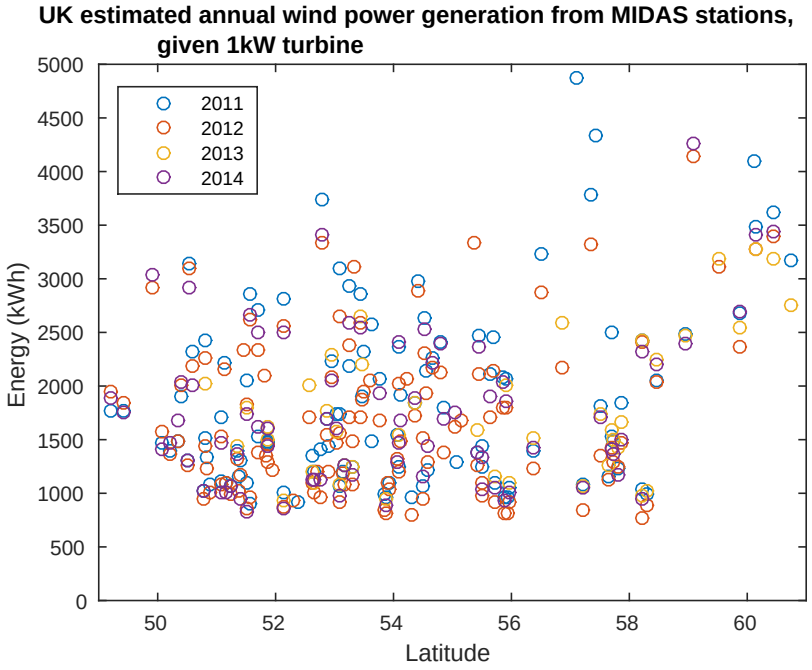

Figure 3.7: Wind power annual energy generation, simulated using wind speed data from different locations around the UK, years 2011 to 2014. Wind power up in the north of Scotland tends to be high, but other than that there is no real correlation with latitude.

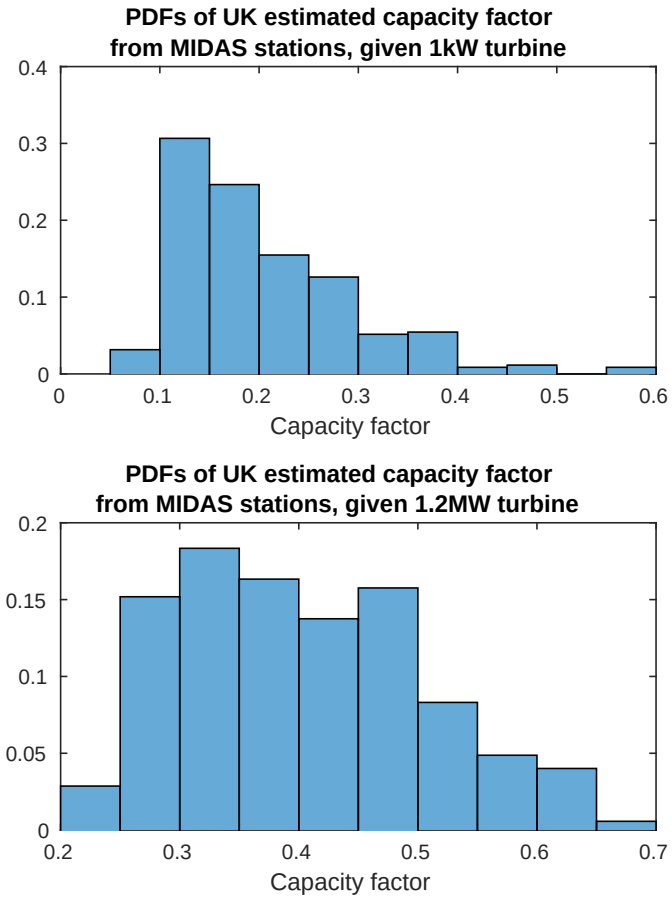

Figure 3.8: Probability distribution functions showing the capacity factors of simulated wind power across the UK, for wind turbines of small (1kW, hub height 10m) and large (1.2MW, hub height 60m) capacity, where wind shear exponent is assumed to be constant at 0.2. Capacity factors are higher for larger wind turbines.

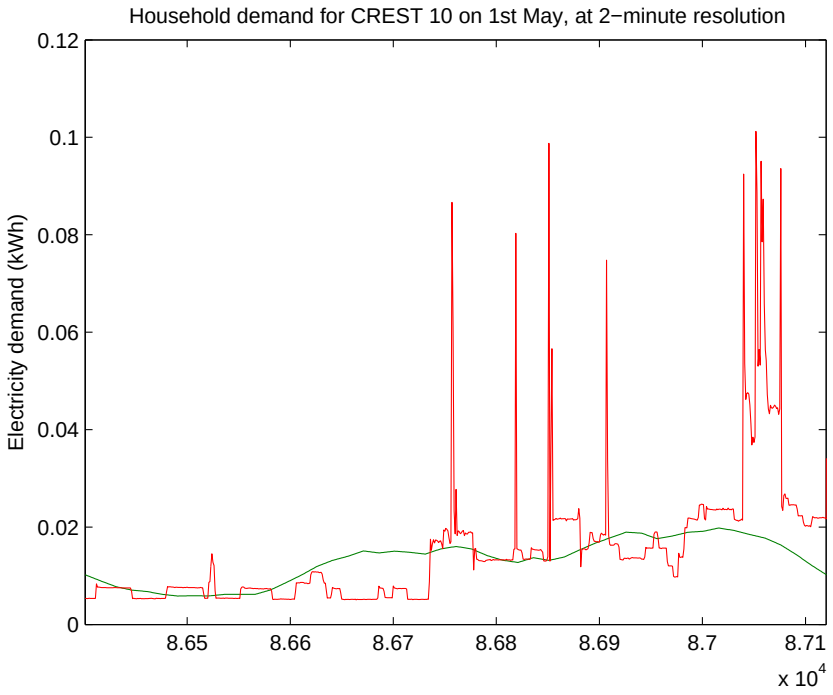

Figure 3.9: Graph showing a day of one of the household demand time-series at high temporal resolution (red) and the average UK household load (green). Intermittent spikes occur in the single household load, but these are completely smoothed out by the adding together of all the nation's households.

so it was assumed that their hub height was 10m, the height at which wind speeds had been recorded. Thus for these systems the wind speed was not altered.

3.2.3 Demand data

There is a large variation in demand data, so it was important to get a wide range of demand time-series from different sources. Crucially, while average demand data was readily available, the smooth average is not typical of an actual household's demand, which demonstrates sudden peaks in power demand. The smooth average curve shown by the green line in figure 3.9 only exists for a large aggregation of households, and is not suitable for modelling a single household because its characteristics would only occur when energy storage or demand-side management is applied.

As household electricity demand simulation is still experimental, relying upon extensive data collection that is not yet readily available [212] such as occupant behaviour [213], it was decided that real recorded data was essential to return accurate security results. The majority of available household electricity demand data was drawn from the CREST survey in Loughborough, comprising of 22 houses with demand data at 2-minute temporal resolution over the years 2008-9. These were chosen randomly in a monte-carlo simulation to give average metric results for a single household, as explained in section 3.3. The sample of households has a higher than average number (12, or 55%) that use the Economy 7 tariff, where off-peak electricity use is incentivised by lower electricity prices. Two of these households had incomplete data where only half of one year out of the two was usable, so the total number of households with usable data was 20, 10 of which are on an Econ 7 tariff. The difference in average daily demand profile of the households with a standard tariff are

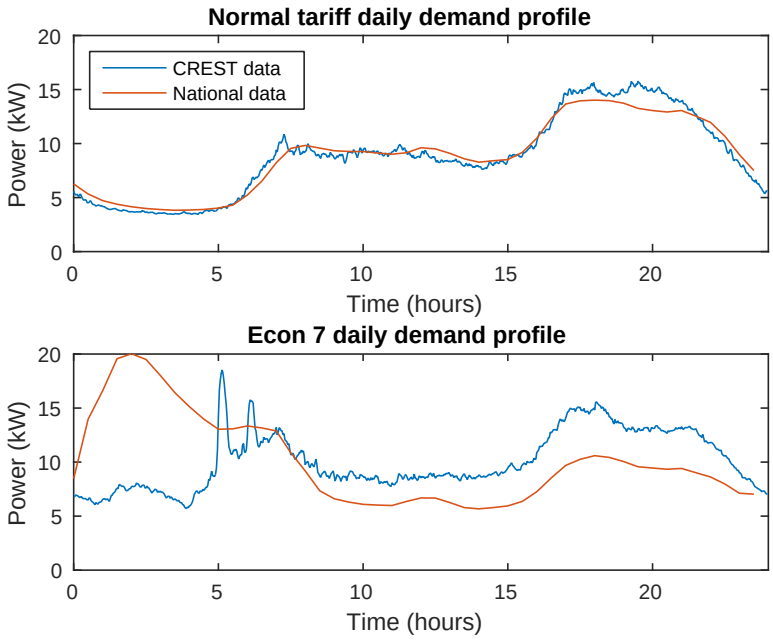

Figure 3.10: Graphs showing 2-minutely daily demand profile of the used household data, alongside half-hourly national average demand profiles. The choice of tariff has in theory a big effect on the shape of the demand profile, as many households with the Econ 7 tariff use electricity strategically in the morning (off-peak) to reduce their demand later in the day, but this is not as apparent in the sample data as in the national data.

compared to the households with an Econ 7 tariff in figure 3.10; there is actually not much difference other than power spikes in the morning of the daily profile for Econ 7 sample households (these mostly appear in one household) and some increased consumption at around 2am, while the national average has a much higher demand peak at 2am. The maximum power use is on average slightly higher in households with an Econ 7 tariff, shown in figure 3.11, but there is some overlap and anomalous points, so the difference is not too significant. The average annual demand is lower than average at $3.77MWh$ per year, and their distribution of demand is shown in figure 3.12.

A survey was taken of all the households to establish the nature of their energy use, which showed that all households had gas or oil heating, and only three used electric heating in addition to that. Two of these households happened to be ones that had incomplete data, so only one of the available time-series includes heating as an energy demand. As electricity was not the primary source of heating in that household, and battery electric vehicles were very rare at the time of measurement, it could be assumed that the household demand time-series generally were not linked to any other energy sectors such as heating or transport.

In addition to the household demand there were 15 different non-domestic demand time-series available, their annual demand shown in figure 3.13 and the type of buildings summarised in table 3.3. The sources of these time-series are varied, but most are public buildings located in Sheffield, London or Bristol.

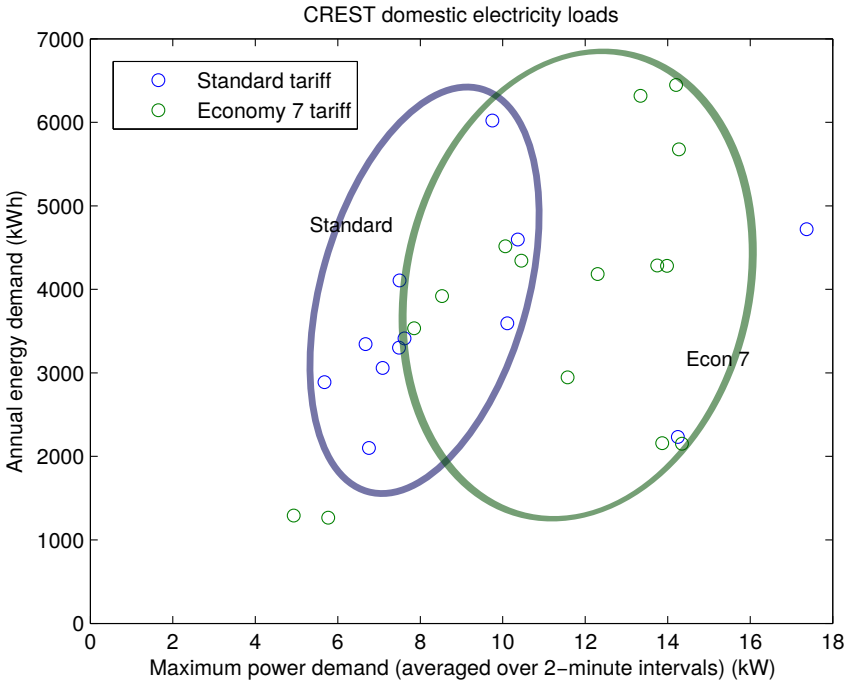

Figure 3.11: Maximum power demand in sample of household demand time-series, at their maximum recorded resolution of 2 minutes. Households with Econ 7 tariffs tended to use a larger amount of energy, but there is some overlap, and the average annual demand is still lower than the average UK household's demand despite there being higher than usual number of households with the Econ 7 tariff.

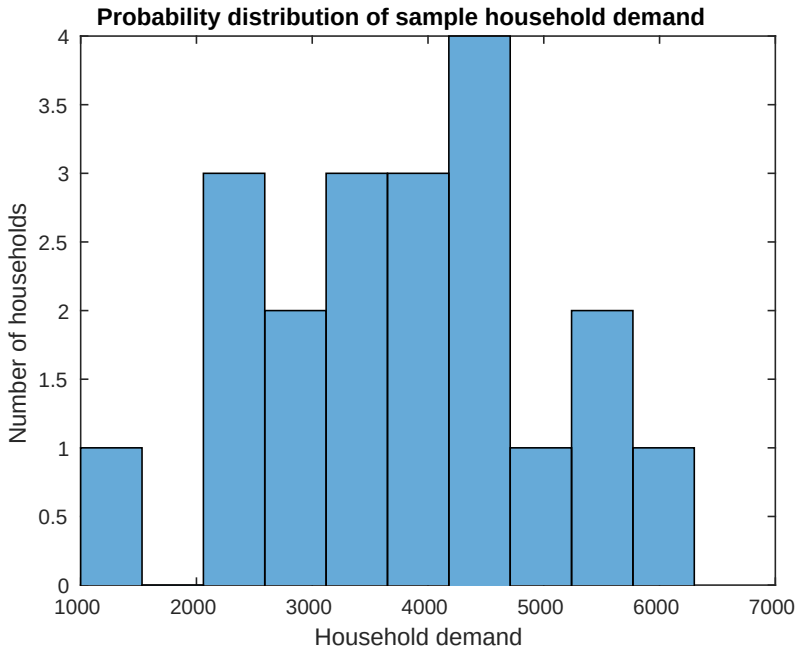

Figure 3.12: Distribution of average annual demand for all sample households, where the average demand is $3.77MWh$ per year.

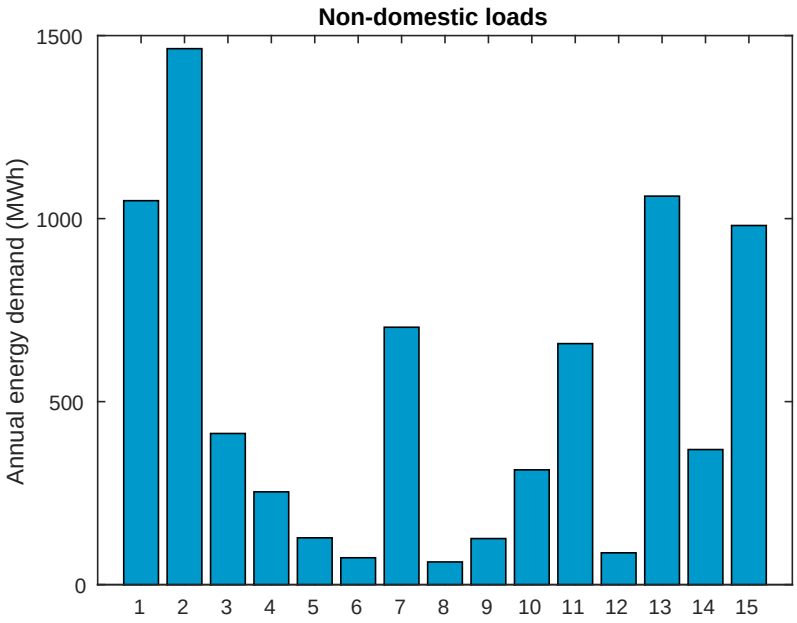

Figure 3.13: Non-domestic annual loads. The difference between loads is so large that the battery capacity has to be scaled to demand.

	Data source
1	Downing St
2	Hicks (university building)
3	School
4	Carbrook 3
5	Carbrook 4
6	Carbrook 5
7	Office building
8	Joinery workshops
9	Leisure centre
10	Swimming pool
11	Government building 1 (Bristol)
12	Government building 2 (Bristol)
13	Government building 3 (Bristol)
14	Government building 4 (Bristol)
15	Government building 5 (Bristol)

Table 3.3: Non-domestic demand sources. Most are office buildings.

3.2.4 Thermal demand

For the household system model containing a heat pump, the thermal load had to be modelled with respect to the household's electricity demand load. Given that the intent of this model was to examine how the additional heat load is handled by the system, it was not possible to simply add a thermal load from an unrelated household. In lieu of existing heat demand data for the households that supplied the electrical demand time-series, the heat pump was assumed to be the average size of $3.5kW$, and the load was crudely simulated using an occupancy method as follows.

For each household, the electrical demand time-series was analysed to find days where the household was unoccupied. It was assumed that if the total electricity use in that day dropped below 50% of that household's daily mean consumption, then the household was unoccupied or in low use (there will always be some consumption from fridge-freezers etc). This was judged to be realistic given that daily demand rarely dropped below 50% of the mean (see figure 3.14), and that none of the households used electric sources for their primary heating system. Furthermore, it was assumed that the household would be well insulated, so would only require full heating during the winter period of December to February inclusive, where this load would be continuous to maintain a steady indoor temperature. During the warmer spring and autumn months (March to May and September to October) the heat pump would be operated from mid-afternoon to the evening, to account for higher thermal demand in the evening and night. This operational schedule is shown for one of the households in figure 3.14

While the hot water tanks (cylinders) were included in the embodied energy value for the heat pump installation, their usage was not explicity modelled in this time-series, as such a simulation would require more accurate thermal demand time-series.

3.3 Ensemble building and statistical sampling

3.3.1 System organisation

Once input time-series and simulation of the energy storage technologies were established, they were assembled together to create samples of energy systems. These energy systems were designed to run over lifetimes of 25 years, allowing for a large sample of electricity generation time-series and the modelling of battery degradation. Given the dependence of system performance on weather patterns, and the large range of weather conditions that would exist over the UK across 4 years of data, repeated measurements of systems with different energy inputs were taken, with the aim of giving generalised results for UK systems. This approach varied depending on the particular system that was being modelled, however for all systems it was assumed that the demand pattern would remain constant year-to-year, while solar and wind availability would change between years. This fixing of annual demand is a simplification, but backed up by the available household demand data that shows notable similarity between years of the same households.

The energy systems are to be optimised with respect to two main variables: storage capacity and power generation capacity. Storage capacity is varied by running the system model over an array of different storage capacities, referred to by variable k in figure 3.1, where the range of values of k depend on the depth of discharge of the chosen battery technology. The total storage capacity range is always 0-50kWh, but the usable capacity range would be $0 - 25kWh$ for lead-acid batteries due to the setting of depth of discharge at 50%, for example. Power generation capacity is varied by running the model multiple times for differently sized inputs; results comparison is made possible by either comparing between systems using identical generation time-series, or by using large enough samples of different generation time-series. It is important

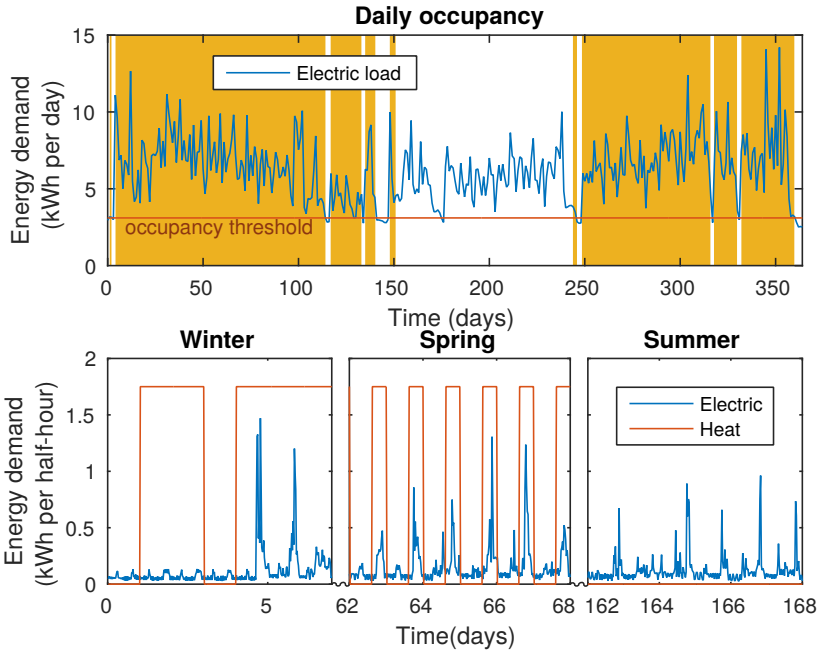

Figure 3.14: Top graph shows the daily electricity demand for one of the households, where dropping below the occupancy threshold (half of the mean daily demand) indicates that the house was not occupied that day. Combining that with non-heating during summer, the yellow sections indicate which days the heat pump will be operated. The bottom graphs show the operation of the heat pump at a half-hourly resolution during the winter, spring and summer months: constant during winter (except when unoccupied), in the evening during spring (except when unoccupied), off during summer. Autumn has the same operational schedule as spring.

Generation as proportion of annual demand	PV=0	0.2	0.4	0.6	0.8	1	1.2	1.4	1.6	1.8	2
Wind=0	0	0.2	0.4	0.6	0.8	1	1.2	1.4	1.6	1.8	2
0.2	0.2	0.4	0.6	0.8	1	1.2	1.4	1.6	1.8	2	2.2
0.4	0.4	0.6	0.8	1	1.2	1.4	1.6	1.8	2	2.2	2.4
0.6	0.6	0.8	1	1.2	1.4	1.6	1.8	2	2.2	2.4	2.6
0.8	0.8	1	1.2	1.4	1.6	1.8	2	2.2	2.4	2.6	
1	1	1.2	1.4	1.6	1.8	2	2.2	2.4	2.6		
1.2	1.2	1.4	1.6	1.8	2	2.2	2.4	2.6			
1.4	1.4	1.6	1.8	2	2.2	2.4	2.6				
1.6	1.6	1.8	2	2.2	2.4	2.6					
1.8	1.8	2	2.2	2.4	2.6						
2	2	2.2	2.4	2.6							

Table 3.4: Table showing each generation mix scenario (93 in total including the null scenario with zero generation). White cells show annual energy generation as a proportion of annual demand; greyed out cells were not used as scenarios due to excessively large generation capacity for grid-connected systems

to note that while power generation capacity has been referred to previously in the text, system samples have been grouped by their estimated annual energy production rather than rated power. This was necessary to be able to compare between solar and wind sources, which have different patterns of production over time, and different capacity factors. Furthermore, because of the large range in size of annual energy demand values, most strongly across non-domestic buildings but also between domestic households, annual energy production was normalised to be a ratio of annual energy demand. It is thus referred to as generation/demand ratio (or generation proportion), and its ranges are shown below in table 3.4; total generation ratio ranges from 0 to 2.6 as a proportion of annual energy demand, while the contribution of wind and solar range from 0 to 2. This approach of scaling generation to demand was not only taken for convenience, but is realistic as the size of renewable energy installations are generally dictated by the expected demand.

Three different sampling approaches were taken. Firstly results for each non-domestic building demand load were taken separately to give preliminary results. Secondly the model was run where 200 sample systems were taken for each generation mix scenario, and results were averaged to give typical metric results. This was done for single household systems, and networked households to simulate a neighbourhood. Thirdly the model was run for the Stocksbridge case study, using only the load representing the entire area's demand, and generation time-series simulated using only weather data particular to the area's location. For the Stocksbridge case study a different approach was taken with the generation mix scenarios; instead there was a base scenario of rooftop PV generation, and additional renewable sources were added by using local land for wind and solar farms. These approaches are summarised in table 3.5.

3.3.2 Single demand load analysis

The simplest ensembles were for single demand loads, where a single electricity demand time-series was selected and used with generation data of different temporal resolutions from Sheffield. Here the power generation time-series were not simulated using weather data, but were real solar and wind power generation data. More precise temporal resolutions (up to 2-minutely) were

System	Annual energy demand (MWh)	Number of data input combinations considered per generation/demand ratio	Technology included in systems	Source of input data
Single household	4.13	1	PV array, PbA	Household demand time-series, PV generation time-series
Single non-domestic load	61.9 - 1,464	15 (individually, one for each load)	PV, wind turbine, all battery technologies	Commercial load time-series, UK weather data 2011-2014
Average household	3.73 (average of all available households)	200 (results averaged over Monte Carlo simulation)	PV, wind turbine with 10m hub height, all battery technologies	Household demand time-series, UK weather data 2011-2014
Average networked load	7.46 - 74.59 (2 - 20 households)	12-100 depending on network size	PV, wind turbine, all battery technologies, PHS for largest communities	Household demand time-series, UK weather data 2011-2014
Stocksbridge case study	21,500 domestic + 5.5 commercial	1 (inputs are pre-defined due to location)	PV, wind turbine, all battery technologies, PHS	National demand time-series for domestic and commercial loads, school and leisure centre demand time-series, Sheffield PV time-series, Bradfield wind speed data

Table 3.5: All tested energy scenarios

used to examine the sensitivity of results to data accuracy, which necessitated the use of PV generation data from the Hicks building solar array. There was no available wind power data available at temporal resolution smaller than 10 minutes, so unfortunately the highest resolution results were only available for PV systems. The limited volume of generation data at higher resolutions was was the reason for not using a larger sample of generation data.

3.3.3 Averaging using Monte Carlo sampling

It was desired to return results that were representative of an average system in the UK, given the usual lack of hourly household demand time-series, and the inability of forecasting an entire year of generation. The model and its results are characterised by the variability/intermittency in demand and generation time-series, so the inputs could not be aggregated, as this would simulate a network of energy demand and generation with increased security. Thus instead multiple samples of energy systems were simulated, individually measured for their sustainability and security, and then these measurements were averaged over the samples with knowledge of their statistical characteristics. Choice of energy input data varied depending on the particular system that was being modelled. When modelling a single or networked household system with wind and/or solar generation, and battery storage, it was assumed that the household(s) would have a similar demand pattern year-to-year, while solar and wind availability would change between years. Demand data from households with standard and Econ 7 tariffs were mixed in the samples, as there was less difference between their demand profiles than would be expected (see section 3.2.3). The process for building the demand and generation time-series is shown in figure 3.15, for a fixed proportion of solar and wind production.

The process is nearly identical for systems with more than one household, quantity n up to 20 households, the only difference being that the demand time-series is created from n randomly chosen household demand time-series. This creates a new time-series that is again repeated over 25 years. Locating weather stations within $50km$ of the initial station required conversion from latitude and longitude to km. The following formula of the Spherical Law of Cosines was used to find distance d between two points with latitude ϕ_1 and ϕ_2, and longitude θ_1 and θ_2 (unit radians):

$$d = 6371 \arccos(\sin\phi_1 \cdot \sin\phi_2 + \cos\phi_1 \cdot \cos\phi_2 \cdot \cos(\theta_1 - \theta_2)) \tag{3.7}$$

Finding weather stations within $50km$ of any random weather station did not necessarily always return solar irradiance data, due to there being less available time-series, so the available area was widened to within 2 degrees latitude. The correlation between latitude and solar irradiance is high (see figure 3.5) so this would still return a pool of solar data that is similar in annual irradiance.

A similar procedure was followed for non-domestic demand, but different demand sources were separated out due to their much wider range of demand sizes and profile shapes. This procedure is outlined in figure 3.16. Given the considerable range of annual non-domestic demands from less than $100MWh$ to nearly $1500MWh$, results were not averaged between different loads, and battery capacity was sized to fit the demand. This was done in the model by dividing annual demand by average household demand, and taking this result as the number of batteries in the system, where each battery has the usual range of $0 - 50kWh$ storage.

All these results were collated using a biharmonic surface fit to find representative results with respect to PV and wind power capacity. A biharmonic fit does not find a polynomial equation to fit the three-dimensional data, but uses locally weighted linear regression to smooth data. The Matlab function *fit* was used with model type *biharmonic* to find this, which interpolates scattered points. The goodness of fit was measured using the R-squared

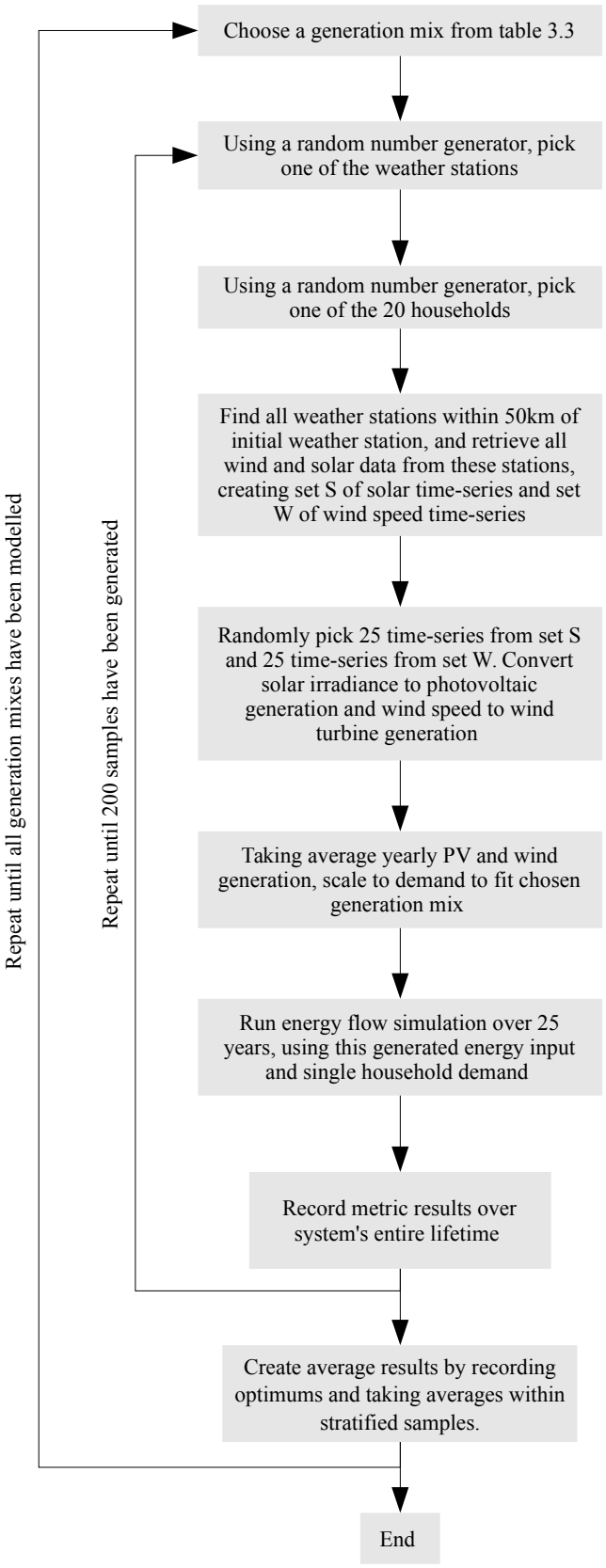

Figure 3.15: Flow chart illustrating the sampling procedure for an averaged household model. Note there are two years of demand data for each household, which are concatenated alternately to create 25 years.

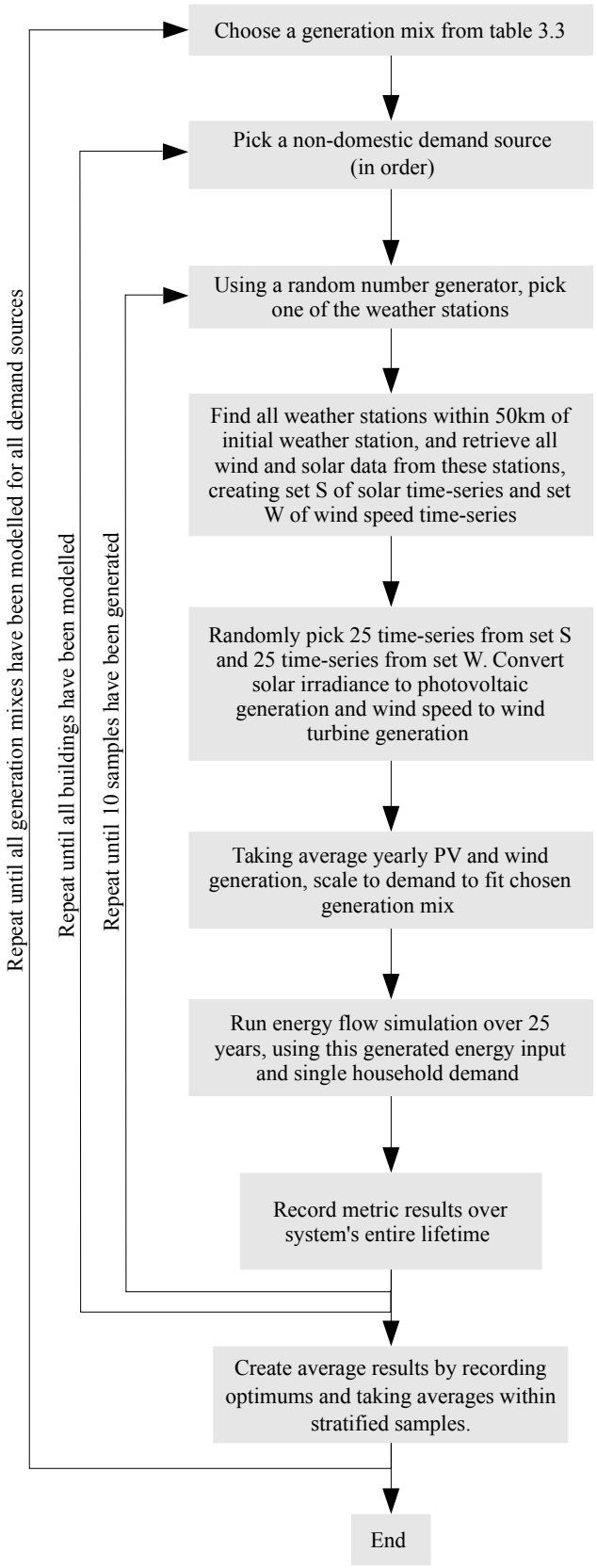

Figure 3.16: Flow chart illustrating the sampling procedure for systems with non-domestic demand.

value. Accuracy in general was improved by using a large number of system samples for all types of system scenarios.

3.3.4 Stocksbridge scenario

The largest system, the Stocksbridge case study, uses a different method of generating data inputs given both its considerably larger size and fixed location. Stocksbridge has an estimated 6,120 households and total domestic annual demand of $27GWh$, so the sample was considered large enough to use annual national demand time-series in combination with some known time-series, scaled to $27GW$h. This was repeated over the 25 years of the system lifetime. Photovoltaic and wind generation time-series were created from Sheffield data as discussed in sections 3.2.1 and 3.2.2. Different generation scenarios were modelled from a baseline of having half of the roof-space devoted to PV installations, expanding capacity through differently sized wind farms, solar farms and three types of energy storage.

3.3.5 Alternate scenarios

Two alternate scenarios were tested using the single household model: where a domestic heat pump was added to the load, and where hydrogen was used to store excess generation. These were simulated using limited sources of data, which is why they were not expanded to be part of the main results. However, these limited investigations allow for a wider evaluation of the technology available, and a long-term view of the potential energy transition.

3.4 Analysis and results interpretation

There were multiple lines of inquiry for the analysis: finding suitable metrics for energy security and sustainability, choosing optimisation methods given certain metrics, sensitivity analysis on certain error-prone variables, and analysis of the initial data to ensure that results were representative of realistic energy systems.

In order to optimise the systems, metrics were required to measure and judge chosen characteristics of the systems. For reasons outlined in the introduction - chiefly pertaining to longevity and performance of the energy systems - sustainability and security were chosen to be the most important system values. However, there is still a wide range of metrics available to measure and illustrate these, as previously discussed in the literature review.

3.4.1 Energy security metrics

Two metrics measuring energy security/reliability were chosen for implementation, being the most applicable and commonly used in the literature, and in electrical engineering practice. Both metrics LOLP and EIR provide a measurement of the periods that the system cannot meet demand, the former measuring the length of those time-periods, and the latter measuring the energy shortfall during those periods.

Loss of Load Probability

The most common metric used for energy system reliability evaluation, $LOLP$ (Loss of Load Probability) is a dimensionless ratio that gives the proportion of time that the system suffers from loss of load:

$$LOLP(n, c) = \frac{LOLH(n, c)}{H} \tag{3.8}$$

for a system with energy storage of size n and generation capacity c, run over a period lasting H hours, where $LOLH(n,c)$ refers to the LOLH (loss of load hours - number of hours of underproduction) result. $LOLP$ is most relevant to systems that are disconnected from the grid, and therefore have to completely meet demand, but focusing on only $LOLP$ can risk unnecessary energy wastage when generation capacity is oversized in order to meet demand. Lower levels of $LOLP$ indicate higher security.

$LOLP$ for a system's full lifetime was calculated from the model's output time-series in Matlab as so:

```
>> for year=1:lifetime
>> --run model--
>> for k=1:lenSB
>> lolprun(year,k) = length(find(imp(k,:)>0))./l_gen;
>> end
>> end
>> lolp = mean(lolprun);
```

where *l_gen* is the length of each year's time-series (leap years are ignored), *imp* is the time-series of unmet (imported) demand (created by the model), and *lenSB* is the length of the battery capacity array.

Energy index of reliability

There was some concern that measuring loss of load periods by their duration rather than energy generation deficit may lead to inaccurate results, particularly when the time intervals are long, as an interval with a small generation deficit is judged to be as equally underproducing as an interval with zero generation and large demand. To see how much of a difference this makes, metrics that measure the energy dimension rather than time were introduced. To measure underproduction, the energy index of reliability EIR is defined as:

$$EIR = 1 - \frac{EENS(n,c)}{D} \tag{3.9}$$

where $EENS(n,c)$ denotes the needed energy not supplied over its lifetime where the system has energy storage size n and generation capacity c, and D denotes the total electricity demand of the system over its lifetime. EIR ranges from 0 to 1. EIR therefore shows the proportion of energy demand not supplied over the system's lifetime.

3.4.2 Sustainability metrics

As was outlined in the introduction, embodied energy was chosen as the measure of the sustainability of the technology, being a cost-effective assessment of environmental impact [162]. The level of embodied energy is correlated strongly with GHG emissions [27] and allows for a dimensionally consistent analysis with energy generation [179]. Energy return on investment ($EROI$) is a dimensionless net energy analysis metric that has been applied to a broad range of energy sources [214], such as fossil fuels [215], biofuels and renewable energy [27]. The $EROI$ of an energy source is defined as the ratio of the generated energy to the lifecycle energy costs [216].

If all energy is normalised to primary energy - i.e. the amount of energy currently required to generate the equivalent quantity of electrical energy - using the coefficient $\eta_G = 0.31$ to represent the average efficiency of the EU-25 grid, [166] then a renewable energy device with lifetime L, total energy generation without curtailment E_{out} = total system energy output over

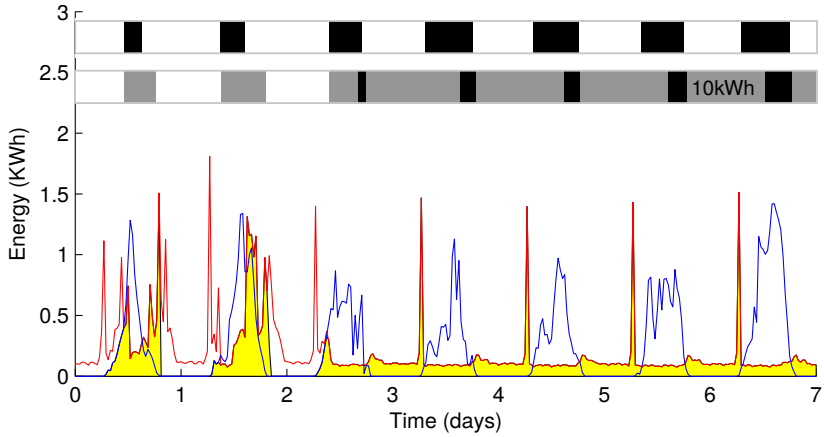

Figure 3.17: Demonstration of security metrics: bars at top show periods of under- (white) and overproduction (black) periods for a system without storage (upper) and $10kWh$ PbA battery storage (lower). Yellow shaded area shows the locally used energy $EENS(t)$ when a $10kWh$ PbA battery is installed, matched by grey periods of system balance on the lower bar when all demand is met. For a given system of storage k, $LOLP$ calculation sums the white periods, and EIR sums the yellow area and divides by demand (area under red line).

lifetime L and lifecycle embodied energy costs EE, has an $EROI_{out}$ calculated as follows [52] [177]:

$$EROI_{out} = \frac{E_{out}}{EE \cdot \eta_G} \tag{3.10}$$

This is a net energy ratio, as energy lost in the system (e.g. in battery energy conversion inefficiencies) are not included in E_{out}. The coefficient η_G is important to preserve energy quality in the analysis; while most of the energy input for technology manufacturing is thermal, mostly derived from fossil fuels, the energy output is in the form of electricity, a high quality form of energy. In a future system powered significantly by non-thermal renewables, the value of this coefficient would increase proportionally, keeping consistently comparable $EROI$ values across time.

In $EROI_{out}$ the system boundaries are defined such that any energy generated and not lost in the system is counted as E_{out}. However, in certain systems such as grid-connected PV in a network with high solar penetration, surplus generation is of limited use, and thus counting it as part of E_{out} will give a misleadingly high $EROI$ result. Therefore in systems where overproduction has to be curtailed, $EROI_{used}$ can be used instead, where:

$$EROI_{used} = \frac{EENS}{EE \cdot \eta_G} \tag{3.11}$$

and $EENS$ = used energy, i.e system demand that is met by local generation. Note this was previously used in equation 3.9 for the security metric EIR. Then the EROI metric using E_{out} as the numerator can be redefined as $EROI_{out}$, and $EROI$ can be used as a generic term for both metrics.

The two different net energy ratios: $EROI_{out}$ and $EROI_{used}$, can be applied to different types of energy systems where different outcomes are desired.

The embodied energy values used in the E_{in} calculation are shown in table 3.6. Values for PV modules are reduced to account for the separate calculation of inverter EE, which is

Component	Embodied Energy	Range		Units
		Min	Max	
PV module (mono-Si)	1,614**	474	3,098	kWh/m^2
PV module (multi-Si)	1,063**	280	1,842	kWh/m^2
Wind turbine	$-0.8P + 3081$**	-*	-	kWh/kW_{cap}
Lead-acid battery	321 [137]	200	500	kWh/kWh_{cap}
Lithium-ion battery	454 [137]	300	600	kWh/kWh_{cap}
NaS battery	488 [137]	370	630	kWh/kWh_{cap}
ZnBr battery	505 [137]	450	550	kWh/kWh_{cap}
VRB battery	694 [137]	600	850	kWh/kWh_{cap}
Pumped hydro storage	$104C + 0.0068E_{del}^2$ [123]	-	-	kWh
Inverter	$(-36.8\log(P)+256)P$	-	-	kWh/kW_{cap}
Charge regulator	$(-36.8\log(P)+256)P$	-	-	kWh/kW_{cap}
Heat pump (3.5kW)	$2130kWh$	-	-	kWh
Hydrogen electrolyser	756	-	-	kWh/kW
Hydrogen fuel cell (10kW)	36340	-	-	kWh
Hydrogen cylinder	644	-	-	kWh

Table 3.6: Embodied energy for all system components. Note P = power capacity, C = storage capacity, E_{del} = energy delivered over lifetime.
*Range was not determined for all wind turbine capacities due to lack of data, but section 5.5 discusses range for micro wind turbines.
**Not including inverter.

addressed in the next section. Range of values is taken either from the literature or (in the case of PV and wind) from minimum and maximum values used when finding the mean in section 2.4.6. Note that pumped hydro storage has a lifetime of 60 years [123] but this is not accounted for in the value chosen for analysis, so the final $EROI_{out}$ values of pumped hydro will be slightly higher than if the system was used for its full 60 year lifespan. This approach was taken because it could not be confirmed that a theoretical pumped hydro system would remain in use after the generating units had reached the end of their lives.

Inverter embodied energy

Embodied energy for inverters and charge regulators with power rating P is calculated using the formula $EE = (-36.8\log(P) + 256)P$, as discussed in the literature review in section 2.4.6. An energy system may contain many inverters and charge regulators; namely one inverter per household PV array and one per wind turbine. The power rating of these components is unlikely to precisely match the power rating of the PV array or wind turbine, as there are limited choice of inverter sizes available. Therefore the power rating is taken as the closest available size above

or equal to power generation capacity of the particular generation technology. This discrete relationship is shown in figure 3.18, where power rating is is more precise for smaller inverters, but there is less choice of selection the larger they become.

Using these conventions alongside the established embodied energy in table 3.6 can allow us to consider how each component of an energy system contributes to its total embodied energy. Three test systems, each of total power capacity 6kW, are shown in figure 3.19 with the embodied energy of each component made clear. This demonstrates the much higher embodied energy required for PV systems in comparison to wind, but since the inverter and charge regulator sizes remain the same, this gives them more proportional embodied energy when wind is included in the system. These higher proportions show why it was important to calculate inverter embodied energy separately, considering how embodied energy cost decreases per kW as the systems grow.

3.4.3 Primary energy scaling

It was noted in the literature review that using the coefficient η_G (life-cycle energy efficiency of the electric grid) cannot simply be taken at face value. To evaluate the effects that different coefficients may have, the main results were calculated using $\eta_G = 0.31$, and then compared to secondary results using a higher value of η_G (applying to a grid with an already high penetration of RE), or simply not using η_G at all.

To estimate a reasonable value of η_G for the secondary results, first the life-cycle efficiency of a 1.2MW wind turbine was calculated, with the assumption that any high penetration of renewables in the UK would likely be from medium to large wind turbines. Indeed, the "Gone Green" scenario in the National Grid's UK Future Energy Scenarios [3] suggests by 2036 a 34% wind penetration in terms of power capacity, and 40% in terms of annual energy production, with only minimal solar input. Using average wind production from all over the UK, based on the wind speed data used in the main model and and 95% inverter efficiency, life cycle efficiency of the 1.2MW turbine was calculated to be 0.94. At 40% production penetration of the grid, the grid's life-cycle efficiency is estimated to be 56%. This is an improvement of 81%, or 25 percentage points. However this is a very rough estimate, as the National Grid scenario includes many new generation technologies such as new nuclear and carbon capture & storage, whose efficiencies and embodied energy are fairly unknown. Additionally, if utility storage is widely implemented on the grid, then new sources of inefficiencies will be introduced. This future value of η_G is much higher than the estimate of 42% given by Raugei [176] for a grid with 20% PV, as it is based on a larger penetration of wind, which itself has a more efficient lifecycle than PV.

Due to the optimisation methodology, it is not possible that a different value of η_G would change the system optimisation results; however the EROI value at those optimums would be lower, which may have an impact on their acceptability. These projections in higher η_G values were used in conjunction with estimated reductions in PV embodied energy of up to 80%. These embodied energy reductions are examined in more detail in the sensitivity analysis.

3.4.4 Metric aggregation

Installing electronic energy storage alongside the renewable energy sources will inevitably reduce $EROI$ results [208], so there needs to be a way to tell if this drop in $EROI$ is worth the increase in energy security, i.e. a method of combining or comparing the sustainability and security metrics. Any methods applied need to be able to both indicate a set of optimal systems, and to assist in describing system performance as variables are changed.

Rather than taking metric results separately or setting minimum thresholds, it was decided to combine $EROI$ and $EROI_{used}$ with the mentioned security metrics, to form two-dimensional composite indicators that can be maximised as part of an optimisation

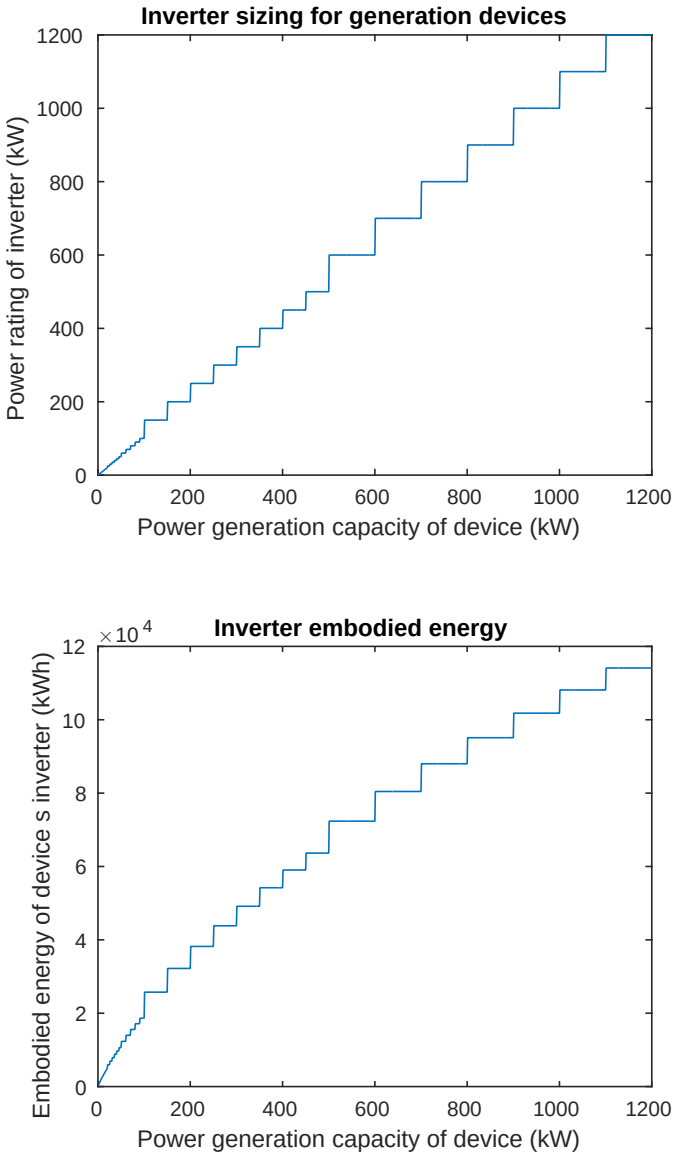

Figure 3.18: Upper graph shows convention for inverter sizing according to the device it is connected to (PV or wind turbine). Lower graph shows the embodied energy of said inverter, using a log relationship between the inverter's power rating and its embodied energy.

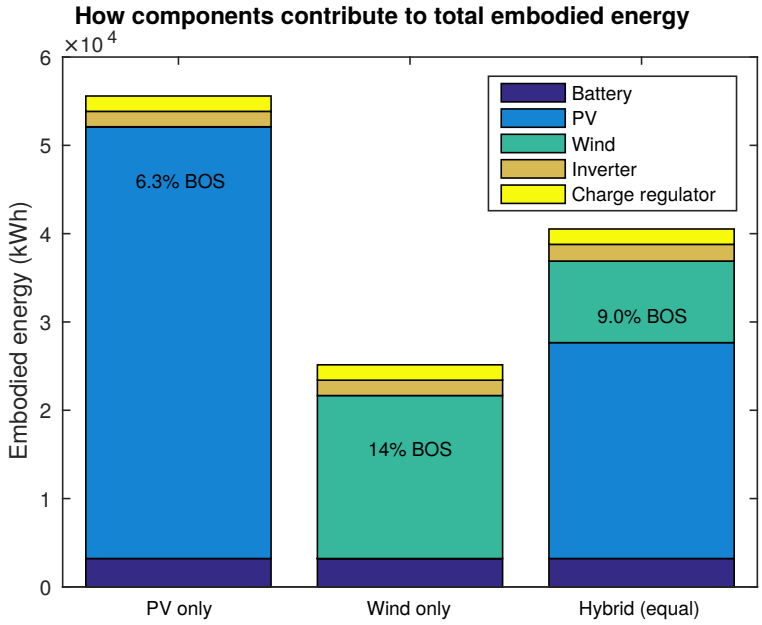

Figure 3.19: System embodied energy for three theoretical systems: 6kW PV, 6kW wind turbine, and hybrid with 3kW PV alongside a 3kW wind turbine. All systems have a 10kWh capacity PbA battery. BOS here refers to the inverter and charge regulator only.

process. These indicators are chosen with the context of the particular energy system: if the VPP exists in a grid where exporting energy to the wider grid is permissable, then $EROI$ can be used, but if all overproduction must be curtailed then $EROI_{used}$ must be used instead. This curtailment may be the result of either local connections only having limited capacity, or where the grid has such a high renewable penetration that there is no guarantee that exported electricity will be usable. These systems will therefore have a lower indicator result than those using the $EROI$ measure, as some energy output will have been lost.

When choosing how to combine the metrics, the following factors were considered: weighting, normalisation, and method of aggregation. Sustainability and security are judged to be of equal weight in the study. The normalisation for $LOLP$ is a simple subtraction from 1 to ensure that all metrics return a larger value for higher performing systems. The method of aggregation was chosen to be geometric, as recommended by the literature [217] to avoid the bias that weighted addition methods can bring, but alternative optimisation methods were investigated as shown in section 3.4.5. Composite indicators are therefore defined as follows:

$$ELOLP = EROI_{out} \cdot (1 - LOLP) \tag{3.12}$$

$$ELOLP_{used} = EROI_{used} \cdot (1 - LOLP) \tag{3.13}$$

$$EEIR = EROI_{out} \cdot EIR \tag{3.14}$$

$$EEIR_{used} = EROI_{used} \cdot EIR \tag{3.15}$$

Identifying positions of optimal values, and the behaviour of the indicators, gives insight into the performance of the systems. This method will return Pareto optimal solutions, and the theory behind this is further explained in section 4.1. Thus the composite indicators are also *objective functions*, and will be referred to as such in the results.

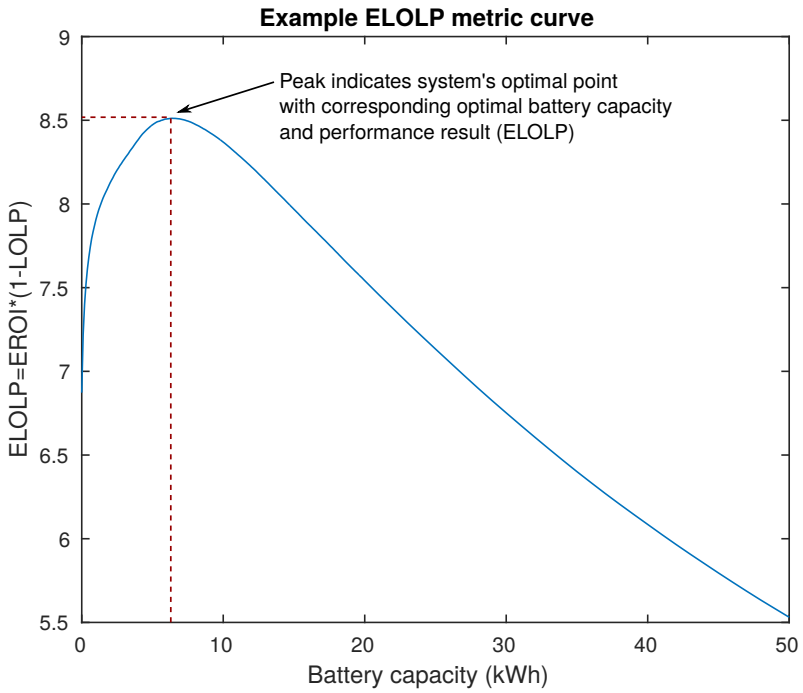

Figure 3.20: $ELOLP$ metric curve for a domestic hybrid lead-acid battery system with PV capacity $1.52kW$ and wind turbine capacity $1.2kW$. Optimal battery capacity according to $ELOLP$ is $6.4kWh$.

The results of the four indicators can be compared, showing the effect of different types of systems and/or measurement methodology. For example, $ELOLP$ and $ELOLP_{used}$, or $EEIR$ and $EEIR_{used}$, can be compared to see how generation curtailment affects the performance and value of storage, while $ELOLP$ and $EEIR$ can be compared to see whether the choice of time or energy measurement makes a difference to the results.

Difficulties may occur in optimisation if there is no peak observed when plotting the composite indicator against generation or storage capacity. This peak refers to the curve having a maximum point located at a capacity that is not the minimum or maximum of the range, e.g. in figure 3.20 the example system has a peak for $ELOLP$ where battery capacity is 6.4kWh, so the optimal battery capacity for that system is 6.4kWh. If $ELOLP$ is a constantly increasing or decreasing curve, conclusions can be more difficult to draw; this would generally require either an expansion of the range of capacities (where the curve is increasing) to identify a larger optimal point, or an improvement in resolution (when the curve is decreasing) to identify an optimal point smaller than the current resolution. However, if the curve is decreasing this may simply indicate that the optimum occurs where $x = 0$. See section 4.1 for more detail on determining how peaks occur with this method of aggregation.

3.4.5 Alternative optimisation methods

As was mentioned in section 2.1.3, the most common methods of optimisation have generally been some form of linear programming, or sometimes using multiobjective optimisation (which is often nonlinear). Linear programming is particularly applicable to economic optimisation, which can incorporate energy security requirements by setting constraints on security measurements (e.g. $LOLP < 0.05$). A similar approach could be taken with energy sustainability metrics. Alternatively multiobjective optimisation can be used to minimise with respect to security and

sustainability simultaneously. These optimisation methods are more subjective than would be expected, as the choice of weighting values or other similar inputs have a significant impact on the optimal result. As the geometric aggregation method summarised above is capable of automatically weighting the metrics, there was no reason to seek an alternative multiobjective optimisation method.

Linear programming

[What was the point of this?]

To optimise systems using linear programming, the objective function must be constructed by summing the cost functions, using appropriate weighting for all inputs. However, as $EROI$ and the security metrics are ratios on different size scales, where $EROI_{out}$ can range from having 8 or 80 as its maximum boundary, it is impractical and likely to cause unavoidable errors if fixed weights are applied. Instead, it makes more sense to choose the objective function to either the sustainability or security metric, and then to apply the complementary metric as a constraint. Constraints can be set on both underproduction and overproduction levels.

Therefore, constraints were set on energy security levels, and the $EROI_{out}$ value was maximised as follows where EEG is excess energy generation (proportion of generated energy not used by local system):

$$\begin{aligned} &\text{maximise } EROI_{out}(S) \\ &\text{where } EIR(S) > \alpha \\ &\text{and } EEG(S) > \beta \end{aligned}$$

This ensures a result where underproduction and overproduction are restricted, and the choice of their constraints α and β have a large impact on the results. The constraints must be carefully chosen to ensure that an optimum exists. The metrics EIR and EEG have been chosen because of EIR's greater accuracy than $LOLP$. Preliminary results also suggest that this may lead to smaller optimal battery capacities due to this increase in accuracy.

3.4.6 Sensitivity analysis

The metrics $EROI_{out}$ and $EROI_{used}$ are subject to certain errors, being based upon calculations of embodied energy that are highly sensitive to multiple variables. Therefore it was considered necessary to carry out uncertainty analysis so that the difference between systems could be well understood in terms of their statistical significance, and that the results are not made worthless by the errors involved in LCA data.

In particular, embodied energy is expected to decline in the future due to increased efficiency of manufacturing and alternative cheaper materials (for example organic solar cells) [186]. These are incidentally caused by economic pressures, but this process can be accelerated if reduction in energy use is specifically targeted by governmental policy, such as reducing transportation distances and using more energy-efficient manufacturing processes that are not necessary economically beneficial. Adversely, there is some dispute in life-cycle analysis about which input processes should be included. For example, energy use of the workers involved in manufacturing (such as transport to work) is not currently included, and other energy inputs may be poorly recorded or underestimated. Thus it is useful to test higher embodied energy values than the ones used in the main model, in addition to the extrapolated lower values that may be available in the future.

This analysis will also be useful to understand the differences between different storage technologies, as they are characterised in the model by their embodied energy values, energy

conversion efficiency, depth of discharge and lifetime. These are all prone to error to a certain degree, often given by a range of values in the literature, so carrying out a secondary sensitivity analysis with respect to their efficiency will provide more understanding into how choice of storage technology affects the system's performance. Lifetime uncertainty was not studied directly because it only affects the embodied energy (as the embodied energy is calculated over the system's entire lifetime rather than just the battery's lifetime), which is already addressed. However variation in the lifetime may result in a wider range of possible embodied energy, and it should be considered that using a greater depth of discharge with batteries will likely decrease their lifetime.

Chapter 4

Methodology validation and preliminary results

This chapter on methodology validation sets some required initial results. These show that the methods of analysis and energy system simulation are robust and working as expected. Section 4.4 shows the impact of model resolution on results using a single household load, and presents how the objective functions behave for a single system.

4.1 Optimisation methodology validation

When combining two metrics to create a objective function, it is useful to know if this method will actually produce an optimal result in practice: i.e. if an observed peak is a Pareto optimal point, and whether it is a global as well as local optimum. To ensure that this was the case, mathematical analysis was performed on generalised curves that share the fundamental properties of the investigated metrics. It can be assumed that these curves are smooth beause the analysis takes place over the entire lifetime of the systems.

Let $f(x) = EROI(x)$ where x can be any quantifiable system value that can be classified as a security intervention, most likely storage or generation capacity, and EROI can refer to either $EROI_{out}$ or $EROI_{used}$. EROI will either be a decreasing curve with no maximum ($f'(x) < 0$), or an initially increasing curve with maximum point $EROI = E_{max}$ at $x = P$ and decreasing for $x > P$. These are indicated by the curves $f_1(x)$ and $f_2(x)$ in figure 4.1. No optimal results will be accepted for $f(x) < 1$.

Let $g(x)$ be a security metric normalised such that larger values indicate better security, so can be $1 - LOLP$ or EIR. The function $g(x)$ will be an increasing function ($g'(x) > 0$), because otherwise the technological intervention implied by increasing x is unnecessary. In a case where $g(x)$ has a decreasing section for some values of x, the system can be evaluated by either taking the lowest storage capacity size, or by only looking at the sections of g where $g'(x) > 0$. For all values of x, $g(x) \leq 1$ and $g''(x) < 0$ because security interventions typically have diminishing returns.

To carry out an optimisation study, we know that increasing x will eventually decrease sustainability due to oversizing of the system or cost of the intervention, and we are only interested in situations where increasing x will increase security, because otherwise the security intervention is useless. Therefore for a system where small values of x improve security more than sustainability is reduced, a Pareto optimal solution can be found at the limit where a small increase in x will decrease sustainability more than security is increased. These changes in sustainability and security must be weighted appropriately, with the most sensible option being to express the change in terms of a ratio to the total sustainability or security.

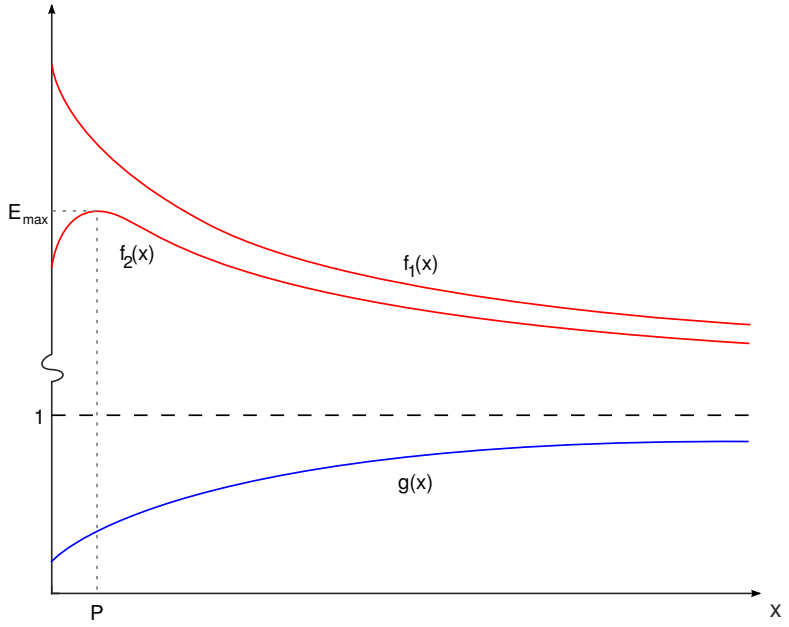

Figure 4.1: Plot of generic sustainability metric f (with alternate versions f_1 representing $EROI_{out}$ and f_2 representing $EROI_{used}$) and security metric g.

In terms of the functions f and g, a Pareto optimal point at $x = Q$ exists where Q is the largest x for which

$$-\frac{f'(x)}{f(x)} \leq \frac{g'(x)}{g(x)} \tag{4.1}$$

where the left-hand side is increasing and the right-hand side is decreasing, i.e. $-{}^{f'(Q)}/_{f(Q)} = {}^{g'(Q)}/_{g(Q)}$ and $-{}^{f'(x)}/_{f(x)} > {}^{g'(x)}/_{g(x)}$ for all $x > Q$. Rearranging equation 4.1 gives

$$f'(x)g(x) + f(x)g'(x) \geq 0 \tag{4.2}$$

The left hand side of this is simply $(fg)'(x)$, so $x = Q$ where $(fg)'(x) = 0$, i.e. the Pareto optimal exists at the peak of $fg(x)$, as shown in figure 4.2. Note that when $f(x)$ has a peak at $x = P$, $f'(x) > 0$ for all $x < P$, so $(fg)'(x) > 0$ for all $x < P$ also. Therefore the optimal exists where $x > P$, which makes sense. In the opposite situation where the decrease in sustainability is very high for even small x, it may be possible to see a curve with no peak, shown as the trivial result $(fg)_0(x)$ in figure 4.2. This can also occur when the gradient of $g(x)$ is small for all x, i.e. when increasing x makes little appreciable difference to the security. For such systems, the optimum is at $x = 0$. This result cannot exist for systems with the $f_2(x)$ curve or when $g(0) = 0$, but it will likely be a rare case regardless of the metrics chosen. If in practice a large number of systems return the trivial case, this is either an indictment of the cost of the security intervention, or of the metrics chosen for the analysis.

To ensure that finding the peak of $fg(x)$ is a robust method of optimisation, the local optimum must also be a global optimum; i.e. this peak must be either the only peak, or the highest. Otherwise if a peak is observed within a certain range of x, it will be unknown if a better optimal solution exists for a larger value of x outside the range.

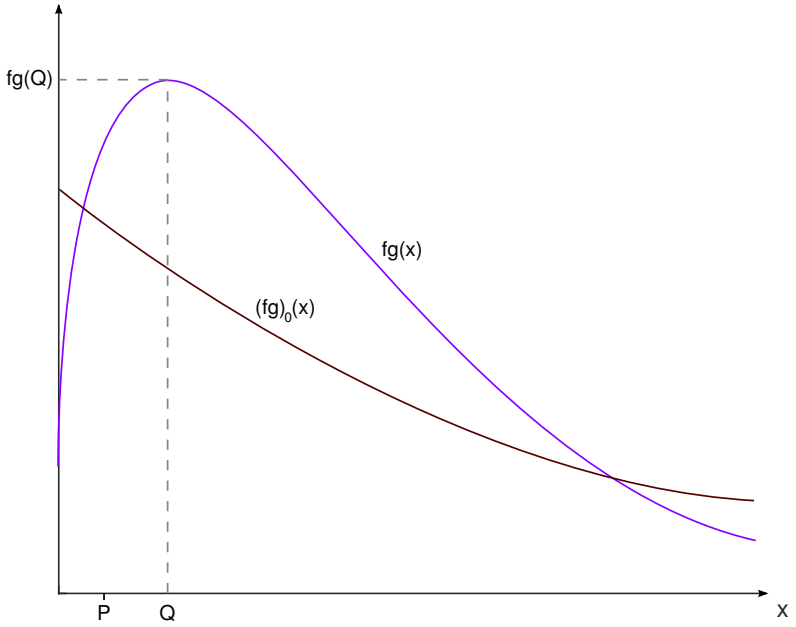

Figure 4.2: Plot of generic objective function fg, showing a peak at $x = Q$. Trivial result with no peak is also shown, where the optimum is at $x = 0$.

To show that Q is the global optimum, suppose another peak exists where $x = R > Q$. Then

$$\begin{aligned} f'(Q)g(Q) &= -f(Q)g'(Q) \\ \text{and } f'(R)g(R) &= -f(R)g'(R) \end{aligned}$$

Divide these (the denominator is by definition non-zero) to give

$$\begin{aligned} \frac{f'(Q)g(Q)}{f'(R)g(R)} &= \frac{f(Q)g'(Q)}{f(R)g'(R)} \\ \frac{f(R)g(Q)}{f(Q)g(R)} &= \frac{f'(R)g'(Q)}{f'(Q)g'(R)} \end{aligned}$$

But we know $f'(Q) < f'(R)$ and $g'(Q) > g'(R)$, so

$$\begin{aligned} \frac{f(R)g(Q)}{f(Q)g(R)} &> 1 \\ f(R)g(Q) &> f(Q)g(R) \end{aligned}$$

and since $fg(Q) > f(R)g(Q)$ and $f(Q)g(R) > fg(R)$, it follows that

$$fg(Q) > fg(R) \tag{4.3}$$

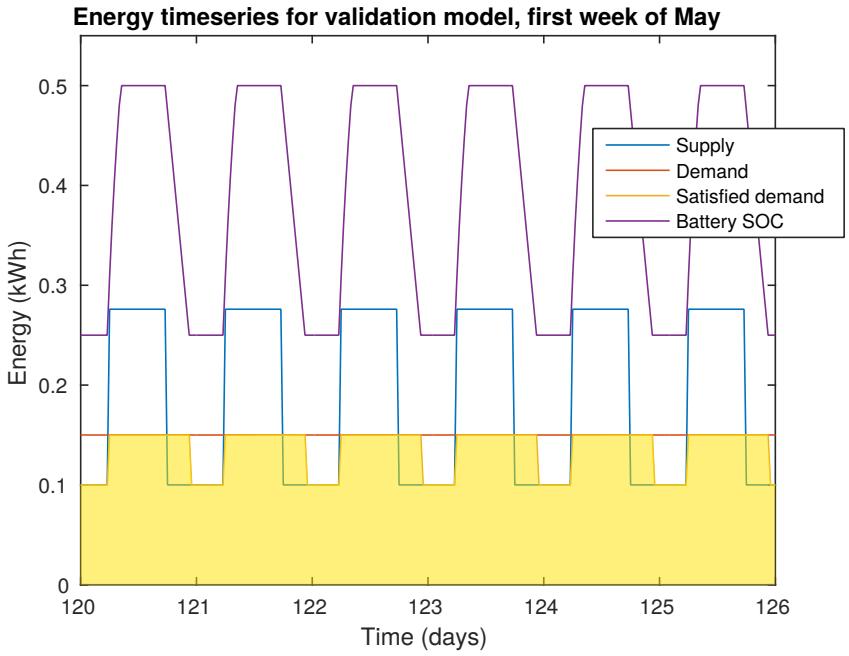

Figure 4.3: Energy time-series for the initial test of the model, with Pba battery capacity $0.5kWh$. Demand is a flat line, and the yellow fill shows how much demand is met by direct supply and battery.

so the peak at $x = Q$ is higher and therefore the global optimum. It has therefore been shown that finding the first peak of the curve fg will give the global Pareto optimal solution for the system with respect to sustainability and energy security.

When comparing optimum results from multiple systems, it is still viable to choose the highest fg results as the optimum over all those systems. However this cannot be assumed to be the global optimum, as the behaviour of f and g are more complex, dependent on some dynamic properties such as storage capacity sizing.

4.2 Model validation

Before moving to the generalised results, an initial test was carried out with simplified input data to ensure that the model was working correctly. The demand data was approximated by a flat demand of $0.15kWh$/half-hour, photovoltaic (PV) generation by a daily square wave with peak $1.75kWh$/half-hour, and wind generation by a flat supply of $0.1kWh$/half-hour. These time-series, alongside the satisfied demand and battery state of charge for a $0.5kWh$ PbA battery, are shown in figure 4.3. Here it is shown that when supply exceeds demand, the battery is charged until it is at 100% charge, then once supply drops below demand the battery discharges to meet demand with a minimum at its depth of discharge at 50%.

The degradation of PV panels and each type of battery is also shown to perform as expected. Figure 4.4 shows that while annual wind energy remains constant over the lifetime (note in the model using real data this would vary due to weather), annual solar energy drops linearly as was defined in the methodology by 0.5% each year (note this is percentage points, not cumulative). Battery degradation follows two patterns: their depth of discharge drops each year by an average of 1.35% of the original depth, modelled by the normal distribution $D \sim N(0.0135, 0.0015)$ (this appears close to linear in the graph), and they also have a rate of failure modelled by the Weibull

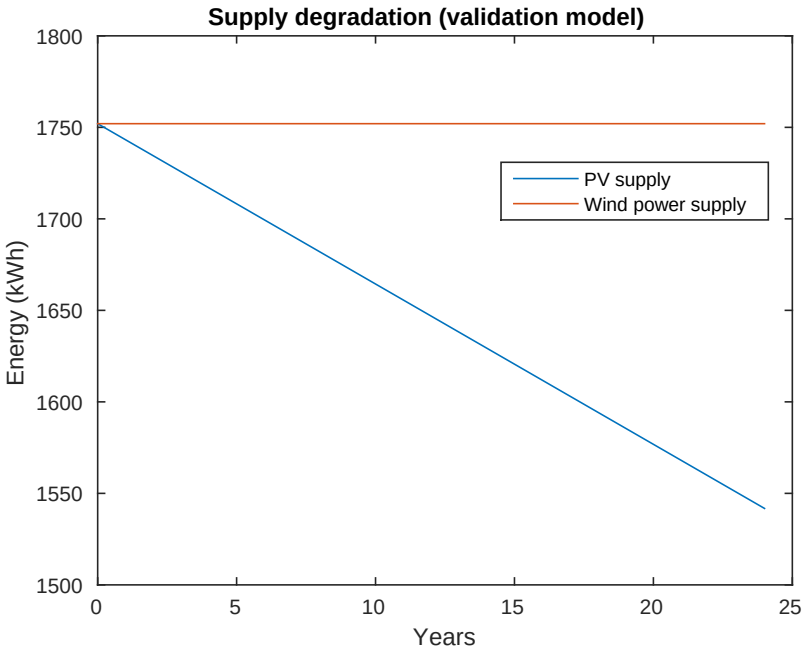

Figure 4.4: PV and wind power supply over lifetime of system, using fixed supply to show linear degradation of PV module performance ratio.

distribution as shown in the methodology in figure 3.3. Figure 4.5 shows batteries of all five types degrading their usable capacity over time and being replaced by new batteries when they either reach the end of their life or drop below 80% depth of discharge. The graphs show that lead-acid (PbA) batteries are replaced so often that their depth of discharge never reduces by much, while batteries with very long lifetimes such as vanadium redox (VRB) may be replaced before the end of their life. This gives a surprise benefit to batteries with high rate of failure, as their usable capacity suffers less degradation, however their rate of replacement is accounted for in the embodied energy values, so the cost of the system reflects this.

All components and energy flows of the model behave as required, so the model works as expected and can be used to find results for real electricity demand and weather time-series.

4.3 Time-series preliminary analysis

To get a clearer idea of how the model is affected by the variability and intermittency of the energy time-series, for both renewable generation and household demand, there was a small amount of analysis done to determine these characteristics and relate them to the system results. As this was carried out prior to the running of the model, the results are presented here.

4.3.1 Fourier transforms

Performing a Fourier transform displays the typical frequencies of the time-series, and can illustrate major differences between different types of generation and demand. It is expected that PV generation and household demand would both show daily frequency patterns, but this does not mean they match because correlation is not indicated.

Comparing wind power and solar power generation Fourier transforms in figures 4.6 and 4.7, you can see that while they both have daily frequencies, the solar diurnal pattern is very strongly

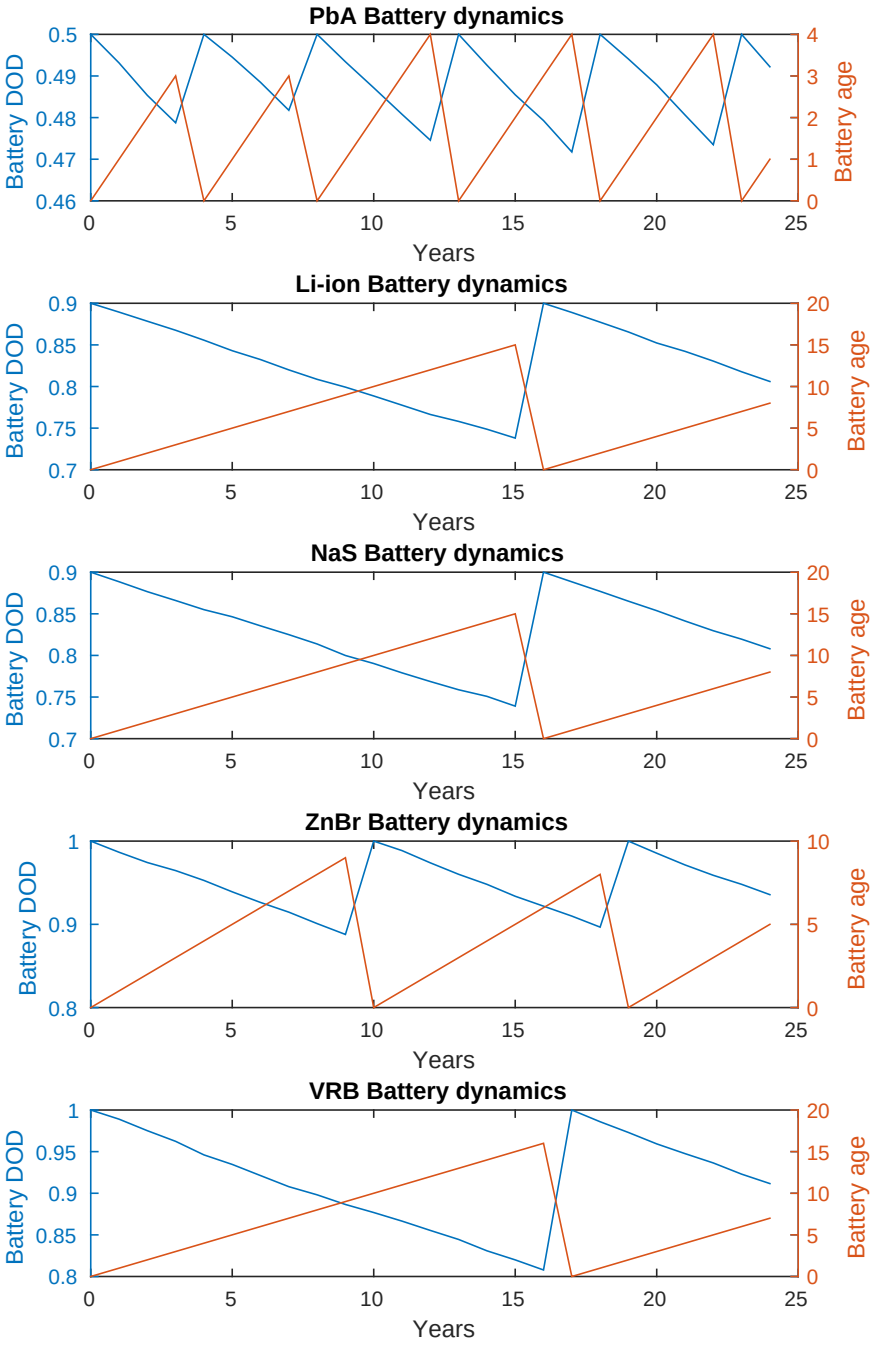

Figure 4.5: Battery degradation of depth of discharge (DOD) and rate of replacement over lifetime of system. Sharp peaks show when a battery is replaced, so age and DOD are reset.

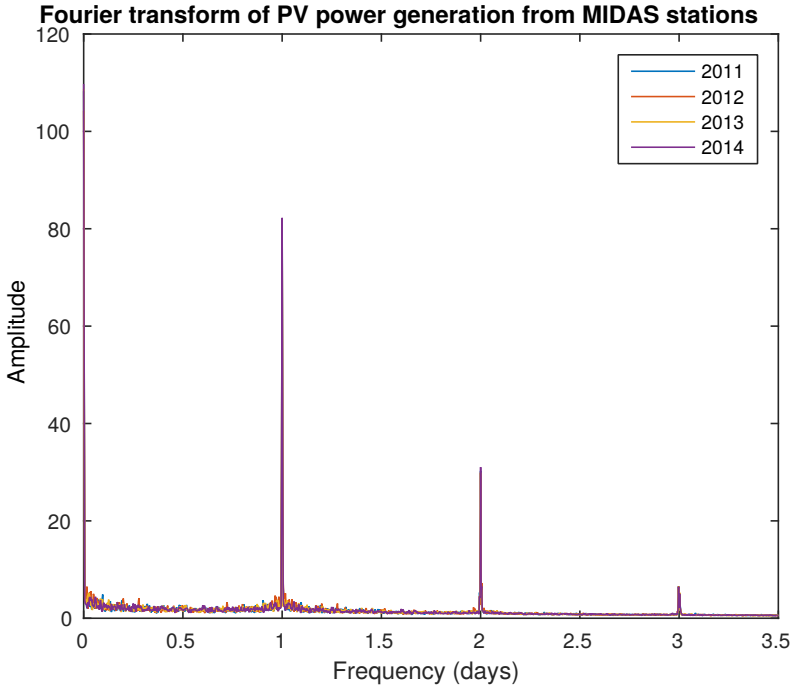

Figure 4.6: Fourier transform of PV power generation in the UK. The only major frequency is daily, but cloud cover etc is a big enough factor that frequencies of more than two days are very low.

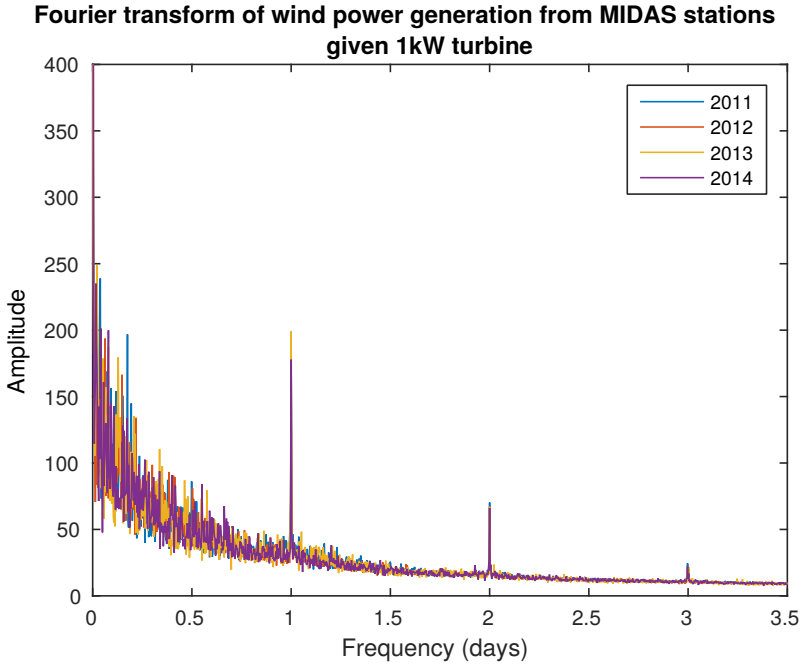

Figure 4.7: Fourier transform of wind power generation in the UK. Frequencies higher than daily ones can be observed in abundance, which decline in amplitude as frequency increases. Rather than have daily cycles like solar power, wind power at a given time has more in common with the most recent previous measurement than any other measurement. This is why it is difficult to predict wind power accurately more than 2 days in advance.

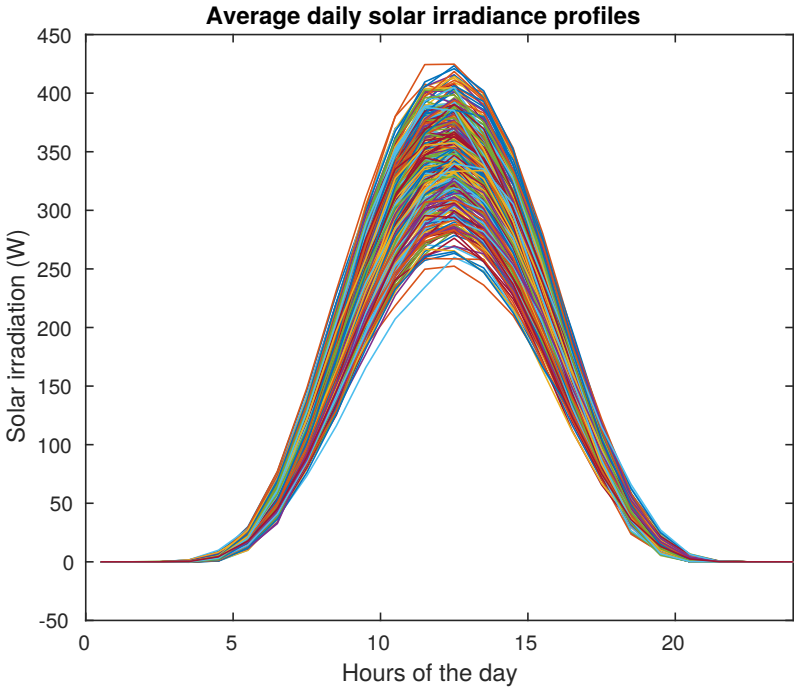

Figure 4.8: Average daily profiles of solar irradiance in UK data. A simple peak at noon is observed for all weather station locations.

pronounced, while wind power has significant patterns at an hourly or minutely scale. So while wind power is affected by day and night, this is only one of the many variables affecting wind availability. The average daily profiles of solar and wind availability are shown in figures 4.8 and 4.9. Wind speed exhibits a peak at 3pm, which is unexpected, while solar exhibits a much larger peak at noon.

The Fourier transform of domestic demand in figure 4.10 shows similar daily patterns to solar production, however smaller peaks indicate other patterns present in the data. Non-domestic demand has a similar result, shown in figure 4.11 with more non-daily frequency peaks present. There is generally more variation between non-domestic building demands, and depending on the particular building, they may not follow a standard daily routine in electricity use.

4.3.2 Integral time scale

A common metric in wind power analysis, the power integral time scale is the average time over which fluctuations are correlated [218] [211]. First we must calculate the normalised autocorrelation function R with time-lag m of energy time-series $S(t)$ with variance σ^2 and mean μ:

$$R(m) = \frac{\mathrm{E}[(S(t) - \mu)(S(t+m) - \mu)]}{\sigma^2} \tag{4.4}$$

The initial zero crossing C can be inferred from $R(m)$, which is the value of m where the line $R(m)$ first crosses the x-axis. Then the power integral time scale $PITS$ is calculated by integrating $R(m)$ between 0 and C:

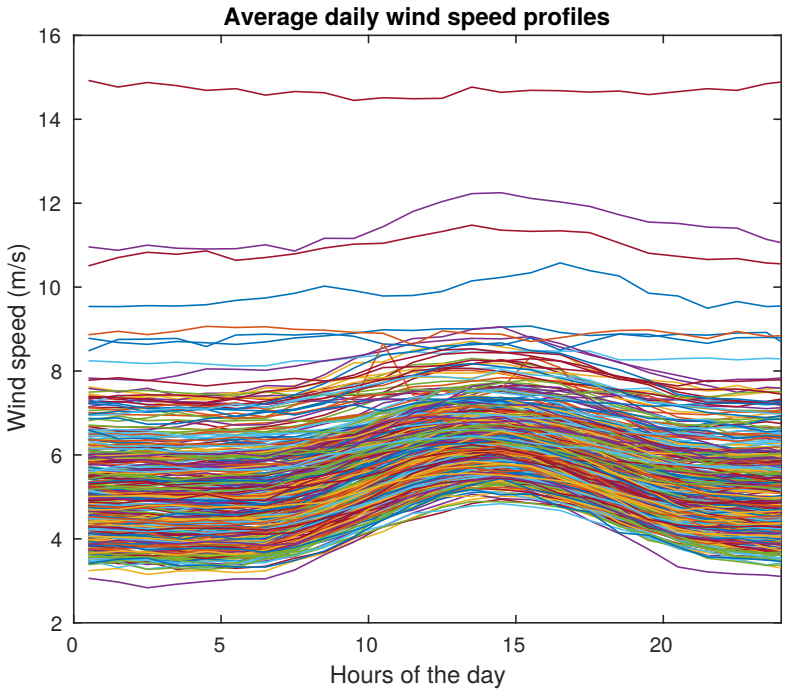

Figure 4.9: Average daily profiles of wind speed in UK data. A small peak at 3pm is observed for many of the weather stations, particularly those with low typical wind speed.

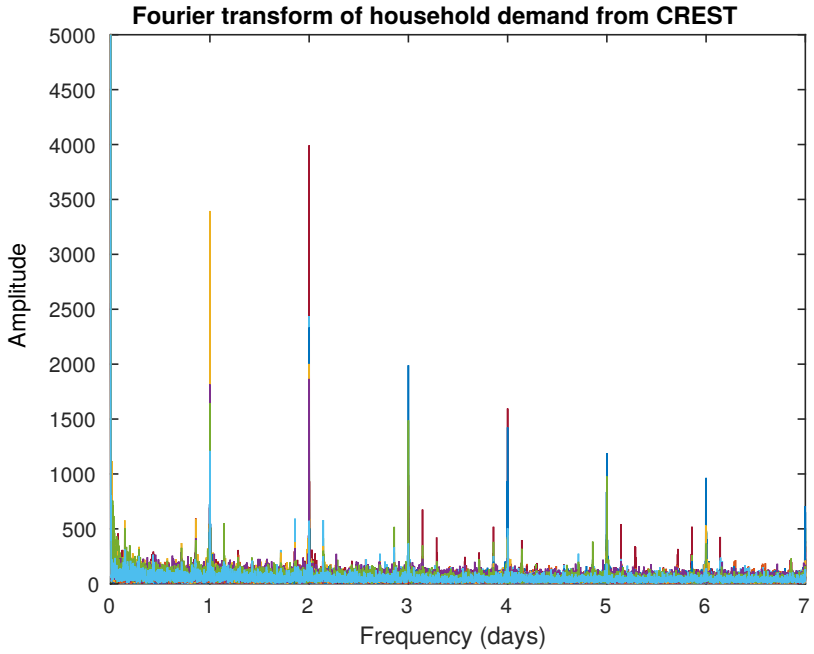

Figure 4.10: Fourier transform of sample household demand. The strongest frequencies are daily, and are also some multiple-day cycles observed, so the demand within a week is generally fairly similar. Higher frequencies are less strong, so each day experiences large changes in demand between each hour.

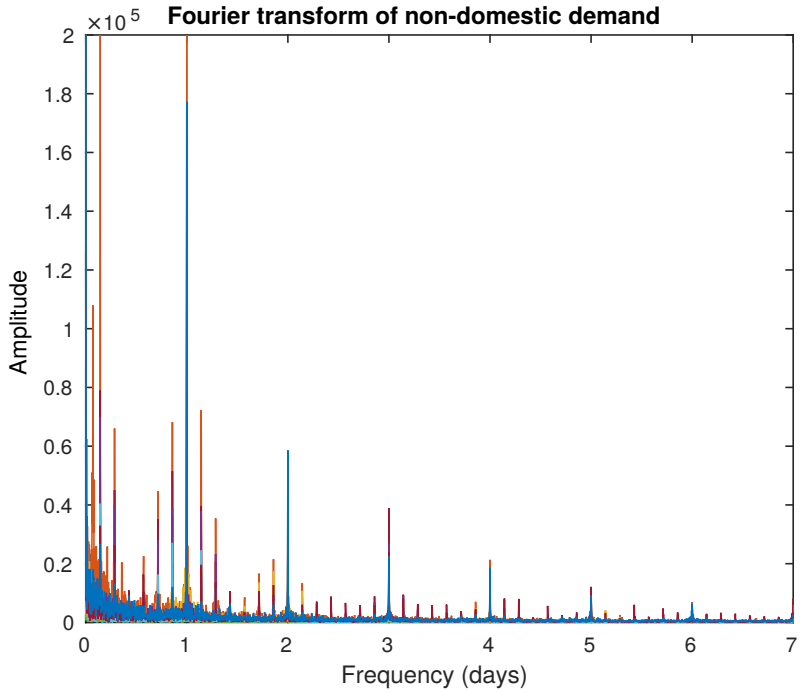

Figure 4.11: Fourier transform of sample non-domestic demand. Daily frequencies are observed as with household demand, but also hourly frequencies, showing a generally flatter demand.

$$PITS = \int_{m=0}^{C} R(m)\,\mathrm{d}m \tag{4.5}$$

Plotting the autocorrelation functions of wind and solar power production is very useful in illustrating the difference in their fluctuation behaviour and predictability, shown in figures 4.12 and 4.13 where each autocorrelation function is plotted up to their corresponding initial zero crossing. Solar power is generally more consistent, but wind power has large variability in both the initial zero crossings and also within each individual autocorrelation function. This is because wind power typically has much more variation in the lengths of productive time periods. Sometimes there will be days of constant production (i.e. near-constant wind speed at the same direction), sometimes short periods of unpredictable gusty weather, sometimes long periods of nonproduction caused by low or non-existent wind speeds. This is highly relevant in optimising wind systems for electrical energy storage, as the length of time storage is required for will be difficult to predict in most locations. However note that the smoothness and uniformity of autocorrelation in fig 4.12 does not mean that PV production is totally predictable and uniform, but merely that the diurnal pattern of solar is consistent. In fact, the larger values of integral time scale for wind production is indicative of wind power‘s predictability, and wind power production can currently be predicted with good accuracy for up to two days ahead.

As there are so many wind power time-series included, it is difficult to pick out individual values of their initial zero crossings, so their probability distributions are graphed in fig 4.14. The variation between years, and the wind range within years, really shows how variable wind power can be. Finally, the power integral time scales are shown for solar and wind in figures 4.15 and 4.16. Thus the average time that fluctuations are correlated is around 4 hours for solar power, and 10-200 hours for wind power (but clustered mainly around 20-50 hours). Note that

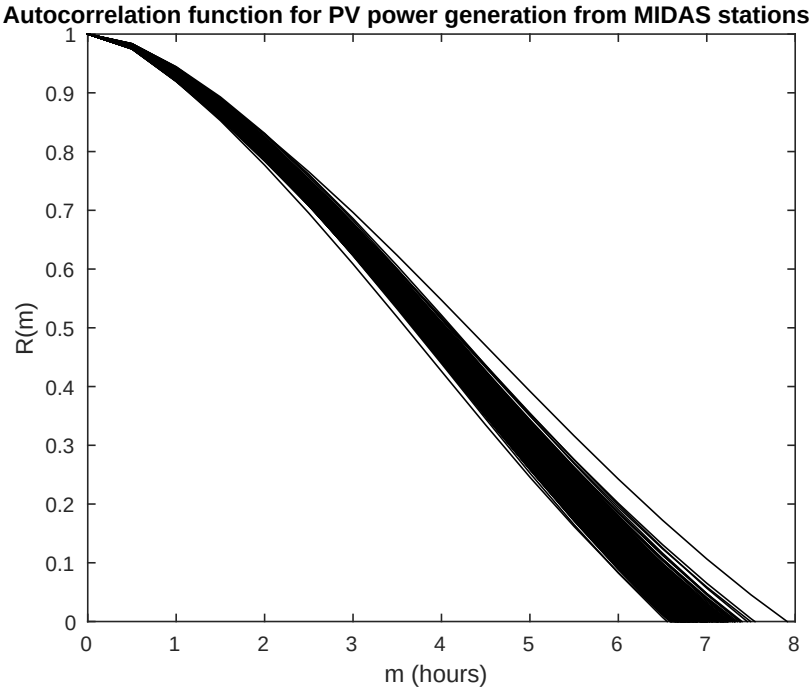

Figure 4.12: Autocorrelation of modelled PV power generation in the UK, showing a correlation scale of hours. The results of all weather stations are very similar to each other.

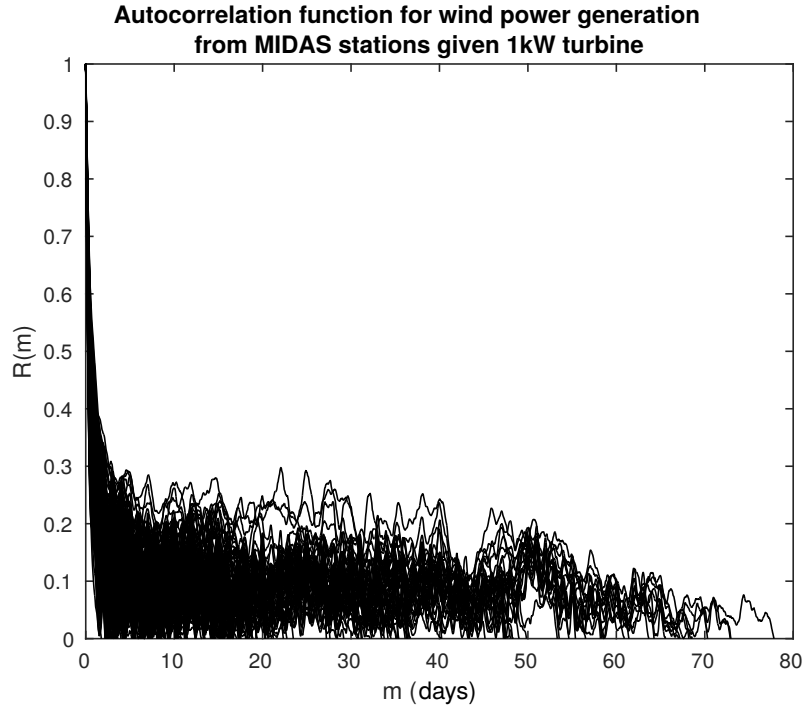

Figure 4.13: Autocorrelation of modelled wind power generation in the UK, showing a correlation scale of days, evidence of multiple-day long constant production. Results vary widely, and autocorrelation is often sinusoidal in shape due to repeating patterns in production.

this result is influenced by the fact that wind and solar data was measured hourly, which gives larger PITS results [218]. However, regardless of this, these figures show that wind typically experiences slower fluctuations than solar time-series.

The power integral time scales for demand time-series are shown in figures 4.17 and 4.18. Household demand has the fastest fluctuations with typical PITS of value 1-2 hours, while non-domestic demand has fluctuations of a similar speed to solar, at 5-10 hours. Anomalies at 34 hours show where the autocorrelation is so high between days that an extra 24 hours has been added to the time-scale, so can be considered similar to a time-scale of 10 hours. Non-domestic demand profiles shows no evidence of smoothing for larger buildings/demand, possibly because even the smallest buildings already have a relatively smooth demand.

4.3.3 Probability distribution function

Plotting the PDF of a power time-series shows the likelihood of certain levels of power being required (in the case of demand time-series) or supplied (in the case of generation time-series). Comparing solar and wind power PDFs in figures 4.19 and 4.20 shows a similar proportion of time not producing for both, but removing those instances of non-production shows that PV modules very rarely produce their top level of power in the UK, while wind turbines can be at full capacity up to 10% of the time. However there is much greater variability between locations for wind power, as was demonstrated by the results earlier in this section and by the total production in fig 3.7.

Comparing the PDFs of solar and wind to household and other building demand can give an idea of the difficulty of matching supply to demand, as a mismatched distribution of supply power can only meet demand through load shifting. Plotting the PDFs of household and non-domestic demand in figures 4.21 and 4.22 shows that the shape in power demand is quite different to that of supply, as there is a more gradual decline in the distribution as power demand increases, in contrast to the much larger proportion of time that wind or PV supply is very low or at zero. Again, this reinforces the need for time shifting of loads.

PDFs for the $1.2MW$ wind turbine show a lower proportion of time spent at low or zero production than the $1kW$ turbine; this is due to the stronger wind speeds at higher altitudes being captured by wind tubines with greater hub height.

4.3.4 Capacity factor

Capacity factor of the generation available is useful to know alongside system performance, as it gives insight into how applicable the results are to real world systems. Typical capacity factor values for PV installations in the UK are around 10%, using the data from figure 3.5, and this is matched by the low latitude results in figure 4.23. Typical capacity factor values for micro wind turbines are also around 10% [197] and this is matched by the data in figure 3.8, however some locations show very high capacity factors. Capacity factors are expected to be much higher for medium to high power wind turbines, and using the power law profile in equation 3.5 to model production by $1.2MW$ turbines shows a much more suitable range of 25-50% capacity factors, with less clustering around the lower values. These results are likely to overestimate slightly as changes in wind direction are unaccounted for, as is time required for wind turbine maintenance. Note that wind capacity factor is unaffected by latitude unlike solar capacity factor, as local climate is a bigger factor, depending on many variables such as proximity to coast, roughness of terrain etc.

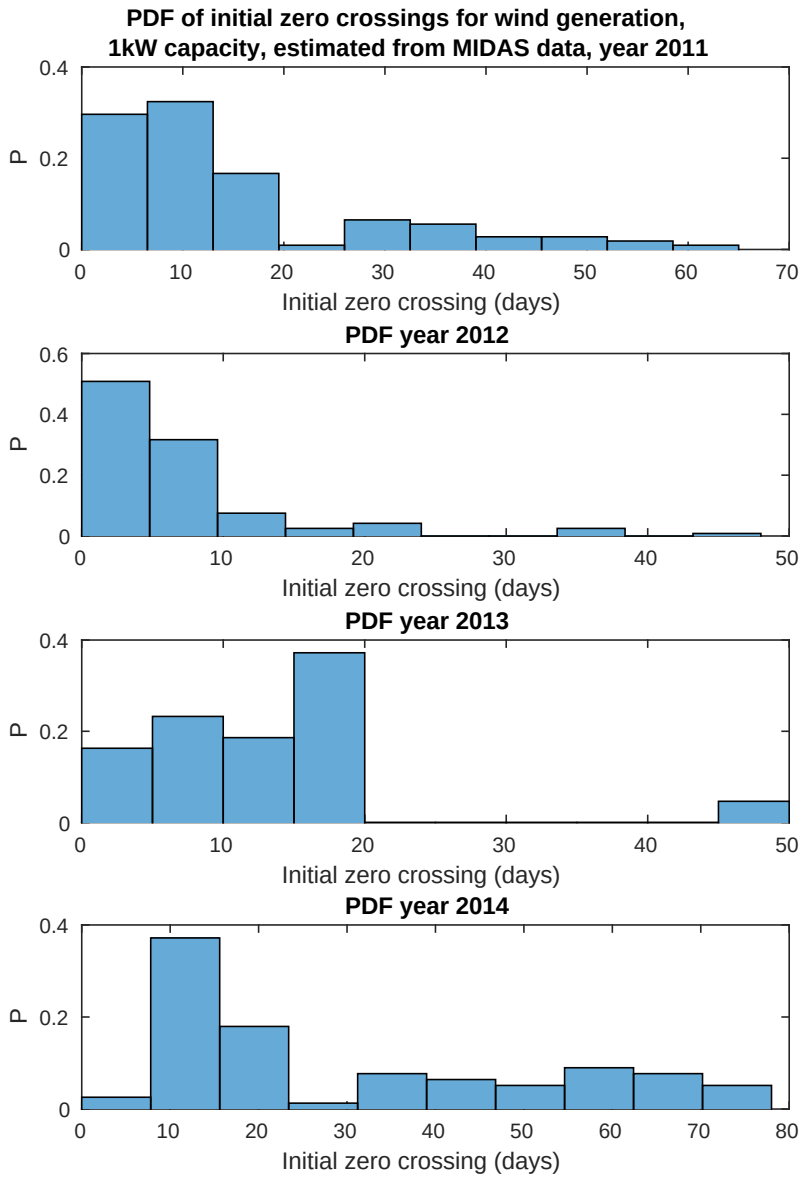

Figure 4.14: Probability distributions showing initial zero crossings of modelled wind power generation in the UK. Each year has a different distribution, but all show an initial zero crossing of around 10 days being typical.

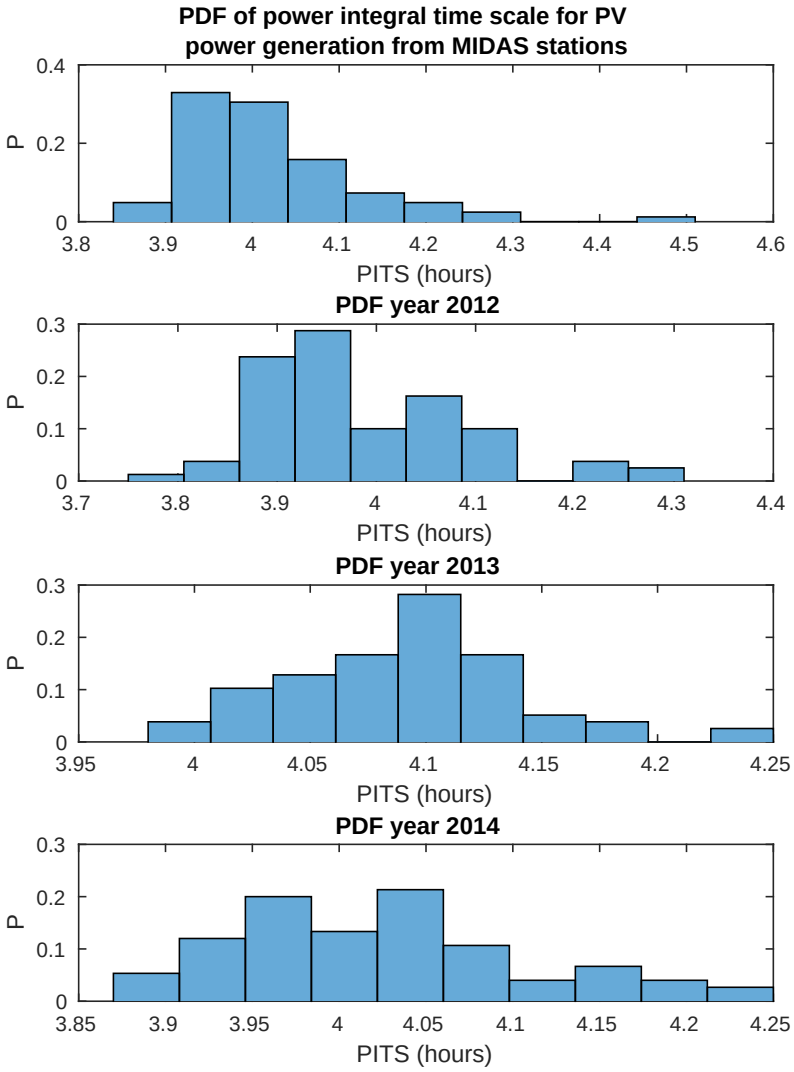

Figure 4.15: Probability distributions showing power integral time scale of modelled PV power generation in the UK. The time scale is generally around 4 hours.

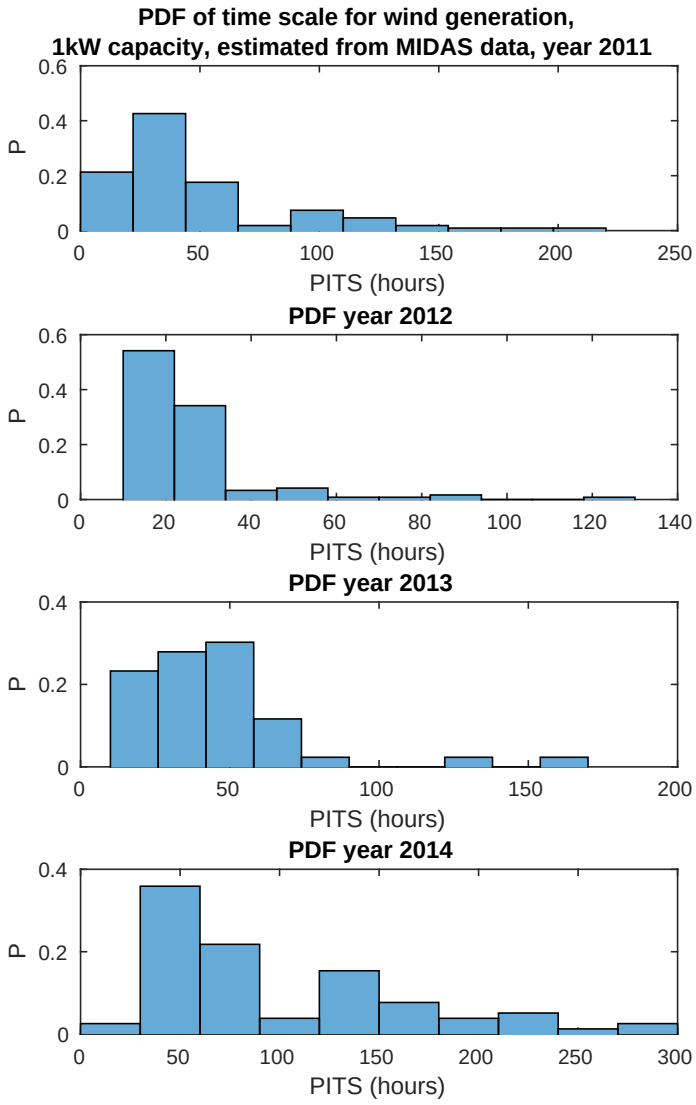

Figure 4.16: Probability distributions showing power integral time scale of modelled wind power generation in the UK. The time scale can range up to 300 hours, but below 100 hours is usually typical.

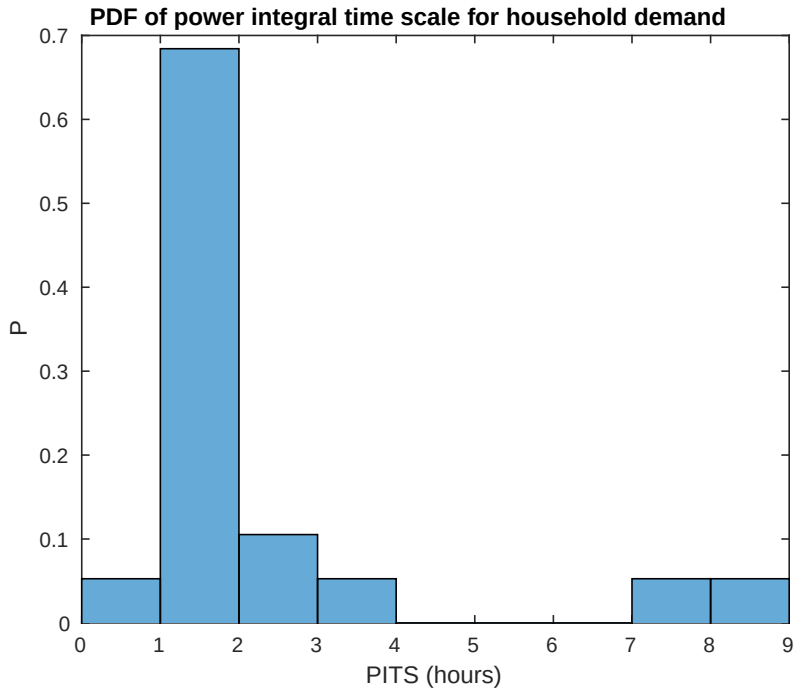

Figure 4.17: Probability distributions showing power integral time scale of sample household demand. Most have a time-scale of around 1-2 hours, showing a demand that fluctuates very quickly.

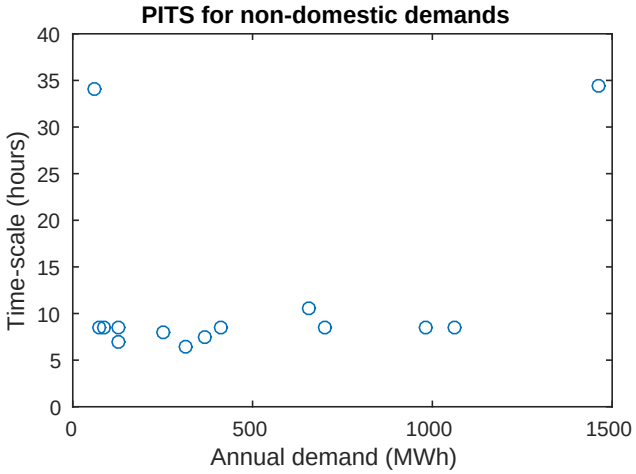

Figure 4.18: Power integral time scale of sample non-domestic demand. The longer PITS shows that non-domestic demand is more smooth and predictable than household demand, as they fluctuate over a time period of 5-10 hours (the working day) rather than hourly. Unrelated to size of annual demand, so larger loads are not necessarily smoother.

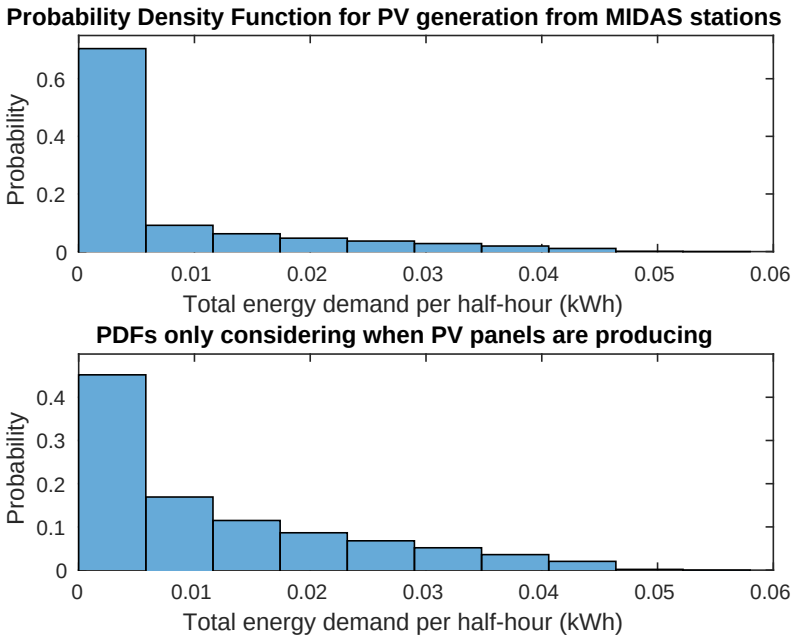

Figure 4.19: Probability distribution function of modelled PV power generation in the UK. They spend over half their time either not producing or producing at low levels.

4.4 Varying temporal resolution

There were some concerns that running the model only over half-hourly resolution would remove important fluctuation detail from the data, particularly in light of security issues such as frequency and voltage quality which take place over very short time periods from seconds to minutes. For instance, figure 4.24 shows the maximum power demand for all households where changing from a half-hourly resolution to 2-minutely can double these values per time interval. As the household demand data was accurate to a resolution of 2 minutes, and some 2-minutely PV generation data was available, some brief results were obtained from this data to analyse the PV model resolution's effect on results.

The household with its demand load closest to the national average of $4kWh$/year was chosen for this test. The system has household with average annual demand of $4,131kWh$ (peak power demand $0.1-0.2kW$ per two minutes), a $4kW_p$ PV array composed of 22 $1.3m^2$ mono-Si panels (Sharp NT-185U1 [219]) each with rated power capacity 185W at 14.2% efficiency, and varying size of PbA battery. The usual energy system model was run with these inputs over a lifetime of 30 years (estimated lifetime of PV) for different temporal resolutions of this input data to see the effect on objective function results. The resulting objective function curves are displayed in figure 4.25, and their corresponding optimal battery capacities shown in figure 4.26.

Important points from these results are that as resolution increases in accuracy, optimal battery capacity decreases when using all objective functions except possibly $EEIR$, which is mostly flat. It was concluded that as resolution increases, the model can account for smaller fluctuations in supply or demand, so the battery is utilised more for these smaller amounts, resulting in smaller optimal storage capacity. Crucially, this is the reason that the energy-based security metric EIR is mostly unaffected by the resolution, as size of fluctuations can be better detected when accounting for size of energy losses. The $ELOLP$ results are close to those of $EEIR$, however suggest a need for up to 2kWh more storage at low resolution, and up to 1kWh

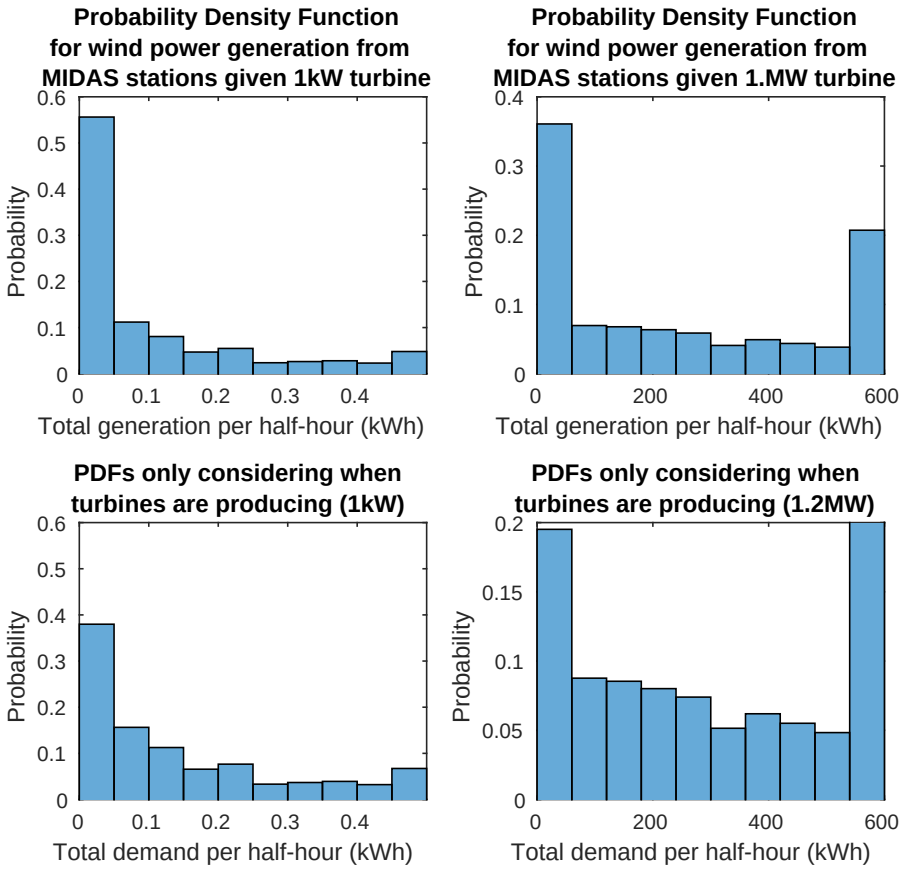

Figure 4.20: Probability distribution function of modelled wind power generation in the UK. Larger wind turbines spend more time producing at their highest levels than small ones, and also spend less time producing at low levels, but both spend about 20% of the time not producing.

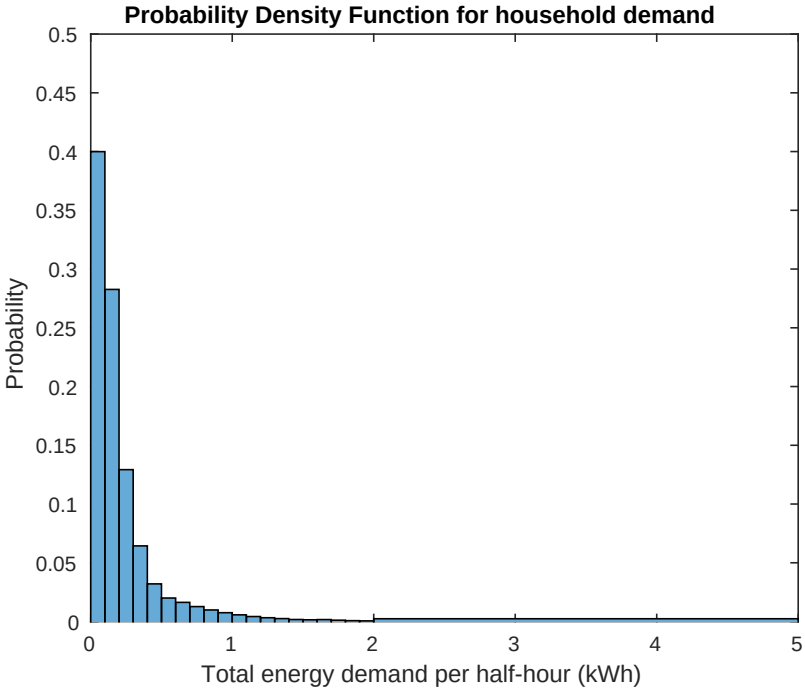

Figure 4.21: Probability distribution function of sample household energy demand. The majority of the time is spent requiring less than 0.2kWh per half-hour, but households can require up to 5kWh of demand on very rare occasions.

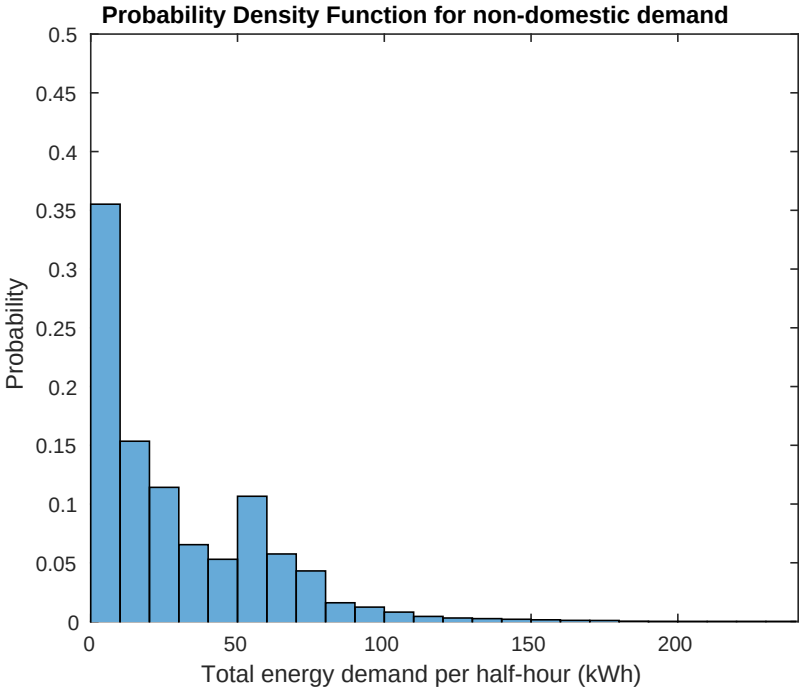

Figure 4.22: Probability distribution function of sample non-domestic energy demand. The PDF is more spread out due to variation in demand loads.

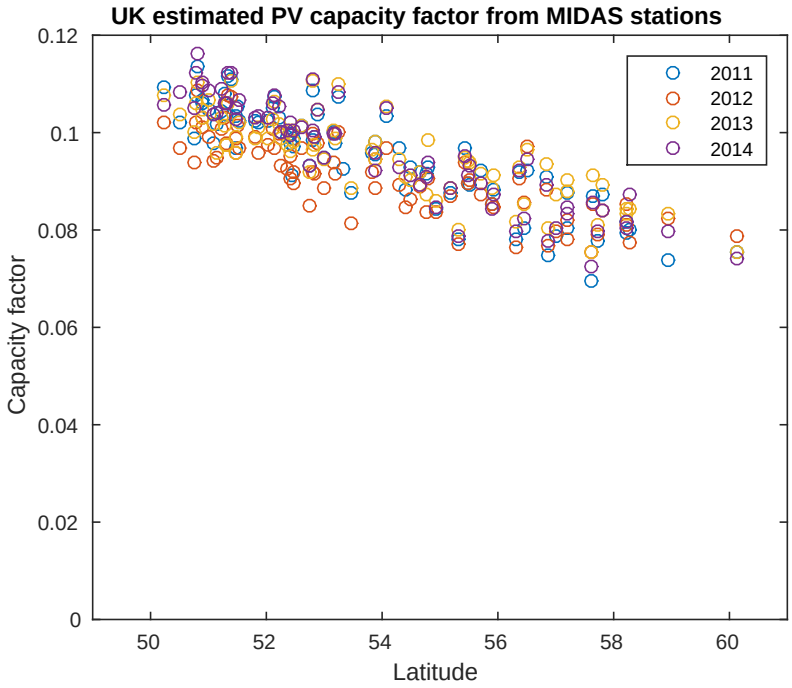

Figure 4.23: Capacity factor of modelled PV power generation in the UK. There is high negative correlation with latitude, and capacity factors range from 0.12 to 0.07.

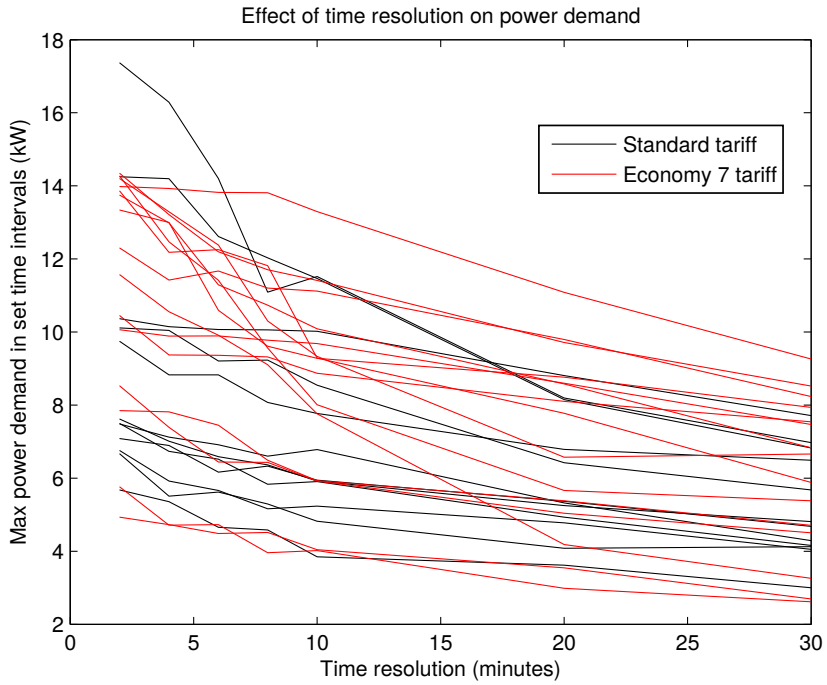

Figure 4.24: Max power draw from the available households (using years with complete data) with relation to their temporal resolution. Reducing resolution smoothes out intermittent peaks, reducing max power demands. Resolution is measured by length of time intervals rather than number of observations per hour.

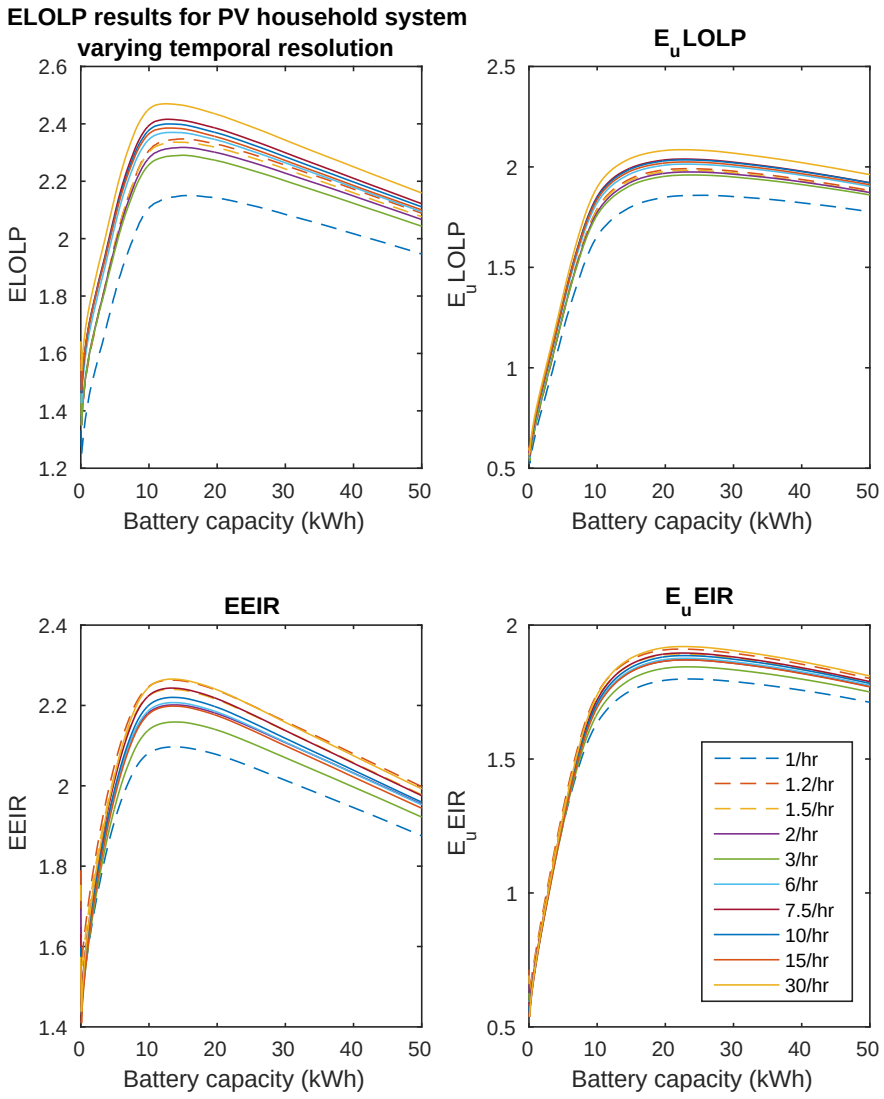

Figure 4.25: Performance results for a single household PV-only system with varying temporal resolution, where resolution is denoted by number of observations per hour. Peaks show optimal battery capacity, and while resolution makes a difference to the x and y positions of the peaks, the level of difference is dependent on the chosen objective function.

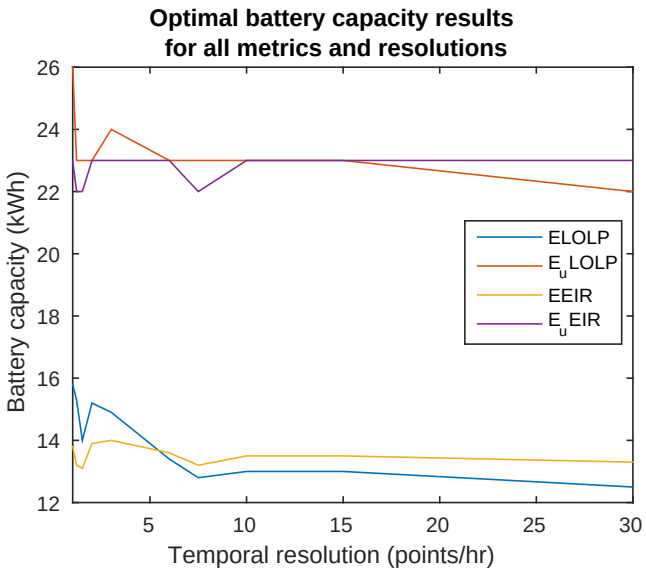

Figure 4.26: Optimal battery capacity results for a single household PV-only system with varying temporal resolution. The higher the resolution the more accurate the model is expected to be, so if there is a large change then this objective function is likely to be more prone to errors when using low resolution data. Using low resolution appears to push $LOLP$-derived optimisation towards larger batteries than necessary.

less storage capacity at high resolution. The objective functions that account for under- and overproduction (E_uLOLP and E_uEIR) give higher optimal battery capacities, but otherwise show a similar pattern with E_uLOLP decreasing while E_uEIR remains mostly static. The crossover point for both pairs of results is at 6 points per hour (10-minutely).

Looking at the curves in the top two graphs of figure 4.25, it is also apparent that as resolution improves, the system appears to have higher performance for all battery capacities. The most likely reason for this is that when resolution is poor, loss of load periods may appear longer than they actually are: e.g. if a loss of load period is only be ten minutes long, and supply is not sufficently high enough before or after that period, an entire half-hour period may be thought to suffer from loss of load if that is the minimum resolution available. The opposite could also occur: a short loss of load period may be obscured by low resolution if power supply exceeds demand afterwards, but this appears to be less likely, or only occurring for shorter periods. This order is not followed as strongly by the results that use the EIR security metric, showing that accounting for energy losses reduces this possible error. They still show some variation in curve height, but this could be due to a number of variables relating to the choice of load, as there is no logical order to the height.

These limited results suggest that LOLP-based objective functions are less accurate than EIR-based ones. This applies to both optimal battery sizing and the actual objective function values. However even when there is reason to suspect error arising from low resolution, this doesn't necessarily mean that models must be run (or real life systems monitored) at a 2-minute resolution, as there is little difference between 8-minutely resolution (7.5 points/hr) and 2-minutely results. Using EIR as the energy security metric may also reduce a great deal of this error.

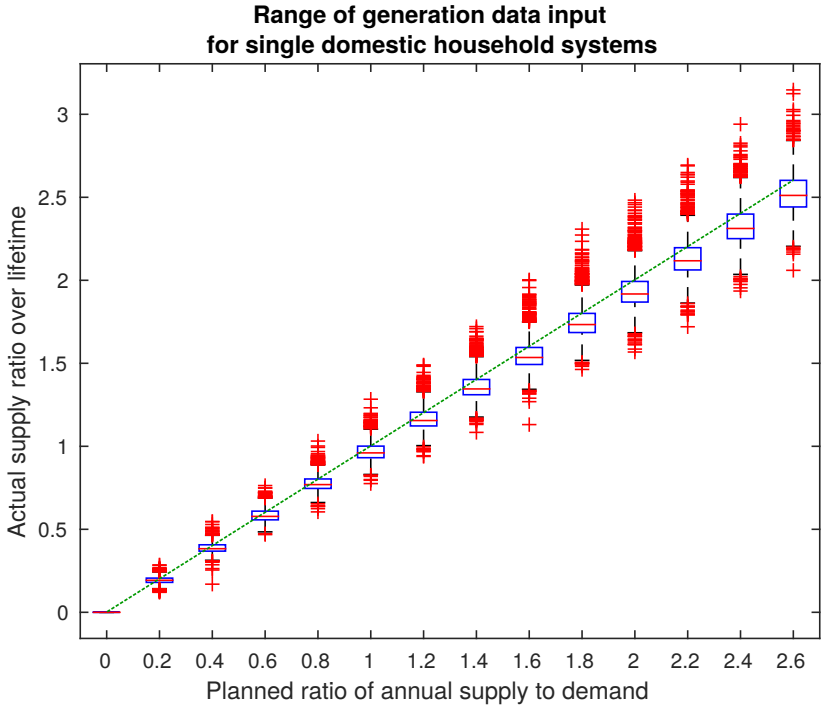

Figure 4.27: Boxplots showing discrepancy between planned annual supply (green dotted line) and actual supply (boxplots).

4.5 Power generation capacity

In the methodology it was mentioned that samples of energy systems were stratified by their annual energy production from wind power and PV, as a proportion of the household's annual energy demand. These samples were shown in table 3.4. Due to practicalities of the methodology, the actual supply to demand ratio over a system's lifetime did not necessarily match its expected production. There were many reasons for this: variability in solar and wind availability from one year to the next, limited availability of sizes (PV arrays were rounded to the nearest panel area, and wind turbines were rounded to the nearest 0.2kW), PV panel degradation over time, and variability between the two available years of each household demand data. This can be observed in figure 4.27 where the average supply is typically smaller than expected (below the dotted green line) and the level of scatter above and below the mean is high. This is realistic given the unpredictable nature of wind on an annual time-scale.

It is also useful to relate these supply:demand ratios to actual power capacity of the technologies involved. Given that the total of annual household demand ranges from 1266kWh to 6446kWh, in addition to the variability in renewable energy availability, this leads to a wide range of possible capacity sizes. These ranges are shown in figure 4.28.

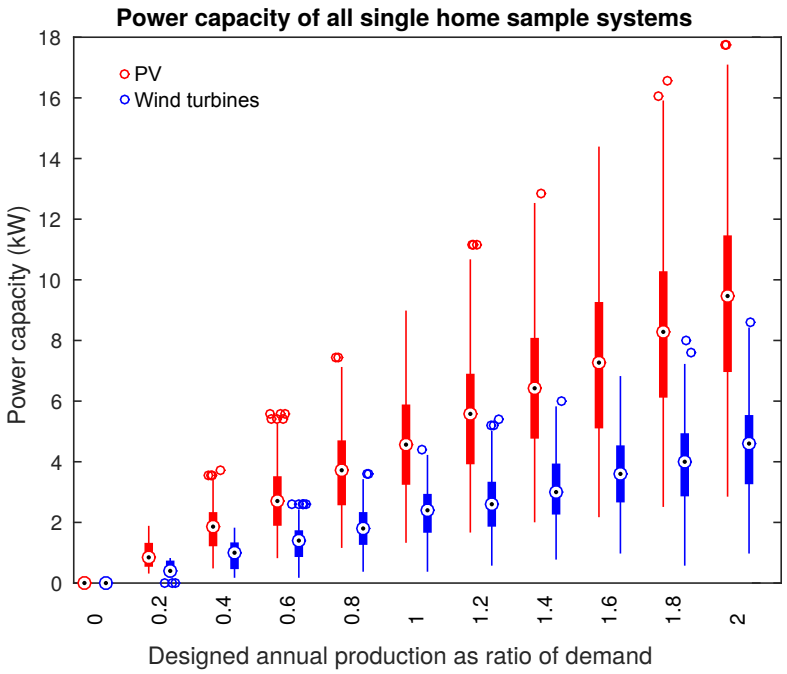

Figure 4.28: Boxplots showing actual power capacity of PV and wind turbines, given their estimated annual production as a ratio of household demand. PV requires a higher top-end of power capacity because of its lower capacity factor, especially in the north of the UK.

Chapter 5

Generalised results

The majority of energy system scenarios investigated in this thesis used a generalised model, where randomised samples of energy systems were generated using solar irradiation and wind speed data from across the UK, in combination with electricity consumption data from 20 households or non-domestic loads. The system scenarios differ according to their type of demand and their choice of technology:

- Single households with battery storage:
  - Lead-acid (Pba) batteries
  - Lithium-ion (li-ion) batteries
  - Sodium-sulphur (NaS) batteries
  - Zinc-bromine (ZnBr) flow batteries
  - Vanadium redox flow batteries (VRB).
- Networks of up to 20 households, using PbA batteries only.
- Non-domestic systems (mostly commercial and public buildings, some industrial) using PbA batteries only.
- Single households with hydrogen storage using electrolysis and PEM fuel cells for hydrogen creation and utilisation.
- Single households with heat pump load, using PbA batteries.

All these systems optimise across a full range of PV, wind turbine and storage capacities, scaling these capacities appropriately to facilitate fair comparison between systems of different sizes.

The single household systems with batteries are also analysed in further detail to investigate the correlation between sustainability and security, testing the commonly assumed hypothesis that they are necessarily the inverse of one another. This is followed up in the larger energy systems of networked domestic demand and non-domestic demand. There is also an evaluation of the methodology: first finding the correlation between security metrics to decide whether one is more suitable than the other, then finding the sensitivity of results to the uncertainty of input data.

This sensitivity analysis touches many strands of concern, and leads to significant results regarding future technologies and how the makeup of the electricity grid affects primary energy scaling. The analyses are as follows:

Objective function	Security concerns	Dimension of security measurement	Sustain-ability metric	Security metric
$ELOLP$	Underproduction	Time	E_{out}	$LOLP$
E_uLOLP	Underproduction and overproduction	Time	E_{used}	$LOLP$
$EEIR$	Underproduction	Energy	E_{out}	EIR
E_uEIR	Underproduction and overproduction	Energy	E_{used}	EIR

Table 5.1: Objective function summary.

- Uncertainty analysis of component embodied energy, using ranges of embodied energy values from the literature.
- Uncertainty analysis of battery cycle efficiency, again using ranges of battery efficiency from the literature.
- Sensitivity analysis of estimated future reduction in PV embodied energy.
- Sensitivity analysis of potential future grid efficiencies.
- Alternative results without using primary energy scaling.

All the standard optimisation analyses are performed using the four objective functions in table 5.1, but the uncertainty analysis, reflection on the similarity of results, and conclusions from the high-resolution tests in section 4.4 allow the investigation to proceed using only the security metric EIR. Therefore only $EEIR$ and E_uEIR are used to analyse the hydrogen and heat pump systems, and the case study in the next chapter only uses E_uEIR.

The chapter is concluded with a comparison of the results to a more traditional optimisation, where strict EIR constraints are chosen to give a more rigid choice of low energy cost systems. This allows for a more open discussion on how the choice of methodology reflects the aims and objectives, and how results and conclusions are affected.

5.1 Results for single household systems

This section examines the optimisation of systems composed of a PV array and/or wind turbine, supplying a single household and balanced using a battery (PbA, Li-ion, NaS, ZnBr or VRB) of varying size. The four objective functions in table 5.1 are each used to find optimal results, and these results are compared to give an idea of the optimal systems and the viability of each objective function. Graphs show results for systems with PbA batteries, but results are compared in the text to systems with other battery technologies, and all result graphs are shown in appendix B.1. Optimal results for systems with all batteries are discussed in section 5.1.5.

Size of components (PV array, wind turbine and battery) are all scaled to the system to allow for reasonable comparison between samples. Therefore PV array and wind turbine are shown as a measure of their total expected average output across the system's lifetime, divided by the household's average demand (this is the same metric used to create the samples) and the optimal battery capacities are shown as the total battery capacity (kWh) divided by the system's total power capacity (kW). This can be conceived as a measure of battery-hours: the amount of time the battery would take to charge from 0% to full charge when the generation is running at full power capacity. This was considered a more realistic scaling than using the annual demand as

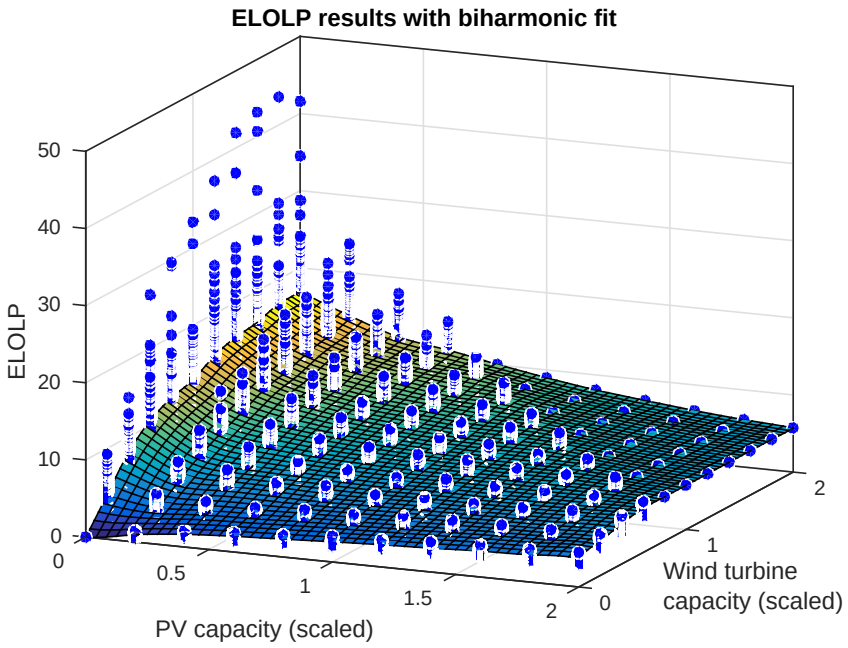

Figure 5.1: Optimal results for ELOLP for a PbA system, using the biharmonic method to fit the data. This particular fit has $r^2 = 0.90$, where the biggest scatter is for systems with majority wind input. The fitted surface is shown more clearly in figure 5.2 using 2D contours.

the denominator, or annual energy output, as the battery works on time-scales of hours rather than years, and is going to be in the most use when the system is producing at full capacity. Furthermore, the battery-hours unit also expresses the value of the battery to the system: for example, a system requiring twice the number of battery hours of another system means that the value of storage is doubled.

The analysis proceeds as follows:

1. Find optimal storage capacity for each combination of PV and wind power capacities.

2. Optimise these results with respect to relative size of generators.

3. Compare results between choice of objective function and battery type.

The results for each battery type across all system input variable are displayed using two graphs per objective function, the first displaying the optimal battery sizes and objective function results (performance), the second displaying these optimal systems' sustainability and security values (using appropriate metrics). These results are for all systems optimised with respect to battery capacity, and it is predefined that for all metrics, the performance for a system with zero inputs is 0. All surface plots are fitted using the biharmonic interpolation method within Matlab, which uses weighted linear least squares regression. The biharmonic method was chosen because the results do not necessarily fit a polynomial surface, and there are a large enough enough number of sampled systems that fitting by interpolation gives a fairly smooth surface. The biharmonic fit of optimal battery results determined by *ELOLP* are shown in figure 5.1 to demonstrate how the fitted results generally look.

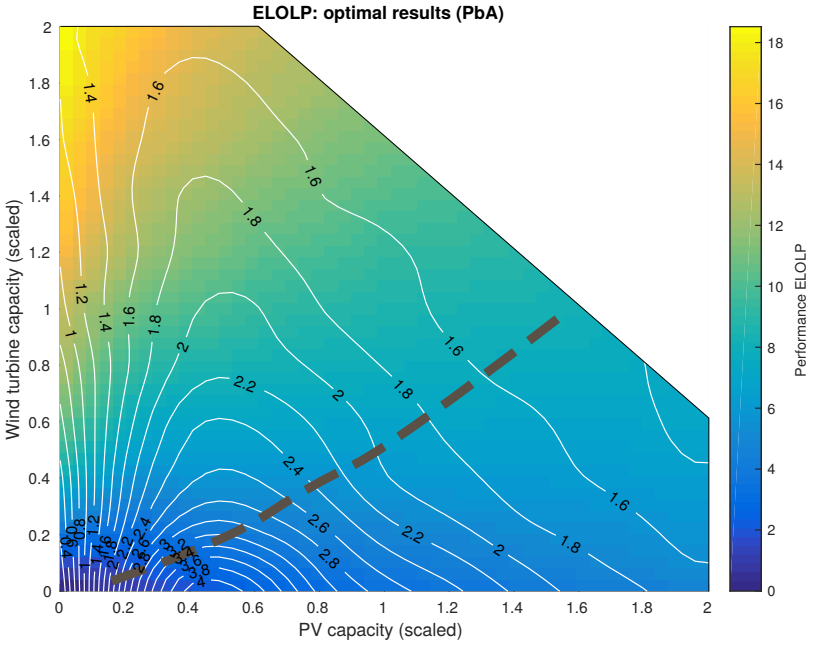

Figure 5.2: *ELOLP* results showing optimal PbA battery capacity (contours) and system performance (shading) for all input capacities. Best security results lie along dashed line, and best performance is at large wind-only systems, while worst is for small PV systems.

5.1.1 Results from *ELOLP* analysis

Plotting the optimal results with respect to wind and PV capacity in figure 5.2, it is clear that large wind-dominated systems give the highest *ELOLP* results, and reducing this wind capacity results in lower *ELOLP*-performance. Adding in PV capacity reduces this performance even more quickly, unless wind capacity is at zero.

Wind-dominated systems also show less need or suitability for storage, as increasing wind capacity alone gives a very slow increase in optimal battery capacity, while increasing PV capacity alone gives an immediate requirement for storage, reaching its peak at 0.5 and decreasing slowly thereafter. For small hybrid systems, increasing PV and wind input equally has more of a complex effect, where systems with low PV input (below 50% of demand) behave more like wind-only systems, and all systems with higher PV input will increase their optimal battery size when extra capacity is added, regardless whether the capacity is PV or wind.

The thick dotted line in figure 5.2 shows the combination of PV and wind that provides the best security for a given total capacity, taken from the contours in figure 5.3. Systems existing on this line have hybrid energy sources, but rely more on PV input than wind, with reduced reliance on battery storage as generation capacity increases, which is matched by a gradual increase in performance *ELOLP*.

When comparing single-source systems, PV-only have better security than wind-only systems, as increasing to maximum capacity results in an *LOLP* of 0.4 for wind, but 0.25 for PV. However increasing all types of generation capacity has diminishing returns on security, showing that for these systems there are always going to be loss of load periods where additional capacity cannot solve the problem.

PV may bring more security to the systems, but the wind-only systems have a much greater

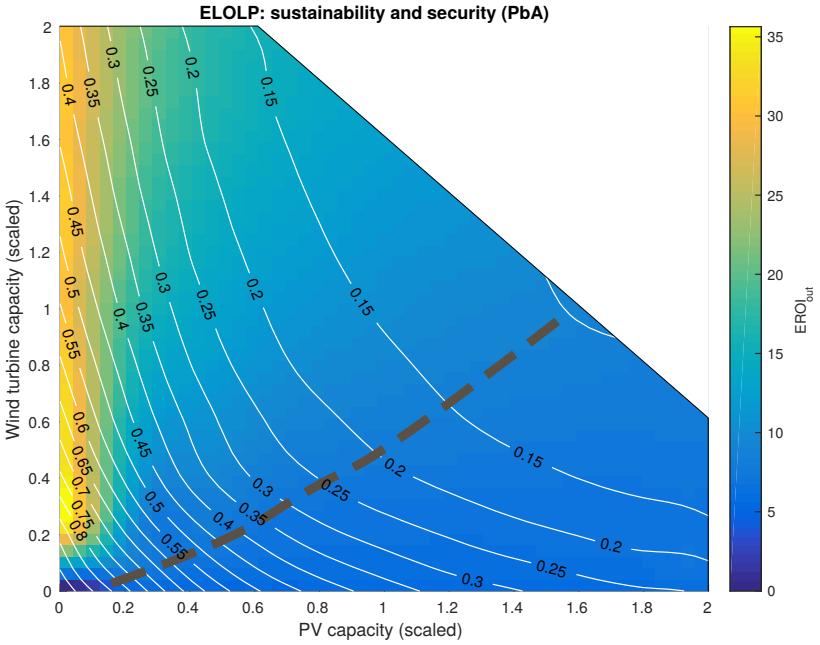

Figure 5.3: $EROI_{out}$ (shading) and $LOLP$ (contours) results for optimal PbA energy systems. Dashed line shows where best security exists for total energy supply, and best security overall is for large hybrid systems, skewed towards those with a larger PV input.

advantage in terms of their $EROI_{out}$, having a range of values over triple of the PV-dominant systems. This $EROI_{out}$ has a peak for small wind turbines with an output of 40% of total demand, which only have an $LOLP$ of 0.7-0.75 and therefore a low (10) $ELOLP$ value in comparison to the larger wind-dominant systems. This interplay between the $EROI_{out}$ and EIR values shows a certain amount of anti-correlation, however it is not true that increasing one necessitates a decrease in the other, as in many cases increasing PV capacity has a negligable effect on $EROI_{out}$ but an improvement in $LOLP$ values.

Analysing all systems across all batteries, it is apparent that while wind turbines facilitate higher EROIout results, some combination with PV is useful to reduce LOLP. However, at the current embodied levels of PV technology, adding battery storage to wind is actually a more cost-effective intervention, as moving to the right on the graph in figure 5.3 gives a very quick decline in EROI.

These results are for PbA batteries, which are presumed to be the worst performing batteries tested here. Other batteries succeed in reaching 0.1 $LOLP$ with fewer resources, namely Li-ion requires $12kW_p$ PV, $4.5kW_p$ wind and $10kWh$ battery, NaS requires $10kW_p$ PV, $3.5kW_p$ PV and $10kWh$ battery, ZnBr requires $8.5kW_p$ PV, $3kW_p$ wind and $10kWh$ battery, and VRB requires $10kW_p$ PV, $3.5kW_p$ wind and $10kWh$ battery. Analysing all systems across all batteries, it is apparent that while wind turbines facilitate higher $EROI_{out}$ results, some combination with PV is useful to reduce $LOLP$. However, at the current embodied levels of PV technology, adding battery storage to wind is actually a more cost-effective intervention, as moving to the right on the graph in figure 5.3 gives a very quick decline in EROI.

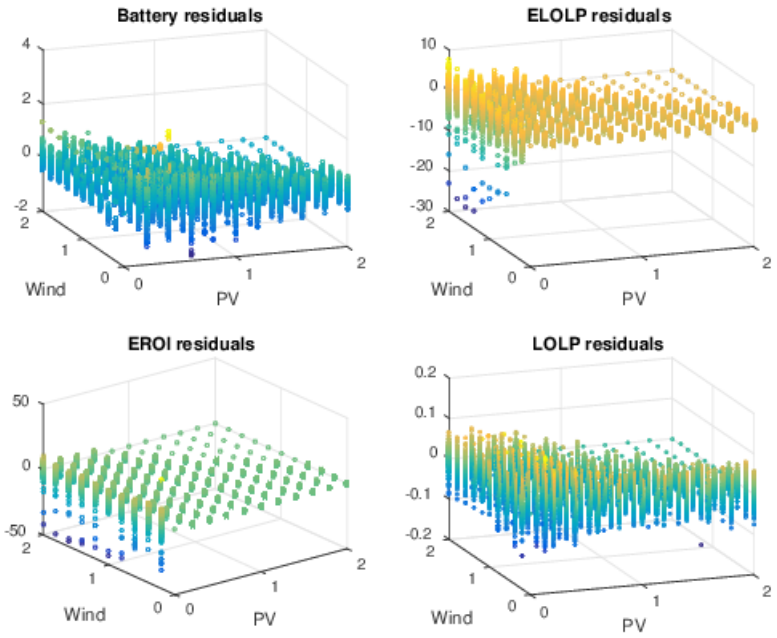

Figure 5.4: Residuals for the $ELOLP$-optimal fits. While there is some negative scatter for ELOLP and EROI residuals for wind-only scenarios, caused by a small number of very high EROI results, this is not systematic enough to suggest a bad fit of the data.

Goodness of fit

The biharmonic fit shown in these graphs is a good fit to the results, as shown by the residuals in figure 5.4. A bad fit would display systematic deviation from 0 in the residuals, but these show an even cluster around $r = 0$, with the exception of some wind-only systems with unusually high EROI values. These are not numerous enough to suggest a bad fit, however are not anomalous thus have not been removed either. These residuals also show that there is much more range in the optimal results when one energy source is dominant over the other (i.e. in high-PV or high-wind scenarios) in general. The fit to $ELOLP$ and optimal battery size have $r^2 = 0.90$ and $r^2 = 0.78$ respectively.

5.1.2 Results from E_uLOLP analysis

Using the EROI metric $EROI_{used}$ gives the performance of a system when its excess energy is not usable by the external grid, resulting in a lower performance if there is unnecessary overproduction. It is not expected that any of these systems will be able to reach good levels of $LOLP$ without producing too much energy at some points in time, so the $EROI_{used}$ results will always be lower than $EROI_{out}$ unless the system is severly under capacity. A less direct result of the $EROI_{used}$ metric is to add value to the batteries; now instead of merely contributing to security via decreasing $LOLP$, they can also improve the system's sustainability by reducing energy losses.

This added value of the batteries is immediately apparent in the greater optimal capacity of batteries in figure 5.5, where even wind-dominant systems utilise up to 4.6 battery-hours of storage, and PV systems have a peak of 5.4 battery-hours. Unlike the $ELOLP$ results, there is a second peak of battery capacity for wind-dominant systems, with twice the performance of the peak for small PV-only systems. The E_uLOLP values are also much lower and more spread

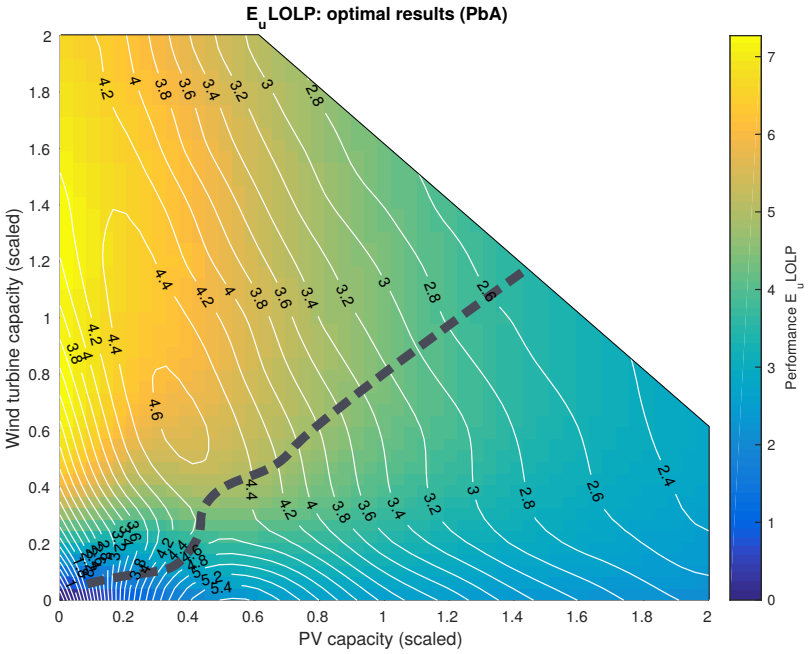

Figure 5.5: E_uLOLP results showing optimal PbA battery capacity (contours) and system performance (shading) for all input capacities. Optimal battery capacities are much bigger than when using $ELOLP$, particularly for wind-dominated systems. Less stark variation in performance exists, but medium-sized wind-dominated systems have best performance and large PV-only systems have the worst. Best security results lie along dashed line.

out than $ELOLP$, such that the highest performing systems are mid-large size wind-dominant rather than large wind-only systems, and PV-dominant systems are able of showing over half the performance of the best wind-dominant systems, unlike the steep differential seen with $ELOLP$. These E_uLOLP results and their similar battery sizes suggest that wind-dominant systems are more prone to periods of overproduction, an observation that is borne out by energy export results in figure 5.6. Therefore when a wind system is unable to export excess production, it has more to gain by adding additional units of PV or storage capacity.

The dashed line of best security results has a similarly shallow gradient to that in the $ELOLP$ results, with the exception of a detour at PV$\approx$ 0.5, where the second peak of battery capacity is exhibited. This also shows a slight preference for more equal large hybrid systems; now the wind turbines are matched by a larger battery capacity, their EIR results become comparable to PV.

This explains the more symmetrical nature of the $LOLP$ results in figure 5.6, but PV-dominant systems still have a slight edge over wind-dominant ones, reaching 0.2 $LOLP$ in comparison to 0.3. All of the $LOLP$ values are better when optimising with E_uLOLP, benefitting from the larger storage capacity. Their sustainability is however much decreased, PV-dominant systems in particular having an $EROI_{used}$ of less than 5. Large wind-only systems also have much lower EROI, as so much of their production is lost, and they have the extra cost of larger batteries.

When measuring the systems for exported energy in figure 5.7, the difference between $EROI_{out}$ and $EROI_{used}$ is less obvious than you would expect, with only around 500kWh saved annually under E_uLOLP-optimisation. However while comparing systems with the same generation capacity shows little difference, the optimisation towards smaller wind

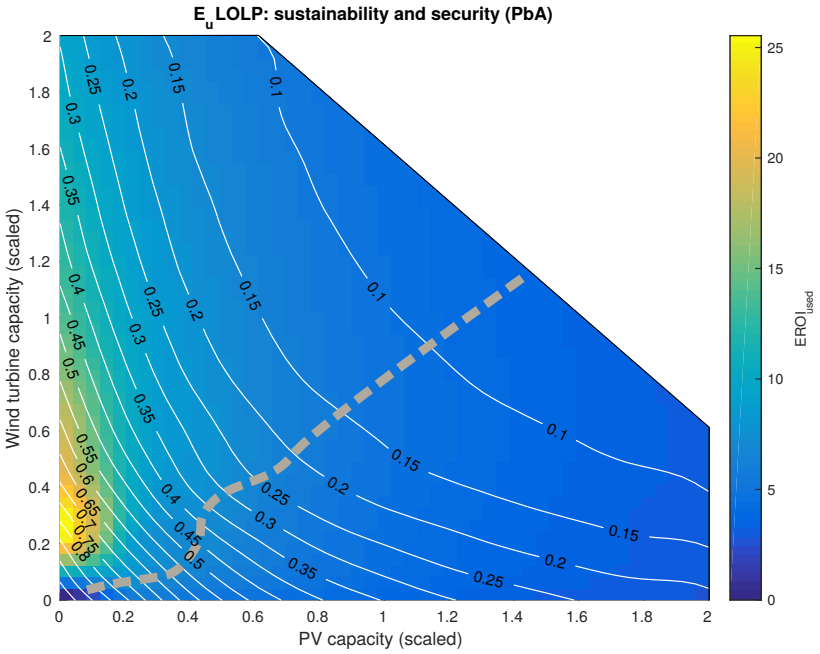

Figure 5.6: $EROI_{used}$ (shading) and $LOLP$ (contours) results for optimal PbA energy systems. Large hybrid systems give best security, while small wind-only systems give best sustainability.

turbines means that an E_uLOLP-optimal system will curtail less than half the amount of energy exported under $ELOLP$. The process of optimisation does change the total exported energy for wind-only systems, as the contours close to the y-axis gain a negative gradient. However curtailed energy for wind-dominated systems still exceeds that of PV-dominated systems, despite larger battery capacity for some of the systems. It must be noted here that as the battery capacity is scaled to the generation power capacity, and wind turbines on average have a higher capacity factor than PV, the absolute battery capacity in kWh would be lower for all wind systems, so their overproduction is a side-effect of their higher capacity factor.

The graphs in figure 5.7 also illustrate the difference between PV and wind fairly well, as adding a small amount of PV to a mid-sized wind-only system will not increase the amount of unusable generated energy (despite an increase in overall production), whereas adding a small wind turbine to a PV-only system will generally result in increased excess. However once the wind-only systems are producing over 150% of annual demand, the system becomes saturated and PV no longer has that effect.

Seasonal results show the relationship between wind and PV more clearly; summer (June to August) has the best security as long as there is substantial PV capacity, and winter has the best $LOLP$ results for wind-dominant systems, but still has a respectable showing for PV-dominant systems which are able to contribute 0.5 $LOLP$ when no wind is present. This is admittedly small, but contradicts the commonly held assumption that PV is completely useless in winter. When taking all seasons into account, PV does appear to deliver the most security to the system; however given that winter is the period of greatest demand, there is reason to give it more weight. The overall E_uLOLP optimal result of wind-only systems would give a result of 0.3-0.35 $LOLP$ in winter, which is slightly better than the security over all seasons. Therefore this optimal result is better than it may seem, as it delivers more security when it is most needed.

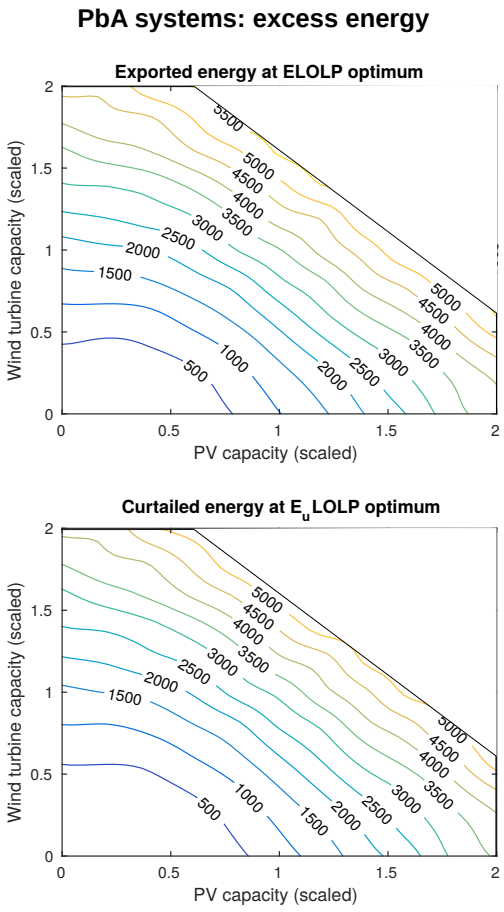

Figure 5.7: Exported energy (kWh per year) of single household systems.

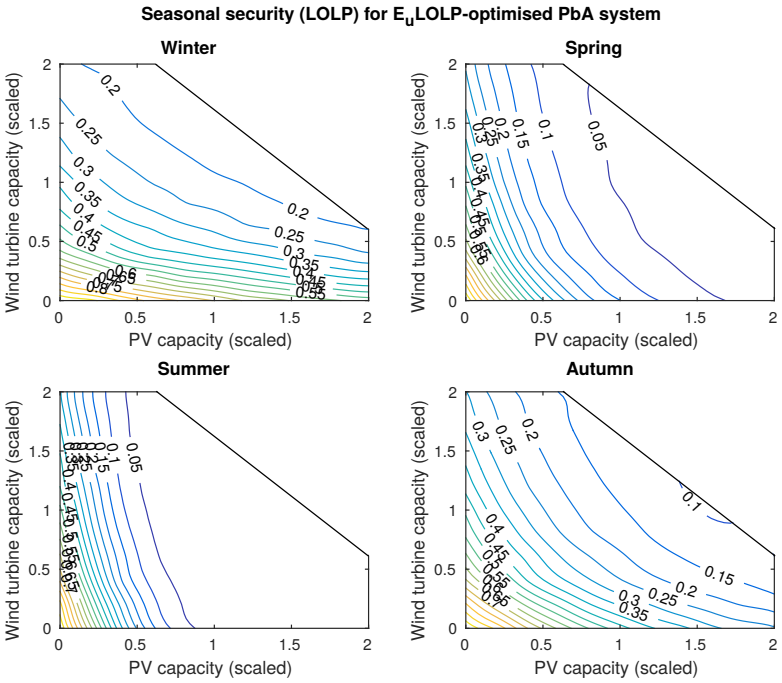

Figure 5.8: Seasonal $ELOLP$ results for optimal PbA energy systems. Summer shows the best $LOLP$ results, with PV systems being able to utilise the more predictable solar power, but winter months show the best $LOLP$ for wind-dominant systems and spring.

Goodness of fit

The residuals from the fits were plotted as with $ELOLP$, shown in figure 5.9. There is much less deviation from the fit in these results, particularly for the E_uLOLP result itself, however some highly negative residuals are again observed for wind-only systems. Fit for E_uLOLP and optimal battery size have $r^2 = 0.88$ and $r^2 = 0.86$ respectively.

5.1.3 Results from $EEIR$ analysis

It is expected that optimisation using the EIR metric rather than $LOLP$ would result in similar outcomes to above, however the EIR metric may be better at accounting for the severity of loss of load periods, as it quantifies the energy shortfall rather than just their lengths. This is also more relevant in these systems where it is possible to import energy from the grid, rather than a national grid where energy shortages may result in a blackout.

The reason for using both metrics was to compare and contrast results, to see how strong a relationship they truly have. Indeed, the $EEIR$ performance results in figure 5.10 show a very similar shape to the graph in figure 5.2, with a peak for the largest wind-only systems and a similar range of battery capacities. This result is repeated for the $EROI_{out}$ and EIR results in figure 5.11, which shows very little difference to the $ELOLP$ graph.

Using the same system inputs as mentioned in the $ELOLP$ section to compare results at high levels of security, a PbA system with $10kW_p$ PV, $3.5kW_p$ wind capacity reaches nearly 0.9 EIR with around $19kWh$ storage. For other battery technologies, a Li-ion system with $12kW_p$ PV and $4.5kW_p$ wind reaches nearly 0.9 EIR with around $8kWh$ storage, and a NaS system with $10kW_p$ PV and $3.5kW_p$ wind capacity reaches nearly 0.85 EIR with around $8kWh$ storage. The flow battery systems show that a ZnBr system with $8.5kW_p$ PV and $3kW_p$ wind reaches

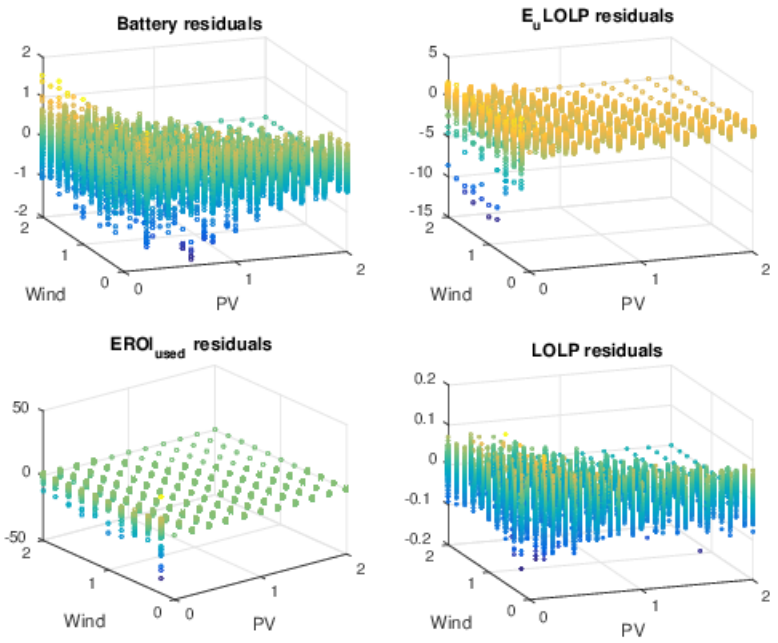

Figure 5.9: Residuals for the E_uLOLP-optimal fits. The scatter is generally lower than that seen in the $ELOLP$ results.

nearly 0.9 EIR with around $10kWh$ storage, and a VRB system with $10kW_p$ PV and $3.5kW_p$ wind reaches nearly 0.9 EIR with around $11kWh$ storage.

A summary of the differences between $EEIR$ and $ELOLP$ results is in table 5.2, and more detailed differences in the security results are shown in figure 5.12. The security metrics $LOLP$ and EIR are not expected to perfectly match, however mapping their variation in difference can show how they detect levels of security given different ratios between PV and wind power input. The graphs of these differences show a systematic difference where security is measured as better (+0.4) for mid-sized wind-only systems when using $LOLP$, corresponding with a larger battery capacity (+0.5) for those systems. There is not a consistent difference in battery capacity across all systems, as using $EEIR$ for hybrid systems results in a slightly smaller (-0.1) battery capacity than when using $ELOLP$. Therefore the high resolution results from section 4.4 may not necessarily hold when wind is included in the system. However this does not mean that EIR is not more accurate than $LOLP$.

Goodness of fit

The residuals from the fits are similar to those found with $ELOLP$, and are shown in figure 5.13 where wind-only systems again have the highest level of scatter for $EROI_{out}$. Fit for $EEIR$ and optimal battery size have $r^2 = 0.89$ and $r^2 = 0.77$ respectively.

5.1.4 Results from E_uEIR analysis

As $EEIR$ can be compared to $ELOLP$, so can E_uEIR results with E_uLOLP. Again, the optimal battery sizes in figure 5.14 show a similar pattern to that of E_uLOLP-optimal results, with a double peak for small PV-only and mid-sized wind-dominant hybrid systems, and a similar range of battery capacities. Regarding E_uEIR performance, mid-sized wind-dominant systems again have the highest value at $E_uEIR = 0.7$.

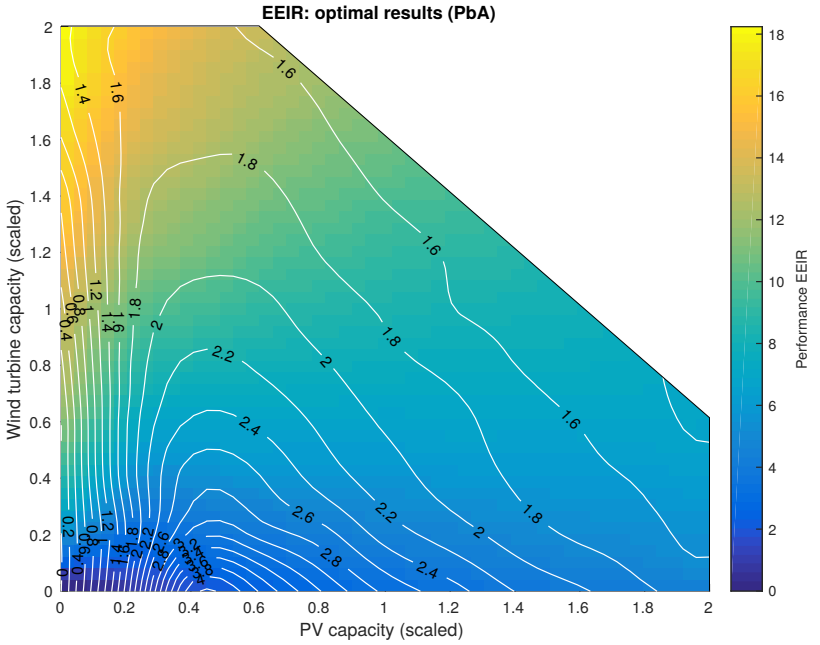

Figure 5.10: *EEIR* results showing optimal PbA battery capacity (contours) and system performance (shading) for all input capacities. Results are very similar to when using *ELOLP* optimisation, except for slightly smaller battery capacities.

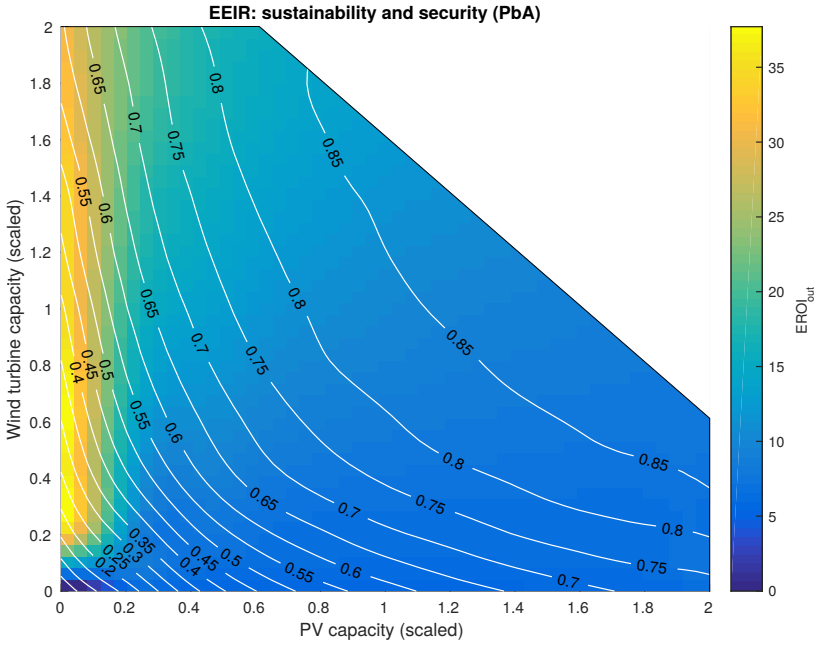

Figure 5.11: $EROI_{out}$ (shading) and *EIR* (contours) results for optimal PbA energy systems. Again, results are very similar to when using *ELOLP*.

Parameter	Optimal results in common	Differences
Battery capacity	Similar range of battery capacities and shape of fitted surface.	$ELOLP$ gives larger optimal battery capacities than $EEIR$ when PV input is low.
Objective function	Identical position, similar gradient.	No significant differences.
$EROI_{out}$	Similar location of peak and shape of fitted surface.	No significant differences.
Security	Similar range and shape of fitted surface (comparing $1 - LOLP$ and EIR).	$1 - LOLP > EIR$.

Table 5.2: Comparing results between the underproduction analyses $ELOLP$ and $EEIR$.

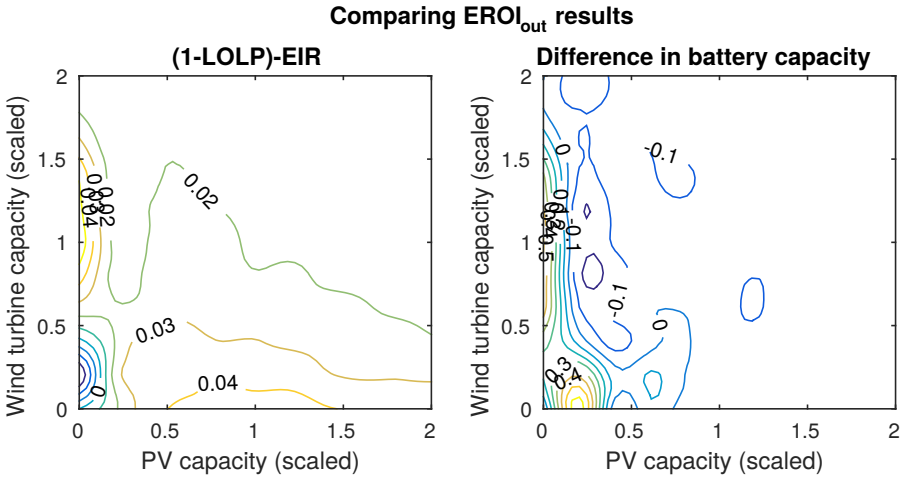

Figure 5.12: Differences between the security metric results and optimal battery capacity, when comparing $ELOLP$ and $EEIR$. $LOLP$ is normalised to $1 - LOLP$ to better compare with EIR. The differences are very small, however these graphs show a systematic difference where security is measured as better for mid-sized wind-only systems when using $LOLP$, corresponding with a larger battery capacity for those systems.

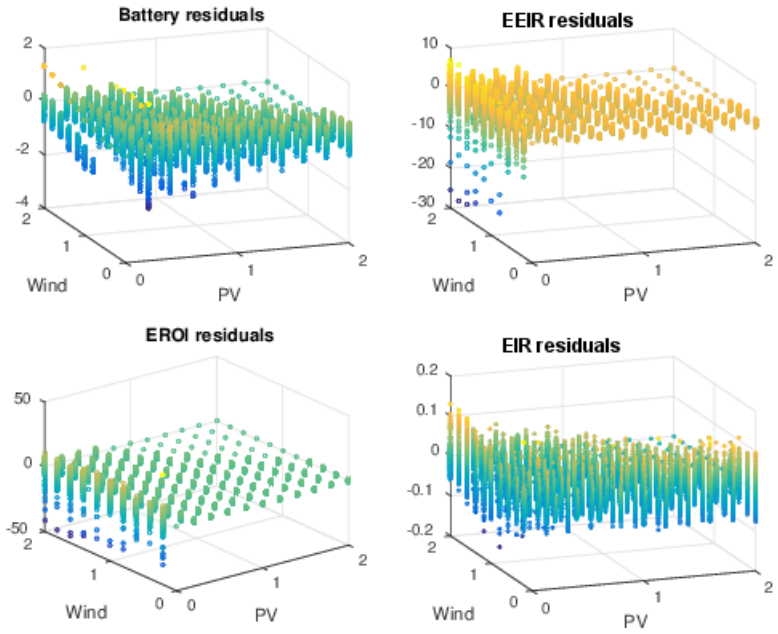

Figure 5.13: Residuals for the $EEIR$-optimal fits. The patterns of scatter is almost identical to that seen in the $ELOLP$ results.

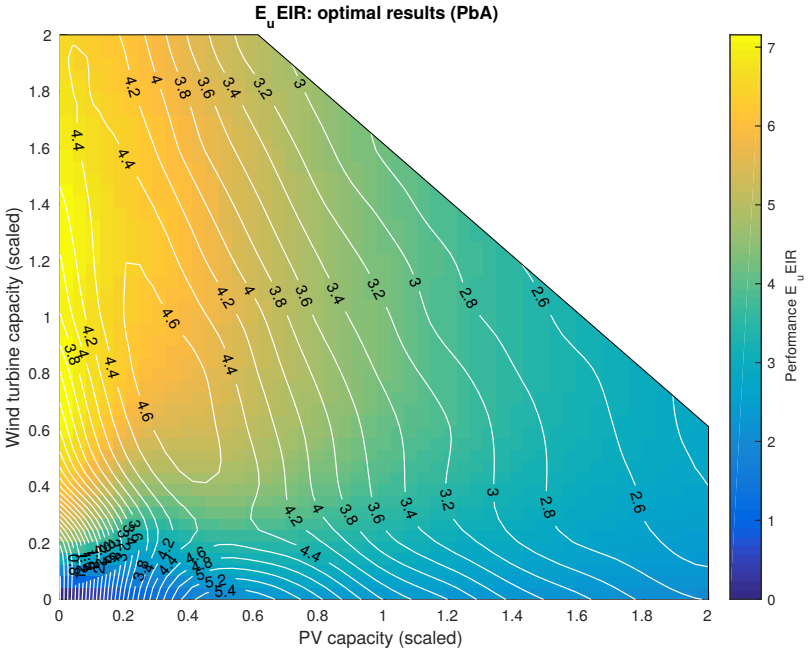

Figure 5.14: $E_u EIR$ results showing optimal PbA battery capacity (contours) and system performance (shading) for all input capacities. Battery capacity reaches a plateau for high power capacity, and gives larger batteries for wind-dominated systems than PV. Performance is highest for small wind-dominated systems.

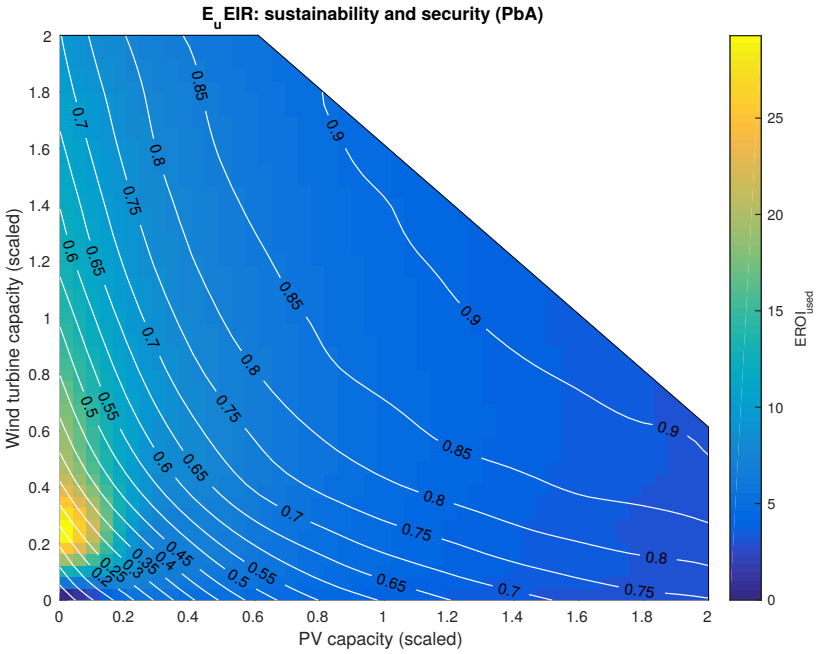

Figure 5.15: $EROI_{used}$ (shading) and CC (contours) results for optimal PbA energy systems. Best security exists for medium-sized hybrid systems, and best sustainability for small wind-only systems.

In figure 5.15 the $EROI_{used}$ values show a similar pattern to the E_uLOLP-optimal results, with a very strong peak for small PV-only systems, and the security measured with EIR again looks stronger than the $LOLP$ results.

While this difference is only small, it is likely caused by a number of loss of load periods where the energy shortfall is only small, and therefore appear as less significant when measured with EIR as opposed to $LOLP$.

A summary of the differences between E_uEIR and E_uLOLP results is in table 5.3, and differences in security metrics and optimal battery capacities are shown in figure 5.16. The differences are very similar to when $EROI_{out}$ is used in the optimisation: security measured by $LOLP$ shows a slight preference (+0.04) towards PV-only systems, and there is little difference in battery capacities.

Goodness of fit

The residuals from the fits are shown in figure 5.17 where wind-only systems again have the highest level of scatter for $EROI_{out}$. Fit for E_uEIR and optimal battery size have $r^2 = 0.87$ and $r^2 = 0.78$ respectively. Compared to the fits for E_uLOLP results, the battery fit is not as strong (E_uLOLP had $r^2 = 0.86$) which is visible in the wider range of battery residuals.

Impact of $EROI_{used}$

It is apparent that when excess energy is curtailed (applying the EROI metric $EROI_{used}$) performance decreases, optimal battery capacity increases, EROI reduces and the increased battery capacity leads to an increase in security (measured by EIR). However, comparing graphs of outcome by eye does not accurately display the variation in these differences depending on the type of system.

Parameter	Optimal results in common	Differences
Battery capacity	Similar range in battery capacities.	None.
Objective function	Peaks exist for similarly sized wind-only systems.	Peak for E_uEIR is steeper, and as more households are added the optimal power capacity increases faster for E_uLOLP than E_uEIR.
$EROI_{used}$	Peak exists at similar location.	No significant differences .
Security	Hybrid systems show the best security.	Best E_uLOLP is for large PV-dominated hybrid systems, but best E_uEIR is for small hybrid systems around $3-4kW_p$ capacity.

Table 5.3: Comparing results between the objective functions E_uLOLP and E_uEIR, which both account for under- and overproduction.

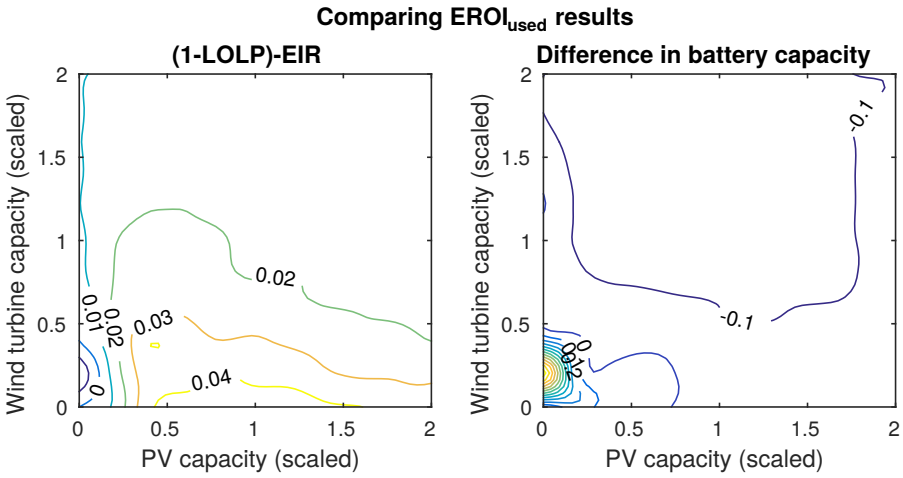

Figure 5.16: Differences between the $LOLP$ and EIR results when optimising with $EROI_{used}$. $LOLP$ security shows preference to PV systems, but there is little notable difference in battery capacity other than for small wind-only systems where $LOLP$ oversizes.

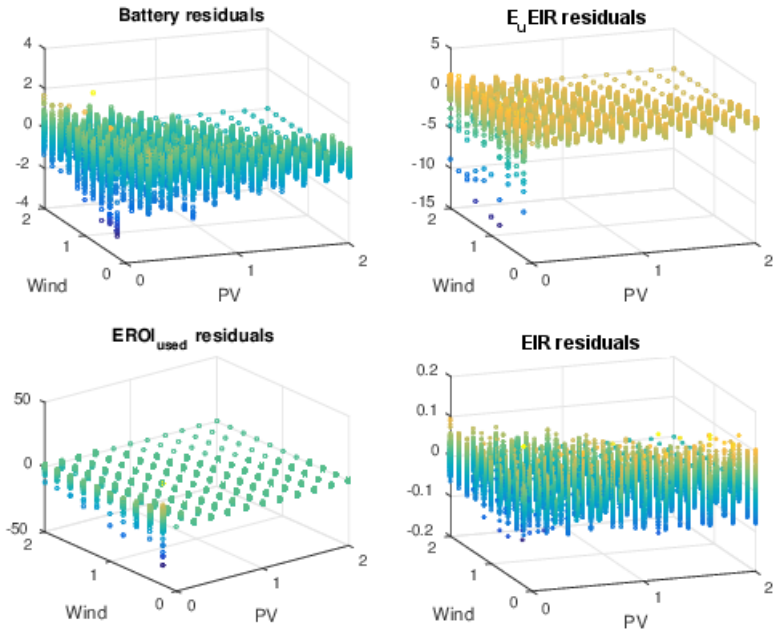

Figure 5.17: Residuals for the E_uEIR-optimal fits. The patterns of scatter is almost identical to that seen in the E_uLOLP results, except for the battery fit residuals where there is increased scatter, especially for small wind-only systems.

Figure 5.18 shows how moving to a non-exporting system has the biggest impact on systems with wind power sources, as their overproduction leads to a proportionally lower performance and $EROI_{used}$ value. The $EROI_{used}$ is further reduced by adding battery capacity of up to 3.4 battery-hours (greatest for wind-only systems), which has the benefit of increasing EIR by up to 0.12 (see figure 5.19). PV-dominated and hybrid systems show the lowest addition of battery capacity per unit of production, and therefore experience the fewest changes in sustainability or security.

The excess energy for $EEIR$ and E_uEIR optimisation are virtually identical to those of $ELOLP$ and E_uLOLP (shown in figure 5.7), so instead of repeating those results, figure 5.20 shows the difference in excess energy when moving from a $EEIR$ optimisation to a E_uEIR optimisation. All systems have some reduction in excess energy, however it is the wind-only systems that benefit the most. Their increase in EIR also shows that the excess energy is not simply being lost in the battery, but stored and used by the household demand when instantaneous generation is not enough.

5.1.5 Full optimisation across all input variables

Optimal system results are shown in table 5.4, where the systems are optimised with respect to their generation capacity as well as battery capacity, for each type of battery technology. These results are calculated by finding the highest performance across all optimised systems for each objective function. The four other different battery technologies all give very similar results in terms of the shape and peaks of their output variables, but the specific values will be slightly different.

All optimal systems include zero PV capacity (this is not included in the table), and a wind capacity that supplies twice the annual demand when using the $EROI_{out}$ metric, or around

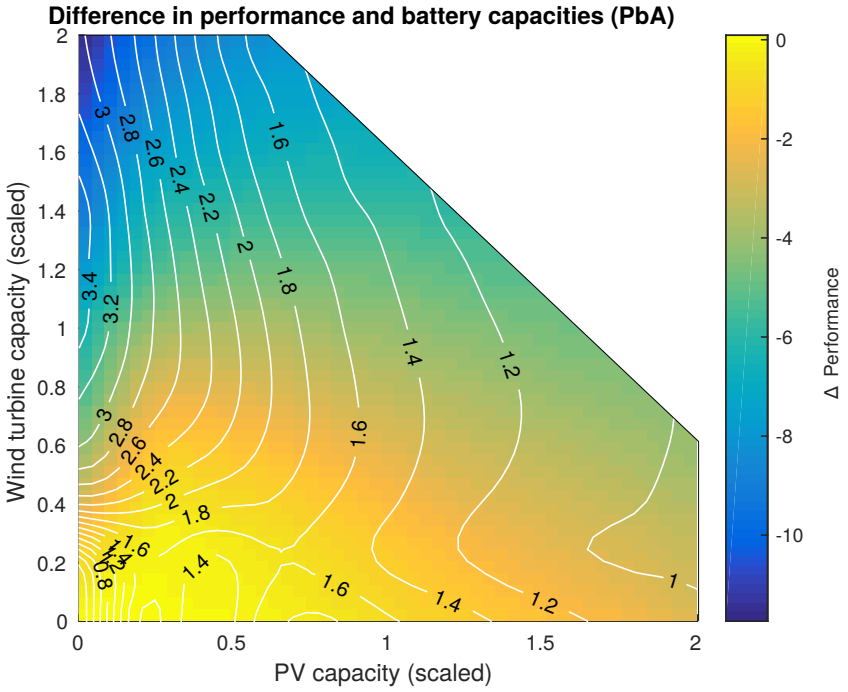

Figure 5.18: Difference in performance (shading) and battery capacities (contours) when optimising with $E_u EIR$ rather than $EEIR$. Large wind-dominated systems show the biggest drop in performance as their overproduction becomes penalised, and they are given much larger batteries to curb excess generation.

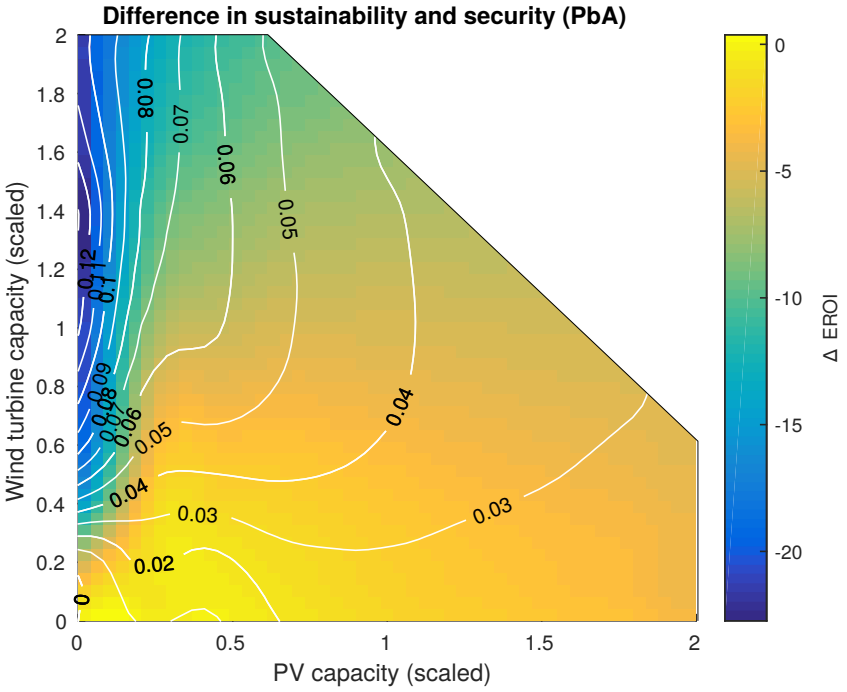

Figure 5.19: Difference in EROI (shading) and EIR (contours) when optimising with $E_u EIR$ rather than $EEIR$. Wind-only systems show the biggest drop in EROI as their overproduction becomes penalised, and they are given much larger batteries to curb excess generation, which increases their security.

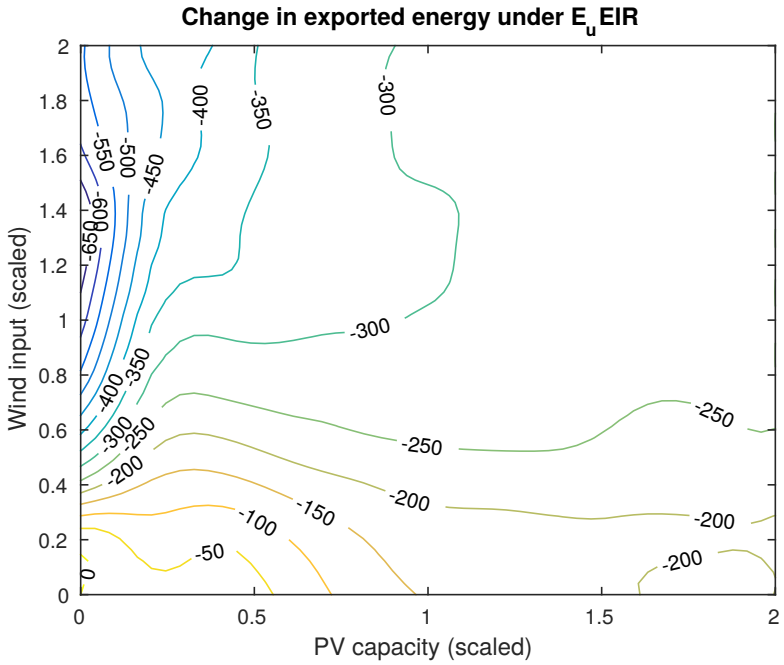

Figure 5.20: Difference in excess energy when moving from $EEIR$ optimisation to $E_u EIR$ optimisation. Contours show the difference in kWh per year, where the difference is the greatest for wind-only systems.

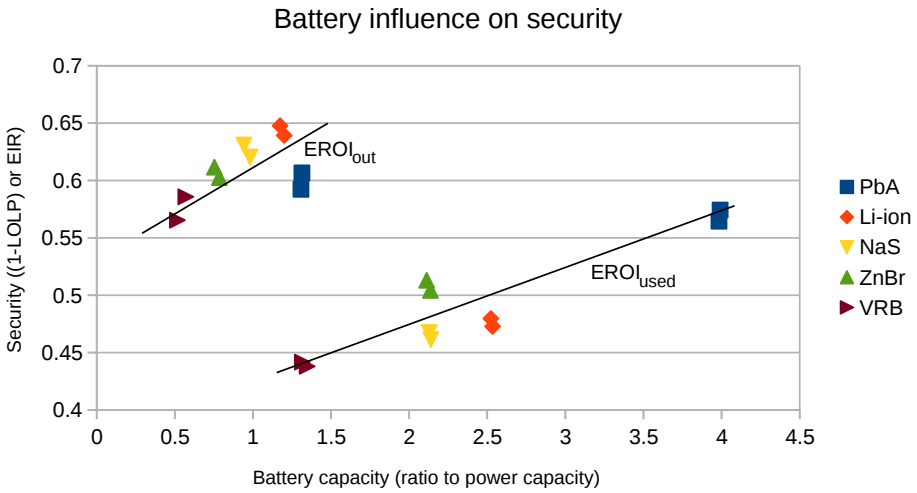

Figure 5.21: Optimal battery capacity and security results for all single household systems. When energy exporting is disallowed, battery capacity has higher value, but lower security is achieved as energy input is roughly halved.

the same as annual demand when accounting for curtailed energy using the $EROI_{used}$ metric. The biggest difference between systems with different battery types is in their optimal battery capacities, where PbA always requires the largest capacity (having low DOD and low EE), and VRB the least (having high DOD and high EE). However the higher capacity of PbA batteries are not necessarily enough to ensure better security, as shown in figure 5.21.

The consistency of giving wind-only systems for all optimisations shows that advantages in EROI are more likely to trump advantages in security, as PV is demonstrated to bring security advantages to the system. However it cannot be assumed that the performance metrics are entirely governed by the EROI result, as they always return an optimal system with wind capacity higher than the EROI alone would suggest. Therefore it can generally be concluded that a reduction in $EROI_{out}$ from increasing wind capacity (this reduction in $EROI_{out}$ comes from the associated increase in battery storage rather than the turbine itself) brings more cost-effective security benefits than bringing in new/additional PV capacity. The same can be said for $EROI_{used}$ results, except that the increase in battery storage is greater, and $EROI_{used}$ is directly impacted by the excess energy of larger wind turbines.

This combination of EROI and security within the objective functions means that the maximum points of performance are much broader plateaus than the steep peak of EROI values (whether $EROI_{out}$ or $EROI_{used}$. These plateaus are widest in the y-axis (wind capacity) but do also show some breadth in the x-axis. For example, increasing PV capacity by 0.2 (per unit of total system demand) will decrease the maximum $EROI_{used}$ from 29 to 9, but will decrease the maximum E_uEIR from 7.1 to 6.4. Therefore while wind-only systems are shown to be optimal, the strength of this optimality is weaker than if $EROI_{used}$ was applied alone.

Comparing objective functions

For all battery technologies, objective functions ELOLP and EEIR return identical results for power generation inputs, being the maximum wind input available. Given no cap on excess energy production, and the improving energy return for wind turbines as they increase in

Objective function	Wind turbine output	Battery capacity	Sustain-ability	Security	Perform-ance	Annual excess energy (kWh)	Goodness of fit
PbA							
$ELOLP$	2.0	1.31	30.5	0.39	18.5	4672	0.90
E_uLOLP	1.2	3.99	12.6	0.43	7.3	1955	0.88
$EEIR$	2.0	1.31	30.9	0.59	18.2	4683	0.89
E_uEIR	1.2	3.98	12.6	0.56	7.1	1959	0.87
Li-ion							
$ELOLP$	2.0	1.17	30.3	0.35	19.7	4644	0.90
E_uLOLP	0.8	2.52	16.6	0.52	8.0	981	0.87
$EEIR$	2.0	1.20	30.2	0.64	19.3	4635	0.89
E_uEIR	0.8	2.53	16.6	0.47	8.0	983	0.85
NaS							
$ELOLP$	2.0	0.94	30.9	0.37	19.5	4913	0.90
E_uLOLP	0.8	2.13	16.5	0.53	7.7	1075	0.87
$EEIR$	2.0	0.98	30.8	0.62	19.1	4901	0.89
E_uEIR	0.8	2.14	16.5	0.46	7.6	1077	0.86
ZnBr							
$ELOLP$	2.0	0.75	31.4	0.39	19.2	4580	0.90
E_uLOLP	1.0	2.11	14.2	0.49	7.3	1342	0.89
$EEIR$	2.0	0.78	31.3	0.60	18.9	4570	0.90
E_uEIR	1.0	2.14	14.2	0.50	7.2	1338	0.87
VRB							
$ELOLP$	2.0	0.57	30.4	0.41	17.8	4807	0.89
E_uLOLP	0.8	1.32	16.3	0.56	7.2	1073	0.86
$EEIR$	2.0	0.52	31.4	0.57	17.6	4867	0.89
E_uEIR	0.8	1.35	16.3	0.44	7.2	1070	0.86

Table 5.4: Summary of optimums for all single household systems, where all optimums have zero PV capacity. Wind turbine output is measured as a ratio of annual demand, and battery capacity as a ratio of wind turbine capacity. Goodness of fit is measured using r^2.

capacity, this would likely always be the case no matter how large they were permitted to be in this model. The $EROI_{out}$, measured security and exported energy results are also fairly consistent across all battery types, possibly because the optimal battery capacity is minimal. Performance using the $EROI_{used}$ metric similarly show very little difference between each other for each type of battery system.

When comparing the results using $EROI_{out}$ against the ones using $EROI_{used}$, it is immediately apparent that wind turbines suffer greatly from having their excess production curtailed, as many of the systems optimise to under-capacity. Furthermore, much larger (from 2 to 3 times the size) batteries are required to capture the excess energy, despite the systems being considerably smaller. This increase in battery capacity leads to improved security, however it is not enough to offset the massive reduction in EROI, so performance overall drops to less than half for all systems.

For all systems and objective functions, the fit to the data is fairly good, with r^2 values from 0.86 to 0.9. Given the range in absolute capacity sizes of the systems, this is notably high.

Comparing battery technologies

Optimal battery capacities are strongly dependent on which battery is used. For all objective functions, energy systems with PbA batteries require larger battery capacity, and systems with VRB storage require the smallest battery capacities. However, their optimal systems retain similar levels of sustainability and security regardless of battery size. This is the result of optimisation skewing battery capacity to reflect similar outputs.

The three variables that likely affect battery performance here are embodied energy, depth of discharge and efficiency. Large PbA batteries are required because of their small usable capacity and low efficiency, and their low embodied energy makes large batteries less of a hindrance. However for batteries like VRB with their large usable capacity and high embodied energy, only smaller batteries are needed/possible. When comparing the actual performance of the optimal systems, Li-ion batteries always give the highest performance regardless of applied metric, and VRB systems show the worst, but the difference between them is not very big.

5.2 Results for networked systems

To simulate networked households as part of a network/virtual power plant, the available household demand time-series were randomly combined to create networks of up to 20 households. As the number of households increases, the smoother the demand load becomes. While 20 households is not a large enough network to give a smooth demand like in figure 3.10, combining these households does give a flatter daily profile, as shown in figure 5.22. Running the model with this increased load can find how the optimal component sizing of the system depends on its number of loads, and how this affects the system's sustainability and security. Depending on the objective function, the battery size required could go up (to account for higher power spikes), go down (as smoother demand means less need for storage) or stay roughly the same in proportion to demand. The system is modelled with the assumption that each household has a battery of equal size to each other, and this individual household battery is the capacity that is optimised.

Limits to this model come from the shortage of household demand time-series: there will be less variation in the demand samples as system size increases because only 20 demand time-series exist. This must not be mixed up with the phenomenon of smoothing, which would occur for any size of population. Because of this lower variation, and to reduce computational demand, the sample sizes are reduced for larger systems, as shown in table 5.5. These sizes are

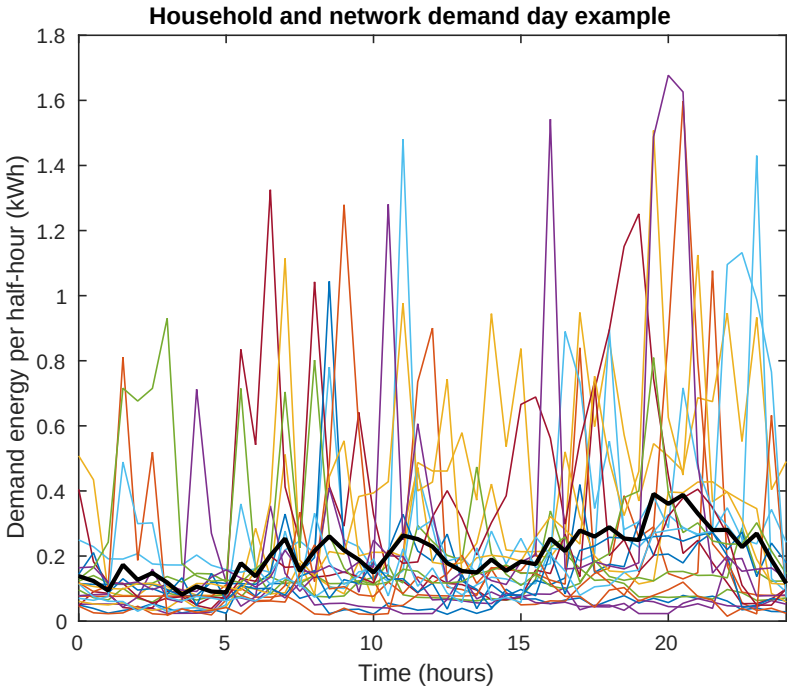

Figure 5.22: Demand time-series of all available households for a day in early March. Thick black line shows the average demand from these households, which is flatter and more predictable than each individual household, but not enough households are included to give the smoother national average profile.

Number of households	Sample size	$ELOLP$ r^2	E_uLOLP r^2	$EEIR$ r^2	E_uEIR r^2
1	200	0.90	0.88	0.89	0.87
2	150	0.90	0.88	0.89	0.87
3	100	0.91	0.89	0.90	0.89
4	100	0.91	0.88	0.89	0.87
5	100	0.91	0.88	0.89	0.86
6	100	0.91	0.88	0.89	0.88
7	100	0.91	0.88	0.89	0.86
8	100	0.92	0.88	0.90	0.87
9	100	0.91	0.89	0.90	0.87
10	100	0.92	0.90	0.91	0.88
11	100	0.92	0.89	0.91	0.88
12	100	0.92	0.91	0.91	0.90
13	100	0.92	0.91	0.91	0.91
14	100	0.92	0.89	0.90	0.87
15	100	0.92	0.89	0.91	0.88
16	100	0.92	0.91	0.91	0.89
17	100	0.92	0.88	0.90	0.86
18	100	0.92	0.89	0.90	0.88
19	100	0.93	0.91	0.92	0.90
20	100	0.93	0.92	0.92	0.92

Table 5.5: Sample size of the domestic grid systems and goodness of biharmonic fit (r^2) for their optimal battery size.

for the 92 samples stratified by supply ratio to demand, shown in table 3.4, so the total number of tested systems is 92 x sample size, plus the null system with zero inputs. The goodness of fit measured by r^2 shows a slight increase as the number of households increase, possibly as the samples begin to converge to give a more regular domestic load profile. The increase in network load (averaged over the systems' 25 year lifetimes) is shown in figure 5.23.

All sizes of network returned optimal systems with zero PV capacity and wind capacity high for $EROI_{out}$ performance, or mid to large-sized wind capacity when using $EROI_{used}$, similar to with single households. Wind capacity is shown in figure 5.24. There is possibly a trend of increasing wind turbine capacity for E_uLOLP-optimal systems, but the results are so erratic that very little can be strongly observed. These erratic results can be explained by viewing the overall systems result for the largest networks in figure 5.25. While the plateau for maximum E_uEIR performance has been narrowed with respect to PV capacity (recall E_uEIR results had a wide plateau for maximum performance) there is still a broad range of wind-only systems that achieve very similar E_uEIR results. Therefore very small changes in input sample data can shift the maximum point of this plateau from 0.6 up to 2 without much of a change in performance.

Optimal battery capacities show a stronger relationship to the size of the network, decreasing logarithmically as network size increases. Here there is also more visible difference between the different security metrics, as $LOLP$ derived optimals use notably larger batteries than with EIR for all sizes of network. It was expected that larger networks would add to the system's security by diversifying the load, reducing the need for batteries, and this graph shows that batteries do indeed offer much less value to the system when the network is larger. However they are still useful, unless using $EEIR$ results.

All performance measurements of the networks (figure 5.27 showed improvement as more households were added. These improvements mirrored the sizing of the batteries, as the

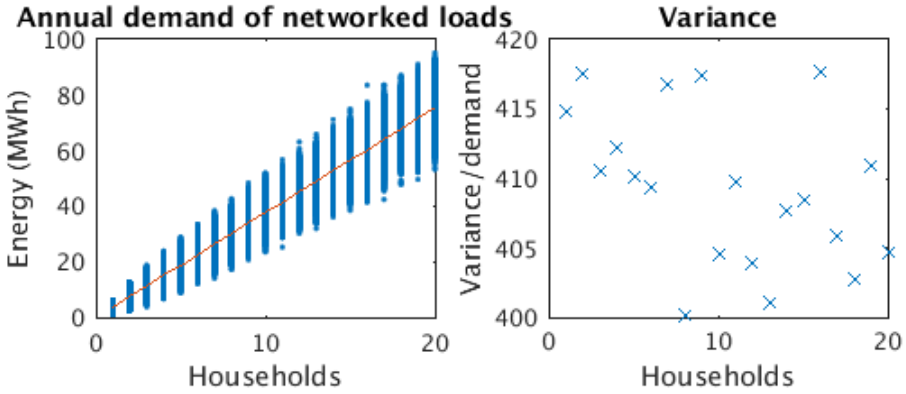

Figure 5.23: Demand samples for the network models. As the network increases in number of households, the spread of annual demand increases, but variance shows no significant change when size of demand is taken into account.

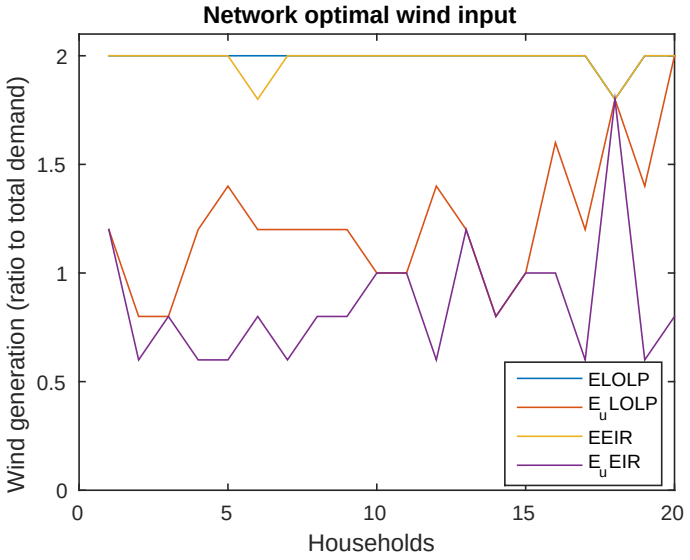

Figure 5.24: Optimal wind capacity for networks of increasing size. Wind capacity remains at 200% of demand for $ELOLP$ and $EEIR$-optimised systems, and shows some increasing under E_uLOLP but not E_uEIR.

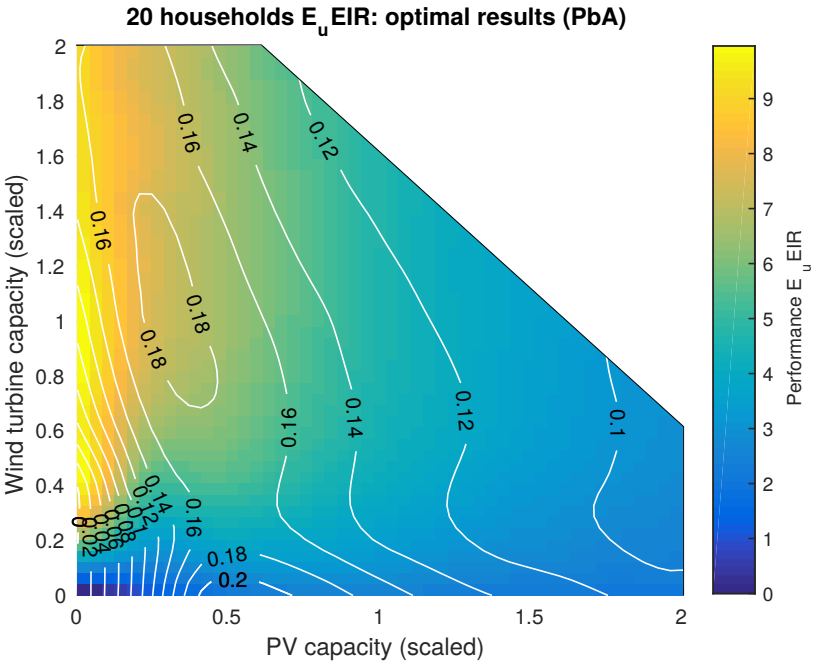

Figure 5.25: Optimal wind capacity for networks of increasing size. Wind capacity remains around 200% of demand for $ELOLP$ and $EEIR$-optimised systems, and shows some increasing under E_uLOLP but not E_uEIR, but results are not strong enough to make this a convincing trend.

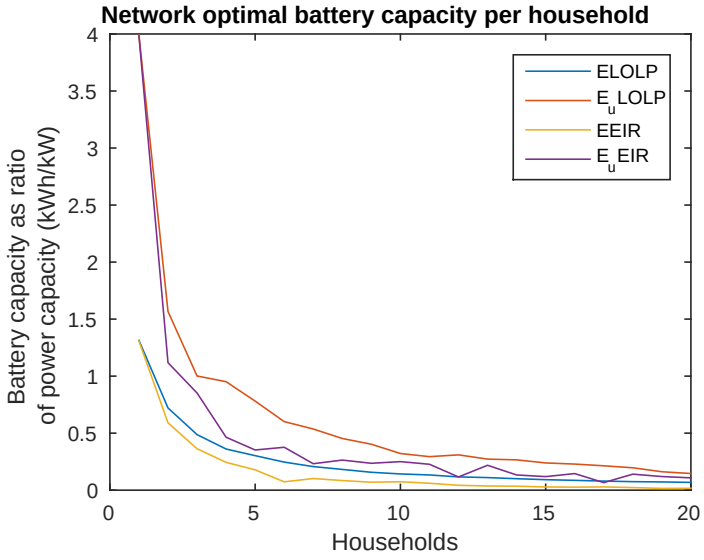

Figure 5.26: Optimal battery capacity per household for networks of increasing size, where all optimisations show a logarithmic decline.

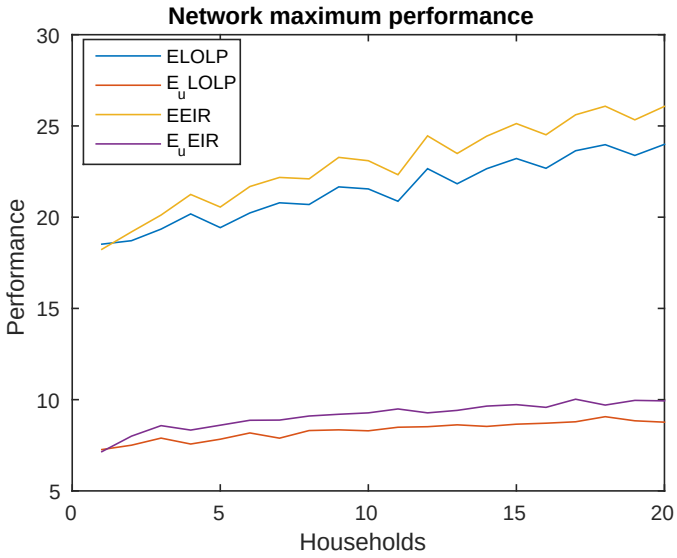

Figure 5.27: Performance at the optimum for networks of increasing size. Performance measured by $ELOLP$ and $EEIR$ increases slightly erratically, while E_uLOLP and E_uEIR are smoother but show less of an increase.

optimisations with smallest batteries had the greatest increase, and vice-versa.

However splitting the performance into EROI and security gives much less clear results when $EROI_{used}$ is involved, as their values are much more sensitive to the erratic optimal wind capacities for each network. While $EROI_{out}$ increases regardless of the security metric applied, $EROI_{used}$ fluctuate, showing a non-significant increase, and their security results show no particular overall trend.

Plotting these security results against the optimal wind capacity shows that it is indeed the fluctuating wind capacity giving these results, and that the larger wind capacities are giving higher security. The correlation ρ between $LOLP$ and E_uLOLP-optimal wind capacity is -0.99, and the correlation between EIR and E_uEIR-optimal wind capacity is 0.99, while the equivalent correlations with battery capacity are 0.13 and 0.22 respectively, showing almost no relationship.

Returning to figure 5.29, security for grid-exporting networks (using $EROI_{out}$ actually decreases as more households are added. This decrease is caused by the drop in battery capacity; while networked demand provides some level of security, this does not entirely replace the security lost by reduced battery capacity.

Finally, systems allowed to export to the grid show some proportional increase in exported energy as more households are added to the networks when using $EEIR$-optimal systems; this is due to their smaller batteries. $EEIR$ and $ELOLP$-optimal systems end up exporting a great deal of energy, such that more is exported than used. This however is to be expected when the systems produce 200% of demand. When using the $EROI_{used}$ metric this level of export is lower, particularly when using E_uEIR optimisation which remains below 50% excess (as a percentage of annual demand).

Overall, the results show that added extra households to the system offsets an amount of battery capacity, however this substitution of load flattening is not as effective as the battery capacity lost, especially when it comes to limiting excess energy. EROI results do benefit greatly as the battery cost is reduced, however the costs of interconnection and smart-grid technology are unaccounted for in the analysis. To remain an improvement, this management network for

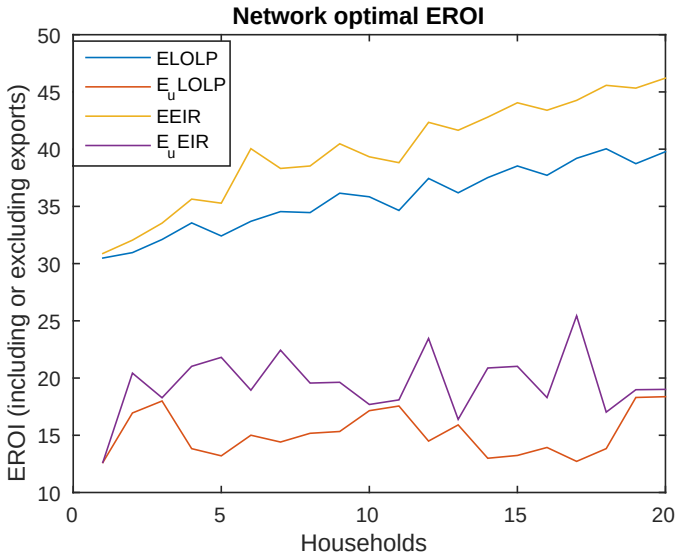

Figure 5.28: EROI values at the optimum for networks of increasing size. $EROI_{out}$ increases noticably, while $EROI_{used}$ changes erratically but shows no overall trend up or down.

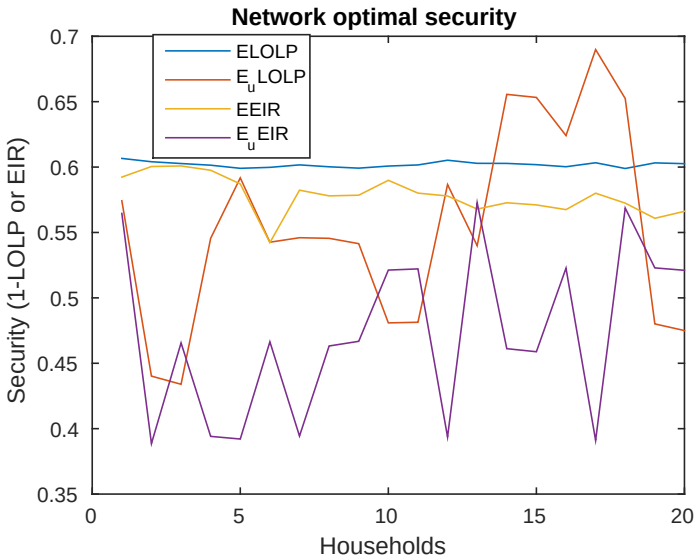

Figure 5.29: Security for optimal non-domestic systems. Security is erratic when $EROI_{used}$ is part of the optimisation, and shows little change otherwise. This is likely because of the choice of wind turbine size (see figure 5.30).

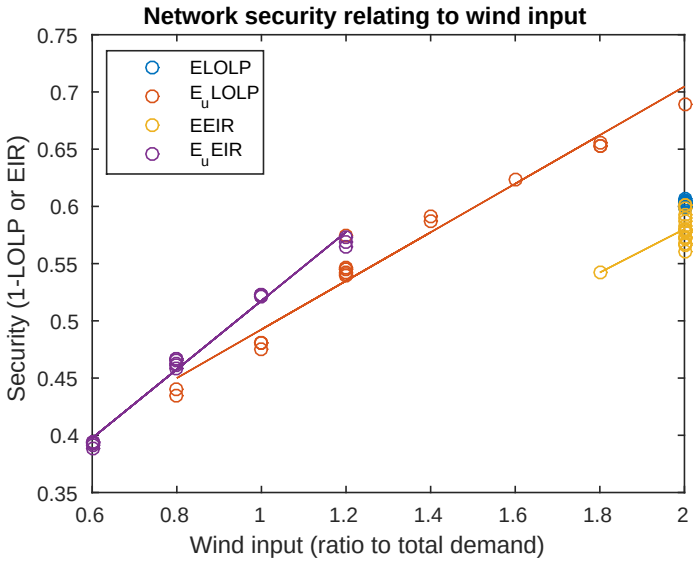

Figure 5.30: Security for optimal non-domestic systems, plotted against wind capacity. There is a stronger correlation between wind input size (which was shown to be unrelated to demand size) and security, so these results are shown instead of plotting against demand size. Note $LOLP$ is normalised to $1 - LOLP$ to better compare with EIR.

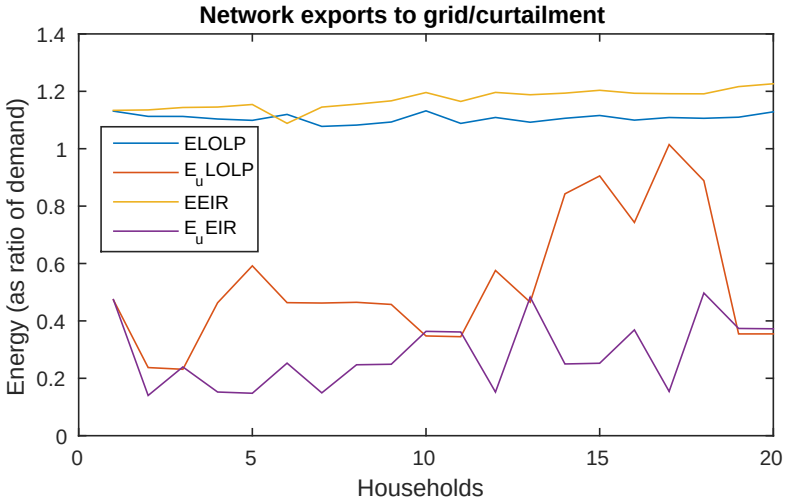

Figure 5.31: Energy exports/curtailment at the optimum for networks of increasing size. Results are scaled to energy demand, to better compare networks at different sizes. Only systems under $EEIR$ optimisation show any noticeable increase in excess energy. Using $EROI_{out}$ optimisation produces very high rates of excess energy, above 100% of demand.

n households cannot exceed an embodied energy cost of xkWh, where

$$x = E_{in}(n) \cdot \left(\frac{P(n)}{P(n)} - 1 \right)$$

with P being network performance measured by $ELOLP$, $EEIR$, E_uLOLP or E_uEIR, and E_{in} being the embodied energy of the network. Both are functions on the number of households.

5.3 Non-domestic systems

5.3.1 Characteristics of non-domestic load

The model was also run using non-domestic building demand. This was considered a necessary part of the analysis because household demand has a typical daily profile where evening demand is highest (shown in figure 3.10) but as non-domestic and industrial buildings are places where people work, the electricity demand is greatest during the daytime. Regarding the specific loads used in the model, all household average daily profiles are shown in figure 5.32, which can be compared to the daily demands of the non-domestic loads in figure 5.33 (both at a half-hourly resolution). These household demands show peaks of demand in the morning in addition to the evening, from households with Econ 7 tariffs which incentivise off-peak electricity use. In contrast, most of the non-domestic loads have either a flat demand from mid-morning until the evening, or a rounded peak around noon. This means that these buildings will be better positioned to use solar generation. There is also a much greater variation in size of demand between loads. The yearly demand for households, shown per day in figure 5.34, is at its lowest during the summer and highest during December and January, so when the sun is shining brightest their electricity demand is lowest. Non-domestic buildings have more differences between them in their daily demand across the year (figure 5.35, but around half show a similar dip in summer, while a couple show peak demand in summer and others are more erratic or have a fairly consistent demand across the year. This will depend on the use of the building, for example the gaps in demand for Load 3 match to holidays, as it is the electricity demand of a school.

Therefore using these alternate demand time-series in the model can show how much of an effect the daily profile has on the system's optimal state, particularly in relation to PV capacity. A secondary consideration, referring back to section 4.3, is that non-domestic demand is less variable hour by hour than domestic demand. This is shown by the longer power integral time scales of non-domestic demand (3-6 hours rather than 1-2), and the greater number of frequencies picked out by Fourier analysis at non-daily frequencies. This is why the daily profiles in figure 5.33 are much smoother than those in figure 5.32, and so this analysis can be compared to the network systems of the previous sections. Comparing battery requirements and security levels can therefore explain to what extent batteries can be useful for unexpected peaks in demand typical of small household loads, in comparison to predictable regular demand.

5.3.2 Results for non-domestic system model

As the difference between different non-domestic annual demand loads is considerable, and the tested range of battery capacity is scaled to annual demand, results are not averaged between loads as with the domestic demand, but taken separately and compared to demand size, similar to the network results. Figure 5.36 shows the optimal wind power capacity of thes non-domestic systems, which has some similarities to the networked household systems. Optimisation with $ELOLP$ continues to give maximum wind capacity, however $EEIR$ shows some systems with smaller optimal wind capacities. These systems also have no battery capacity.

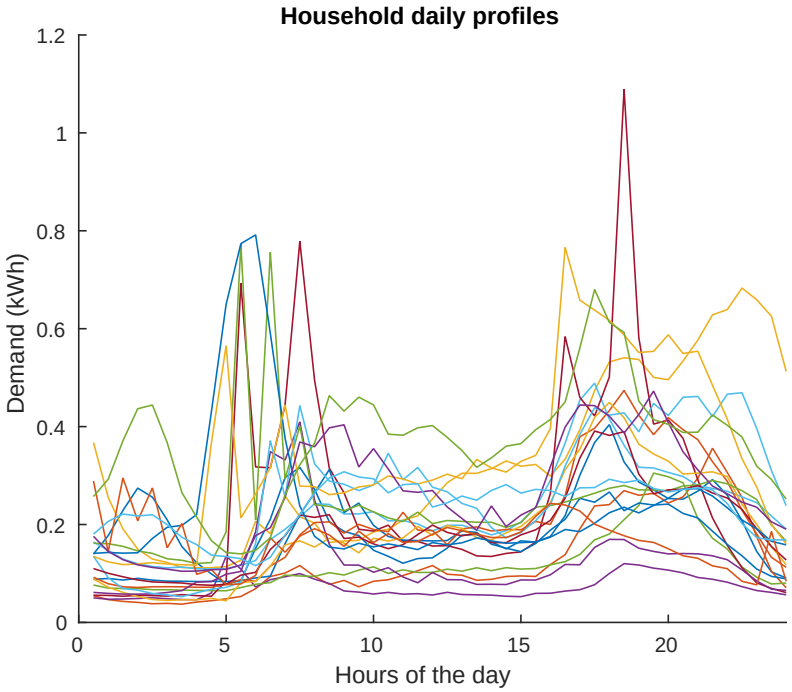

Figure 5.32: Average daily profile over year 2008 for each household. Peaks exist in the morning and the evening, showing a level of anti-correlation with PV generation.

Wind capacities are all lower when optimising with E_uLOLP or E_uEIR; the former still provides a total energy supply of around 100% annual demand, however the latter frequently shows significant underproduction, with a reduction in supply for some larger loads. There is a group of smaller loads that show higher wind capacity, and it is shown below that these also use a higher battery capacity. The considerable scattering of these results shows an increased sensitivity of E_uEIR to the specific load, there being a differentiation between these loads that did not exist for the generalised household model.

Observing optimal battery capacities in figure 5.37, it is notable that $EEIR$ optimisation gives zero optimal battery capacity for nearly all non-domestic systems. E_uEIR optimisation also gives zero battery for some systems, and a rapid decline in capacity for the non-zero results as annual demand increases. In contrast, $ELOLP$ and E_uLOLP show some decrease in battery capacity, but always return non-zero results. All trends here are linear or unclear, a direct contrast to the logarithmic decreases for network results in figure 5.26, because there is no smoothing of the load as annual demand increases.

To investigate the reason for the zero battery optimisations, $EEIR$ results for all wind and PV capacities were viewed for non-domestic load 1 in figure 5.38. This shows that battery capacity is only ever suggested for systems with more than a certain PV capacity, and the change is very sudden from zero to $100kWh$ optimal capacity. Load 1 is chosen here as an example, but this is exhibited for all non-domestic loads. If wind capacity is also included then battery capacity is required for smaller PV capacity, but otherwise the results show that batteries are only required for high PV use. This suggests that underproduction poses less of an issue for non-domestic loads, but that $LOLP$ is not precise enough to pick up on this. In fact, the $ELOLP$ and E_uLOLP optimal battery capacities are lower than would be expected if comparing to domestic systems, but higher than large domestic networks; they are roughly

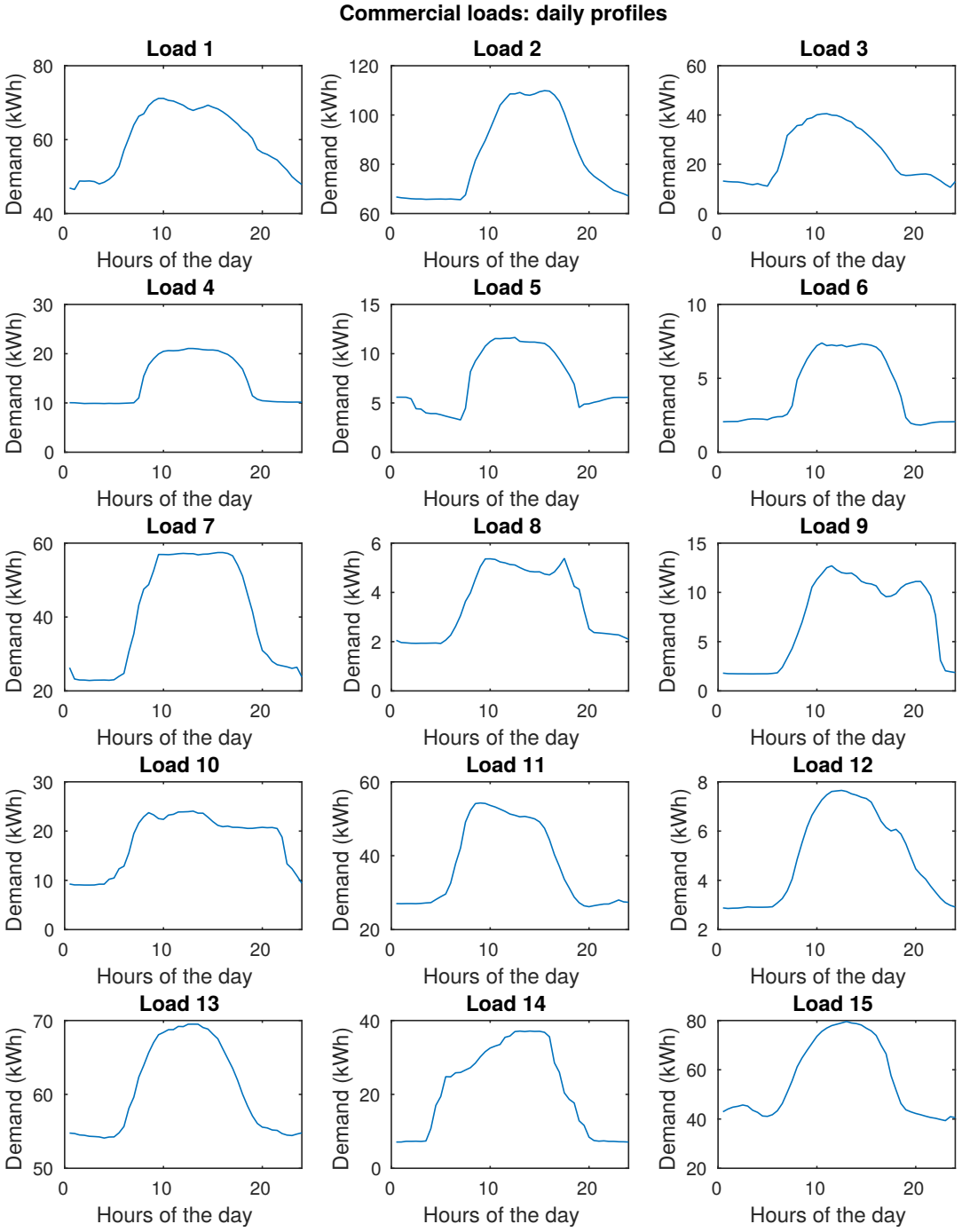

Figure 5.33: Average daily profile for commercial loads. Peaks generally exist at or around noon, giving high correlation with PV generation.

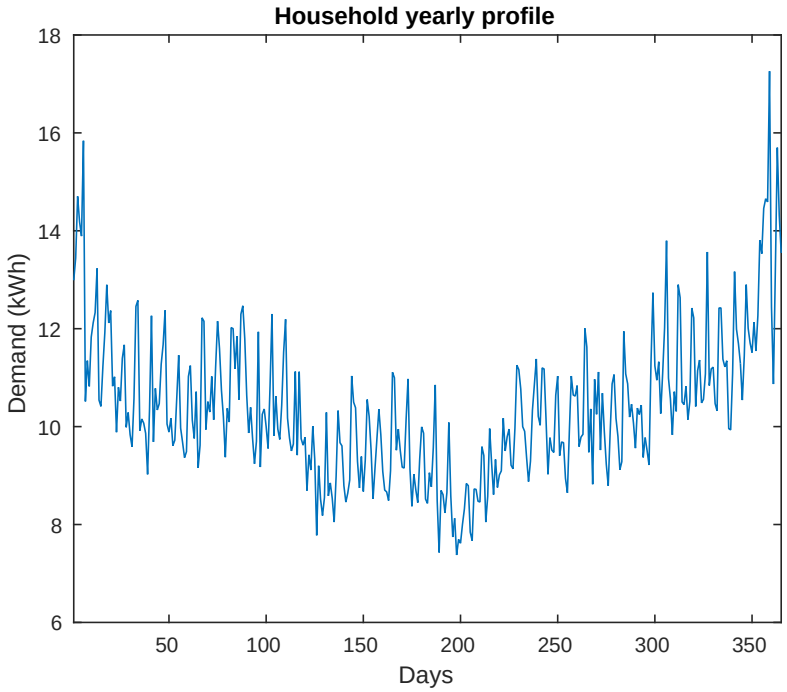

Figure 5.34: Daily time-series over the year for averaged household loads. Demand is lowest in summer and highest in winter, so is again anti-correlated with PV generation.

comparable to networks of 2 households.

This can be explained by returning to the demand profiles. While non-domestic loads with larger annual demand do not have a flatter demand profile in the same way as networked systems, the non-domestic demand is inherently flatter than non-domestic demand, as was shown by the time-scale analysis of non-domestic demand loads in section 4.3. There it was shown that the time-scale of household demand was 1-2 hours, while the time-scale of the non-domestic loads was 5-10 hours, defined by the length of the working day. This means that fluctuations in the non-domestic load are much slower than fluctuations in the household demand, giving a more steady and consistent load that is less reliant on energy storage. In particular, EIR is very sensitive to this reduced dependency on batteries.

The reduced optimal battery capacity under other optimisations cannot be explained by any flattening of the load, as the PITS results showed no positive correlation with total demand, so the reduction in battery capacity must be caused by something else. Further investigation shows that

Figure 5.39 shows increase in performance similar to that seen in domestic grids in figure 5.27, excluding the initial sharper incline, as no notable smoothing of demand occurs. This increase in performance for $ELOLP$ and E_uLOLP comes mostly from their sustainability levels (figure 5.40), as energy security results in figure 5.41 show a high level of scattering, and even a decrease in security under E_uLOLP. The strongest increase in security (in terms of fit strength $r^2 = 0.7$ and gradient steepness) comes from $EEIR$ optimisation, where batteries are unused for all optimal systems. $EEIR$ optimisation also gives the highest $EROI_{out}$ values, as does E_uEIR for the highest $EROI_{used}$ values.

In fact, EIR shows an increase in security whether using $EROI_{out}$ or $EROI_{used}$, whereas $LOLP$ always shows stagnant or decreasing security. Given that battery capacity does not

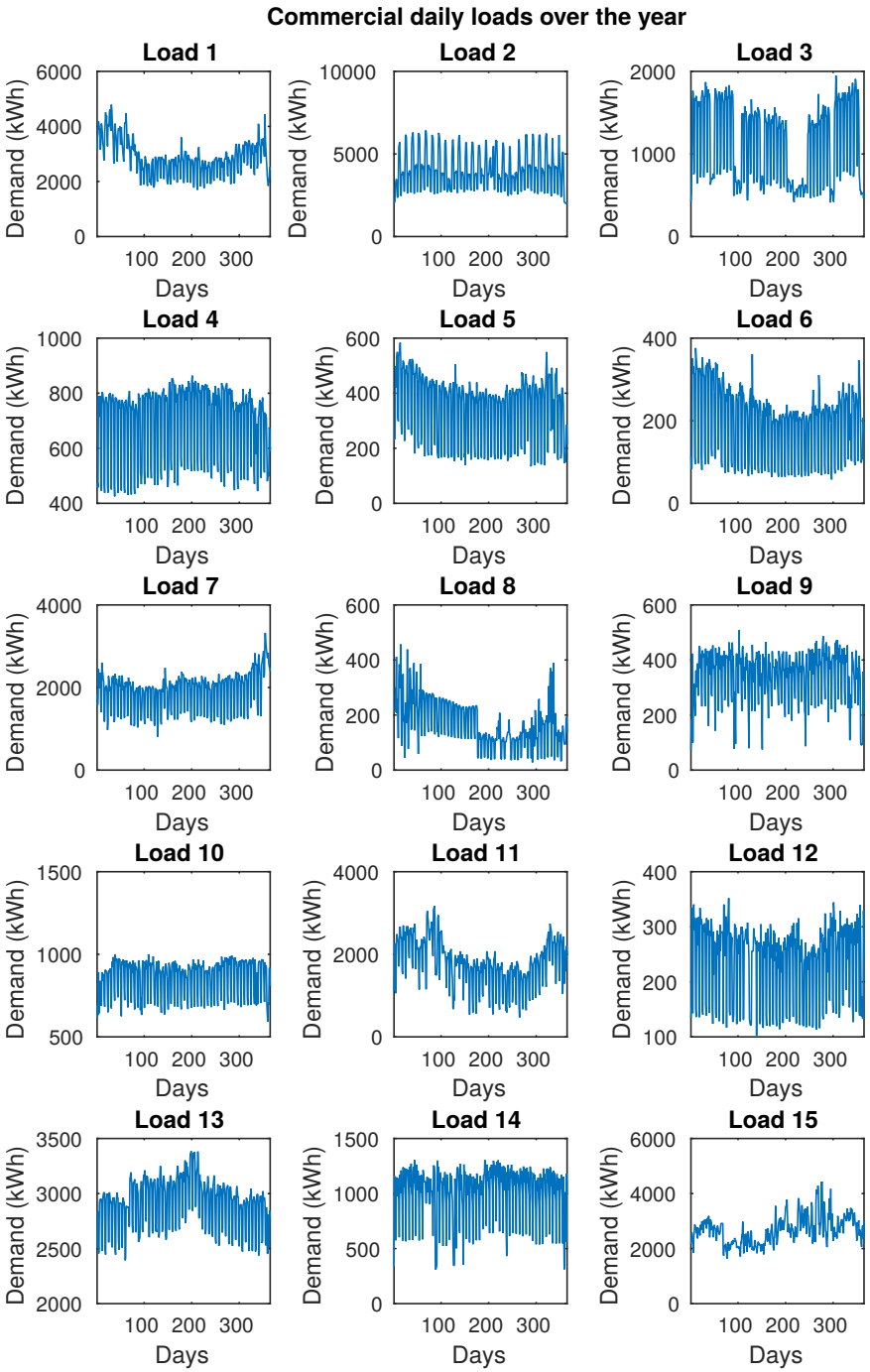

Figure 5.35: Daily time-series over the year for commercial loads. Much variety exists; while most have less demand in summer, some peak in summer and others are erratic or consistent over the year.

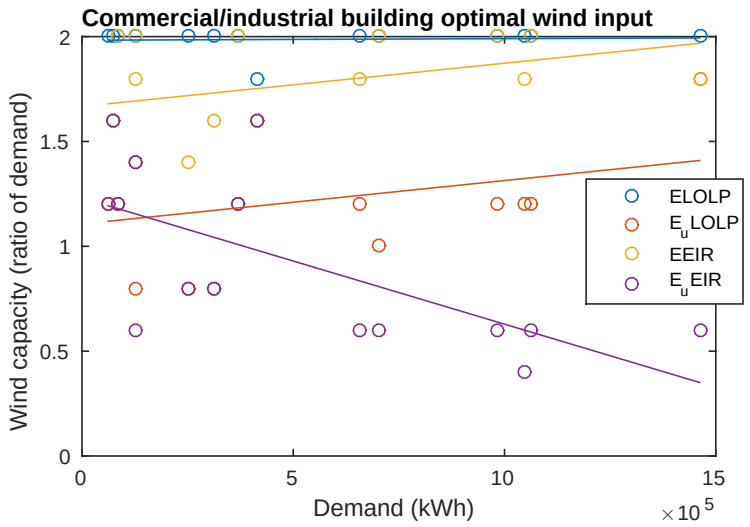

Figure 5.36: Optimal wind capacity for non-domestic systems, plotted against annual demand. $ELOLP$-optimisation gives the maximum 200% wind input for nearly all loads, but $EEIR$ appears more sensitive to specific loads, showing lower wind capacity for some smaller loads. When forced to curtail excess production, wind capacity is reduced further, especially when optimising with E_uEIR, resulting in under-capacity for most of the systems, especially the largest loads.

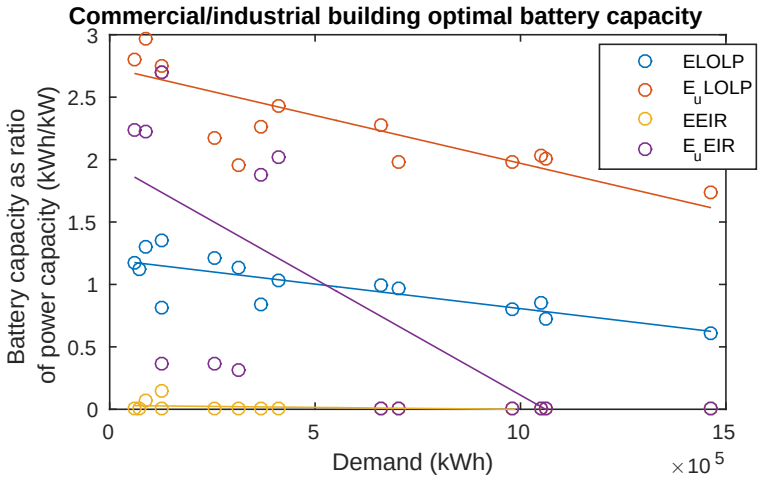

Figure 5.37: Optimal battery capacity for non-domestic systems.

Load ID	$ELOLP$ r^2	E_uLOLP r^2	$EEIR$ r^2	E_uEIR r^2
1	0.94	0.91	0.93	0.89
2	0.96	0.96	0.97	0.96
3	0.95	0.94	0.94	0.94
4	0.92	0.88	0.91	0.86
5	0.93	0.88	0.91	0.84
6	0.93	0.92	0.92	0.92
7	0.96	0.95	0.96	0.94
8	0.93	0.91	0.91	0.90
9	0.93	0.93	0.93	0.93
10	0.94	0.92	0.93	0.92
11	0.96	0.94	0.96	0.94
12	0.94	0.92	0.93	0.91
13	0.95	0.93	0.95	0.93
14	0.93	0.92	0.92	0.91
15	0.95	0.94	0.95	0.94

Table 5.6: Non-domestic loads and their annual demand, and r^2 goodness of biharmonic fit for their optimal performance.

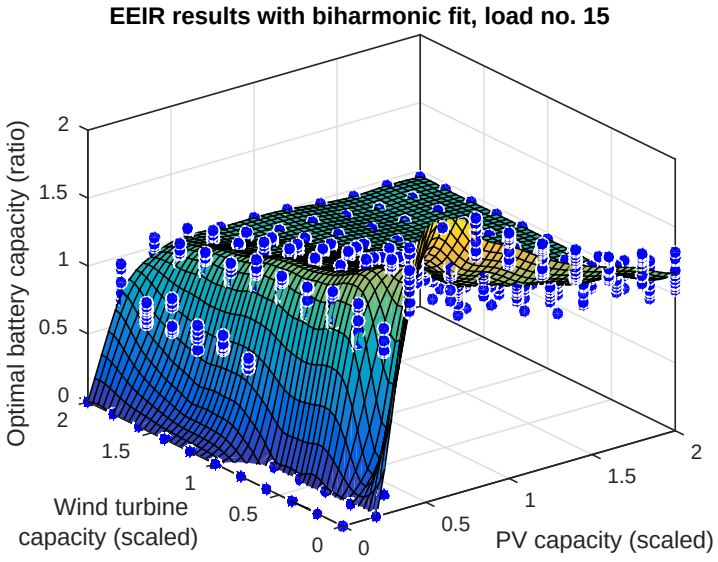

Figure 5.38: Example $EEIR$ optimal battery capacity results for non-domestic system samples with load 15. Systems with low PV capacity always give an optimal battery capacity of zero, and the change to include battery capacity is very abrupt once a minimum threshold of PV capacity is reached.

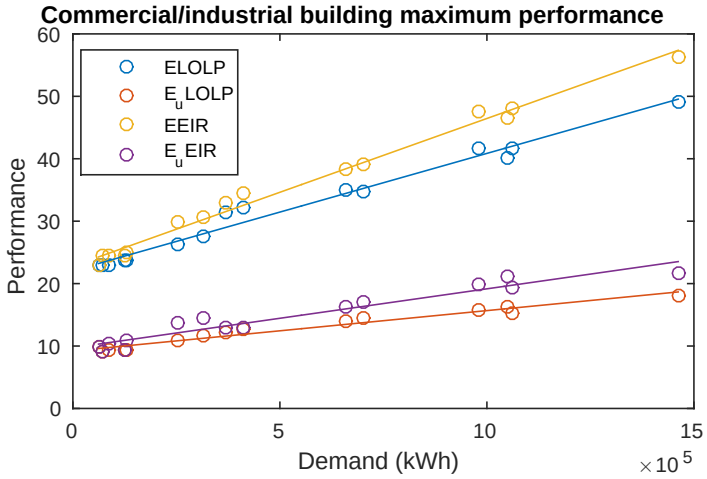

Figure 5.39: Performance at the optimum for non-domestic systems. Performance increases slowly for all objective functions.

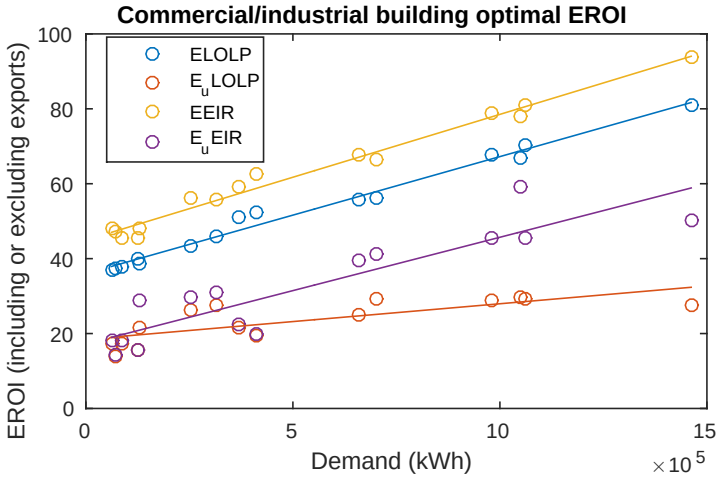

Figure 5.40: Sustainability for optimal non-domestic systems, which always increases.

increase with demand, and remains zero for almost all $EEIR$ results (where security has the strongest increase), this increase is more likely to be linked to an increase in supply, hence why $ELOLP$ and E_uEIR show no increase.

This link between wind capacity and security is made clearer in figure 5.42 where the security results for $EROI_{used}$-derived optimisations are shown to be more related to their wind capacities, as with the networked household systems. However specific demand still does play a part, for example in the E_uEIR optimal results where loads are split into two types: those that optimise to give good security through high wind and battery capacity, and those that optimise for underproduction and zero/small storage, but give higher $EROI_{used}$. The former systems tend to be smaller, but the latter types can be all sizes. Furthermore, the small sample of possible loads cannot possibly represent all types of commercial and industry electricity loads, as there is much diversity in the types of buildings and their functions. Examining the daily or yearly profiles in figures 5.33 or 5.35 does not show any obvious reasons that they would differ, as the loads 3, 6,8 ,9 12 and 14 (those with larger optimal

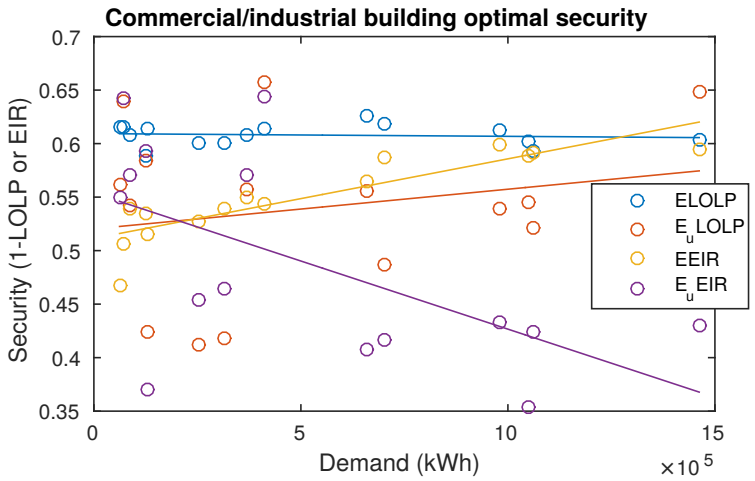

Figure 5.41: Security for optimal non-domestic systems. EIR increases but non-exporting systems show much scatter of security results, and $LOLP$ either decreases or stays the same. Goodness of fit r^2 is shown in brackets for each metric in their legend.

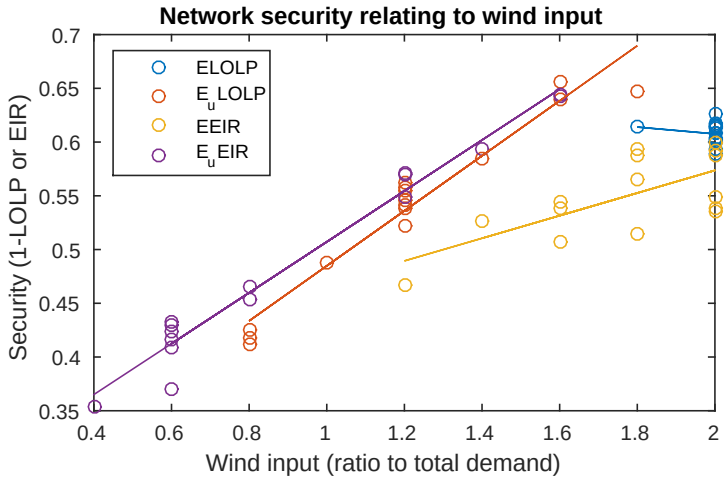

Figure 5.42: Security for optimal non-domestic systems, plotted against wind capacity. The more varied wind capacities under $EROI_{used}$-derived optimisation show the most correlation with security.

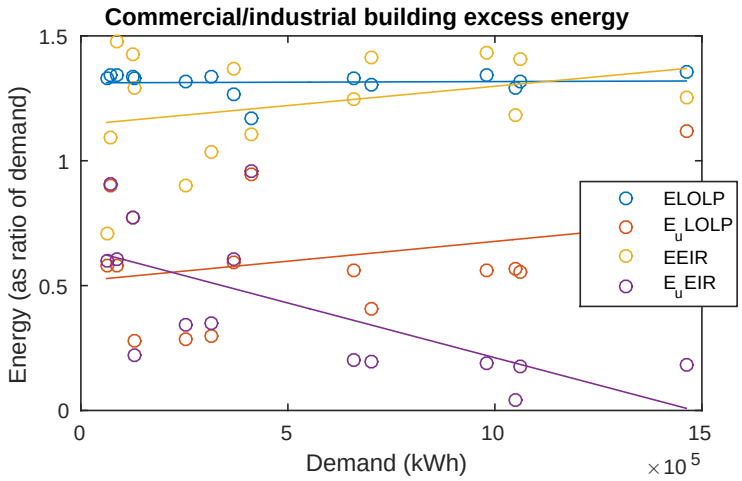

Figure 5.43: Energy exports/curtailment at the optimum for non-domestic systems. In contrast with networked household systems, excess energy production never increases as a proportion of demand.

capacities) show no great difference to the other loads. Furthermore, their time-scale (PITS) are in the same range as the others, so their time-series are not noticably more variable on an hour-by-hour basis.

The systems' excess energy levels shown in figure 5.43 are similar to those of networked household systems, but with more variation for the $ELOLP$ results (however it has a flat linear fit like the networked systems) and decreasing excess energy for the E_uEIR results. This decrease is due to the very low wind turbine capacities, so is indicative of underproduction rather than good levels of security.

In summary, these results show that even if there is not visible flattening of the demand load when demand increases, larger systems generally have increased EROI and increased EIR. EROI results are increased much more than for the networked household systems, with even $EROI_{used}$ reaching 50, up from 12 for single household systems. This linear growth in EROI is partly due to more efficient larger wind turbines, and partly from the reduced reliance on battery storage.

One negative result is particularly important: even though the loads were observed to have a demand profile well suited to PV supply, with a peak at mid-day, PV was still too costly to be included in the optimal systems. Two possible reasons are that winter months will still underproduce with a PV system unless the system is oversized, and that batteries are capable over of spreading PV production to meet overnight demand (as seen in the summer months for household systems) so that the actual demand profile becomes less important.

5.4 Correlation analysis for single household systems

Certain relationships between variables have already been noted from the results so far, such as a tendency for PV capacity to decrease EROI and increase security, or wind capacity to do the opposite. The strength of these relationships was evaluated in this section by using correlation analysis. This allows us to compare how size of solar and wind generation inputs affect the system's optimal results; whether it is just as simple as there being more correlation between solar capacity and storage requirements, or if more complexity is involved. The correlation is measured using Pearson's correlation coefficient ρ:

$$\rho_{X,Y} = \frac{\text{cov}(X,Y)}{\sigma_X \sigma_Y}$$

This correlation measures linear relationships, but using the graphs in section 5.1 can show whether a low correlation is due to a non-linear relationship or simply no interdependency.

Finding relationships between the results from each objective function is also useful in order to evaluate their usefulness. It has already been observed that the $ELOLP$ and $EEIR$ objective functions produce very similar results, and further investigation is required to decide which objective functions should be carried on for later use.

5.4.1 Correlation of inputs with outputs

This section discusses the correlation levels between system inputs and the characteristics of each optimised system, over all 18,400 modelled single household systems. Results for PbA systems are shown in table 5.7 as representative of all types of battery systems. Note that when interpreting this table that it shows correlation between the results when optimised for battery capacity, so these patterns are not necessarily indicative of the technology by itself, but how it behaves when optimised for battery capacity.

Note that the battery capacity itself is normalised to generation power capacity as in the graphed results; therefore positive correlation of any variable X with battery capacity does not merely mean that when X increases as does absolute battery capacity, but that an increase in X gives more value to the battery, so its capacity increases per unit of power generation.

These correlation results demonstrate how complex the outcomes can be when optimising the energy systems, as very few strong correlations exist. Two of the strongest are the ones between wind capacity and $EROI_{out}$-derived performance, being 0.87 and 0.86 for $ELOLP$ and $EEIR$ respectively. However wind capacity is less well correlated with the individual EROI and security metrics. In direct contrast, PV capacity is not particularly well correlated with $ELOLP$ or $EEIR$, but is better correlated with the EROI and security metrics; these are cancelled out as it is negatively correlated with EROI but positively correlated with security. These results suggest that when optimising for wind or PV, wind provides added $EROI_{out}$ and a little security, performing well overall, whereas PV provides much more security, but at large cost to $EROI_{out}$, ultimately bringing the performance down.

Results with the $EROI_{used}$-derived metrics are similar, but with some noted differences. Wind capacity has a stronger relationship with security than $EROI_{used}$, but both have a positive correlation. This gives a positive correlation between wind capacity and E_uLOLP or E_uEIR, but here PV has a stronger correlation, showing that PV performs better when excess energy is discouraged. The correlation with excess energy is strongest with total generation, but is notably stronger with wind input than PV for all battery technologies.

When PV and wind capacity are considered together, we see that this total capacity is strongly correlated ($\rho \approx 0.87$) with security in all cases, but is less well related to performance - with no correlation when $EROI_{used}$ is involved - due to its anti-correlation with EROI, however this relationship is not particularly strong because of the complex relationships involved.

The most complex relationships exist with the optimal battery capacity. In particular, the relationship between PV capacity and battery capacity cannot be summarised using these correlation values, as there is a strong non-linear relationship that they do not detect. The graphs in section 5.1 showed a peak in battery capacity when PV provided 50% of annual demand, so this is where batteries are able to provide the most value to the system for any given wind input. The relationship between wind and battery capacities is also complex; when PV input is low (below 50% of demand), increasing wind capacity gives more value to the

Output	PV	Wind	PV + wind
$ELOLP$-optimal results			
$ELOLP$	-0.47	0.87	0.37
$EROI$	-0.69	0.51	-0.16
$LOLP$	-0.66	-0.29	-0.86
Battery	0.04	-0.40	-0.33
Excess	0.35	0.54	0.80
E_uLOLP-optimal results			
E_uLOLP	-0.73	0.63	-0.09
$EROI_{used}$	-0.73	0.14	-0.54
$LOLP$	-0.59	-0.37	-0.87
Battery	-0.58	0.00	-0.52
Excess	0.38	0.52	0.81
$EEIR$-optimal results			
$EEIR$	-0.48	0.86	0.35
$EROI$	-0.68	0.47	-0.19
EIR	0.65	0.31	0.87
Battery	0.12	-0.32	-0.18
Excess	0.34	0.54	0.79
E_uEIR-optimal results			
E_uEIR	-0.73	0.63	-0.09
$EROI_{used}$	-0.70	0.12	-0.53
EIR	0.57	0.42	0.89
Battery	-0.49	0.06	-0.39
Excess	0.38	0.52	0.81

Table 5.7: Correlation between input variables of power capacity and all optimal results for PbA battery systems, including excess energy generation (whether that is exported or curtailed).

Output	$ELOLP$ vs $EEIR$	E_uLOLP vs E_uEIR
Performance	-0.99	-0.99
Optimal battery capacity	0.92	0.99
EROI	0.99	0.99
Security	-0.99	-0.99

Table 5.8: Correlation between $ELOLP$ and $EEIR$ optimal results (first column), and ${}_uELOLP$ and E_uEIR optimal results (second column). EIR and $LOLP$ show almost perfect correlation, except for optimal battery capacities with $EROI_{out}$.

Metrics ρ	$EROI_{out}$	$EROI_{used}$
$1 - LOLP$	-0.47	-0.68
EIR	-0.49	-0.64

Table 5.9: Correlation between security and EROI optimal results within all four objective functions.

batteries, but when PV input is higher, increasing wind or PV capacity actually decreases the batteries' value. Therefore the most important factor in the batteries' value is PV availability.

5.4.2 Correlation between objective functions

All four objective functions are designed to evaluate performance with respect to sustainability and security, so it was expected that they would have highly related results. Measuring these relationships is therefore a necessary part of metric evaluation. Furthermore, measuring the relationships within these objective functions - namely between their sustainability and security - brings a new perspective on the difficulty of satisfying the trilemma.

Firstly, when comparing the security metrics in table 5.8, it is clear that they are strongly correlated with $\rho = 0.99$ in almost all cases. The only exception is for battery capacity, which was noted in section 5.1 where the difference between $ELOLP$ and $EEIR$ optimal battery capacities reaches a maximum of 0.5 for several sizes of wind input (see figure 5.12). However using $EROI_{used}$ removes this discrepancy, and correlation is still very high at $\rho = 0.96$.

While this does not mean that using either metric will always return the same results, it does mean that the trends in energy security are represented equally well by $LOLP$ or EIR. This can also be seen in table 5.7 where $ELOLP$ and $EEIR$ return very similar correlation results, although there is slightly more difference between the E_uLOLP and E_uEIR results.

This similarity means that the choice of security metric can be made freely, on the basis of which is more well suited to the scenarios. Therefore in the light of EIR being potentially more accurate, and more appropriate for grid-connected systems, any future analyses will use EIR rather than $LOLP$.

Moving onto the relationship between EROI and energy security, table 5.9 shows that while they are not directly related, they experience some negative correlation of around -0.48 when using $EROI_{out}$, or around -0.66 when using $EROI_{used}$. There is a stronger negative relationship when the system cannot export excess energy, as increased generation capacity improves security but reduces $EROI_{used}$ through risk of overproduction. This does back up the argument that as renewables penetration of the grid increases, security is more at risk when sustainable sources are put as the main priority, however the lack of a very strong correlation means that this is not absolute.

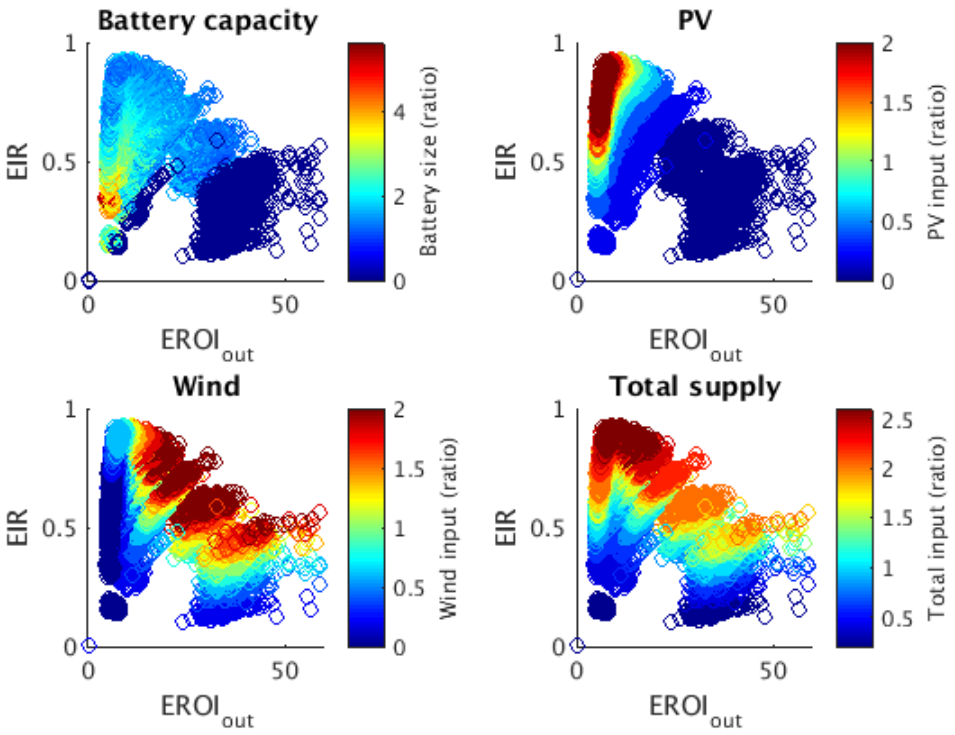

Figure 5.44: Plots of all the systems' $EROI_{out}$ and EIR results, when optimised with respect to battery capacity. Each graph shows the same position of points, but systems are colour-coded differently to illustrate trends in battery capacity, PV, wind and total supply.

These relationships need to be plotted to fully understand their complex relationship. These results are shown for $EROI_{out}$ and EIR in figure 5.44, where it can be seen that increasing PV capacity has different impacts on the metrics depending on wind capacity, and vice-versa. Increasing PV capacity can improve $EROI_{out}$ and EIR if no wind is included in the system, however in some hybrid systems, adding PV capacity can reduce $EROI_{out}$ with only a marginal increase in EIR.

The graph shows segmentation between systems with different PV capacities, most notably for the systems with lowest PV capacity. When PV is increased, these segments become narrower and shift diagonally upwards and left, reducing in $EROI_{out}$ and increasing in EIR. This segmentation shows that adding PV to the system creates significant change, and the narrowing of segments shows that wind-only systems are more diverse in their optimal results.

Plotting $EROI_{used}$ against EIR in figure 5.45 shows a similar pattern, but the wind-only systems are more ordered and the wide segment at the top of the graph has gone. This segment contained a number of systems that showed relatively higher $EROI_{out}$ results for their EIR result, so by disallowing energy exports, these systems have dropped in performance. These were systems with good energy resources, so were producing slightly more energy and using that to gain high EIR at lower cost. However this means that their $EROI_{used}$ result would be much lower, moving them to the left.

PV-only systems (on the far left) are largely unchanged, however they already exhibited negative correlation and the changes noted above are enough to increase the graph's negative correlation, giving the $\rho = -0.68$ result.

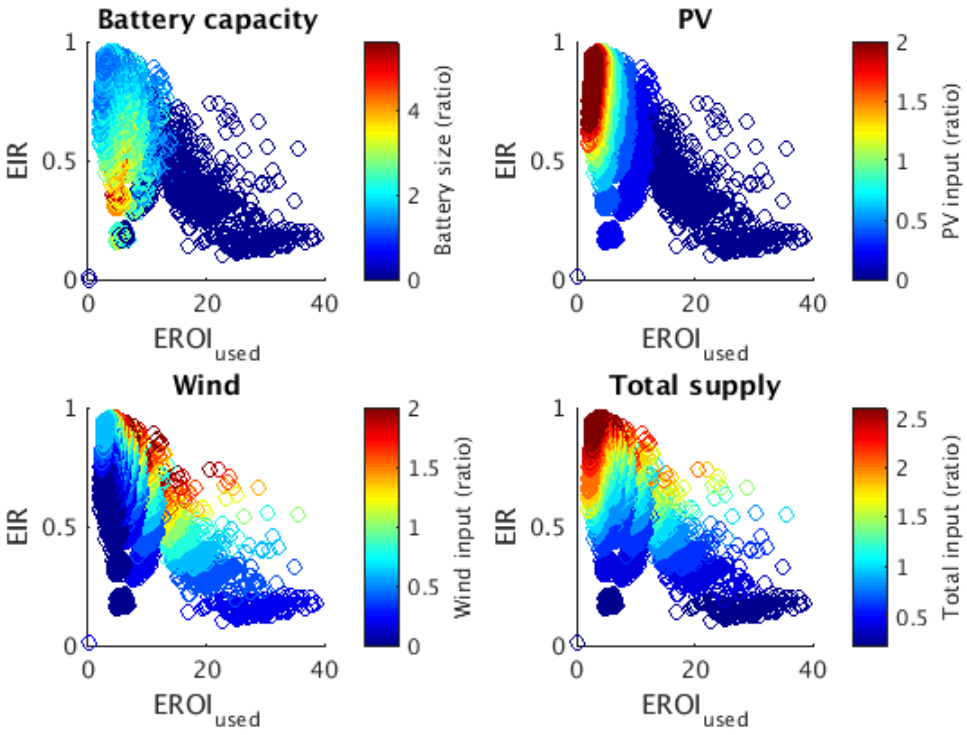

Figure 5.45: Plots of all the systems' $EROI_{used}$ and EIR results, when optimised with respect to battery capacity. Each graph shows the same position of points, but systems are colour-coded differently to illustrate trends in battery capacity, PV, wind and total supply.

5.5 Uncertainty and sensitivity analysis

The largest source of error in all of these optimisation results comes from the embodied energy values. As mentioned in section 2.4.6, these can vary widely depending on the calculation methods used, the boundary of the energy accounting, or the individual process. While the numbers chosen for this analysis were from similar methods of accounting, there will still have been small variations between each lifecycle analysis due to individual methodology or the depth of data available. All sections of the supply chain can be suspect to change, as different factories will have different energy intensities in their process, transport from different countries has a significant impact, and different materials will have different recycling levels. Uncertainty analysis can evaluate how the accuracy of the results is affected by these errors/variation within the lifecycle analysis. Different objective functions may be more sensitive to these errors, so understanding this variation can further help picking which methods are the most suitable to be carried forward.

There is also uncertainty in the values used for battery cycle efficiency. While in reality the mechanisms behind battery efficiency is very complex, depending on charge level, current, voltage, temperature etc, this simple model was unable to apply such mechanisms due to only measuring energy flows and running at a half-hourly resolution. However the possible ranges of average cycle efficiency are known, and were applied in an uncertainty analysis to find the impact of these values on the results.

Another form of sensitivity analysis was performed on the grid efficiency η_G value, itself valuable in determining the EROI but dependent upon the makeup of the grid. Additionally, as was discussed in the literature review, there are some doubts about whether it should be used at all. Results from these perspectives are presented to allow for a fuller discussion of η_G's implications.

5.5.1 Uncertainty analysis of embodied energy

Uncertainty analysis was applied to the embodied energy of all major system components (PV module, wind turbine and battery), using the range of values specified in table 3.6.

Uncertainty of PV embodied energy

The range of a multi-Si PV module's embodied energy was estimated to be $280 - 1,842 kWh$ per m^2, at -75% to +68% of the average value used in the main analysis. Running the model with these levels of embodied energy gives the level of uncertainty in the optimal system's component sizing, shown in table 5.10. In particular, reducing the embodied energy of a PV module results in a system with increased PV capacity and reduced wind capacity, while increasing it makes no difference as the PV capacity remains at zero. A wind turbine of capacity $10kW_p$ has embodied energy of $31MWh$, while a $10kW_p$ PV array with the lower embodied energy has total embodied energy of $22MWh$, which explains the system's preference for cheap PV. PV also brings added security to the system, as was noted in section 5.1, but these results show that only $EROI_{used}$ shows an increase as a result of reduced PV EE, while $EROI_{out}$ decreases, resulting in a lower increase in overall performance.

Indirect effects of lower PV EE include a reduction in wind capacity when using $EROI_{used}$, reduced from 1.2 to 0.6 when using E_uLOLP or E_uEIR. This is matched by an increase of PV by 0.6, so the total level of annual energy input remains the same. The optimal battery capacity is also reduced by 33%. Therefore when cheaper PV modules are used in non-exporting systems, it is no longer the case that you are better off increasing battery capacity than PV

Metric	Bound	PV Δ	Turbine Δ	Battery Δ	EROI Δ	Security Δ	Performance Δ
$ELOLP$	Lower	0.6	0	-13.7%	-7.4%	35.4%	25.0%
	Upper	0	0	0.0%	0.0%	0.0%	0.0%
E_uLOLP	Lower	0.6	-0.6	-32.7%	15.0%	30.9%	50.1%
	Upper	0	0	0.0%	0.0%	0.0%	0.0%
$EEIR$	Lower	0.6	0	-12.7%	-8.4%	35.7%	24.2%
	Upper	0	0	0.0%	0.0%	0.0%	0.0%
E_uEIR	Lower	0.6	-0.6	-32.6%	15.0%	28.0%	47.1%
	Upper	0	0	0.0%	0.0%	0.0%	0.0%

Table 5.10: Uncertainty results when taking upper and lower bounds of PV embodied energy with a PbA system. $LOLP$ is normalised to $1 - LOLP$ to allow comparison to EIR, so a positive change is an increase in security for either metric.

capacity to ensure improvements in security. Sustainability $EROI_{used}$ also increases overall, so performance increases by half.

The $EROI_{out}$-derived results are less sensitive, as there is no reduction in wind capacity (their overproduction suffering no penalty) and optimal battery capacity is only reduced by 13%. This being a proportional battery capacity, the total increase in power capacity means that there would be an absolute increase in optimal battery kWh capacity. This is the reason for the reduction in $EROI_{out}$, and greater increases in security. Ultimately $ELOLP$ and $EEIR$ are only increased by a quarter for cheaper PV modules.

Security metrics $LOLP$ and EIR are similarly sensitive to the increase in optimal PV capacity from reduced PV cost. They become less sensitive when the system cannot export excess energy (under $EROI_{used}$), increasing by a factor of approx 30% rather than 35%. However in general, the system's security is the most sensitive output when decreasing PV EE.

Uncertainty of wind turbine embodied energy

Determining the range of embodied energy values for wind turbines was difficult, as it was originally calculated in relation to the turbine power capacity, and there were not enough points to find the lower and upper boundaries over all power capacities. However, as the embodied energy of the wind turbines was chosen by a fit to the data, the upper and lower bounds of embodied energy were chosen to be the upper and lower bounds of that fit, giving the lower bound as $EE_l = (-1.5P + 2567)P$ and the upper bound as $EE_u = (-0.13P + 3595)P$. For a wind turbine of power capacity 10kW (the typical capacity required for the $ELOLP$ optimal, supplying 200% of demand), this would give the lower bound of embodied energy as 25.5MWh, upper bound as 35.9MWh, and a percentage range of ±17%.

While the range in uncertainty may be smaller than PV's, varying wind turbine embodied energy has a much greater effect on optimal battery capacity. This is shown in table 5.11, where taking the higher value results in a larger PbA battery capacity (by up to 44% depending on objective function) and taking the lower value reduces the optimal battery capacity by up to 94%. This is repeated for other battery technologies, and can be explained by considering that the energy cost of the wind turbine essentially gives its generated energy an imbued cost: the greater the cost, the greater the loss if this energy is unused. Therefore if wind turbines have a greater embodied energy, there is an incentive to use larger batteries to store more of this energy. This in turn has an effect on the sustainability and security of the system, as all security metrics show a slight loss in security with lower embodied energy values, and a slight gain for higher values. The gain in security for greater embodied energy values appears very small in comparison to the gain in storage capacity, except for the E_uLOLP optimised systems, but this

Metric	Bound	PV Δ	Turbine Δ	Battery Δ	EROI Δ	Security Δ	Performance Δ
$ELOLP$	Lower	0	0	-17.52%	17.17%	-2.24%	14.49%
	Upper	0	0	17.86%	-12.89%	2.05%	-11.04%
E_uLOLP	Lower	0	0	-16.09%	14.15%	-2.18%	11.69%
	Upper	0	0	16.37%	-10.86%	1.95%	-9.13%
$EEIR$	Lower	0	0	-38.01%	25.19%	-7.31%	15.10%
	Upper	0	0	22.36%	-14.18%	3.08%	-11.10%
E_uEIR	Lower	0	0	-15.71%	14.12%	-2.12%	11.71%
	Upper	0	0	15.79%	-10.82%	1.89%	-9.15%

Table 5.11: Uncertainty results when taking upper and lower bounds of wind turbine embodied energy, for PbA systems.

is because there are only small marginal gains to be made from increasing battery capacity for wind-only systems.

Sustainability is greatly improved by using lower wind turbine embodied energy values, but this is mostly caused by the reduction in battery capacity rather than the wind turbine itself. Sustainability is only slightly impacted when the larger embodied energy value is used, and optimal battery capacity is only slightly increased.

The greater uncertainty seen by varying wind turbine embodied energy rather than PV can be explained by observing that the original optimal systems are all wind-only, so changing the wind turbine's embodied energy has an immediate effect on the system. In contrast, when PV's embodied energy is varied, this has an effect on both PV capacity and wind capacity, because the system is radically changed by introducing PV capacity. The size in uncertainty of wind turbine embodied energy is greatest when using $ELOLP$ and $EEIR$ optimisation, as was noted with PV embodied energy uncertainty, but E_uLOLP still has a large uncertainty in battery capacity. E_uLOLP is also the only objective function that results in any use of of PV when high wind turbine embodied energy is used, but the its power capacity is still fairly small at less than $1kW_p$. A PV module of $10kW_p$ capacity has $84.5MWh$ embodied energy at the average value, while a $10kW_p$ wind turbine at the high embodied energy value has total embodied energy of $42.5MWh$, which is still smaller than PV.

There is little change to wind capacity, and there are three likely reasons for this. Firstly, the optimal wind capacity under $ELOLP$ and $EEIR$ is already very high, close to the maximum. Secondly, the wind turbine's embodied energy is so low, even at high estimates, that there are no real incentives to reduce wind capacity. Finally, the limits that keep wind capacity low when optimised by $ELOEP$, E_uLOLP or E_uEIR are not caused by its embodied energy, but by the risks to security caused by its oversizing. Reducing embodied energy will make no difference to these system costs caused by its security risk.

Uncertainty of battery embodied energy

The five different battery types (PbA, Li-ion, NaS, ZnBr, VRB) all have different embodied energy values, with ranges taken from the literature in table 3.6. The proportional range in these values is as follows:

- PbA: -38% to 56%
- Li-ion: -34% to 32%
- NaS: -24% to 29%

- ZnBr: -11% to 9%
- VRB: -14% to 22%

When taking the upper or lower bounds for their embodied energy values, the impact on system component sizing has been varied. There is no impact on the capacity of PV or wind, so these have not been shown here. This negative result shows that the barriers to including PV in the system are more to do with PV's high energy costs, rather than any need for battery backup for PV, as if that was the case then reducing battery embodied energy may have caused the system to include some PV capacity.

Table 5.12 shows that for all objective functions, using a lower embodied energy for the batteries gives a larger optimal storage capacity, and vice versa. However the size of this change depends on the batteries involved, where batteries with a wider range of uncertainty have a larger impact from that uncertainty.

PbA systems have the largest changes in battery capacity, however this is unsurprising as PbA batteries also have the widest range of embodied energy uncertainty. This trend remains consistent across all types of batteries for most metrics, as shown by the linear relationships in figure 5.46 between change in battery EE and optimal battery capacity; it can be inferred that EROI is generally the biggest determinant of ideal battery capacity, regardless of battery type or choice of metrics. $EEIR$ is possibly an exception as it gives some scattering around the fitted line, where the four anomalous points all come from either PbA or VRB systems. The only characteristic these two share is a higher embodied energy per usable capacity ($642kWh/kWh_{cap}$ and $694kWh/kWh_{cap}$ respectively), so $EEIR$ appears to be more sensitive than other objective functions when this value is higher.

The considerable increases in optimal battery storage are matched by a linear increase in security for all systems with reductions in battery EE (see figure 5.47), however this increase is small in comparison to the security increases seen in section 5.5.1 where security increased by up to 36% by having more PV capacity. Note the anomalous decrease in security for PbA systems under E_uLOLP and E_uEIR optimisation are caused by the reduced wind turbine capacity for those optimal systems.

Overall performance is always improved by reducing battery embodied energy, even when the subsequent increase in battery capacity causes a drop in EROI. This is to be expected from the optimisation mechanism, however the small percentage changes are notable in showing that the system's overall performance is less sensitive to battery embodied energy than any other component. Performance increases range from 1% to 9%, depending on battery type, whereas performance increases of up to 50% were seen with reduced PV EE, and up to 15% with reduced wind turbine EE.

Uncertainty of all components' embodied energy together

There are two main reasons for uncertainty in the embodied energy values, coming from either the supply chain in general (particularly manufacturing processes or materials acquisition), or the method of accounting for energy costs. These can be considered to be the real costs vs the measured costs. When it is the the supply chain management causing variation, then components can be analysed separately as in the previous three sections, as different materials and components are usually acquired from separate companies. However when it is the method of accounting, or if a manufacturer is dedicated to supply chain management in order to reduce their energy intensity all down the supply chain, then all components will be affected in a similar way. Table 5.13 shows results when all lower/highest embodied energy values are used for the system components. Lower embodied energy values give an increase in PV capacity similar to when PV modules were treated separately, however the other results are more mixed.

Metric	Bound	PV Δ	Turbine Δ	Battery Δ	EROI Δ	Security Δ	Performance Δ
PbA							
$ELOLP$	Lower	0	0	72.89%	-2.10%	7.13%	5.04%
	Upper	0	0	-45.00%	2.58%	-6.43%	-4.03%
E_uLOLP	Lower	0	0	67.40%	5.68%	6.86%	12.90%
	Upper	0	-0.4	-50.87%	19.56%	-24.40%	-9.52%
$EEIR$	Lower	0	0	78.02%	-3.38%	8.21%	5.06%
	Upper	0	0	-68.31%	12.42%	-13.55%	-3.25%
E_uEIR	Lower	0	0	69.00%	5.51%	7.03%	12.89%
	Upper	0	-0.4	-49.28%	19.72%	-24.26%	-9.14%
Li-ion							
$ELOLP$	Lower	0	0	56.44%	-1.02%	6.23%	5.32%
	Upper	0	0	-28.45%	1.16%	-4.23%	-3.22%
E_uLOLP	Lower	0	0	55.03%	4.55%	5.20%	9.96%
	Upper	0	0	-27.87%	-2.51%	-3.55%	-5.97%
$EEIR$	Lower	0	0	55.34%	-0.56%	6.09%	5.36%
	Upper	0	0	-27.84%	1.09%	-4.23%	-3.31%
E_uEIR	Lower	0	0	55.48%	4.45%	5.31%	9.92%
	Upper	0	0	-26.40%	-2.65%	-3.44%	-5.97%
NaS							
$ELOLP$	Lower	0	0	37.98%	-1.19%	4.17%	3.10%
	Upper	0	0	-26.48%	0.89%	-3.57%	-2.64%
E_uLOLP	Lower	0	0	36.16%	2.66%	3.34%	6.07%
	Upper	0	0	-26.13%	-2.14%	-3.06%	-5.13%
$EEIR$	Lower	0	0	35.59%	-0.67%	3.94%	3.14%
	Upper	0	0	-28.10%	2.09%	-4.37%	-2.64%
E_uEIR	Lower	0	0	34.92%	2.71%	3.30%	6.06%
	Upper	0	0	-25.15%	-2.21%	-3.01%	-5.15%
ZnBr							
$ELOLP$	Lower	0	0	14.24%	-0.43%	1.53%	1.03%
	Upper	0	0	-10.16%	0.63%	-1.27%	-0.74%
E_uLOLP	Lower	0	0	14.46%	1.05%	1.49%	2.55%
	Upper	0	0	-9.13%	-0.82%	-1.02%	-1.82%
$EEIR$	Lower	0	0	15.01%	-0.65%	1.77%	1.08%
	Upper	0	0	-10.16%	0.56%	-1.32%	-0.76%
E_uEIR	Lower	0	0	13.13%	1.18%	1.38%	2.55%
	Upper	0	0	-9.46%	-0.77%	-1.08%	-1.83%
VRB							
$ELOLP$	Lower	0	0	20.56%	-0.69%	2.16%	1.37%
	Upper	0	0	-24.69%	1.39%	-3.10%	-1.77%
E_uLOLP	Lower	0	0	19.16%	1.12%	1.68%	2.83%
	Upper	0	0	-21.89%	-1.46%	-2.27%	-3.72%
$EEIR$	Lower	0	0	30.59%	-2.92%	3.93%	1.26%
	Upper	0	0	-37.58%	4.86%	-5.87%	-1.39%
E_uEIR	Lower	0	0	18.13%	1.17%	1.66%	2.84%
	Upper	0	0	-22.58%	-0.93%	-2.62%	-3.69%

Table 5.12: Uncertainty results when taking upper and lower bounds of battery embodied energy, for all types of battery systems.

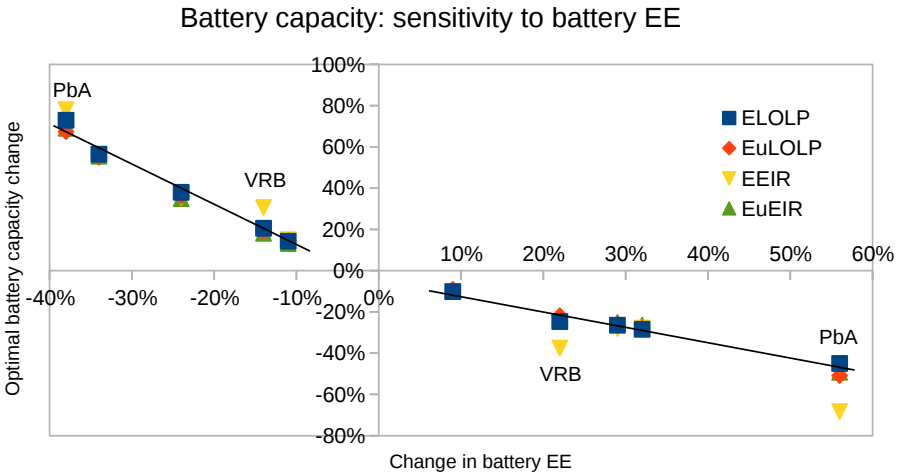

Figure 5.46: Changes in optimal battery capacity when its EE is varied. Optimal capacity value is more sensitive when EE is reduced than increased, but regardless of this direction of change, there is a linear relationship.

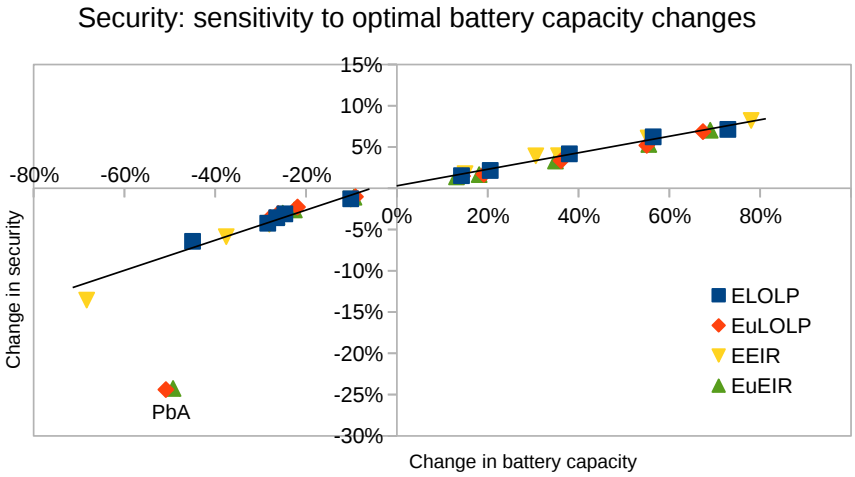

Figure 5.47: Plot showing how the change in optimal battery capacity (caused by changes in battery EE cost) affects system energy security. Increasing battery capacity has less of an impact than decreasing it, due to diminishing returns. Increases in security are smaller than those seen when PV EE costs are reduced.

When the system is unable to export energy, both higher and lower embodied energy bounds result in a small wind capacity. This may seem contradictory, however a possible explanation is that because excess production is penalised, the increase in PV capacity for lower EE drives down wind generation. Meanwhile with universal high EE values the higher cost of wind turbines makes them less worthwhile to install, regardless of the comparatively more expensive PV. As the wind capacity of E_uLOLP and E_uEIR optimised systems at mid-range EE supplies only 120% of demand, this drop of 40% brings the system to undercapacity at 80%.

Change in optimal battery capacity is mixed, increasing only when the system can export energy (under lower EE values), and decreasing under all other scenarios. Optimal battery capacity is therefore sensitive to a number of factors, and to increase their value in the system either their embodied energy must be decreased more than other components, or the system be in a situation where excess energy cannot be exported.

Regarding EROI values, using higher EE values actually increases $EROI_{used}$ by around 6.5% due to the considerably smaller battery size (a reduction in 41-42%) regardless of the security metric used in optimisation. However using lower EE values increases $EROI_{used}$ by a much larger margin of 30.7%, while also reducing battery capacity and substituting some wind production with equal amounts of PV. The $EROI_{out}$ results act in a very different way, dropping by 8-11% for higher EE values and increasing only marginally (2-3%) for the lower EE values. It can therefore be surmised that EROI is more sensitive to embodied energy values when excess energy is curtailed; this holds true when EE is changed for individual components.

Lower bounds of EE result in much improved security, whether this is caused by inclusion of PV capacity or increased battery capacity. As previously mentioned, battery capacity is actually decreased when using $EROI_{used}$, so taking all these results into consideration, increased PV capacity has a stronger effect on increasing the optimal security than increased battery capacity. Furthermore, choice of security metric makes a big difference in recorded security change, as does the choice of EROI. For non-exporting systems, $LOLP$ shows a bigger increase in security than EIR despite giving similar changes in PV, wind and battery capacity, and the negligible change in $EROI_{used}$ means that performance is also more changed, especially for the lower bound of EE values.

Looking at performance overall, it is more sensitive to reductions in EE than increases, particularly when using $EROI_{used}$. This means that if the current EE values are missing out on vital parts of the life cycle costs such as marketing, employee commuting etc, the error involved is less than the potential improved performance that could be achieved by reducing embodied energy across the whole supply chain.

Comparing these results with the previous ones shows that they have the most in common with results when PV embodied energy is varied, particularly in relation to battery capacity, PV capacity and security results. This suggests that the component with the most impact on system optimisation is PV, so PV might be the system component most in need of reducing its embodied energy.

This is backed up by examining the performance uncertainty in table 5.11; while lower embodied energy values of the wind turbine gives the largest increase in performance, this is done by sacrificing security for sustainability. In contrast, reducing the PVs embodied energy increases performance by pushing up security. When optimising with EuLOLP, this also increases sustainability, but if ELOLP or EEIR are used then the increase in battery capacity has a negative impact on sustainability. Therefore reducing battery embodied energy levels are a second priority after PV. The embodied energy levels of PV modules are explored in more detail in the next section.

Comparing objective functions in terms of their sensitivity to embodied energy uncertainties, E_uLOLP and E_uEIR generally appear the most sensitive, particularly regarding PV embodied

Metric	Bound	PV Δ	Turbine Δ	Battery Δ	EROI Δ	Security Δ	Performance Δ
$ELOLP$	Lower	0.6	0	5.60%	3.38%	39.03%	43.68%
	Upper	0	0	-33.45%	-10.86%	-4.47%	-14.78%
E_uLOLP	Lower	0.6	-0.6	-18.21%	30.71%	33.55%	74.10%
	Upper	0	-0.4	-42.40%	6.43%	-23.19%	-18.15%
$EEIR$	Lower	0.6	0	7.90%	2.13%	39.42%	42.79%
	Upper	0	0	-40.53%	-8.50%	-6.56%	-14.74%
E_uEIR	Lower	0.6	-0.6	-17.97%	30.66%	30.73%	70.56%
	Upper	0	-0.4	-41.12%	6.59%	-23.07%	-17.86%

Table 5.13: Uncertainty results when taking upper and lower bounds of all components' embodied energy, for PbA systems.

Metric	Bound	PV Δ	Turbine Δ	Battery Δ	EROI Δ	Security Δ	Performance Δ
$ELOLP$	Upper	0	-0.2	-0.1%	3.3%	-2.5%	0.9%
	Lower	0	0	-6.5%	2.3%	-0.7%	1.5%
E_uLOLP	Upper	0	0.2	12.0%	-13.3%	14.3%	-1.4%
	Lower	0	0.4	12.2%	-17.7%	24.3%	2.0%
$EEIR$	Upper	0	-0.2	-0.6%	3.6%	-2.8%	0.7%
	Lower	0	0	-5.4%	2.0%	-0.8%	1.2%
E_uEIR	Upper	0	0.8	25.2%	-31.2%	43.5%	-2.1%
	Lower	0	0.4	13.1%	-17.8%	24.5%	1.7%

Table 5.14: Uncertainty analysis results for the range of battery efficiencies for lithium-ion batteries (85-95%), showing how upper and lower limits for the battery efficiency affect the optimal outputs. Results are displayed as the percentage difference from the result with 90% efficient batteries. There was no variation in PV size, as all results returned wind-only systems.

energy levels. All objective functions are less sensitive to increases in embodied energy than decreases.

5.5.2 Uncertainty of battery efficiency

Embodied energy is not the only uncertain variable that affects the performance significantly. From comparing the results for each type of battery, it is apparent that the batteries with more efficient cycles offer better performance, however it is difficult to compare these when the different batteries also vary in terms of their embodied energy and depth of discharge. To obtain a true comparison, it is necessary to compare results of the same batteries with different assumed cycle efficiencies.

In practice, a battery does not have constant energy conversion efficiency; this is dependent on a number of factors such as the current, state of charge (SOC) of the battery, temperature etc [144]. However, limitations of the half-hourly model mean that charging efficiency of PbA batteries were modelled as only dependent on SOC, and charging efficiency of other batteries were fixed at their average cycle efficiency.

There were five types of batteries tested in the main set of results, and two were chosen to test how their efficiency affected overall system performance. These two were lithium-ion and vanadium redox batteries, considered to have more potential to improve their efficiency. In particular, VRB are a fairly new technology that are currently estimated to have a low efficiency of 70%, with a wide range of possible efficiencies (60-80%).

The lithium-ion uncertainty results in table 5.14 show that $ELOLP$ and $EEIR$ are not

Metric	Bound	PV Δ	Turbine Δ	Battery Δ	EROI Δ	Security Δ	Performance Δ
$ELOLP$	Upper	0	0	12.6%	-0.2%	3.4%	3.2%
	Lower	0	0	-23.5%	4.9%	-1.9%	2.7%
E_uLOLP	Upper	0	0.2	22.8%	-13.7%	15.1%	-0.6%
	Lower	0	0.4	14.7%	-22.6%	21.4%	-5.8%
$EEIR$	Upper	0	-0.2	10.0%	3.0%	-0.2%	2.6%
	Lower	0	0	-40.9%	9.9%	-6.7%	2.1%
E_uEIR	Upper	0	0.2	17.8%	-13.1%	14.2%	-1.0%
	Lower	0	0.4	13.6%	-22.6%	20.8%	-6.2%

Table 5.15: Uncertainty analysis results for the range of battery efficiencies for VRB flow batteries (60-80%), showing how upper and lower limits for the battery efficiency affect the optimal outputs. Results are displayed as the percentage difference from the result with 90% efficient batteries. There was no variation in PV size, as all results returned wind-only systems.

particularly sensitive to changes in the battery efficiency, however they both reduce the size of the battery when it is less efficient, which leads to the EROI result improving slightly for both the upper and lower limit of cycle efficiency. They also optimise to give a slightly smaller wind turbine when the battery is more efficient, but there is no change for the lower efficiency, however this is not a very meaningful result as the mid-efficiency battery gives the largest wind turbines available. Security is measured as lower by $LOLP$ and EIR for both the high and low efficiency batteries, with the more efficient battery giving lower security because it is paired with smaller wind turbines.

When the system is unable to export energy, the battery efficiency has a much greater effect on optimal results. There is more scope for optimal wind turbine size to increase here, as the original optimal size is not at the maximum boundary; both E_uLOLP and E_uEIR give a large increase in wind input for the upper and lower battery efficiencies. Similarly, both upper and lower efficiencies give larger batteries under those metrics, resulting in decreased EROI but increased security. These largely balance out to give similar performance overall, with a slight increase for less efficient batteries.

These results are surprising, as lower battery efficiency appears to give little hindrance to system performance, and actually increases it overall by all metrics. It is also important to note that the exact battery efficiency is a very important factor in evaluating the system, particularly when using the $EROI_{used}$ metric which places more value on the battery within the system.

Despite the wide ranges in component sizes under $EROI_{used}$-derived optimisation, the overall performance by all objective functions shows only negligible change, suggesting that the system optimises itself to always return to a fixed performance no matter the battery efficiency (within this realistic range). This is particularly interesting in the case of E_uEIR, where wind and battery capacity are greatly increased for the upper and lower bounds of battery efficiency, but all increases in security are offset by reduction in $EROI_{used}$. This is a very different outcome to when embodied energy is targeted for analysis.

Results for the VRB systems in table 5.15 yield similar results for the individual EROI and security metrics, however performance was more sensitive to the battery efficiency. In particular, using lower cycle efficiency batteries for non-exporting systems reduced performance by 6%, and exporting systems showed marginal increased performance by 2-3% whether the batteries were of higher or lower efficiency.

The results are so varied that there is no particular metric that can be shown to be more or less sensitive to battery cycle efficiency.

5.5.3 Sensitivity analysis for PV

Embodied energy values are likely to drop in the future due to improved manufacturing methods, energy efficiency measures and possibly increased sustainability awareness in industry. This may reduce the embodied energy in crystalline PV production by up to 85% from 1998, with more modern projections suggesting 80% [186]. As the optimal results for most systems with current average PV embodied energy levels do not contain PV input (presumably due to their high energy costs) reducing their embodied energy by up to 80% in the model analysis can give insight into whether it is useful to reduce energy costs of PV, and show how the sustainability and security of the optimised systems is affected as a result. Depending on how the systems are affected, this analysis can demonstrate whether research into less energy intensive PV is necessary, and to what extent. Note that PV requires a reduction of around 50% (depending on capacity, but this is accurate at the microgeneration scale) to match wind turbine embodied energy levels per kW_p of rated power capacity.

Using $ELOLP$

Results from $ELOLP$ are shown in figure 5.48 where the reduction in PV embodied energy is shown to have an impact on all outputs: performance and optimal battery capacity, optimal wind and PV power capacity, and sustainability/security. Results are nonlinear, and also exhibit a tipping point behaviour where for small reductions, reducing embodied energy makes little difference. However, once embodied energy drops below 40-60% (where PV becomes more competitive with wind turbines), the optimal system changes drastically, adding up to 80% PV input, giving high $EROI_{out}$ and low $LOLP$. The sideways U shape exhibited is due to initial increases in battery capacity, which are required due to the higher total power capacity. Once the PV capacity increases the battery size also drops, increasing $EROI_{out}$, but never regaining the higher $EROI_{out}$ of the start. The only output parameter that steadily increases or decreases for all battery types is the performance (measured by $ELOLP$), which initially slowly increases, then accelerates as the optimum starts including PV capacity at low energy cost.

Using E_uLOLP

Results from E_uLOLP are shown in figure 5.49, and these show more steady changes than with $ELOLP$ when PV's embodied energy is reduced. While there is a tipping point as before, this occurs much quicker at around 20%+ reduction in embodied energy. As PV embodied energy reduces, wind capacity is gradually replaced by PV capacity, rather than simply adding PV capacity to the existing maximum wind capacity. This results in a mid-sized hybrid system with equal input from PV and wind.

Other impacts are that performance increases and battery size decreases, but performance increases slowly at first and then accelerates, while battery size first drops quickly, then starts to reach a plateau as PV starts to dominate the optimal systems. The behaviour of the optimal systems' sustainability and security is however similar to $ELOLP$ results, as $EROI_{used}$ first decreases in tandem with a decreasing $LOLP$, then once the systems contain some PV input, $EROI_{used}$ quickly increases while $LOLP$ remains fairly stable. This stable $LOLP$ result suggests that the system cannot easily improve its security once PV has reduced its embodied energy by 30-40%, as any gains made by PV capacity are offset by the risk of overproduction and loss of battery capacity. The initial loss in $EROI_{used}$ and steep loss of battery capacity shows how useful PV is to maintaining a high $LOLP$ result; this high security is enough to lift performance overall and require less storage capacity.

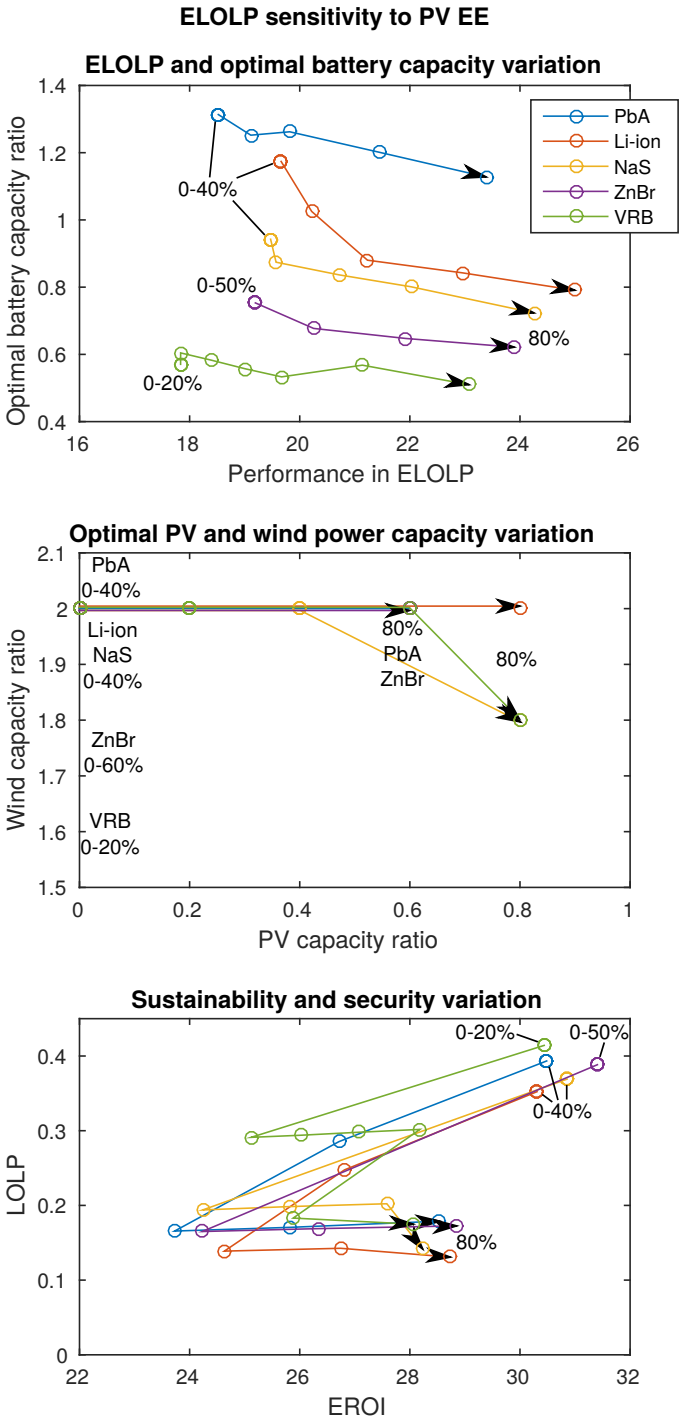

Figure 5.48: *ELOLP* optimal results as embodied energy of PV modules is reduced by 80%. Each marker shows an embodied energy decrease of 10% (percentage points). The change in power capacity inputs (triggered once PV's embodied energy has dropped by 45%) has an influence on the optimal battery capacity, which increases when total power input increases. Sustainability initially decreases, then increases once PV has a lower embodied energy than wind turbines, and security and performance increase throughout.

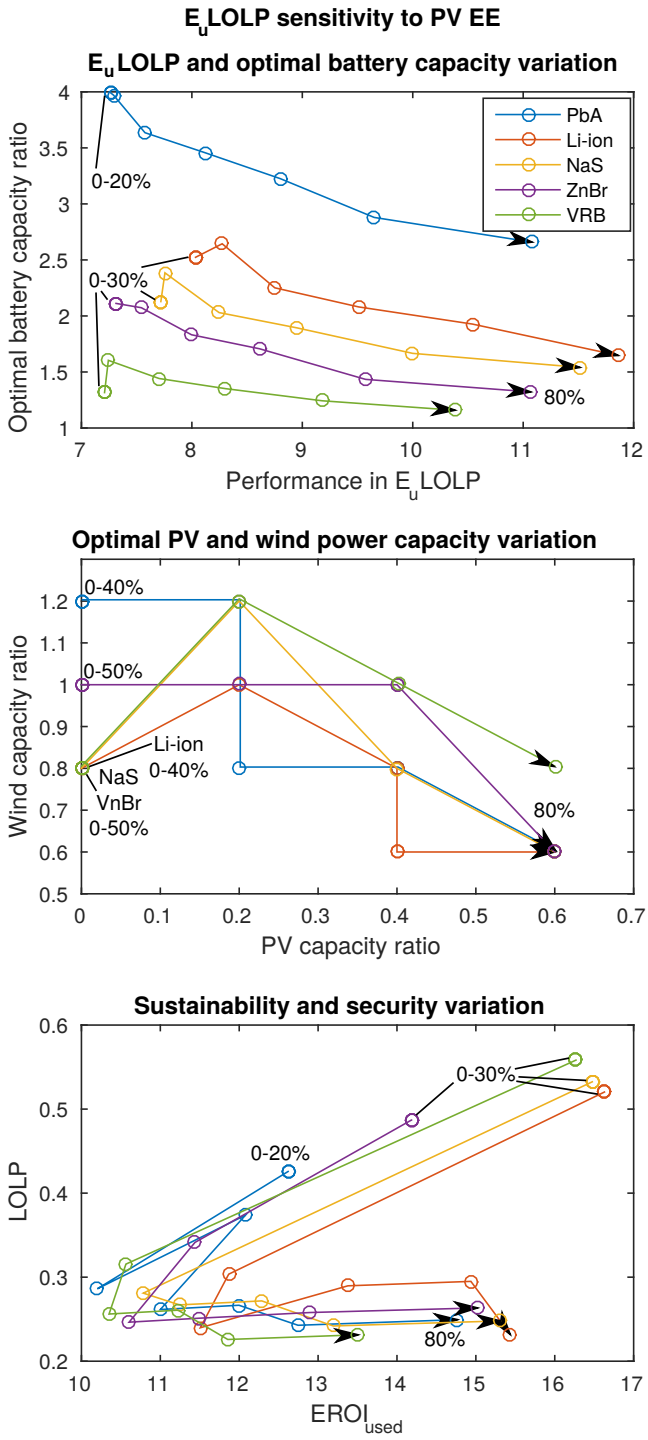

Figure 5.49: E_uLOLP optimal results as embodied energy of PV modules is reduced by 80%. Each marker shows an embodied energy decrease of 10% (percentage points). E_uLOLP gives a more gradually changing generation input than $ELOLP$ did, which results in gradual decrease of battery capacity, but similar sustainability and security outputs.

Using $EEIR$

The results using $EEIR$ are unsurprisingly similar to those of $ELOLP$, given the already acknowledged high correlation between the two sets of results. Shown in figure 5.50, the only notable difference between the two are that $EEIR$ optimisation shows no reduction in optimal wind capacity.

Using E_uEIR

Finally, when using E_uEIR analysis in figure 5.51, the results are almost identical to E_uLOLP results. While the changes in PV and wind power capacity differ, both result in a mid-sized hybrid system with equal input from PV and wind.

Summary

Overall, $ELOLP$ and EIR return similar sensitivity results: they both optimise to add in PV capacity and reduce battery capacity as PV EE drops by 80%. These changes to the system, in addition to the lower EE cost of PV modules, gives improved security and slightly reduced EROI, improving performance by a third on average. When the system cannot export energy, E_uLOLP and E_uEIR also return results similar to each other: they optimise to replace units of wind with PV so that total supply remains the same, and also reduce battery capacity. All choices of optimisation show an initial dropping of sustainability that is matched by a lift in security, and then the trajectory changes direction where further added PV capacity has the effect of improving EROI. However, the final EROI result is never as high as the EROI of the wind-only system at the start.

The choice of battery also matters here. While battery type has little recognisable impact on the optimal PV and wind capacities (other than VRB showing higher wind capacity), it still affects the system's optimal performance and objective function results. PbA systems require the highest storage capacity and give the lowest sustainability across all results, but their security results are average. The batteries remain consistently ordered, where capacity has the order from highest to lowest of: PbA, Li-ion, NaS, ZnBr, VRB. Performance is ordered from highest to lowest as: Li-ion, NaS, PbA, ZnBr, VRB. However, individual EROI and security results are less neat.

5.5.4 Sensitivity to primary energy scaling

There has been much discussion on the necessity of primary energy scaling through the grid efficiency coefficient η_G. Opinions range from believing that it is a misleading normalisation, to alternate methods of defining and calculating it, to conjecture of how it may change when the grid is more reliant on renewable energy capacity. If η_G is defined as the lifecycle efficiency of the grid, then it will increase as renewable energy penetration increases, and EROI calculations using that normalisation will decrease. However, due to the nature of the methodology, and equal primary energy scaling on all system components, the optimal sizing is not affected by the value of η_G.

EROI results without primary energy scaling

EROI results for single-household systems with PbA batteries are shown in figures 5.52 and 5.53. The EROI results are reduced considerably, where some systems have $EROI_{used}$ approaching 1, which would result in a truly unsustainable system; if this were to occur then the energy

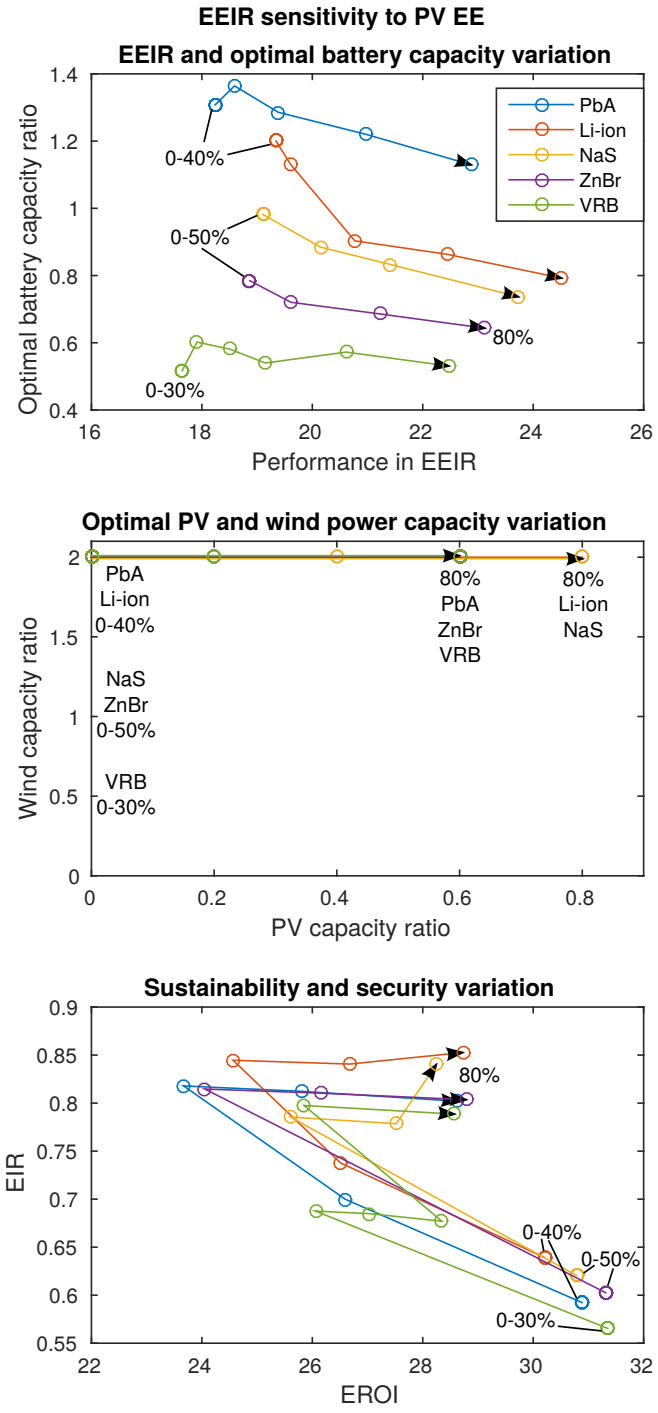

Figure 5.50: *EEIR* optimal results as embodied energy of PV modules is reduced by 80%. Each marker shows an embodied energy decrease of 10% (percentage points). The change in power capacity inputs (triggered once PV's embodied energy has dropped by 45%) has an influence on the optimal battery capacity, which increases when total power input increases.

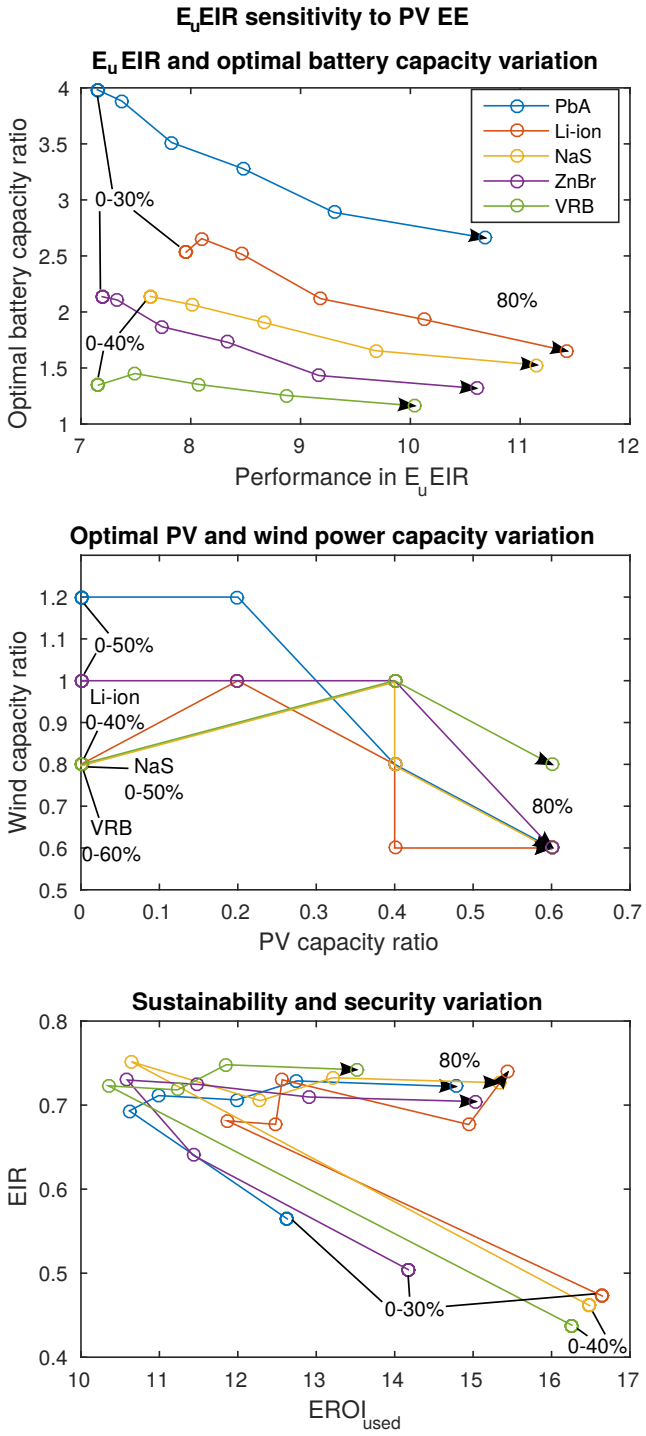

Figure 5.51: E_uEIR optimal results as embodied energy of PV modules is reduced by 85%. Each marker shows an embodied energy decrease of 10% (percentage points). Change in power capacity is more erratic than with E_uLOLP, and initial thresholds of up to 45% embodied energy reductions are required for some system changes.

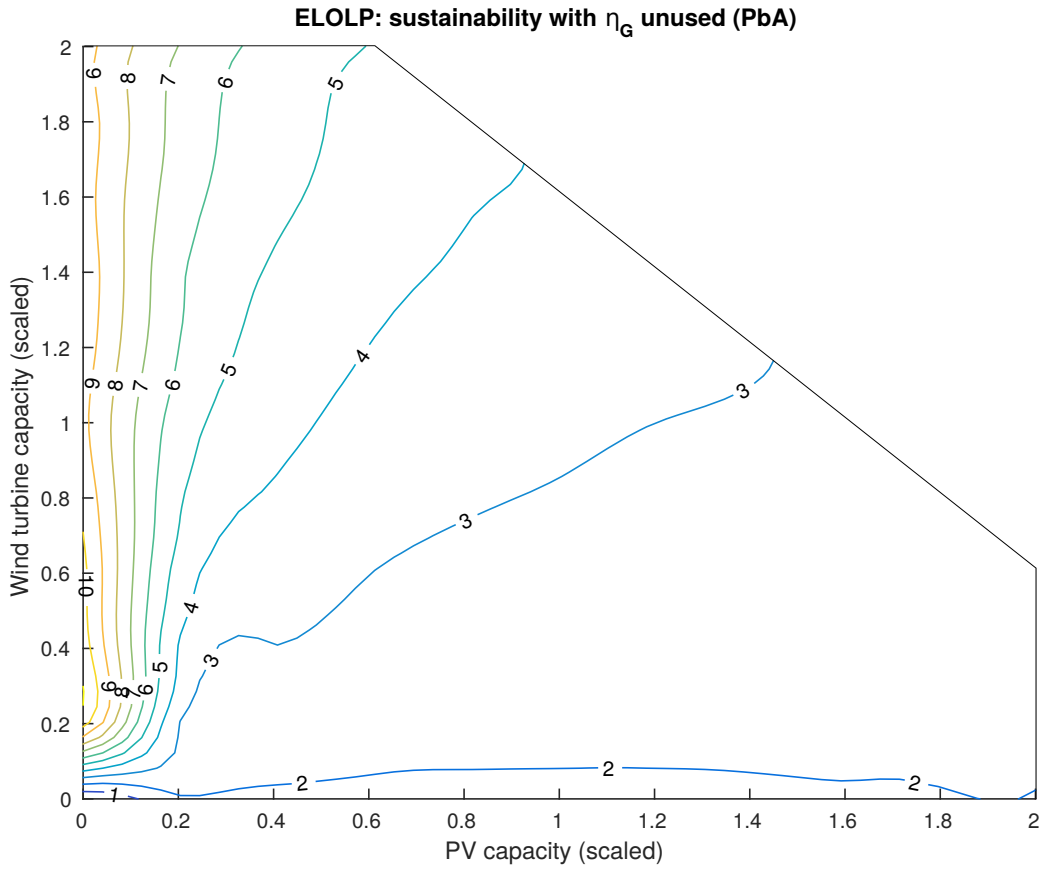

Figure 5.52: $EROI_{out}$ (shading) and $LOLP$ (contours) results for optimal PbA energy systems with no η_G scaling on EROI results. $LOLP$ is unchanged but $EROI_{out}$ is reduced where most results lie in the 2-4 range.

directed towards manufacturing the components was effectively wasted, as it could have been more effective if used directly to supply electricity demand.

For the systems to give an $EROI_{out}$ greater than 5, the energy production from wind sources must be at least 3-4 times greater than energy from solar sources over the year. It is particularly difficult to reach $EROI_{used} > 5$, and essentially requires a wind-only system supplying around 80% of the system's demand over the year, to meet the higher levels of $E_u LOLP$. The actual delivered demand for such a system (measured with EIR) is around 45-50%, or 0.55 LOLP.

Therefore if PE scaling is unused, renewable energy systems appear to be less sustainable, particularly if excess energy production goes unused.

EROI results with improved grid efficiency

If instead primary energy scaling is accepted, then we can consider how grid efficiency will increase as the proportion of generated energy from renewable energy sources grows. For simplicity, this growth was estimated to be a linear progression to 40% wind production in 2040, where wind turbine life-cycle efficiency was calculated to be 94% in section 3.4.3 using the equations in section 2.4.5. This gave an overall grid life-cycle efficiency of 56%, but this is a rough estimate as efficiencies and embodied energy of non-renewable generation technologies

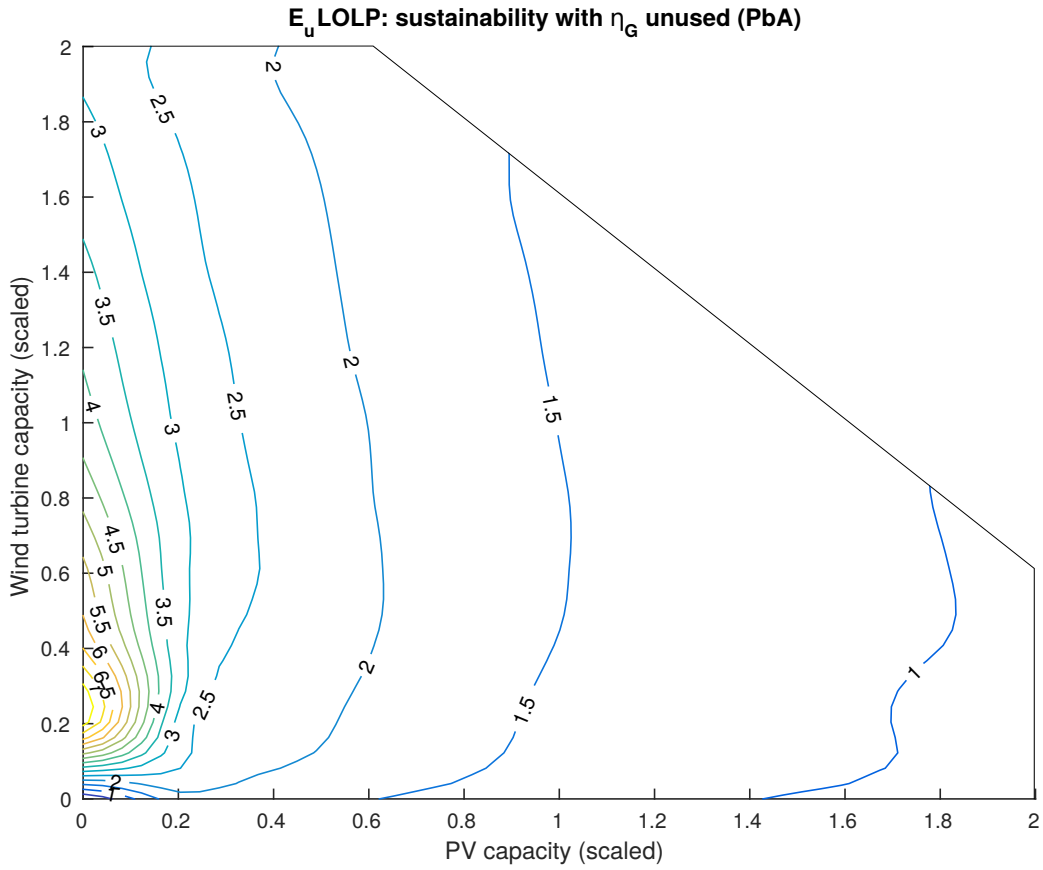

Figure 5.53: $EROI_{used}$ (shading) and $LOLP$ (contours) results for optimal PbA energy systems with no η_G scaling on EROI results. $LOLP$ is unchanged but $EROI_{used}$ is reduced where most results lie in the 1-3 range.

such as new nuclear and carbon capture & storage are unknown. Furthermore, the efficiency of future larger wind turbines are likely to be higher than 1.2MW turbines existing today. However, this estimate is useful for these limited purposes, and can show how the EROI is affected.

Figure 5.54 shows the average EROI values, and how they logarithmically decrease as η_G increases. The samples are averaged with respect to their PV and wind input as a ratio of household demand. As before, wind-dominated systems show the highest EROI results, and systems with no solar input remain with $EROI_{out} > 15$ and $EROI_{used} > 5$ on average. However PV energy systems do not fare as well, resulting in $EROI_{out} \approx 5$ and $EROI_{used} \approx 2$ at the highest grid efficiency.

Given that this is a prediction of future EROI values, it was also considered worthwhile to include improved EE values of PV modules from section 5.5.3, so that PV cost reduces by up to 80% as the grid efficiency is increasing. It was assumed for simplicity that both increase simultaneously. The results are shown in figure 5.55, where energy systems with PV benefit greatly from reduced energy costs. Here, $EROI_{out} > 10$ for all systems (on average) and $EROI_{used} \geq 5$. However, the small wind energy systems still have the highest EROI values, and PV-dominant systems remain with the lowest $EROI_{used}$ values. Note that these results are for optimal systems, so battery capacity is not fixed.

5.6 Alternative systems: using hydrogen or heat pumps

It was discussed in the literature review that there are more innovative solutions to balancing the grid to be considered, such as branching out of the electricity network into other energy systems, or using hydrogen as more flexible means of storage.

The limitations of available data on demand profiles and embodied energy values means that it was not possible to conduct a full study into these systems, however there was a small test on a single household hydrogen system with 100 samples per wind/PV scale, and another on a single household system with a heat pump, also with 100 samples per wind/PV scale. These samples were analysed using only the EIR metric to measure security, as it was shown in the more extensive investigations to be reasonably accurate and more appropriate for these kinds of systems where they are able to import energy during loss of load periods.

5.6.1 Using hydrogen for energy storage

When using a hydrogen system instead of a battery for energy storage, there were considerably more components to be considered within the system, and these had the effect of increasing its embodied energy significantly. These components were the hydrogen electrolyser, which used electricity to produce hydrogen from water and then compress it to be stored; the steel cylinders used to store the hydrogen; and the fuel cell used to generate electricity from the hydrogen. The fuel cell in particular added a great deal of embodied energy to the system, in part because of its very short lifetime (just over a year) and the immaturity of this technology. These contributions to system embodied energy are shown in figure 5.56

This higher embodied energy cost means that there is less incentive for the system to use the hydrogen storage system, leading to zero utilisation when optimising with $EEIR$ (this is repeated for the $ELOLP$ results). However if the systems are restricted to curtail excess energy production, modelled by the use of $E_u EIR$ as the objective function, then some hydrogen storage becomes worthwhile. This is shown in figure 5.57 where optimal storage capacity only rises above 0 once PV contributes to 60-80% of demand. Hydrogen storage capacity is normalised to the energy capacity of the stored hydrogen, dividing by system power capacity, so can be directly

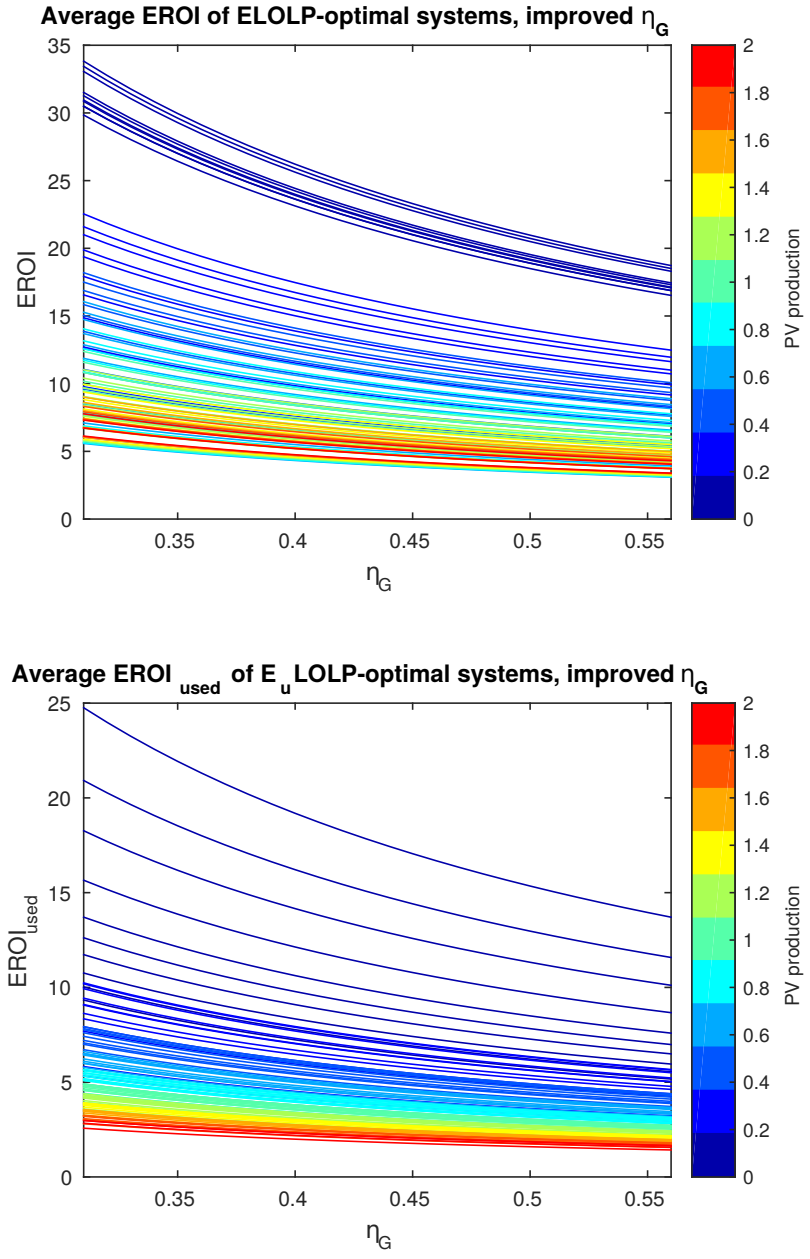

Figure 5.54: Reduction in EROI results when η_G is improved from increased wind penetration on the grid.

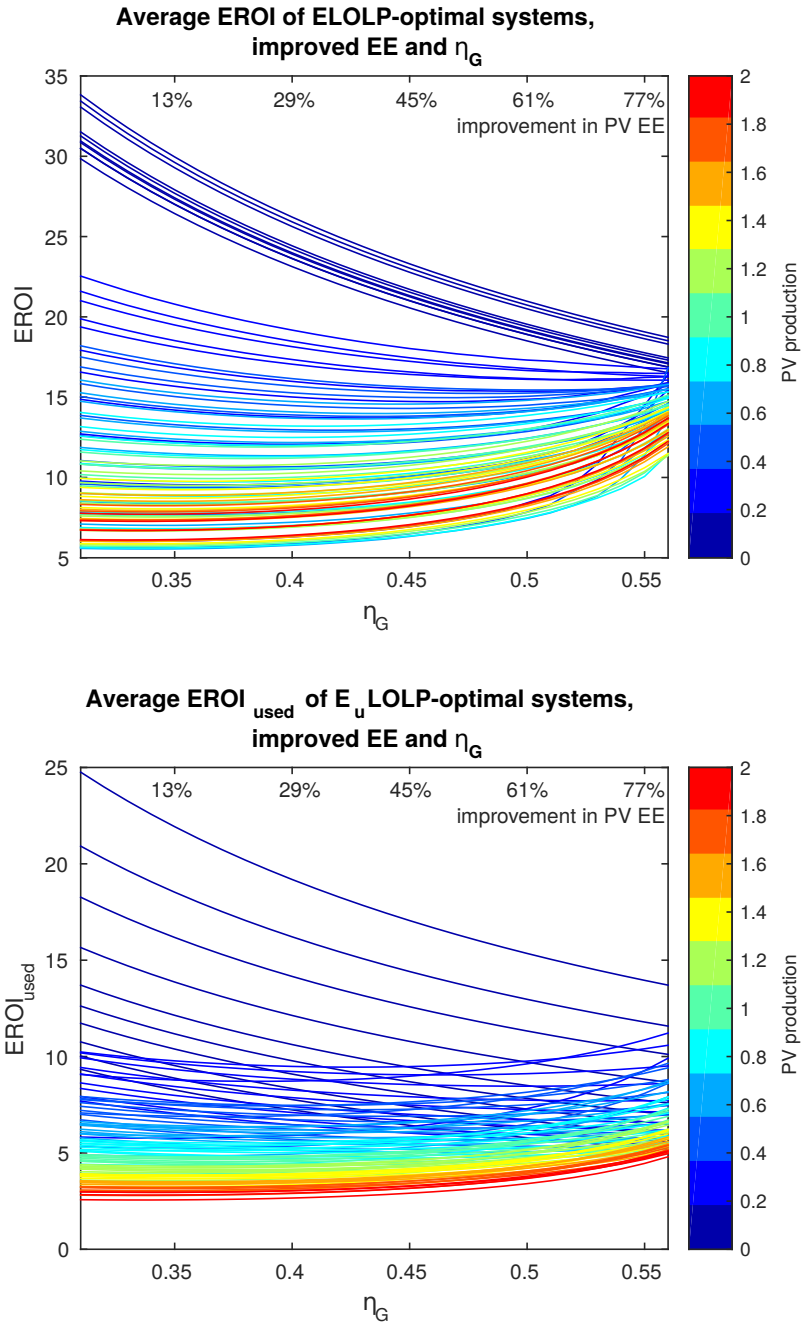

Figure 5.55: Change in EROI results when η_G is improved from increased wind penetration on the grid and PV EE is decreased by 80%, both over the same time-frame. For solar-dominated systems, the improvement in PV EE overpowers the increase in η_G, giving an increase in both types of EROI.

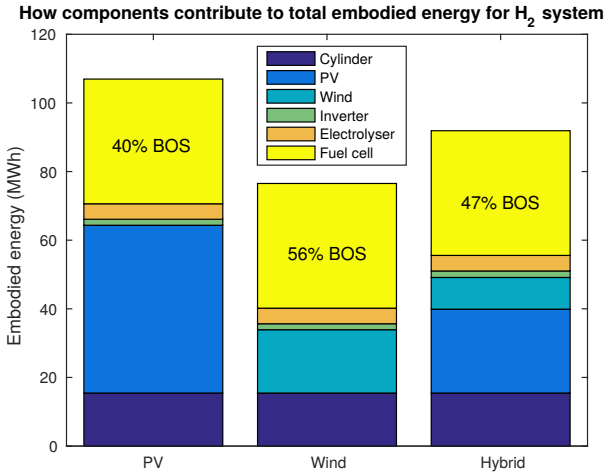

Figure 5.56: Embodied energy of an energy system using hydrogen for energy storage, with one hydrogen cylinder and 6kW generation capacity PV, 6kW wind or 6kW hybrid (3kW PV with 3kW wind). The balance of system (BOS, containing the inverter, electrolyser and fuel cell) makes up a much greater proportion of the embodied energy cost than when using batteries, especially when using the lower costing wind turbines.

compared to the battery system results. Therefore we see that a smaller capacity of energy can be stored with the optimal hydrogen systems than the optimal battery systems, and the peak storage capacity is located at a higher PV capacity - supplying 1.2 times demand rather than 0.5. Wind capacity does not support any type of hydrogen storage, and in fact once PV is producing 100% of demand, added wind capacity competes with storage, reducing the optimal storage capacity.

The performance levels are also reduced, particularly for systems with PV input above half the system's demand. The lack of any storage for wind-dominated systems also reduces their performance slightly, and their performance drops suddenly once any PV capacity is introduced, in contrast to the battery systems where PV provided enough security that performance was only slightly reduced on their introduction as long as their input was small.

These optimal system changes mean that security and sustainability are also changed, as shown in figure 5.58 where EIR is reduced overall, only reaching a maximum of 0.75 for large hybrid systems instead of the 0.9 EIR reached by PbA systems. Increasing wind capacity gives a smaller amount of security to the system (compared to battery systems), with diminishing returns, reaching only 0.45 EIR for the largest wind-only systems as there is no storage support. In contrast, adding PV capacity gives slightly more security, especially once hydrogen storage is added, reaching 0.65 EIR for the largest PV-only systems. However this added storage brings the $EROI_{used}$ value down to below 5, less than when using batteries.

However while EIR is not as high, excess energy is reduced more with hydrogen storage than batteries, resulting in up to 1,500kWh less excess production for PV-dominant large systems (see figure 5.59). However, as EIR security is not similarly affected, it is fairly likely that this is a product of the much lower cycle efficiency of the hydrogen storage system, being at 30% rather than typical battery ranges of 70-90% efficiency. Therefore it is dubious whether such a result can be viewed as positive, as the energy lost in hydrogen conversion might as well have been wasted through curtailment.

While this was only a small test system, as the embodied energy levels are experimental, it is clear to see why hydrogen systems are more generally proposed as transport systems rather than

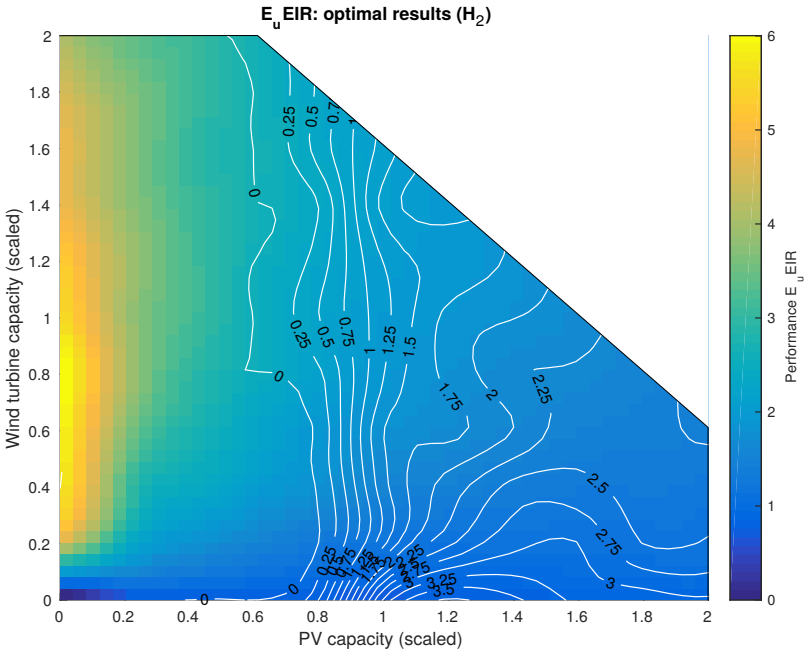

Figure 5.57: E_uEIR results showing optimal hydrogen storage capacity (contours) and system performance (shading) for all input capacities. Performance is highest for mid-sized wind-dominated systems, but hydrogen storage only becomes necessary once PV input is 80% of demand.

as an alternative to batteries. The only advantage hydrogen can offer is through the portability of storage cylinders, whether this is utilised through hydrogen cars or stockpiling of hydrogen to be used for longer term energy storage. However the latter would seem unrealistic as there were no results that showed a large optimal storage capacity, the costs being too great.

5.6.2 Adding heat pump load

For another alternative model, a demand load for a 3.5kW heat pump was added to the existing household loads. This load was fairly simple; lacking data for either the local temperature or household heating demand, the heat pump load was assumed to be flat and either on constantly (during winter) on in the evenings (spring and autumn) or turned off (during summer or while unoccupied). The added flexibility of hot water storage was not modelled, so this is simply an investigation into how the added demand load in colder months affected performance.

An immediate effect of this increased load (an additional 12.3MWh per year, roughly a factor of 4) is a matched increase in generational capacity, requiring an average 20kW PV array or 9.8kW wind turbine to match 100% of the energy demand. This is also a factor of 4 increase on average, so the seasonal variation in demand has not resulted in too much overcapacity. These levels of capacity are shown in figure 5.60

Analysis with $EEIR$

The performance of the systems with heat pump load were measured using $EEIR$ and E_uEIR. While the $EEIR$-optimal battery capacities in figure 5.61 are largely unchanged except for disuse by wind-only systems and lower capacities for large hybrid systems, the $EEIR$ performance overall is generally a third of that shown by the systems without heat

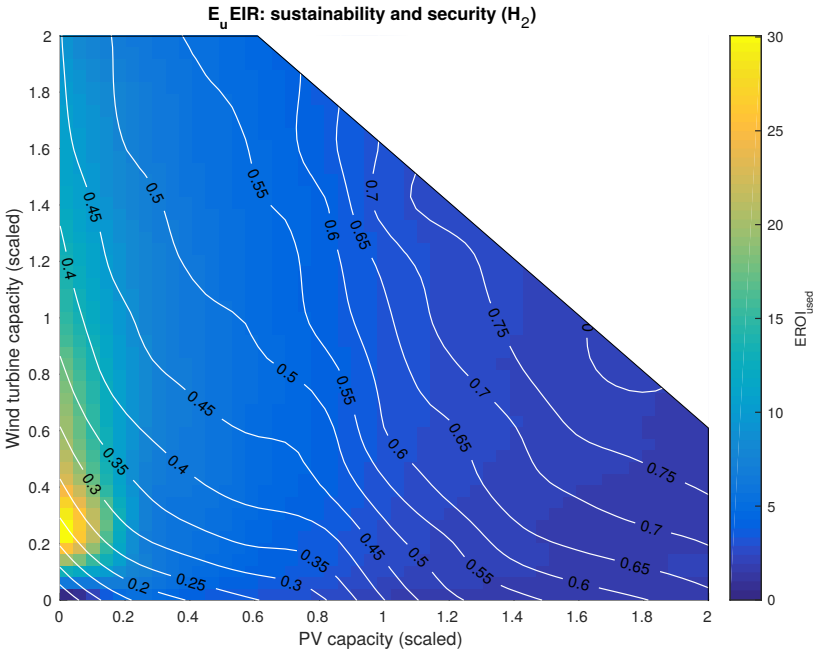

Figure 5.58: $EROI_{used}$ (shading) and EIR (contours) results for optimal energy systems with hydrogen storage. Security increases as input increases, and increases quicker once storage becomes included.

pumps.

The results in figure 5.62 show that the difference is largely due to an equal reduction in $EROI_{out}$ results across the board, however there is also a major difference where large wind-only systems have the highest $EROI_{out}$ results. When heat pumps are not included, the maximum $EROI_{out}$ is obtained by small wind-only systems, due to the cost of larger batteries with the largest wind turbines. However when the heat pump is included, batteries become less important and larger wind turbines manage to give the highest EROI while not suffering much of a security loss. In fact, wind-only systems show better security than PV-only systems, reaching an EIR of 0.55 in comparison to PV's 0.5. The security of hybrid systems never reaches the high EIR results of 0.85 seen when heat pumps are not included, as battery sizes are decreased.

5.6.3 Analysis with $E_u EIR$

When the system is forced to curtail excess energy the wind-dominant systems are changed significantly, ramping up optimal battery capacities and moving the optimal wind capacity to be smaller because of this added battery cost (see figure 5.63. This is very similar to the earlier systems without heat pumps, however the change is bigger as wind turbines were particularly well-performing for $EEIR$. Battery capacities for PV-dominant systems are largely unchanged.

This increase in battery capacity has however had the advantage of improving EIR of wind-dominant systems, see figure 5.64 as they now reach 0.65 in comparison to PV's 0.5 (unchanged from the $EEIR$-optimal results), close to the maximum of 0.75 reached by large hybrid systems. However their $EROI_{used}$ result is much lower than the $EROI_{out}$ results, pushing the maximum $EROI_{used}$ to very low wind capacity. This is similar to the $EROI_{used}$ results for systems without heat pumps.

There are a few notable differences between the wind and PV supply profiles, and the most important in these circumstances is the seasonal difference. Figure 5.65 shows that the summer

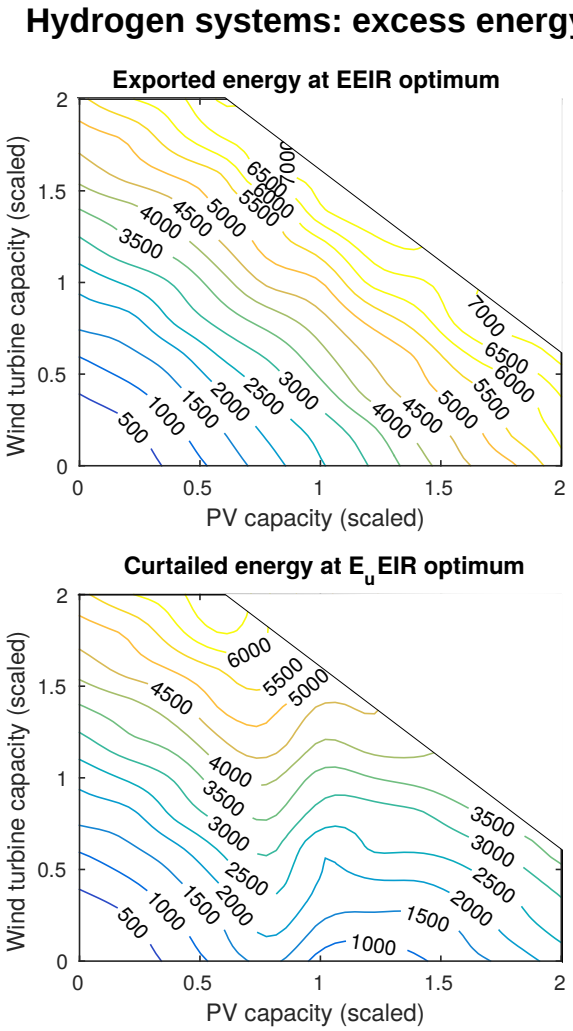

Figure 5.59: Exported energy (kWh) in the hydrogen system, showing results from $EEIR$ for comparison. When hydrogen storage is introduced to the system under $E_u EIR$ optimisation, curtailed energy stops increasing with the increased generation, and actually decreases somewhat for PV-only systems.

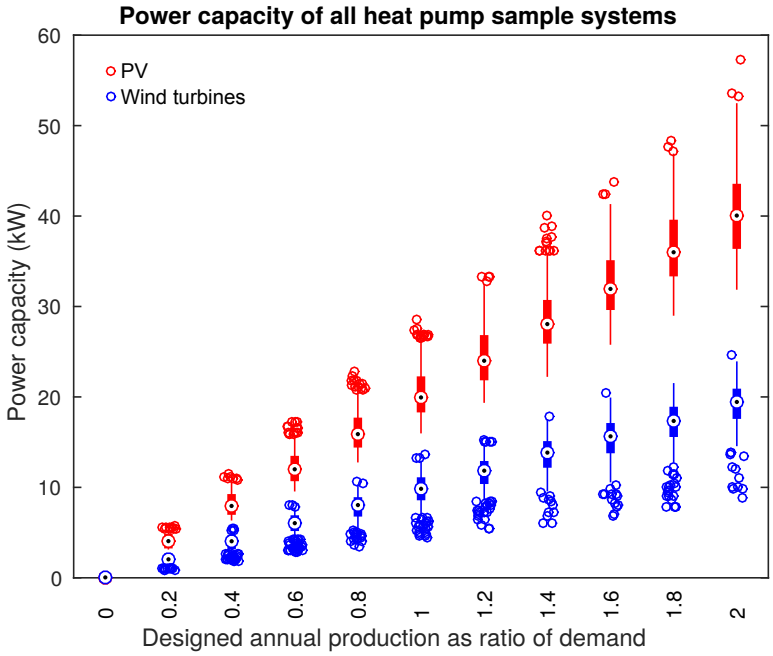

Figure 5.60: PV and wind turbine capacity required to match heap pump demand in the modelled system samples. In comparison the electricity-only samples, generation capacity is considerably larger by a factor of 4.

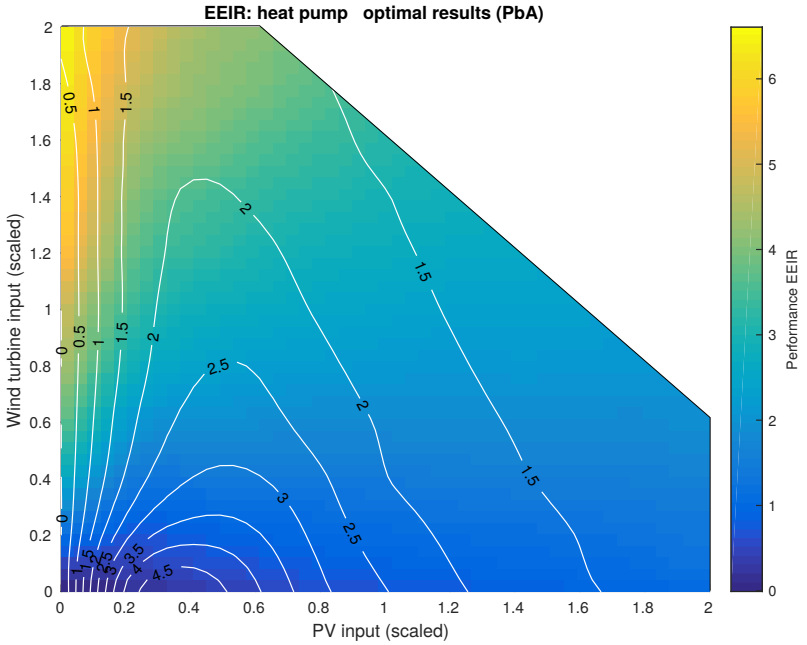

Figure 5.61: *EEIR* results showing optimal hydrogen storage capacity (contours) and system performance (shading) for all input capacities. Performance is highest for large wind-dominated systems, similar to systems without the heat pump.

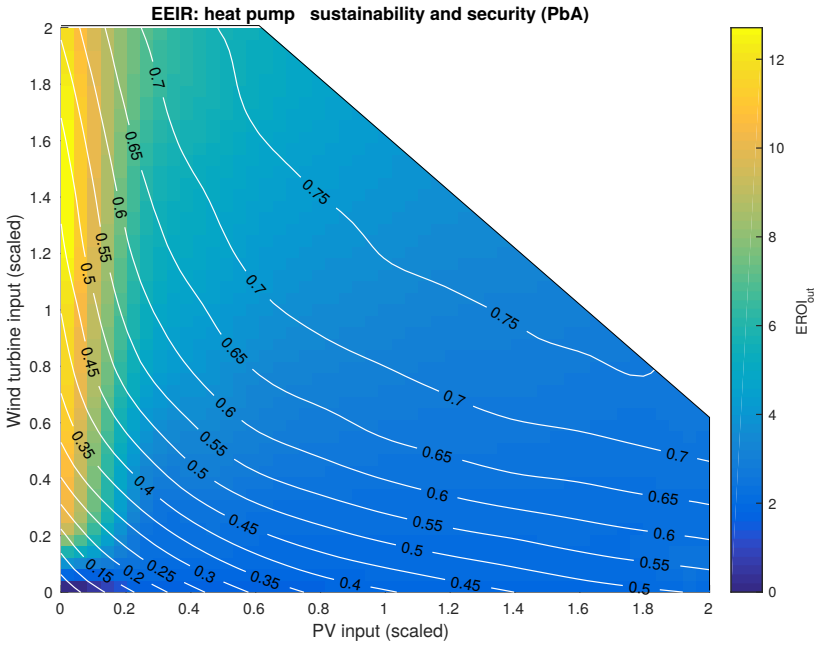

Figure 5.62: $EROI_{out}$ (shading) and EIR (contours) results for optimal energy systems with hydrogen storage. Results are similar to systems without the heat pump, but $EROI_{out}$ results are much decreased from the added embodied energy of the heat pump and extra losses from PV curtailment.

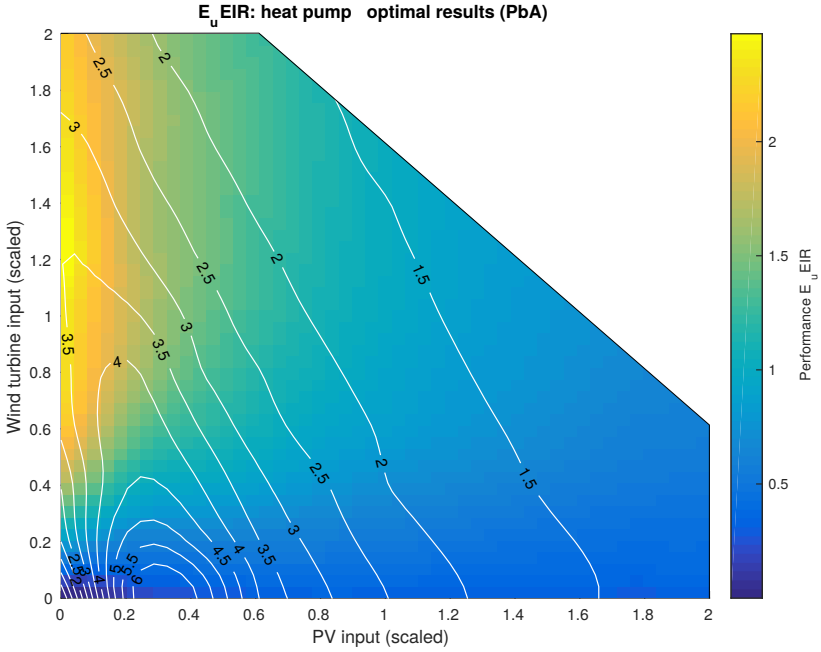

Figure 5.63: $E_u EIR$ results showing optimal hydrogen storage capacity (contours) and system performance (shading) for all input capacities. Performance is highest for mid-sized wind-dominated systems, similar to systems without the heat pump.

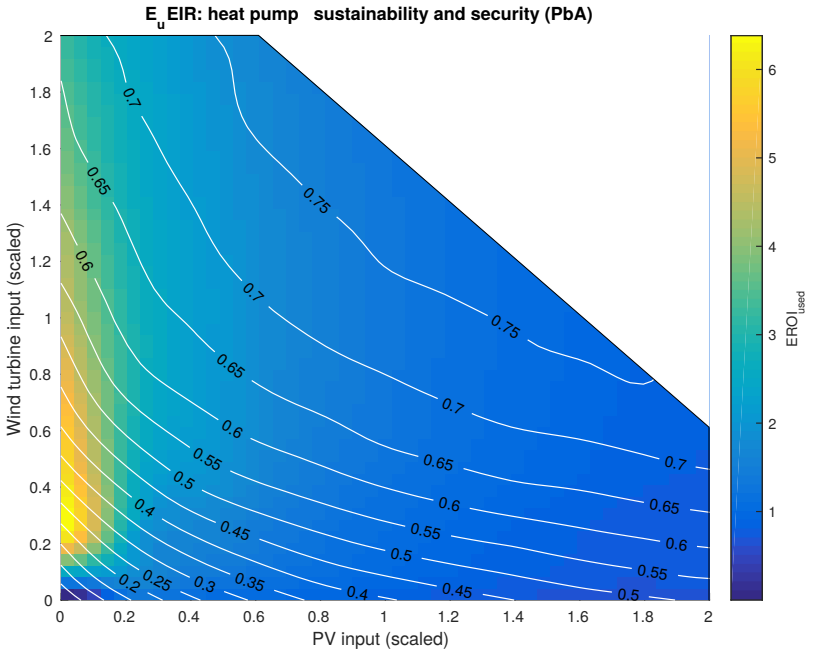

Figure 5.64: $EROI_{used}$ (shading) and EIR (contours) results for optimal energy systems with hydrogen storage. Results are similar to systems without the heat pump, but $EROI_{used}$ results are much decreased from the added embodied energy of the heat pump and extra losses from PV curtailment.

months have very good $LOLP$ results (less than 0.1) as long as annual wind production exceeds annual demand, or as long as PV production exceeds 20% of demand. This is a product of two factors: PV's production being highest in the summer, and thermal load being zero in the summer. Therefore during summer, nearly all sources of energy will be overproducing to meet demand. Spring and autumn give similar levels of $LOLP$ to each other, except that autumn is better for wind power and spring is better for solar power to supply demand; the added heat pump load in the evening means that $LOLP$ values never reach the low values of the non-heat pump systems. Finally winter months, where the heat pump is constantly running, show very little impact from solar, reaching only 0.75 for PV-only systems (they achieved 0.55 with non-heat pump systems) and 0.4 $LOLP$ for wind-only systems. Minimum values of $LOLP$ are consistently not as good as when the heat pump is not included, except for in summer when the system is overloaded.

The necessity to oversize generation capacity in order to meet increased demand leads to much exporting in the summer months. Even when using $E_u EIR$ to optimise the system, only wind production is curbed. This suggests that the level of storage given with $EEIR$ optimisation is already high enough to store all the possible PV generation to meet summer demand, and any more storage will make no difference to excess energy generation. However the increased load in winter can utilise wind generation when additional storage is available.

Therefore it appears that systems including a heat pump load are more well suited to large wind-dominated systems in terms of both their sustainability and security; their performance is less of a compromise than other systems, where PV could have brought in much better security but was too expensive. The actual EROI results are lower for all types of renewable energy due to the added costs of the heat pump, but this is an unfair comparison as the households without heat pumps are do not include their heating costs in the analysis, avoiding the energy

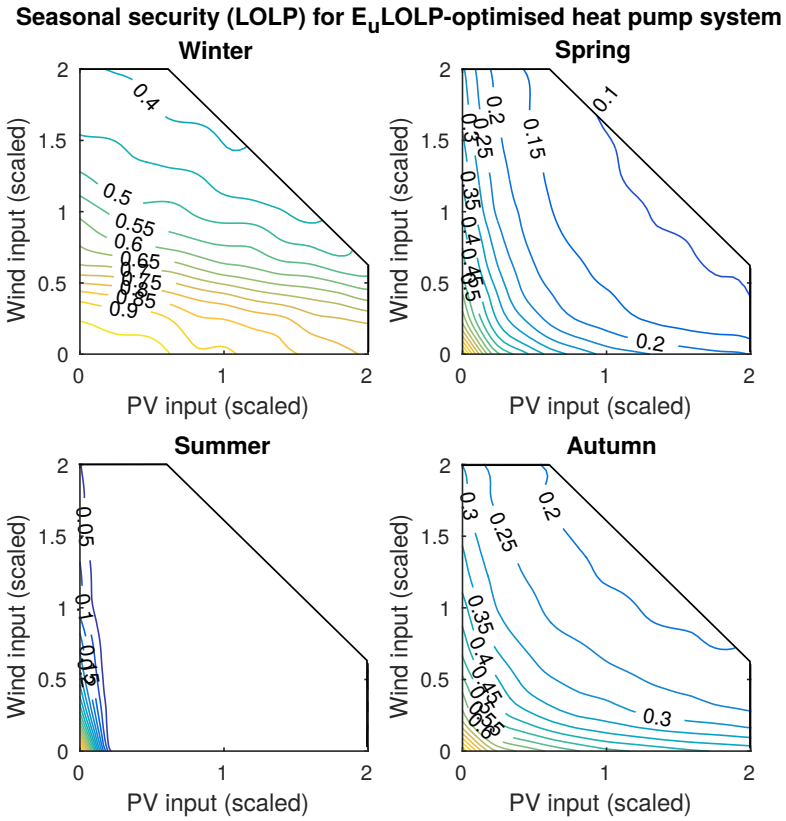

Figure 5.65: Seasonal $LOLP$ results for $E_u LOLP$-optimised systems (these optimal systems are the same as when optimising with $E_u EIR$).

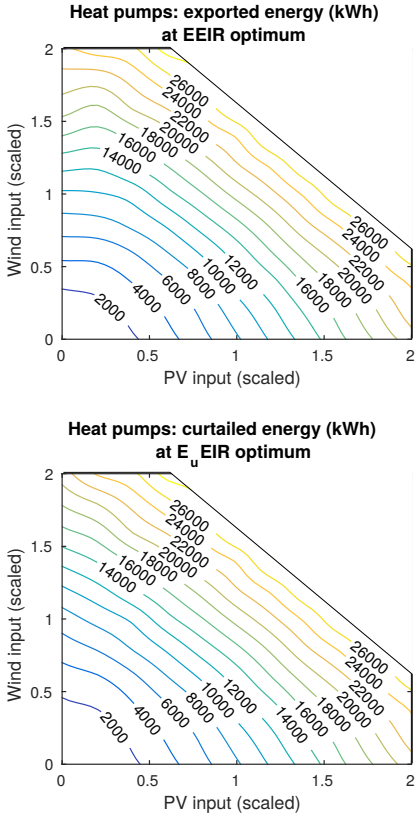

Figure 5.66: Exported energy (kWh) in the hydrogen system, showing results from $EEIR$ for comparison. Annual demand is multiplied by 4 on average, but maximum export increases by a factor of 4-5. This greater factor is caused by overproduction during summer months, and is also the reason why PV is as bad as wind here for generating excess energy.

costs of the auxiliary heating system that would use gas or oil.

Chapter 6

Stocksbridge case study

6.1 Introduction

It was decided that the ideal way to test a larger system would be through a case study, as developing an average community sized system would be unrepresentative of most towns or cities. Only one objective function - $E_u EIR$ - was used, its results in the previous chapter being fairly robust, accurate and encompassing of all necessary metrics.

While most of the new renewables capacity in the UK will come from large-scale deployment, government policy has recognised the importance of community energy schemes by enacting the Community Energy Strategy, stating that they will "work with the community energy sector to set a clear level of ambition for community electricity generation" [220]. This adds to existing legislation in Scotland and Wales to support community energy schemes across the country, with the awareness that community energy projects have multiple benefits to their local areas, and have the potential to contribute significantly to total renewable energy capacity [13].

As community projects are designed to meet local needs, it must still be ensured that energy security with respect to the national grid remains a factor. In some cases, local energy projects may improve energy security in the area, such as when local demand is not reliably met by the grid in remote locations. However, in most grid-connected areas, the two main priorities are similar to those described in the general model:

1. Maximising local use of locally generated electricity from renewable sources, with a long-term view that financial incentives (the Feed-in Tariff) will reduce over time as electricity generated from photovoltaics (PV) approaches grid parity and wind turbines decrease in price.

2. Minimising export of electricity, to limit damage to grid infrastructure not designed to cope with bi-directional energy flows.

Whilst currently PV and wind installations are rewarded for exporting to the grid through the Feed-in Tariff and Renewable Obligation Certificates (ROCs), it is becoming evident that a long-term energy plan would eventually curtail or localise some decentralised renewable energy production, to protect the grid from surges that may damage power quality and make centralised management of the grid more difficult. These incentives have in fact already been reduced significantly, even before such results have come into play, and ROCs for new installations are to be phased out by 2017 [221]. Furthermore, at the local level, transformers attached to areas with high renewable energy production may not be large enough to safely export electricity to the grid during times of peak production, as they were primarily designed for areas of electricity consumption only. Therefore exposing these transformers to bi-directional (import and export) electricity flows is a problem for local energy security.

This chapter evaluates a model of a grid-connected community energy system powered by renewable sources and balanced by energy storage technologies, connected to the wider electricity network as a virtual power plant. The model simulates theoretical energy systems in the small town of Stocksbridge in Sheffield, comparing different power sources and energy storage technologies. The choice to conduct a case study rather than to model an average energy system was made because, given the wide range of areas and possible community schemes, it is not viable to generalise community energy projects. The uncertainties involved in location and variability of supply also make modelling very difficult and prone to error [39]. With this in mind, it is acknowledged that the optimisation results here are particular to this area, but the discussion allows for a wider application of this method to other localised electricity systems with variable renewable sources.

6.2 Stocksbridge

Stocksbridge is a small town in the city of Sheffield, England with a population of 17,120 people in 6,120 households, located in a steep-sided valley running east to west. Most of the housing is situated on the southern north-facing side of the valley, but the northern south-facing side is largely farmland and contains the Upper Don river. The town has a history of industry, and still contains a large steelworks factory owned by Tata Steel, which obtains its electricity through a 400kV transmission substation separately to the rest of Stocksbridge. There is some local interest in renewable energy schemes, and a number of residents (200 households [11]) already have solar PV installed on their roofs independently. Solar power is popular with the residents, and would likely form a large part of any community energy scheme given this social acceptability and the relative ease of installation.

This analysis builds on a wider case study that was held in Stocksbridge to explore different ways renewable technology could be introduced in the area. The participatory research included debates around electricity generation, heat, building regeneration and transport, and aimed to keep solutions local and beneficial to local residents (EPSRC "Solar Energy in Future Societies" EP/I032541/1). These themes were explored during 12 workshops, 2 exhibitions and a number of informal interactions between a group of residents and a group of academics from Sheffield and Durham Universities. While the scenarios discussed in this paper were not entirely arrived at through the participatory process, the inputs and considerations on sizing and choice of technologies were based on opinions of residents, who were also consulted with regards to the results. Unfortunately, as the models only include electricity generation and demand, innovative solutions such as ground-source heating pumps in the local abandoned mines, or district heating from the waste heat of the steelworks, which were proposed by the residents, were unable to be included.

The other projects running alongside this numerical study were designed to be more open; residents of the area had an equal footing with the academics and the focus was more on coming up with visions of future energy/sustainable systems in the area rather than evaluating them to specific criteria. However there was some concern with the residents of how open-ended these projects were, as some wanted more concrete results that they could use to persuade others of their feasibility. Participants also asked for the academics to add their expertise, as they thought it would be more efficient than less experienced individuals taking on large responsibilities [222]. This made the numerical study an important addition to the larger project, as it could give these more solid results and evaluation, while the EROI-based methodology keeps to the ethos of long-term solutions sought by members of the project.

Figure 6.1 gives an idea of possible locations for the chosen technologies of PV, wind turbines and pumped hydro storage, based primarily on the contours of the land and availability of wide

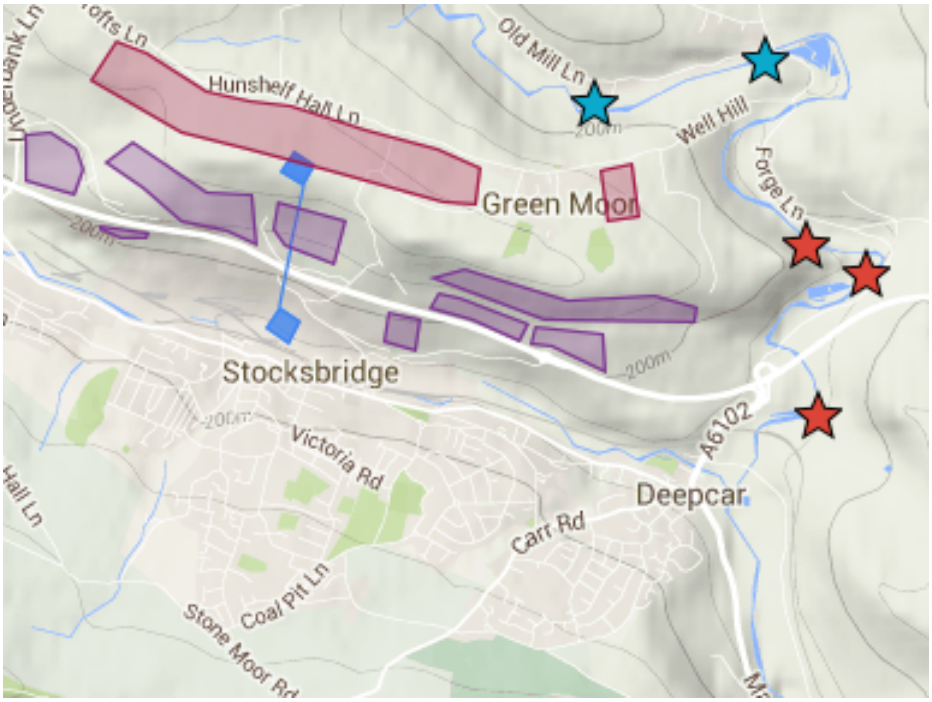

Figure 6.1: Map of Stocksbridge with locations for energy sources. Purple areas = space for PV farms. Pink areas = space for wind farms (combined with existing uses of the fields). Blue squares = possible location for PHS pools. Stars = sites of existing weirs for hydro power.

open areas for generation, however social acceptability also played a significant part. These locations were decided through the participatory process with the local residents, as they held the most knowledge of how socially acceptable certain areas were for generation. The quantities and capacities of generation were based more upon physical possibilities, and optimal results were presented to the residents for further feedback on how the system fit into their visions of an energy future for Stocksbridge. Two examples of such feedback included negative feelings about wind turbines from some residents, and a desire to include the local rivers (previously used in the steel industry) as part of any future energy system.

The location of Stocksbridge brings certain stipulations on any proposed energy system. The main ones are as follows:

1. While wind resources are plentiful, there is limited space to place wind turbines, and planning permission is not guaranteed.

2. Hill steepness gives hydro as an option, whether that be microhydro generation or storage.

3. Solar panels (PV or thermal) are somewhat popular with residents, much more so than wind power.

4. Power demand is mostly from domestic households, so peak demand is likely to occur in the evening, with increased demand overall in winter.

5. The local distribution network has nominal voltage of 11kV, medium availability for increased generation capacity and 0% capability of reverse power flows. There are currently no physical constraints on the primary substation for generation connections.

Items 1) & 2) relate to the physical geography, while item 3) is more socially motivated and 4) & 5) relate to the electricity network. These are all important factors, including the social acceptability, which cannot be ignored or glossed over. For a real community energy scheme, solutions must be worked towards with the community, preferably led by community members. However, members of the community of Stocksbridge did express a need for external knowledge and support, to ensure that they could spend their resources wisely [222].

Stocksbridge demand data

Simulating the electricity demand for Stocksbridge required an alternative approach to that of the generalised model in the previous chapter. To begin, the total annual electricity demand for the region was calculated using UK government data, where Stocksbridge was defined as encompassing the Middle Layer Super Output Area codes E02001611 and E02001612, or Lower Layer Super Output Area codes E01008142-E01008150 (note that this includes Deepcar as part of Stocksbridge) as shown in figure 6.2. It was decided to not include the electricity demand for the Tata steelworks plant, as their electricity use is managed as a one-to-one contract through a separate transformer to the rest of the community, and thus is not publicly published, and also does not add to the normal demand through the main network. Electricity use in Stocksbridge has been declining for the past decade as shown in figure 6.3, but a linear extrapolation cannot be assumed, so demand was modelled to be a total of $27GWh$/year, split into $20GWh$ of domestic load under normal tariff, $1.5GWh$ domestic load under Economy 7 tariff, and $5.5GWh$ non-domestic load. The non-domestic load is then split further into generic commercial/industrial load using average national figures, load from the leisure centre, and load from the three schools in the area. This splitting of the non-domestic load was based upon recognition of very different loads (e.g. electricity use in schools follows a very different pattern to homes and businesses) and what data was available. Stocksbridge's constructed annual electricity demand is shown in figure 6.4.

6.3 Possible scenarios for Stocksbridge

As was mentioned in section 3.2, the choice of renewable energy system paths for Stocksbridge were pre-defined rather than randomly assembled as in the previous chapter. These were based upon the available energy sources of wind and solar, and their generation data was modelled using wind speed data and actual PV generation data located only from the surrounding area. There were five alternate scenarios: PV-only, Wind 1, Wind 2, Wind 3 and Hybrid. These were envisioned along a pathway of increasing power capacity, shown in figure 6.5.

6.3.1 Wind inputs

Rather than having one wind turbine of variable power capacity, each wind scenario has a choice of three wind turbine capacities: $100kW_p$, $500kW_p$ or $1.2MW_p$. These are used in varying quantities, and have different wind power curves as shown in figure 6.6, based up on the power curve in figure 3.6. Their other properties are shown in table 6.1, based on turbines 100kW Air 19/100 [223], 500kW Nordtank NTK, and Autoflug A 1200. These properties are generally representative of other wind turbines with comparable power ratings. The smallest wind turbines were included in the analysis despite their lower efficiencies and EROI values, as locals were concerned with the impact on the landscape brought by taller wind turbines with greter power capacity. The size of the fields available gave an absolute limit of 60m hub height, which was the height of the $1.2MW_p$ turbines.

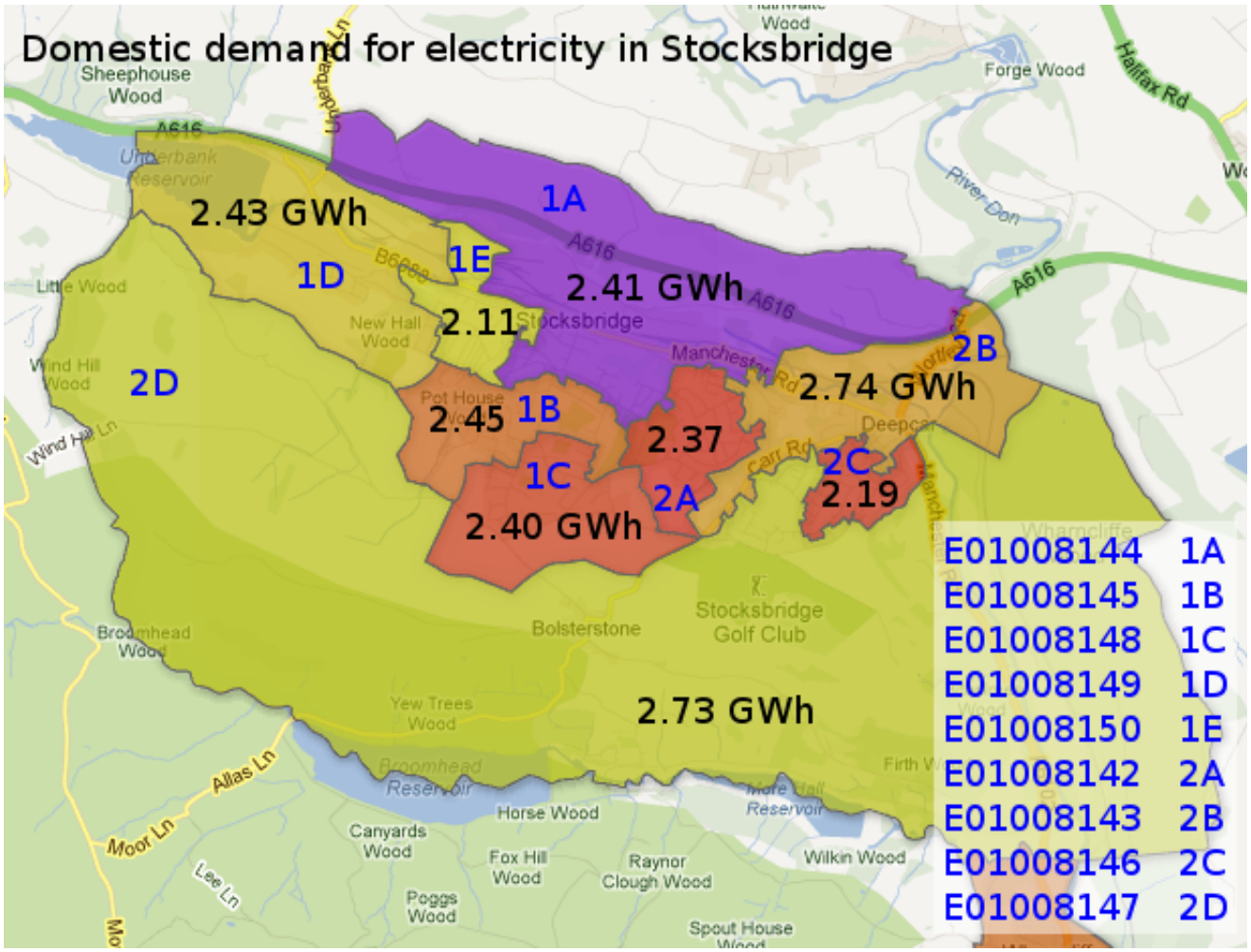

Figure 6.2: Subregions of Stocksbridge and Deepcar, and their annual electricity demand in 2012.

Turbine capacity	$100kW_p$	$500kW_p$	$1.2MW_p$
Hub height (m)	25	35	60
Blade diameter (m)	19	37	61
Cut-in wind speed (m/s)	3.5	4	4
Rated wind speed (m/s)	14	14.9	13
Cut-out wind speed (m/s)	24	25	25
Maximum number of turbines	72	20	6
Maximum estimated total annual generation (GWh)	22	29	27

Table 6.1: Wind turbine specifications for Stocksbridge wind and hybrid energy scenarios. Data taken from website wind-turbine-models.com

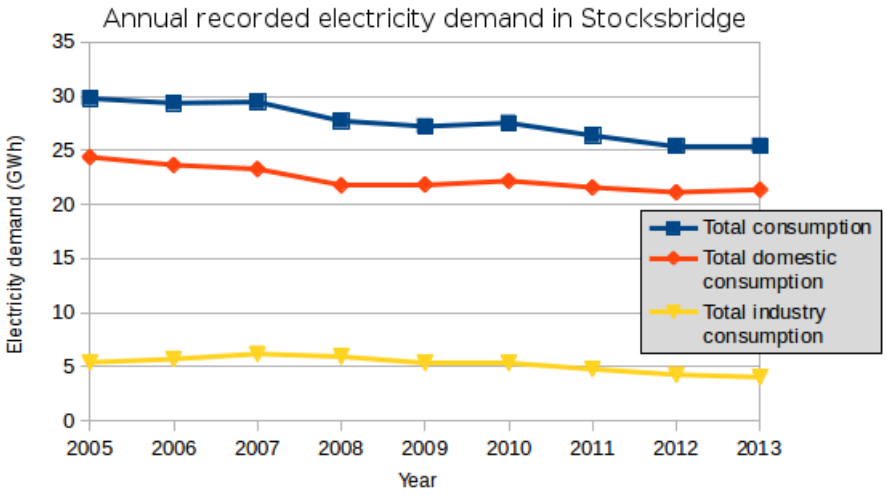

Figure 6.3: Electricity demand for the region of Stocksbridge and Deepcar, showing slow decline for both domestic and non-domestic demand, and a much higher demand for domestic households. This demand was high enough to justify using national average time-series for both domestic and non-domestic demand, scaled appropriately.

The wind turbines were proposed to sit at the top of the south-facing hill, facing south or south-east, to make the best use of the wind resources available. The wind speed data was collected from a nearby location in Bradfield situated on a similar hill to the one in Stocksbridge, with the strongest winds coming from 180-250 deg (see figure 6.7). Air temperature data was collected from another location bordering the Peak District, within a distance of 50km. It was noted that there already exists a small domestic wind turbine on the northern hill in Stocksbridge, of only $10kW_p$ capacity, but there was no further data available for this wind turbine [11].

Air temperature data was collected because the wind shear exponent α used in equation 6.1 is in fact variable throughout the day and year, depending on a number of factors, but particularly air temperature and density (which are themselves related). The relationship between temperature T and α is based upon experimental data from [224], using monthly calculations of air temperature and wind speeds at different heights, and gives wind shear for UK temperatures T at between 0.18 and 0.225 for the years 2011-14:

$$\alpha(T) = -0.001588T + 0.2258 \tag{6.1}$$

This wind shear for Stocksbridge is summarised in the following graphs, which illustrate annual and daily trends, and the typical range of wind shear exponent values. These generally agree with the previous use of $\alpha = 0.2$ for generalised energy systems across the UK.

6.3.2 Solar inputs

For solar generation, two locations of PV were proposed: rooftop installations, and solar fields on the south-facing hill below any potential wind turbines. A baseline level of renewables penetration was set fairly high at 6% of annual electricity demand, supposing that 12% of household roofs have PV arrays at an average of $2.4kW_p$ capacity, giving $1.8MW_p$ baseline capacity. This average capacity was determined using average Sheffield PV installation data obtained from the Sheffield Solar microgen database, so is realistic of available roof space, and is

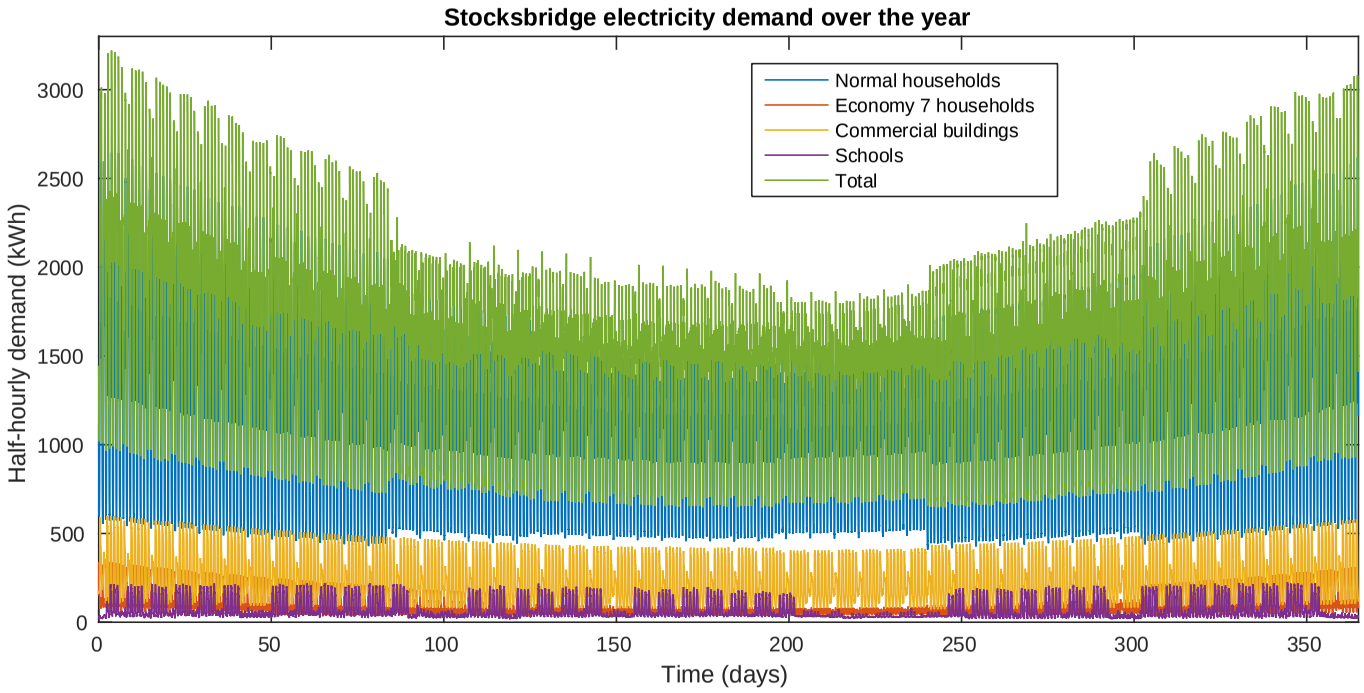

Figure 6.4: Year time-series of Stocksbridge electricity demand. Block of largest demand is households with normal electricity tariff, followed by commercial demand. The curved shape of total demand comes from smoothing out seasonal variation, as it is constructed from national demand time-series (household and commercial) grouped by season.

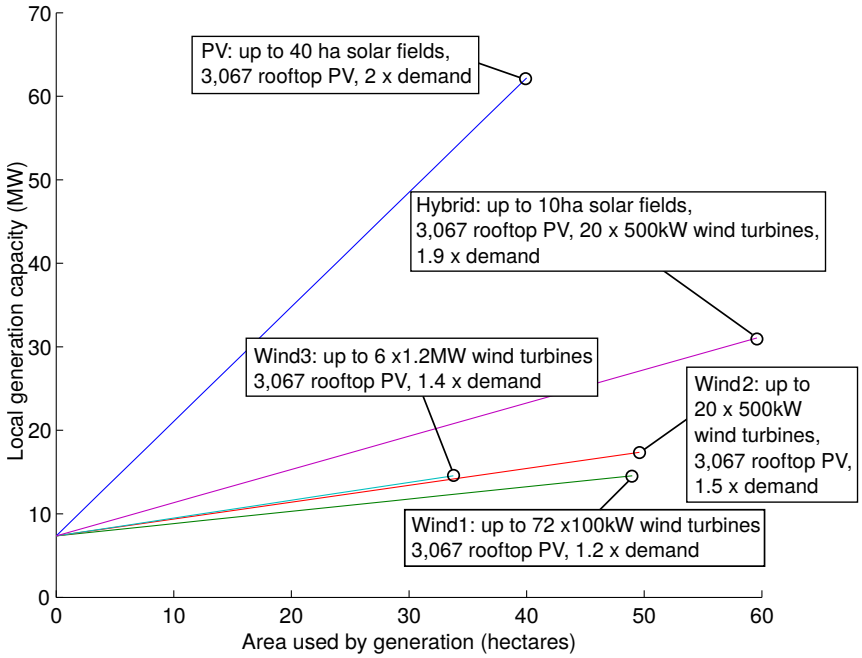

Figure 6.5: Capacity and land use of the five alternate pathways of increasing renewable capacity. The PV scenario is the most efficient user of land with respect to power capacity, but the higher capacity factors of wind turbines means that they will deliver more total energy over the year.

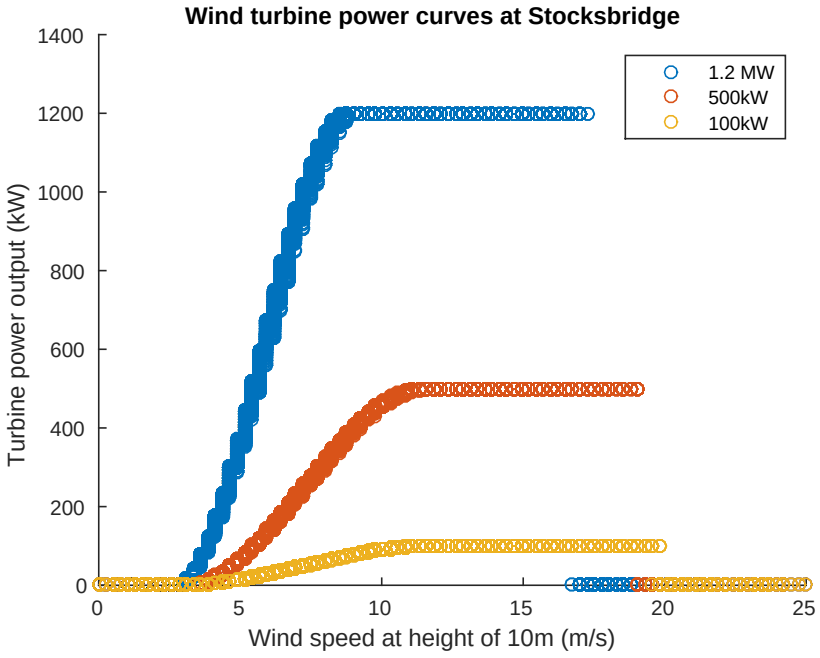

Figure 6.6: Power curves for wind turbines of capacity $100kW_p$, $500kW_p$ and $1.2MW_p$, accounting for differing wind speed at hub height. These power curves show actual output using the locally recorded temperature and wind speed data.

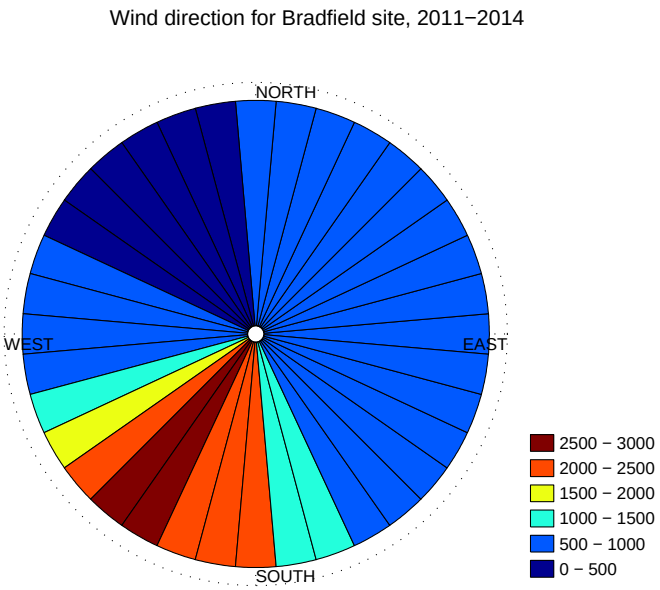

Figure 6.7: Wind rose showing primary wind directions at the location where wind speed was measured. Strongest wind speeds were observed from the south and south-east, which is the direction that the hill in Stocksbridge faces. Key shows length of time (in half-hours) that wind was observed from a certain direction.

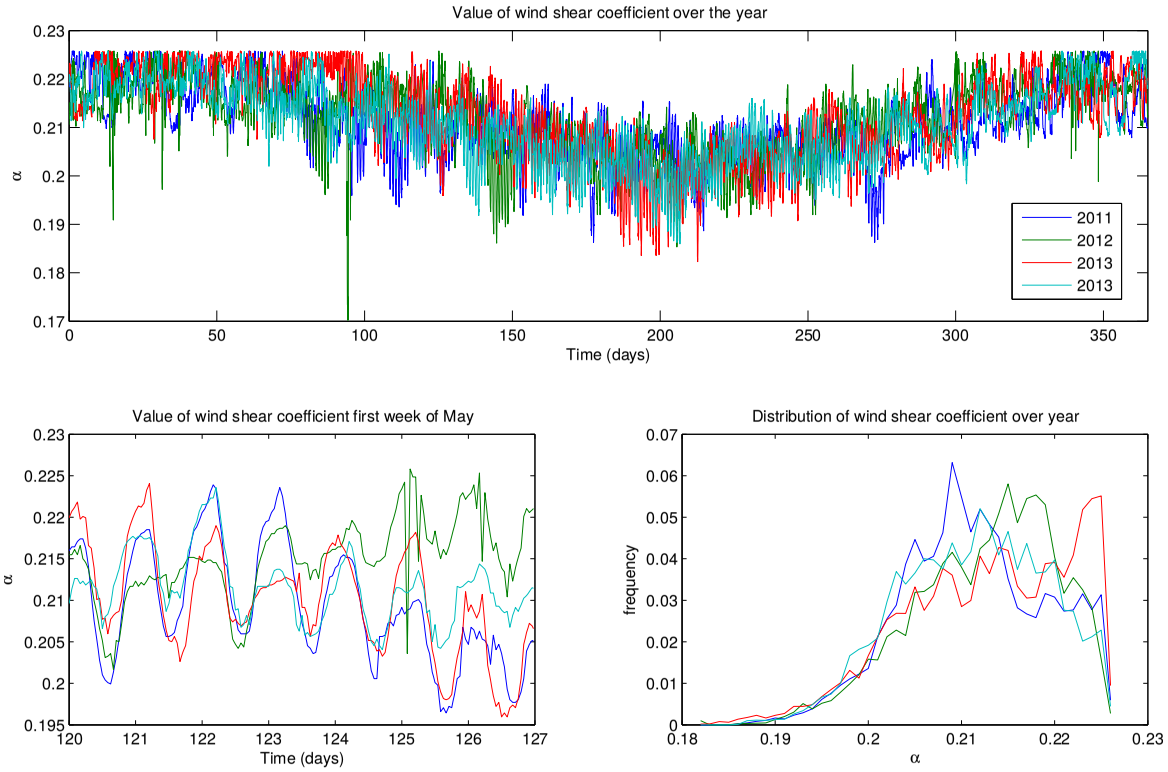

Figure 6.8: Estimation of variable wind shear exponent at the Stocksbridge wind farm location, using air temperature data. Wind shear shows a similar distribution each year, ranging from 0.2 to 0.225.

smaller than the current Stocksbridge average of $3.4kW_p$ because it includes roofs that may not currently be seen as worthwhile due to their smaller size. Rooftop installations were considered as a viable first step towards increasing renewable power generation capacity, as they require no additional land use, can be managed by individual households, and fit into existing incentive policies in the UK (Feed-in Tariffs). The solar fields to the north can add to solar generation, and their capacity was added incrementally in the model as with wind to allow for optimisation of size, up to 40ha of an estimated maximum 60ha of land. It was assumed that the fields, which are currently grass, would be able to support current utilisation such as grazing, in addition to solar generation. PV generation data was collected from four different PV arrays in Sheffield, spanning years 2011 to 2013, array locations spaced 3-7km apart which roughly matches the size of Stocksbridge. These arrays are roughly 10km away from Stocksbridge, so should have a correlation of 0.85 with PV production in Stocksbridge, a good enough approximation for the area [225]. Figure 6.9 shows the map of these locations.

6.3.3 Other components

The final power generation technology to be considered was micro-hydro, using the river Don and its existing weirs. As mentioned previously, there was local interest in using the river for power generation, there being a strong local history of using water power in steel mills. However the estimated production is so small in comparison to total demand, only powering 30 households at most [226] that it was not included in the final model. While micro-hydro can be applicable to small-scale energy systems, it was considered to make so little difference to either the power generation or system security (despite being a flat, fairly dispatchable source of power) that there was little reason to include it in the model. However there was some prospect in using hydro generation for energy storage, albeit not as part of the natural river flow.

To balance the system, different types of energy storage technology were proposed. The first option was household battery storage, using either deep-discharge lead-acid (PbA) batteries or lithium-ion (Li-ion) batteries. These would be installed in every house, and connected to the local grid with exporting and importing between them, to be exploited to their full extent. The second option was large-scale flow battery storage, using VRB units to store electricity centrally. Another centralised option for storage was pumped hydro storage (PHS), using the steep sides of the valley to store gravitational energy in vertically pumped water. There is a potential drop of 100m down the hill situated to the north of Stocksbridge, with no housing in the location, making it a prime location for such technology.

6.4 Results

With five different options for power supply and four different storage technologies considered, this gave a total of 20 possible scenarios with varying areas of land used for generation, whose performance (measured in E_uEIR) is plotted in figure 6.10 and corresponding optimal storage capacities shown in figures 6.12 through 6.16. The performance values for the wind scenarios are much higher than recorded for small household networks in section 5.2, which only reach an E_uEIR of 10, but this can be explained by the use of larger wind turbines with corresponding lower cost per kW of power capacity. The PV-only systems are similar to those PV-dominant systems for the single household systems, remaining below $E_uEIR = 5$.

The scenarios are increased in capacity by adding more generation on land use, building on the initial rooftop PV, so wind scenarios become more wind-dominated as total capacity increases. This can make for difficulty in comparing systems along their pathways, however it was considered more realistic that PV installation would be a precursor to wind turbine

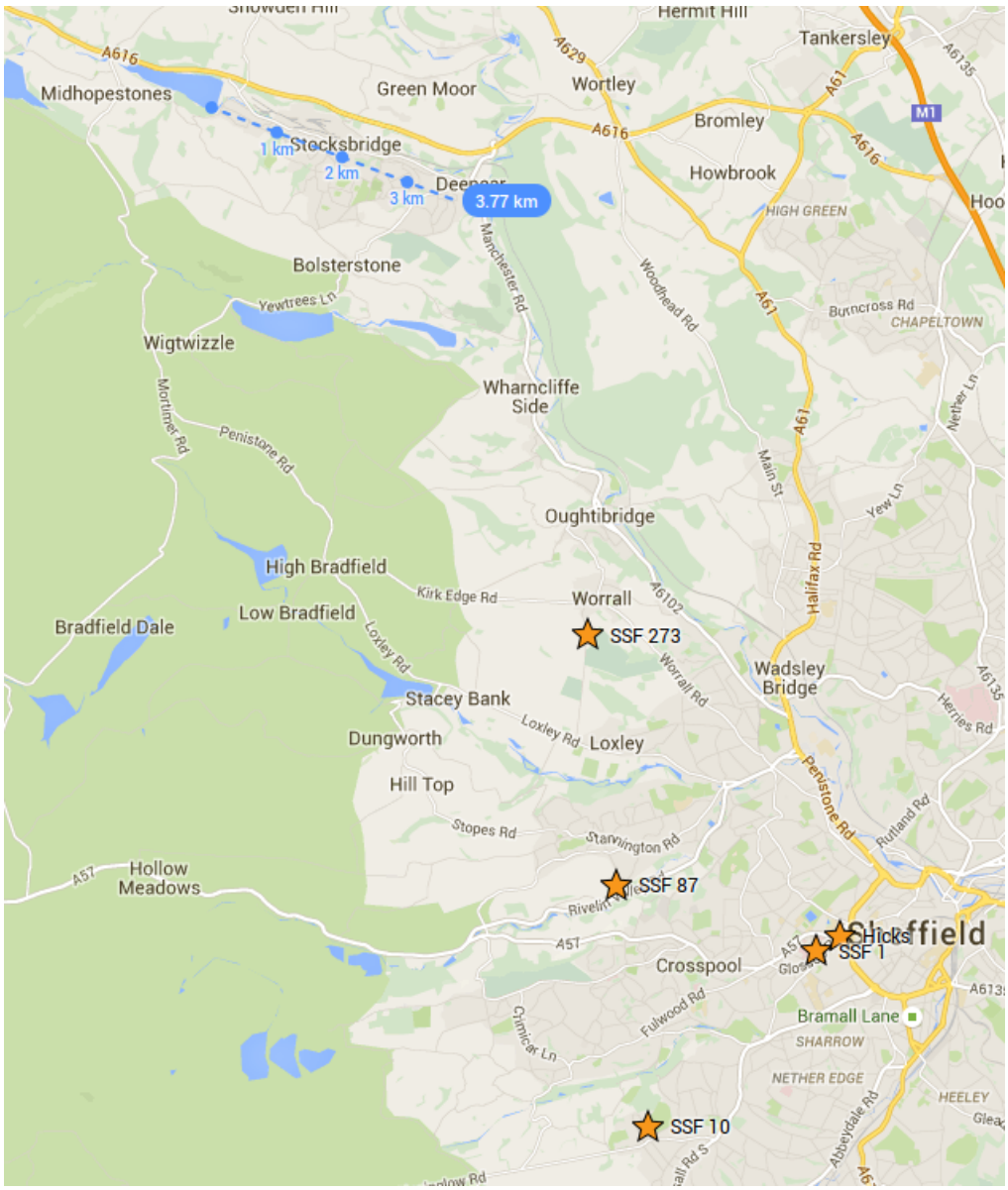

Figure 6.9: Map of PV locations used for PV generation data in the Stocksbridge model, compared to the size of Stocksbridge.

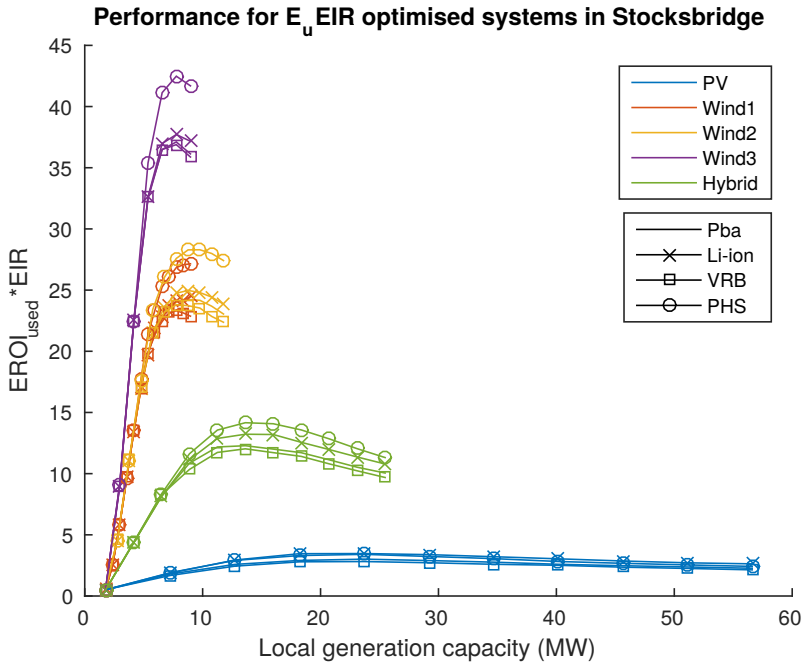

Figure 6.10: $E_u EIR$ results for all Stocksbridge scenarios. These have already been optimised for storage capacity, shown in the next graph.

development, than for both to increase in capacity at the same rate. The best performing systems are for scenarios that include wind. This is for multiple reasons: the lower embodied energy of wind turbines, their combination with rooftop PV giving a more consistent baseline, and their higher capacity factor giving more power per rated capacity overall. Larger wind turbines perform best, as their ratio of embodied energy to generation capacity is lower, and their taller hub heights give even higher capacity factors. It is therefore unsurprising that the best performing system of all is Wind 3 ($1.2MW_p$ turbines) with PHS storage, but even this system reaches a ceiling of maximum generation capacity at 5 turbines ($7.8MW$ total capacity) where adding another turbine would create too much overproduction, reducing performance. In fact all systems have an optimal generation capacity at less than the theoretical maximum, demonstrated by the peaks of the curves in figure 6.10 and summarised in figure 6.11. This also shows the proportion of capacity that comes from solar or wind.

The optimal generation capacities are at least twice the maximum power demand of $7MW$, and most of the optimal systems, excluding PV systems, are able to generate around 100% of annual demand over the year, ranging from 85% to 111% depending on the size of wind turbines. However not all this generation will be matched to demand, due to losses in the system and inability to deliver all the energy where it is needed. Differing capacity factors between wind and solar power make a big difference in the optimal generation sizing, as higher capacity factors for wind (particularly larger turbines) gives them smaller optimal generation capacity that still delivers more energy to the system over the year.

6.4.1 Battery capacity results

When comparing battery systems in figures 6.12 through to 6.16 greater storage capacity is required when PbA batteries are used, despite their higher embodied energy cost. This is likely due to their lower DOD at 50%, so while the maximum stated PbA capacity is higher than the

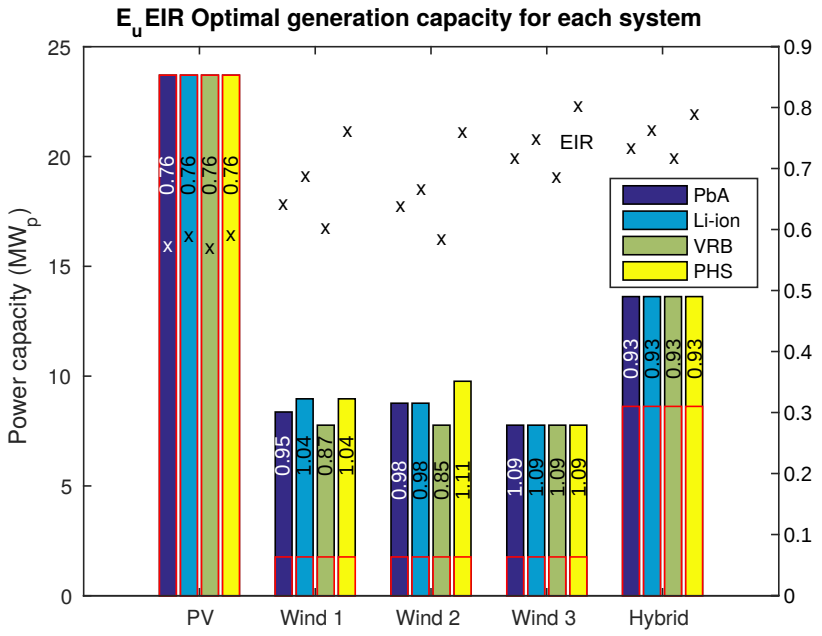

Figure 6.11: Generation capacity for optimal Stocksbridge scenarios, measured on the left y-axis. Red outlined section of the bars shows the amount of capacity that comes from PV, and numbers written on the bars show the ratio of generation to demand (where 1 means that annual demand=annual generation). Plotted x's show EIR for the corresponding system, measured on the right y-axis.

Li-ion capacity at $12.3MWh$ (capacity is total over network), the usable capacities are fairly similar. However the optimal PHS capacity results are higher still when high levels of wind capacity are deployed. Different reasons come into play here; PHS can use its full capacity, but the technology's low embodied energy values means that using the maximum capacity of $160MWh$ provides a cost-effective increase in security. These lower embodied energy values are reflected in the high $E_u EIR$ for PHS systems in figure 6.10 (excluding PV) as $EROI_{used}$ is generally higher and the increased storage capacity gives higher EIR. VRB is shown here to be the worst performing storage technology, as it is only worthwhile using alongside an all-PV system, where the effective "cost" per MWh of electricity is greater, giving more incentive to retain it through storage.

It can therefore be concluded that while both PHS and PbA storage utilises large storage capacities, PHS is more effective at putting that capacity to good use.

It is notable that changing the storage technology makes only a little difference to the optimal generation capacity of each system. However, this could be a factor of having large increments between different generation capacities, which reduces accuracy. The PV scenario has the largest increments, and its peak in figure 6.10 is very flat, so there is actually very little difference in performance between the $18kW_p$ and $24kW_p$ systems.

While PV systems have the largest optimal generation capacity, the estimated annual generation from this capacity is actually the lowest at 76% of annual demand, due to the technology's lower capacity factor in north England's typical climate. This puts an inevitable cap on the potential independence and security of PV-only systems, as capacity must be oversized to meet demand, and this results in overproduction that must be exported if not curtailed. The largest optimal supplies are for the Wind2-PHS and Wind3-PHS systems, which both supply close to 110% of annual demand, while the others often give less than

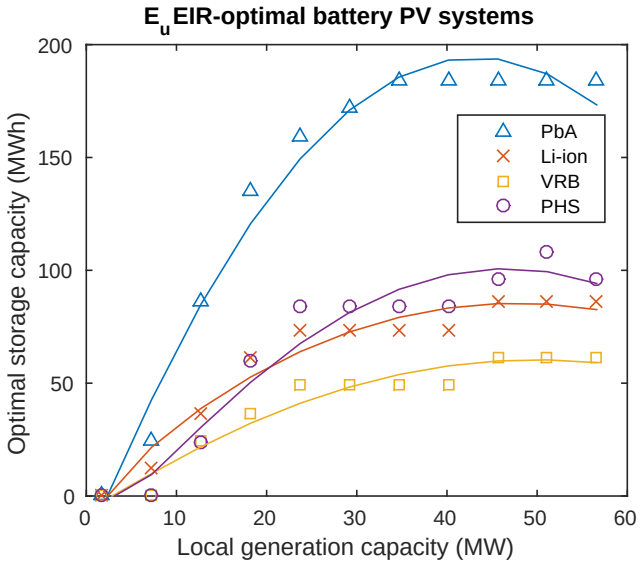

Figure 6.12: Optimal storage capacity for Stocksbridge PV-only scenarios. Increasing PV capacity quickly leads to increased storage capacity for all technologies, the greatest increase being for PbA batteries by a large margin. All reach a cap of maximum storage at $22MW_p$ generation capacity, except PbA systems which reaches the maximum storage capacity allowed at generation capacity of $25MW_p$.

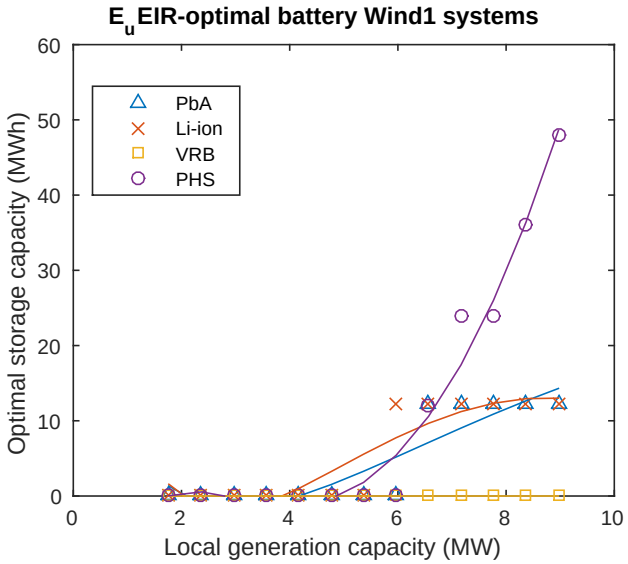

Figure 6.13: Optimal storage capacity for Stocksbridge Wind1 scenarios. Storage only becomes worthwhile at a generation capacity of $6MW_p$, and VRB batteries are never cost-effective enough to be deployed. PHS becomes worthwhile for large-scale deployment beyond $7MW_p$.

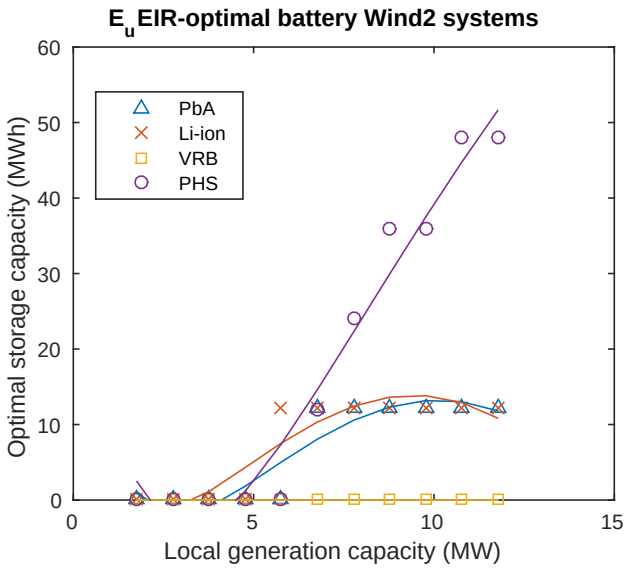

Figure 6.14: Optimal storage capacity for Stocksbridge Wind2 scenarios. Storage deployment is similar to Wind1 systems.

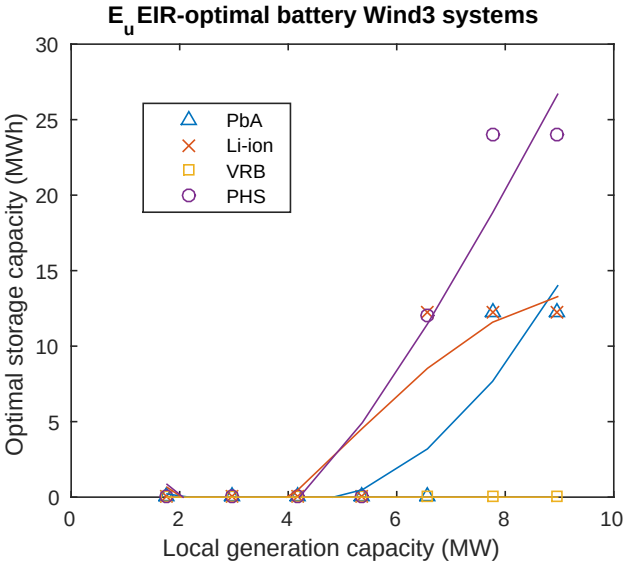

Figure 6.15: Optimal storage capacity for Stocksbridge Wind3 scenarios. Less storage capacity is deployed for the PHS systems than with Wind1 or Wind2, however the batteries exhibit the same behaviour as with those systems.

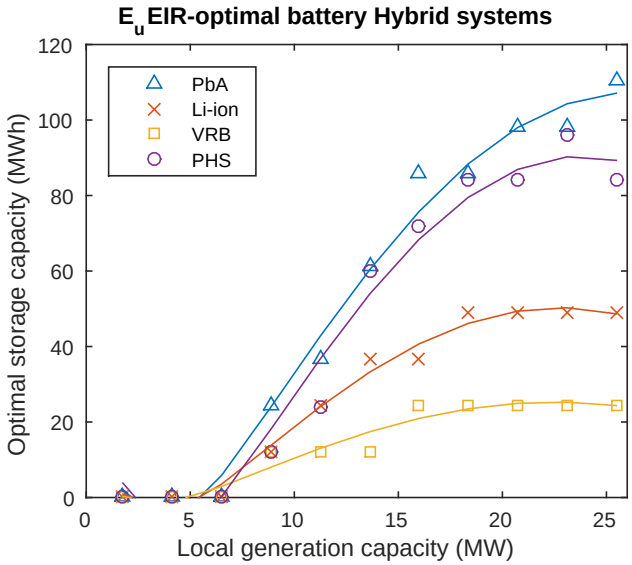

Figure 6.16: Optimal storage capacity for Stocksbridge hybrid scenarios. This bears more similarity to the PV systems than the wind-dominant systems, giving maximum capacity to PbA rather than PHS, and some deployment of VRB storage. However capacities of PbA and PHS are fairly close.

Scenario	Generation capacity (MW)	Storage capacity (MWh)	$EROI$	EIR	E_uEIR
PbA					
PV	23.7	159	5.3	0.57	3.0
Wind1	8.4	12	36.7	0.64	23.4
Wind2	8.8	12	38.0	0.64	24.2
Wind3	7.8	12	52.0	0.71	37.1
Hybrid	13.6	61	16.8	0.73	12.3
Li-ion					
PV	23.7	74	5.9	0.59	3.5
Wind1	9.0	12	35.7	0.69	24.5
Wind2	8.8	12	37.6	0.66	25.0
Wind3	7.8	12	50.8	0.74	37.7
Hybrid	13.6	37	17.4	0.76	13.2
VRB					
PV	23.7	49	5.0	0.57	3.0
Wind1	8.4	0	37.8	0.61	23.4
Wind2	8.8	0	39.1	0.61	24.2
Wind3	7.8	0	54.1	0.68	37.1
Hybrid	13.6	12	16.8	0.72	12.3
PHS					
PV	23.7	84	5.8	0.59	3.4
Wind1	9.0	48	35.7	0.76	27.2
Wind2	9.8	36	37.3	0.76	28.3
Wind3	7.8	24	53.0	0.80	42.5
Hybrid	13.6	60	18.0	0.79	14.2

Table 6.2: Sustainability, security and performance results for all optimised Stocksbridge scenarios.

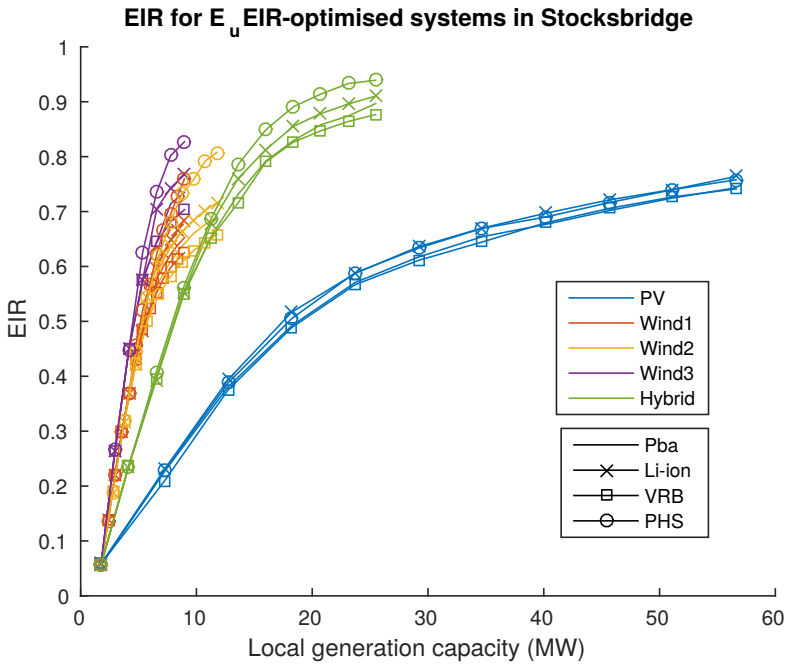

Figure 6.17: EIR for Stocksbridge scenarios optimised by $E_u EIR$. Hybrid systems give the best EIR given their more balanced mix of resources, and PV systems struggle to exceed EIR of 0.7 despite reaching the highest available generation capacity. All systems show a limit to their independence, the curves flattening so that a EIR of 1 is unobtainable without connection to the grid.

100%. Given that the greatest power demand by the system (on a half-hourly averaged basis) is $7MW_p$, this means that the optimal wind systems are capable of supplying this at full capacity, while the hybrid systems could generate twice this maximum demand, and PV systems over 3 times. However, the system will rarely deliver full capacity, and solar is less likely to meet peak demand as that generally occurs in the evening, highest in winter.

6.4.2 System independence

The impact of all these factors on the security/independence of the systems can be seen by investigating the EIR results for the optimal systems, shown in figure 6.17. The independence of Stocksbridge system was fairly important, being seen by some residents as their primary motivation for choosing local sources of energy generation.

The individual EIR results for all systems are heavily dependent on type of generation, with only a small difference seen with choice of storage technology. The results are worst for PV systems, with a maximum EIR of for PV-PHS systems at their maximum generation capacity of $62MW_p$. The high EIR values for PHS systems are caused by their larger optimal storage capacities; comparing lithium-ion batteries with equivalently sized PHS would give better EIR results for the li-ion systems due to their higher efficiency. However it is not feasible to ever reach 100% security with such a small system; the best EIR results obtained (for maximum storage capacity, at non-optimal states due to the cost of the extra storage) do not surpass an EIR of 0.8. The lower EIR results for the hybrid systems in comparison to the wind-dominated systems (when comparing systems of equal power capacity) may be surprising, but this merely suggests that the most secure mixed-source systems have a higher penetration of wind than solar. When alternative mixed-source systems with differing proportions of PV and wind were

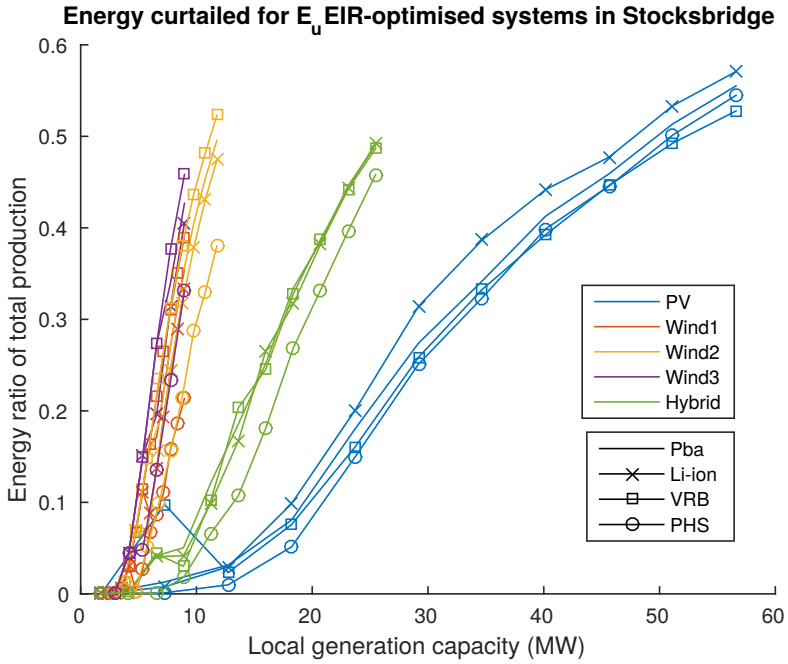

Figure 6.18: Excess energy curtailed, shown as proportion of total energy production. Large wind turbines lead to the greatest amount of curtailment, whereas systems containing more PV, especially using PHS, need to curtail less energy. However the lower cycle efficiency of PHS means that some energy is still being lost.

investigated, the best performing systems had a low PV penetration, closer to the wind scenarios than the chosen hybrid.

Of course, while EIR gives an idea of how independent the system is, it doesn't show by how much the system ended up overproducing in order to supply demand. A complementary calculation alongside EIR is the total excess energy, assumed to be curtailed, shown in figure 6.18. This shows that while the wind-dominated systems return the best EIR values, their level of excess energy is also the highest when compared to their power capacity. By contrast, the systems with higher levels of PV show less need for energy curtailment. This can be partly explained by the greater amount of energy produced by the wind turbines, however the blip shown on the graph for small PV-VRB systems, where there is no storage deployed, gives evidence that the high storage capacities help curb excess energy. As shown in the generalised model, PV works better with storage than wind turbines because day-night cycles of production are more reliable and shorter than wind generation's intermittent patterns, enabling better use of storage to meet demand.

Finally, the metric $EROI_{used}$ shows favourable results for PHS storage and large wind in the Wind 3 scenario. The PV scenario is the only one to continuously decrease in $EROI_{used}$ when new generation is added. This could be caused by the higher embodied energy of PV modules, in combination with the patterns of solar generation; i.e. while more energy is being generated, it is occurring in the middle of the day when households are less able to use it, thus the satisfied demand E_{used} is not increasing as much as it would with wind generation, while embodied energy nonetheless increases at a faster rate than for wind turbines. The $EROI_{used}$ results are more scattered than the other metrics, suggesting that it is more sensitive to chosen data, but they mostly display a peak similar to the E_uEIR and EIR curves, indicating that increasing generation capacity past a certain point can have a detrimental effect on the sustainability, as

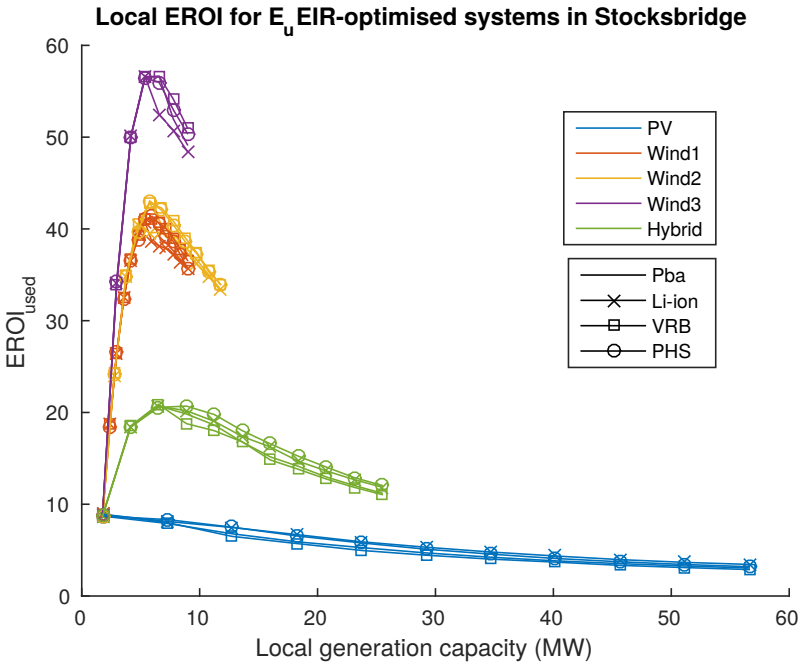

Figure 6.19: $EROI_{used}$ values for Stocksbridge scenarios optimised with E_uEIR. PV is the only scenario to show constant decrease in $EROI_{used}$, and using the largest wind turbines gives the highest $EROI_{used}$.

either the size of the required storage becomes prohibitively energy-expensive, or the increase in generation capacity doesn't create a large enough increase in usable local energy. The actual $EROI_{used}$ values, mostly increasing beyond the initial value of 8.8 (with the only exception being the PV systems), are encouraging as they suggest a good energy return.

6.4.3 Conclusions

These results have given the optimal renewable energy system to be a $1.8MW_p$ network of rooftop PV supported by five $1.2MW_p$ wind turbines, managed with a local pumped hydro storage system of $12.3MWh$ capacity. Furthermore, analysis with the metrics has given an understanding of how this system compares to the others, and some ideas about how such a system would behave in terms of its sustainability and security. It would not be feasible to aim for a fully independent local renewable energy system, this being unachieveable with the technology mentioned (long term storage would be necessary over the winter months and during long periods of wind calms) and far too costly. However, this work has shown that it is possible to create a local security buffer on a virtual power plant level, reducing the work required to be done by the national grid to maintain full energy security.

It must be noted that the optimisation results cannot be taken at face value, as there are more issues to be considered in terms of local acceptability and practicality. In attempting to compromise for affordability, many of the scenarios suggested to the Stocksbridge residents included wind generation using shorter wind turbines (to reduce their visibility), which some were happy with, but others found alienating. One such resident gave this inclusion of wind energy generation as the reason for her eventual leaving of the group, saying "suddenly wind turbines were back on the agenda... this is when I suddenly thought there is nothing more in it for me". [222].

In terms of practicality, there are no current incentives for installing storage capacity on such a large scale, other than potentially the capacity market, which pays generators to export energy at times of peak demand. This would be more practical to apply to the VRB or PHS systems, as they are large centralised units of power, but still would add extra complexity to the system, as they would need to be producing energy at specific times of year with only a few hours notice [227]. The centralised options for energy storage would likely be more logistically practical, however would require planning permission and therefore entail a long planning period beforehand. These are equally barriers to the more general systems studied in the previous chapter, however such barriers are illuminated when relating to a real case study with specific consumption/resources and locality.

Therefore it must be acknowledged that finding a desirable energy system of the future cannot be determined entirely though optimisation; there are more complex nuances to the solutions and results are unlikely to satisfy every party. However results from the participatory process with the Stocksbridge local residents showed that having some form of optimisation and evaluation is necessary, both as part of the decision making process and to give a sense of tangible results.

Chapter 7

Conclusions

This thesis has brought together a number of renewable energy system optimisation studies, all using real world data of electricity generation and demand. In this conclusion the results from across all scenarios are linked together and contrasted, allowing for a broad evaluation of potential renewable energy systems.

These energy systems were posed within the framework of a transition towards decentralised/distributed generation, where the challenge of balancing the grid is distributed into more local energy systems, referred to as virtual power plants (VPPs). In this context, electrical energy storage such as batteries or pumped hydro storage (PHS) becomes relevant as a way to balance electricity generation and demand at the local level. However, there is concern that while this model is designed to work in favour of renewable energy sources, which are naturally distributed geographically, the additional requirements/costs of balancing technology may undermine the primary goal of making our energy systems more sustainable. The trilemma, widely known as the compromise between sustainability, security and financial cost, is ultimately at the heart of this balance. Therefore these optimisations are an approach to studying the trilemma, using the energy parameters of the energy systems to form a physical, rather than economic, evaluation of their performance.

7.1 System optimisation results

7.1.1 Comparing different systems with PbA batteries

While not the most high-performing battery technology, lead-acid (PbA) batteries were used as the baseline storage technology in the evaluated systems. The data available on their performance and embodied energy is the most reliable, being the most mature of the battery technologies, so evaluating results from PbA systems provided a threshold that could then be extended to systems with more modern batteries.

Looking at the results for energy systems with a full range of optimisation (all studies excluding the Stocksbridge scenarios), optimising with all objective functions returned an optimal system that only had one source of power: wind, alongside some energy storage capacity. While solar electricity generation was shown to improve energy security of the system, PV's high embodied energy meant that it was more sustainable for systems to use only wind energy sources, supplemented by battery storage.

Optimal power capacity results for single household systems, whether these be power generation or storage capacity, were not significantly affected by choice of $LOLP$ or EIR, but were by the choice of $EROI_{out}$ or $EROI_{used}$; i.e. whether the system was allowed to export energy to the grid. Optimal battery capacities for non-exporting systems were over twice the

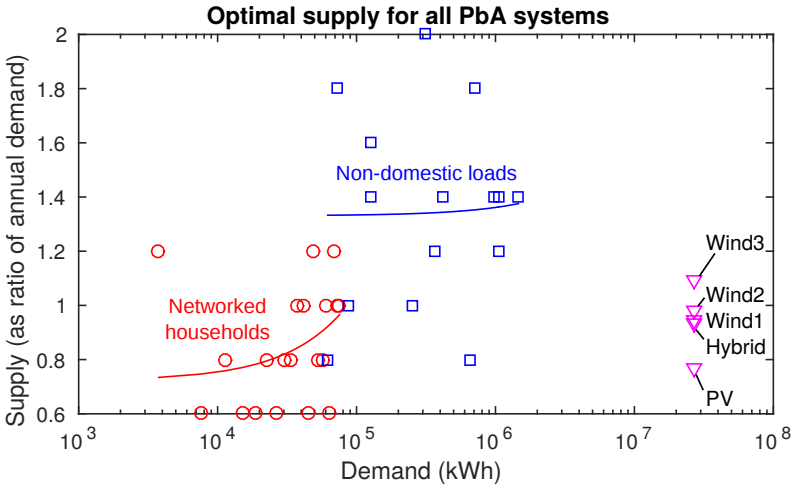

Figure 7.1: Optimal power capacity results for single household systems, domestic networks and non-domestic systems, up to results for Stocksbridge case study (PbA only). Log plot allows for expression of small and large systems, and all fitted curves are linear. These linear fits are not particularly strong: domestic household systems have an initial drop in capacity, Stocksbridge power capacity depends on the power source's capacity factor, and non-domestic systems have no clear trend, likely being more dependent on type of load.

optimal battery capacity for exporting systems, across results for all battery technologies. Similarly, systems returned optimal wind turbines with twice the energy output for exporting systems than non-exporting systems, where they supplied a total energy over the year equal to the total demand. Furthermore, the actual optimal wind capacity under $ELOLP$ and $EEIR$ would be unlimited, as their results simply returned the upper limit imposed by the study. This can be clearly seen as $EROI_{out}$ is only improved by using larger wind turbines, and the security would not be negatively affected from increased generation.

When expanding these results to networked domestic systems, as shown in figure 7.1, exporting systems once again gave optimal results where the largest wind turbines were sized to be as large as possible. However there was a decline in optimal battery capacity, returning almost zero capacity for the largest networks of 20 households. Non-exporting systems showed a sharp drop in wind turbine capacity when a second demand was added to the initial single household system, the result of demand smoothing. Wind turbine capacity was then stagnant for E_uEIR results, but increased under E_uLOLP. Battery capacity dropped more dramatically than for exporting systems, given their initially higher baseline. However their storage capacities were still higher than for non-exporting systems up to the maximum size of 20 households.

Non-domestic systems showed similar trends, but larger non-domestic demands were less likely to be smoother, as their profiles were constructed differently. Rather than being a number of demands added together, which naturally creates a smoothing effect, larger loads were from larger buildings, which may show some smoothing from having a number of different rooms, but the building as a whole would likely adhere to a regular timetable, creating notable patterns of demand that are not smooth. One example is the school load, which shows weekly and term-time patterns of demand. Therefore reductions in battery capacity were linear rather than exponential, guided more by the increase in EROI of the larger wind turbines rather than limited storage functionality.

Figure 7.2 shows the exponential drop in battery capacity for networked households, and

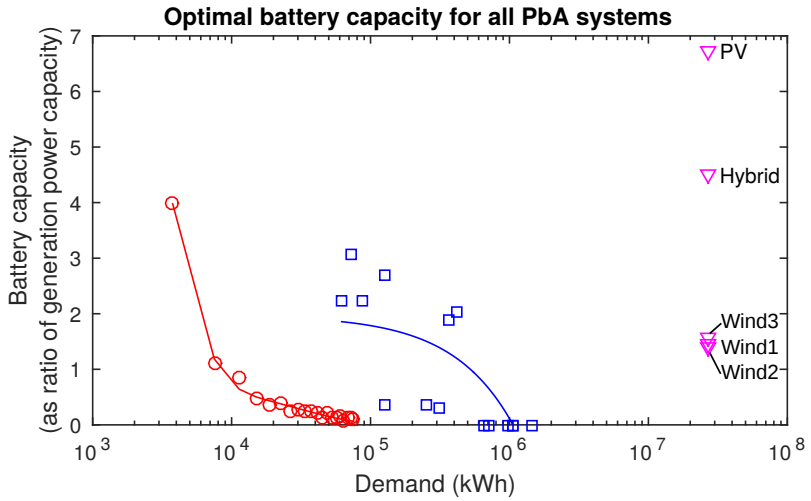

Figure 7.2: Optimal battery (PbA) capacity results for single household systems, domestic networks and non-domestic systems, up to results for Stocksbridge case study. Battery capacity is normalised for non-domestic demand by dividing total capacity by $3.77MWh$ (average household data demand). Both domestic and non-domestic demand have decreasing battery capacity, but Stocksbridge's use of PV brings batteries back into the picture.

the more steady decline for non-domestic systems. Both give zero storage capacity for their largest systems, however the much larger Stocksbridge system returns non-zero battery capacities for all scenarios. This non-linear relationship is interesting, as it shows that medium-sized systems develop a smooth enough demand that the batteries become less valuable, eventually dropping their value below their cost. However the case study is large enough that more complex considerations come into play, and PV becomes an integral part of the energy inputs. This use of more costly PV production increases the value of the generated electricity, making it more worthwhile to store, thereby giving larger battery capacities once more. This is a complicated relationship, as PV generation also improves security by complementing wind production, filling in some gaps of production when wind speed is low but the sun is shining. PV generation is also complementary to storage regimes, as a fixed storage capacity is capable of storing energy during daytime, and using that stored energy at night. It is difficult to adapt this strategy to the more stochastic patterns of wind power generation, where the periods of underproduction do not necessarily match the periods of overproduction.

The effects of these battery sizes can be seen in the security results in figure 7.3 where small domestic networks and non-domestic systems show a small increase, but all the Stocksbridge scenarios have higher security. The case study scenarios benefit from using mixed energy sources, where a 3:1 mix of PV and wind in the Hybrid scenario gives a slightly more independent system than the more equal 6:7 mix (Wind 1/2) or the 5:7 mix (Wind 3) offered by the wind-dominated scenarios, and the PV-only scenario has the lowest security, but not as low as the wind-only smaller systems.

The use of mixed energy sources in the case study was inevitable due to a number of factors: geographical, technical, econonomic and social. Geographically speaking, there is limited land available for large wind turbines. On the technical side, large single-source PV or wind systems run into security problems relating to overproduction, such as harmonics or limits to how much can be exported at a given time. Economic and social factors are more complex: wind turbines were included to allow for economic benefits, but wind-free scenarios also existed to give options

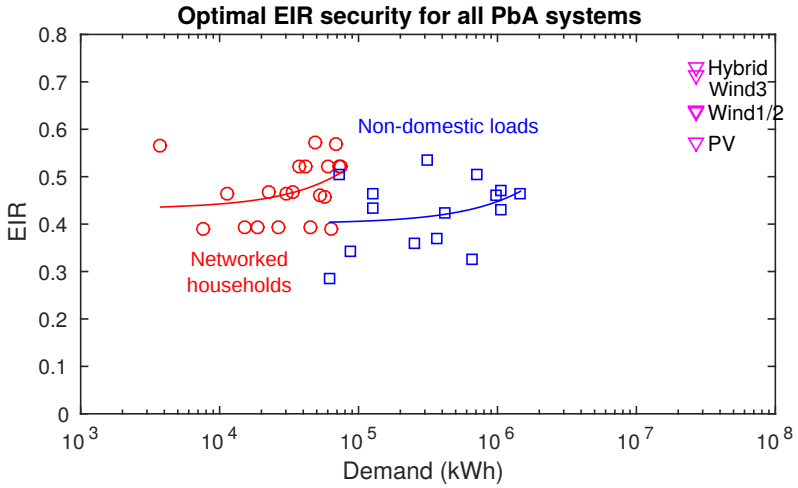

Figure 7.3: Optimal security (EIR) results for single household systems, domestic networks and non-domestic systems, up to results for Stocksbridge case study. Results for PbA battery systems. Increase in EIR for the domestic networks and non-domestic systems is mainly motivated by demand smoothing rather than battery use, as storage capacity decreases for both.

for residents who disliked wind power, as did small wind turbine scenarios for those who were only against tall wind turbines.

These hybrid systems have better energy security than the smaller wind-only systems, as previously noted, but sustainability is not increased any higher than the range of $EROI_u$ reached by much smaller systems (see figure 7.4). This contrasts with the EIR results, where all of the optimal Stocksbridge scenarios are higher than those achieved by the smaller systems. The most secure system is the wind-PV hybrid scenario, but this is only slightly higher than the Wind 3 scenario (which also includes a small percentage of rooftop PV), both surpassing an EIR of 0.7. It can be concluded that a hybrid system with slightly higher power capacity of PV than wind is generally the most secure and independent type of system according to $E_u LOLP$.

Bringing sustainability and security together, $E_u EIR$ performance generally improves as systems increase in size and demand increases, up until the Stocksbridge scenarios, where the lower $EROI_{used}$ values of PV reduces performance. This is because sustainability is generally the strongest factor in deciding performance; increasing sustainability has only a small impact on security, whereas increasing security by using PV or larger storage capacity can have a very large impact on sustainability. This is summarised in figure 7.5, where all the small domestic household networks and non-domestic systems are optimised to be wind-only systems, the most sustainable but least energy secure form of generation. Their performance increases with system size, which is caused by the improved $EROI$ of larger wind turbines and smoothed demand requiring smaller batteries. The Stocksbridge case study also gives preference to large wind turbines, where the Wind 3 scenario (using $1.2MW$ wind turbines) has over 12 times the performance of the PV-only system. Reducing the size of the wind turbines to 500kW or 100kW gives a factor of 8, and the hybrid system has higher performance than PV by a factor of 4. These multiplication factors are seen across all storage technologies, and most of the difference is contributed by the increase in $EROI_{used}$ when wind turbines are used, however a small increase in EIR is also seen.

This result adds to the consistent theme of EROI being easier to increase than energy security, which is understandable given the difference between the metrics. Since 100% security (whether measured as an EIR of 1 or $LOLP$ of 0) would be a perfectly secure system, a goal that

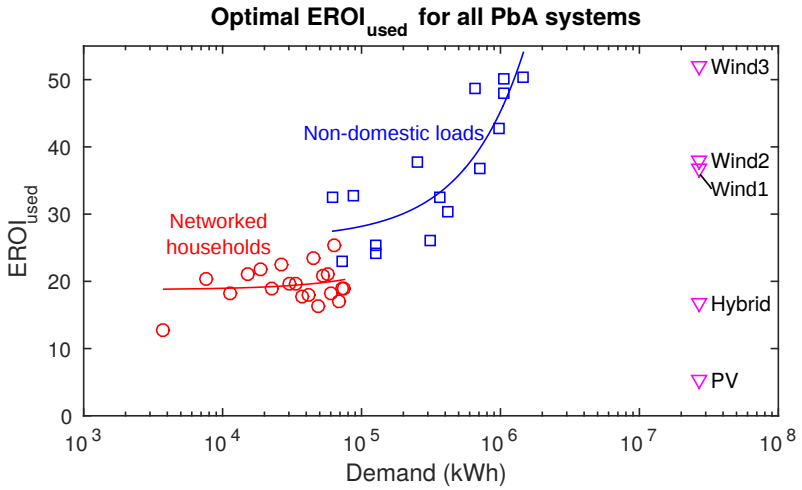

Figure 7.4: Optimal sustainability ($EROI_{used}$) results for single household systems, domestic networks and non-domestic systems, up to results for Stocksbridge case study. $EROI_{used}$ increases until PV is introduced as the baseline for the case study, and the PV-only system has $EROI_{used} < 5$.

is impossible even for the current national grid, this means that we will always see diminishing returns when aspiring towards better security. However there is no "perfect" EROI to aspire towards, and while energy consumption can be split into components that have diminishing returns, e.g. aims for 100% recycling of materials, there is much more space overall for energy use reduction and energy generation gains, and we are not currently at the limits of their improvement.

It must be noted that when it comes to community systems as large as the one considered here, the land available is an important concern, as it may be not big enough or not exposed enough for wind turbine installation. Just as importantly, local perceptions of wind turbines could remove the option of large wind turbines with their better EROI levels, or eliminate wind turbines as an option altogether. However in the case of local opposition, $E_u EIR$ analysis can be used to find a scenario that works to meet local needs while also maximising sustainability and security. For example, there was some support in the participatory workshops for shorter wind turbines, and the Wind 1 scenario with $100kW$ turbines still outperforms the Hybrid and PV scenarios, while using shorter wind turbines than the Wind 3 scenario which used $1.2MW$ turbines. However, Wind 1 required up to 72 turbines, while only 5 $1.2MW$ turbines were required for the optimal result. Wind turbines are not the only factor affected by local conditions; most areas would not have the hills required to support pumped hydro storage, so this would not usually be available as an option. Furthermore, the ease of installing rooftop PV, and the subsidies that used to exist for households that installed PV, meant that there was a strong desire for solar energy inputs despite their higher costs.

Over all PbA systems tested, results showed that when optimising for battery capacity, EIR could reach values of 0.9 for large hybrid systems, regardless of system size; this was seen for the Stocksbridge case study and also single household systems. However these systems showed very high excess energy that would need to be exported or curtailed, so the overall optimal systems had lower inputs, less PV availability, and lower EIR values of 0.75 at most.

When comparing different sources, it was found that wind power is more prone to overproduction, and PV is more prone to underproduction. This can be explained by their capacity factors - wind turbines literally produce more total energy for an equal power capacity - and also by their daily and yearly supply profiles. As wind power has higher

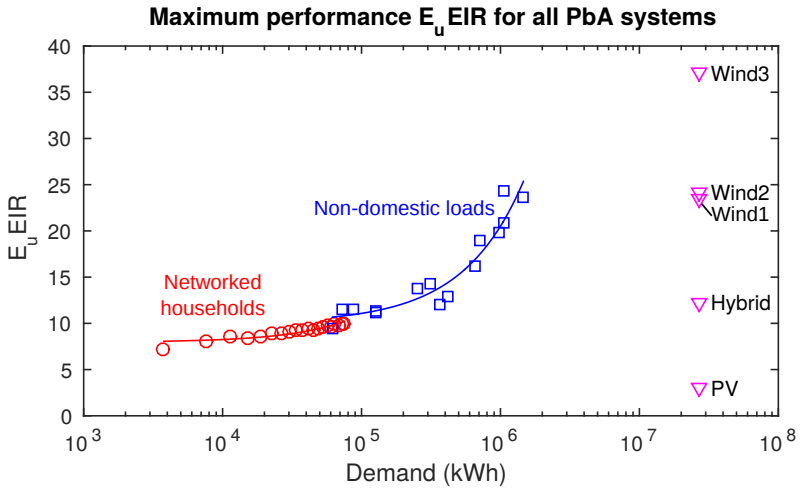

Figure 7.5: Optimal performance ($E_u EIR$) results for single household systems, domestic networks and non-domestic systems, up to results for Stocksbridge case study. Performance increases overall, showing consistency between domestic and non-domestic systems, but decreases for Stocksbridge systems with significant PV use.

capacity factors (even at low hub heights, some areas showed high production) and can generate power during night time when demand is lowest, it is more capable of supplying energy when the system doesn't need it. Furthermore, its stochastic nature means that the battery is less likely to be empty when it is producing at full power, unlike PV whose daily cycle means that the battery will generally have been discharged over night and ready to charge again during the daytime. Therefore wind turbines may continue overproducing when the batteries are fully charged and demand is low, so the only option is to export or curtail production. By contrast, PV production is very low during the winter, so will always underproduce in those months no matter how large the storage capacity is or how oversized the system is (within reasonable limits). Even in summer when a large PV system may be massively overproducing during the day, it will still not provide any power at night (at UK latitudes) so there is a period where storage can discharge and be ready for recharging the next day. This complementary relationship between PV and the battery can be observed in the correlations between system inputs and their optimal sizing, as when only considering one aspect of security - whether underproduction or overproduction - the size of PV capacity is more correlated with the battery capacity. However when considering both aspects of security through the either $E_u LOLP$ or $E_u LOLP$, wind capacity has higher correlation with security, as its tendency to overproduce is now penalised. However, this correlation is still less than PV's with security, and there is no correlation between wind inputs and optimal battery capacity, suggesting that wind generation derives little value from battery storage.

When considering sensitivity of the results to embodied energy values, it was found that the best way to improve sustainability, security and performance is to reduce PV embodied energy. Reducing battery EE was also valuable for improving security, but sustainability was adversely affected, as the system relied on larger battery capacities. Given the positive combination of PV and battery storage, it would make most sense to reduce both in tandem, but giving more emphasis to the reduction in PV EE.

Reducing the wind turbine's embodied energy also improved performance, but this resulted in lower battery capacities and thereby had a slight negative effect on the system's security. There also may be less scope to reducing these values because most of the energy use is from

tower construction (steel or concrete) and these are mature manufacturing processes that would require serious reform to ensure that all factories stuck to low energy techniques. While energy costs for PV manufacturing could be reduced in an economically beneficial way by using more efficient methods or new types of PV such as organic solar cells, reducing steel or concrete energy costs would need changes such as very high levels of recycling or renewable energy powered factories. Therefore reducing PV's embodied energy is a more realistic goal, possibly combined with the reduction of battery embodied energy to ensure that sustainability is not compromised.

It was found that when PV's embodied energy levels were reduced more gradually, optimal system supply was shifted to hybrid systems with a significant PV input - equal to wind inputs under E_uEIR optimisation - and system security EIR was increased from 0.45 to 0.75 for single household systems. However, 0.8 EIR appears to be a natural limit to optimised systems when PbA batteries are used, as reducing PV's embodied energy beyond 60% appeared to make no considerable difference to EIR, only serving to improve $EROI_{used}$. Using Li-ion and NaS batteries could achieve EIR results of 0.85 when PV EE was reduced by 80%, but the other batteries gave similar results to PbA.

7.1.2 Storage technology results

Five different types of batteries were investigated as part of the single household system optimisation, and pumped hydro storage (PHS) was also used in the Stocksbridge case study. PHS was only plausible for the case study because there was much higher energy demand, and a hillside steep enough to consider it as an option. However, this is an unusual case, as there is a shortage of available sites for PHS left in the UK.

Over all types of storage investigated, there were only small differences in their performance (E_uEIR) for single household systems, as shown in figure 7.6. While lithium-ion systems gave the best performance, PbA systems had the best EIR result despite having poorer quality batteries in terms of efficiency, lifetime and depth of discharge. This was because their reduced energy costs allowed for larger wind turbines and more storage capacity, resulting in a lower $EROI_{used}$ result overall and more excess energy.

VRB systems are the least successful, showing the lowest performance and EIR. Their low EIR value is due to a low storage capacity, caused by their high energy cost. Their application in the Stocksbridge case study also returned the worst results, where the wind-dominant scenarios showed no use for the flow batteries at all.

Of course, the most important results to draw from the batteries was how they affected the security of the systems. When it came to the optimised single household systems, all battery types were unable to give an EIR result of above 0.55 without impeding sustainability (i.e. becoming suboptimal), however this limit was also imposed by the systems being wind power only. This upper limit of security was estimated to be 0.85 for Li-ion or NaS systems when the embodied energy of PV was reduced by 80%, and 0.8 for the other battery technologies. For the Stocksbridge case study, a limit of 0.75 EIR existed for large hybrid systems with Li-ion batteries, but PHS systems were able to surpass this with an EIR of 0.8 for large wind and hybrid systems.

Storage is likely to only become a widespread method of balancing renewable energy production if certain technologies are improved. The results of the uncertainty analysis showed that lowering the embodied energy levels of PV modules is the most effective way of improving security and sustainability together. While systems with cheaper PV would require smaller batteries, they can use them more effectively and attain security levels $28-35\%$ higher, or $30-40\%$ higher if battery EE is also reduced. These results are for single household

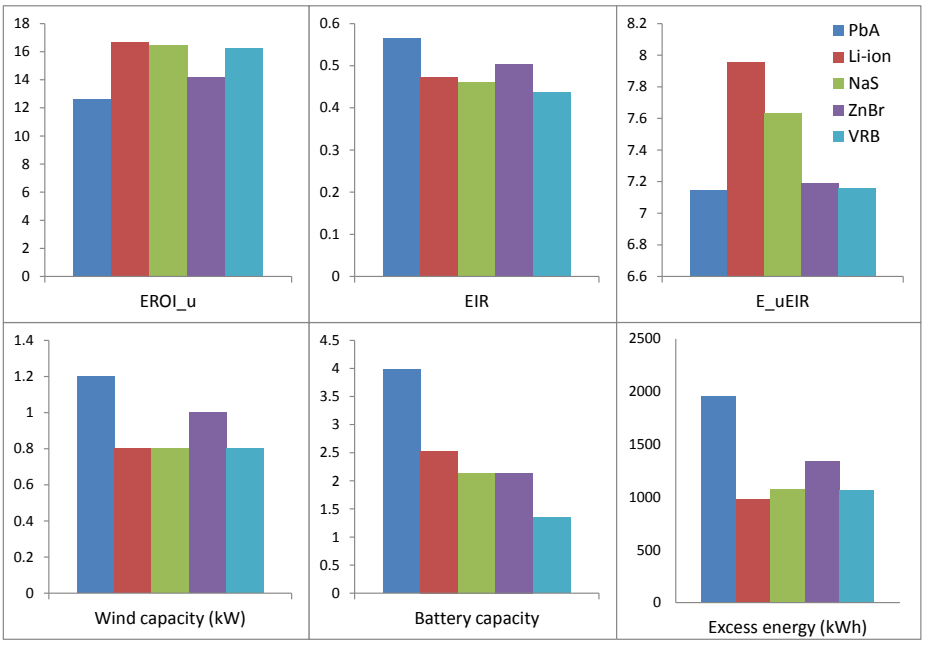

Figure 7.6: Optimal results for single household systems with all battery types, using the objective function $E_u EIR$. Li-ion batteries give the best performance ($E_u EIR$) levels, alongside higher $EROI_{used}$, but PbA systems use larger batteries and increased wind turbine capacity to reach higher levels of security, while producing the most excess energy.

systems, and the margin of improvement is smaller for networked demand where sustainability and security are already improved with less need for batteries.

7.2 Methodology evaluation

Throughout this project, methods were developed for the optimisation of renewable energy systems with respect to sustainability and energy security, using four alternative objective functions that can be maximised to find a Pareto optimal system. These objective functions were designed to compare the changes in the outputs (sustainability and energy security) when one of the system input variables was changed, finding the Pareto optimal system where an increase in one output would only be possible by causing a greater decrease in the other output.

This approach of finding balance between sustainability and security was considered appropriate for the framework of distributed systems, where security is important but not entirely a local responsibility. This approach differs to much of the literature, where $LOLP$ levels are seen more from a whole-system viewpoint, and therefore have much more strict limitations. Using E_uLOLP or E_uEIR is a much more grounded method, as it does not ask how possible it is to return certain security/sustainability levels, but establishes the strengths of the renewable energy systems, and shows how best they may be implemented or what development is required to improve their suitability. It can be used as a policy tool to find the best configuration of renewable energy and storage technologies, thereby showing what kind of deployment should be encouraged and developed in research.

This methodology is based on a number of assumptions; most crucially that the metrics are reasonable representations of the actual sustainability and security of the energy systems, and also that a compromise could be reached where both aspects were maximised without needing to keep above any particular thresholds. It was acknowledged that the metrics $EROI_{out}$, $EROI_{used}$, $LOLP$ and EIR were all limited in their abilities of fully describing the system, but that the practicality of expressing it in a single number was worth the loss in information, and that the combination of metrics still resulted in surprisingly complex outcomes. $EROI_{used}$ showed more complexity than $EROI_{out}$, however the division of systems into exporting and non-exporting was a simplification when many systems are capable of sometimes exporting, and sometimes not, depending on the energy composition of the wider electricity grid. Furthermore, neither include the embodied energy costs of the network management system that would be a requirement for any VPP, and even the single household systems, as this was an unknown quantity.

The four objective functions can be divided into pairs by their approach to how independent the systems were modelled to be: two investigating underproduction ($ELOLP$ and $EEIR$), and two investigating independence (E_uLOLP and E_uEIR). In other words, $ELOLP$ and $EEIR$ (using the metric $EROI_{out}$) were applied to systems that exported to the grid, while E_uLOLP and E_uEIR (using the metric $EROI_{used}$) were applied to systems that cannot export to the grid. Reasons for not exporting could include a grid with a high penetration of renewable energy (and therefore would not be able to use excess energy from wind or solar sources), a poor local connection not allowing for bi-directional electricity flows, or complete disconnection.

When comparing the results of different objective functions, it was generally found that $E_uEIR = EROI_{used} \cdot EIR$ gave optimal solutions that were neither oversized nor undersized for demand, were sensitive to changes in system inputs, and balanced equally the concerns for underproduction and overproduction. Supplementing E_uEIR analysis with a measure of excess energy production was also useful; while the $EROI_{used}$ metric accounted for this by subtracting the excess energy from the total energy output, separation gave more insight into the energy flows of the systems.

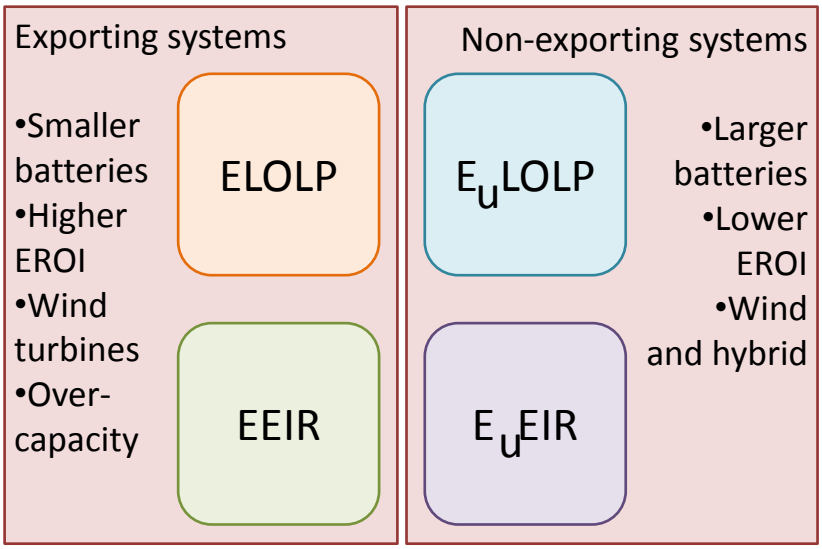

Figure 7.7: Summary of the four objective functions and how their use impacted on the results found. Functions $ELOLP$ and $EEIR$ used $EROI_{out}$ to represent systems that export to the grid, and functions E_uLOLP and E_uEIR used $EROI_{used}$ to represent more independent systems that have limits on their exporting. E_uEIR was found to be the most useful and accurate for maximising system independence, so was the only method used to optimise the case study.

In contrast, using $EROI_{out}$ as the sustainability metric gave oversized systems, limited only by the cap of 200% that was imposed by the methodology. These exporting systems optimised to give an unlimited capacity for the wind turbine, which while encouraging for the use of wind power generation in the UK, was clearly unrealistic and demonstrated the limitations of such an approach.

In addition to the main studies done of renewable energy systems at variable sizes, the methodology was directly assessed, firstly by a study of how temporal resolution affected the results. Lack of readily available high resolution data meant that this investigation could not be taken very far, but the potential for new smart metering and big data approaches means that further investigation into the usefulness of such data would be of value. The system investigated was a single household with PV generation and one type of battery (PbA), using one of the household demand time-series. Results were limited due to low availability of weather or power generation data at higher resolution than half-hourly, but they suggested that measuring energy security by measuring the actual energy discrepancy, rather than length of time that they exist for, gives results that most accurately reflects the behaviour of the system in real time. This is relevant because the most commonly used energy security metric is $LOLP$, which simply measures the length of time that loss of load periods cover, and energy metering is generally no more accurate than half-hourly. While this is good enough for comparing the reliability of most systems, if all analyses use $LOLP$ then they will likely overestimate the size of backup or storage capacity required to fix energy security issues. This would incur additional costs in terms of sustainability and finances.

Further investigation on the metrics themselves included uncertainty and sensitivity analysis, which evaluated the sensitivity of results to the chosen embodied energy values in each system component. All objective functions that account for underproduction are fairly sensitive to the choice of embodied energy values for system components, but their sensitivity depends on what component is being varied. Use of the metric $EROI_{used}$ with E_uLOLP and E_uEIR optimisation resulted in more sensitivity to PV embodied energy values, whereas using $EROI_{out}$ with $ELOLP$ and $EEIR$ optimisation gave results that were more sensitive to wind turbine embodied energy. There was less difference when varying battery EE, but for batteries with higher ranges of EE such as PbA and VRB, $EEIR$ was more sensitive than the other objective functions, giving higher than average performance for lower embodied energy values, and vice-versa. When varying battery cycle efficiencies, there was no consistent difference between the metrics.

High sensitivity can be undesirable when inputs such as embodied energy are known to have a high error/variability, however it is also useful to know that system performance can be greatly improved by reducing embodied energy levels. Therefore sensitivity cannot show the effectiveness of the metrics, however it is useful to know that the performance of exporting systems (i.e. $ELOLP$ and $EEIR$) is more sensitive to wind turbine EE, and that the performance of non-exporting systems (i.e. E_uLOLP and E_uEIR) is more sensitive to PV EE, as this can be taken into consideration when looking at the optimisation results. These differences show that exporting systems draw less benefit from PV being included as part of the system, and actually have lower sustainability despite having to rely less on batteries. However for non-exporting systems, their much larger batteries are reduced more significantly, leading to an improvement in both sustainability and security, and an overall greater increase in performance. In contrast, when wind turbine EE is reduced, none of the optimisations showed any change in wind turbine capacity, so any change in performance is simply down to the reduced cost of the wind turbine. As non-exporting systems have larger optimal batteries, the wind turbine has a smaller contribution to the cost, so reducing that cost has a smaller effect.

All objective functions are more sensitive to the lowering of embodied energy values than their increase. This is extremely important because there are concerns that current calculations are underestimating embodied energy values, as not all sections of the supply chain are available for analysis. This can include the energy costs of employees, research and development, and advertising. Therefore since the results' sensitivity is weaker for increases in embodied energy, any errors in this direction should have less of an impact on the results.

In addition to the standard uncertainty and sensitivity analysis, there was some reflection on the use of the primary energy scaling when applied to the EROI results. Scaling for primary energy has a strong impact on the EROI values, multiplying them by a factor of $\frac{1}{\eta_G} = 3.2$ to account for the fact that wind and solar generation have a purely electrical output, and removing or reducing this multiplier brings down the EROI values significantly. While optimised power and storage capacities were unaffected, this meant that PV and hybrid systems had very low $EROI_used$ values of 1-3.

Therefore it was concluded that the most useful objective function was E_uEIR, unless the system can export to the grid with knowledge that the energy will be of use, in which case $EEIR$ is more applicable. However, if actual half-hourly data is unavailable, the $LOLP$-derived objective functions would be a worthwhile substitute, being only slightly less accurate. Using E_uEIR can evaluate how well matched supply is to demand, where concerns about underproduction and overproduction are equally weighted. The use of the metric $EROI_{used}$ as a component of E_uEIR is also appropriate for national electricity systems with a high penetration of renewables, as it does not assert that exported energy is always usable, thus being applicable to a long-term view of energy systems. Using objective functions such as E_uEIR can establish whether renewable energy systems can provide a reasonable level of sustainability and security to the grid as a whole.

7.3 Final summary

At the beginning of this thesis five questions were posed. These served to address optimisation results, the effectiveness of electrical energy storage, limits to sustainability and security, possible technology improvements, and real world implications. The final summary answers those questions, and offers suggestions and recommendations to follow this work.

1. *Is there an optimal mix of wind and solar technologies in the UK's climate, and what are the implications from any such optimum, now and in the future?*

   From an objective optimisation perspective, where only the energy costs and security of the system are considered, the results overwhelmingly gave optimal systems that were were entirely wind powered, with capacity of generation and energy storage dependent on the situation of the system. For systems that could rely on exporting to the grid, optimal wind power capacity was enough to meet at least twice the system's demand, while non-exporting systems had a smaller optimal capacity, only enough to produce the same total amount of energy over the year as there was demand. This gave less excess generation, but also resulted in a reduced security, as generation patterns did not generally match those of demand, even with larger batteries.

   There were assumptions made in order to give a simple initial model, and these were broken down by questioning how the energy costs of technology will change in the future, how energy systems may entirely change their form and function, and how social implications in the real world can change the options available to us. Key results from these show why PV still has relevance; they include the deployment of PV and increase in system performance once PV energy costs drop by around 50%, and higher acceptance of PV

than wind turbines makes it necessary to include in real-world case studies. Results for other countries would likely differ, given the different availability of certain energy sources, and countries at lower latitudes may need less of a drop in PV embodied energy to enable their deployment.

Therefore the conclusion from these studies is not that PV should be ignored, but that its improvement in energy costs is a very important step in transitioning to a renewable powered future. However, wind power generation is likely to remain the dominant source of renewable energy for a long time.

2. *How effective is electrical energy storage at providing security services to local renewable energy systems, and can this be done in a sustainable way?*

   Despite the high energy costs of energy storage, it formed a fundamental part of most of the optimised systems. Notable exceptions were the most expensive stroage options: hydrogen storage systems, where using hydrogen production for energy storage was only worthwhile for non-exporting systems with PV; also the wind-dominant systems in the Stocksbridge case study gave optimal zero capacity when using high cost vanadium redox batteries (VRB). However, the fact that such cases were so rare was encouraging; the current discussion around batteries frames them as being too costly, so their inclusion in most of the results showed that they do provide enough value to offset their cost.

   When optimising the systems, storage capacity was expressed by converting the optimal storage capacity in kWh to be scaled to power generation capacity; i.e. a battery capacity of n could store n hours worth of peak production. This allowed for more objective comparison between differently sized systems, and ultimately meant that the optimal storage capacity also represented the value that storage brought to the system, because large optimal batteries only occurred when their value to the system was large. When this large value coexisted with high security values, such as for PV-dominant systems, this showed an effective use of battery technology.

   For the single household systems, plotting optimal battery capacity against energy security showed a linear relationship, where optimal systems with larger batteries returned higher security values. Non-exporting systems also optimised to use larger batteries, as their use in constraining excess energy gave them more value in the system, and comparing systems of equal generation capacity showed that security was improved by up to 0.12 EIR. Using $E_u EIR$ rather than $EEIR$ meant that up to 650kWh of excess energy was saved per year, where this maximum occurred for the optimal wind-only systems. PV-dominant non-exporting systems showed less of a change in excess energy or security, despite still having larger batteries.

   The best results were reached by systems using Li-ion batteries or pumped hydro storage (PHS), despite having contrary properties. Li-ion is the most effective per unit of storage, having high cycle efficiency and high depth of discharge but mid-range energy cost, so its optimal systems had smaller capacity but good performance. Conversely, PHS only works for large-scale systems, and its strength is in having less cost per kWh of storage capacity, despite having lower cycle efficiency. So systems using PHS achieve high performance through high storage capacity at lower cost. This variety in results shows that choosing the best storage technology is complex, and depends on many factors.

   More complexities come from the additional sustainability costs of batteries, mentioned in the literature review. These include the toxicity involved in PbA and VRB manufacturing, and the limitated supplies of lithium for Li-ion batteries. If Li-ion batteries are used for

electric grid balancing in addition to battery electric vehicles, then this would put a lot of strain on the world's supplies, and require very high recycling rates.

Battery utilisation was most effective alongside solar power sources; PV-dominant systems were capable of reaching higher security levels than wind-dominant ones, while requiring lower battery capacity per unit of power generation capacity once they were large enough. This effectiveness is caused by solar production being complementary to the day-night patterns of PV production, in contrast to the more unpredictable wind time-series, where the length of consistent production or outages can range from a few minutes to several days. Planning a storage management strategy for such a variable pattern of production is very difficult, and doesn't lead to an obvious capacity size for storage.

There is another factor in the relationship between PV and batteries, however. Since PV has higher EE, electricity produced from solar sources is imbued with more "value", meaning that there is more incentive to capture that energy through storage. This is part of the reason that reducing PV EE gave a drop in battery capacity, and why systems with very high storage costs (hydrogen and VRB systems) only included the storage for systems containing above a certain penetration of PV. However, the patterns of production was considered to be a more important factor. Such a conclusion could be reached because when PV EE was reduced as part of the sensitivity analysis, battery capacity reduction levelled off even as PV became cheaper than wind. These systems with cheaper PV gave higher priority to security, as performance was increased while EROI initially decreased. Therefore a future system of PV and battery storage is a realistic proposition, and one that would become even more viable as the embodied energy costs of both components drop.

Not all storage technologies mentioned in the literature review were tested. In particular, compressed air energy storage (CAES) was ignored as it utilises natural gas. We can assume that, as it has lower embodied energy costs and higher cycle efficiency than PHS [123], it would have given slightly higher performance results than the PHS systems in Stocksbridge. However, such a result would ignore the costs of using fossil fuels. Another possible technology, supercapacitors, were not included as their application was based more around short-term storage for power quality. However, given the reduced need for storage for networked households, and the increased potential for power quality issues over networks with high renewable energy penetration, supercapacitors may be more applicable than batteries for small household networks. This result would also hold for other short-term storage technologies such as flywheels and superconducting magnetic energy storage, however these are likely to be less practical due to their mechanical nature and complexity, respectively.

3. *What limits exist regarding the sustainability and security of distributed energy systems?*

   Both EROI and $LOLP/EIR$ were demonstrated to have hard limits in the tested small systems, but the nature of those limits was different. These were caused by constraints of security upon sustainability and vice-versa, and also from natural constraints imposed by the wider system: eg. variable patterns of generation, supply chains, efficiency of available energy, or recycling rates.

   When looking at the optimal battery capacity sizing over all generation capacities, security values of around 90% (i.e. 0.1 $LOLP$ or 0.9 EIR) were achieved by the largest hybrid systems. Any improvement in security, whether by increasing generation or storage capacity, showed diminishing returns as larger units were required to give smaller increases. Indeed, a key feature of the optimisation was to identify where this increase

had diminished enough to not be worth its additional cost. For these large hybrid systems, $EROI_{out}$ dropped from its optimal value of 30-31 to around 10, while $EROI_{used}$ dropped from 12.6 to around 5. None of the systems reached the high energy security expectation of 95% imposed by other previous studies. This suggests that while those studies were able to reach such levels, the use of PV and storage capacities required to do so are not worth the energy costs required.

When optimising for generation capacity (giving large wind-based energy systems) the security limits were lower at around 57-64% for exporting systems, or 47-56% for non-exporting systems. The lower security for the latter was caused by smaller power and storage capacities, and the highest security was reached by PbA systems due to their larger batteries. It was noted that levels of security depended upon the season, as PV produced mostly in summer, wind produced slightly more in winter, and winter had the highest levels of demand. These seasonal results showed that wind-dominant systems were capable of reaching higher limits of security in winter, despite that period having greater energy demand, and PV systems appearing more energy secure over the year. This greater demand means that winter is more constrained for supply, and therefore that wind power has additional benefits that are not obvious from the non-seasonal analysis.

Larger household networks showed some decrease in security as they increased in size, but the most important relationship was with their wind turbine capacity, where security of the non-exporting systems was improved to 70% when using the largest wind turbines. Similar results were seen with the non-domestic systems, but security was increased no further despite their larger sizes. The largest systems were in the Stocksbridge case study, where introducing PV and cheap PHS enabled higher security limits of up to 80%.

The difficulties in surpassing these energy security limits of course comes from the use of variable power such as wind and solar; even when combining the two together in hybrid systems there is likely to be a shortfall in energy production at some point in the year. Battery storage is not a complete solution to this, as wind generation can be down for a week at a time, and holding such massive reserves of battery storage capacity is an incredibly costly way to fulfil this demand. The only plausible solution would appear to be low carbon reserve capacity, possibly combined with an extreme approach to demand-side management.

By contrast to security results, increasing system size showed a distinct progression in EROI results, up until the Stocksbridge scenarios where the addition of PV reduced $EROI_{used}$ considerably. In general, EROI results ($EROI_{out}$ and $EROI_{used}$) are most constrained by the EROI of the most cost-effective component of the system, which in turn is constrained by external processes such as recycling rates, efficiencies of supply chains, source of energy in manufacturing etc. It was generally seen that improving EROI was easier than improving security, as wind power can be boosted and battery capacity reduced, and the range of possible EROI results - from 1 to 55 - were much wider.

However, this does not mean that EROI is not constrained by security concerns: security is valued when battery capacity is included in the system, which reduces $EROI_{out}$ from the potential maximum of 46.7 (assuming a 4.7kW turbine with capacity factor 0.2, producing twice the annual demand of 4000kWh) to 30.5. Another limitation was enforced through the use of $EROI_{used}$; where previously high-producing systems were rewarded for their output regardless of whether it was used locally, now they were penalised for producing power when none was needed, so the $EROI_{used}$ results were significantly lower than $EROI_{out}$, particularly for wind-dominant systems which

experienced the most overproduction.

Another important limit for EROI is its lower limit. There was discussion in the literature review of whether there is a lower limit to EROI, below which the system would be deemed unsustainable. While results never returned EROI values of less than 1, there were some that dropped below EROI values of 5, such as hydrogen systems and future projections of improved grid efficiency. However for the most part, EROI of most systems plateaued around values greater than 5. This meant that the focus could be overall performance rather than whether sustainability values were too low.

While there is a compromise to be made between EROI and $LOLP/EIR$, it is not as straightforward as it may seem. The metrics behave in different ways at their limits, and plotting EROI against EIR showed a far more complex relationship than simply an inverse correlation, as shown in figure 7.8. This relationship depends on the type of system chosen, where focusing on wind singly does give an inverse correlation, but adding PV makes this much less straight-forward. There is also much scattering of results due to variability in weather patterns over the UK. Furthermore, circumstances may force the use of PV because they are more acceptable, or because open land is not available for wind turbines. While these may seem irrelevant, they are in fact qualitative elements of sustainability: social acceptability is in the sphere of social sustainability, and land is a much depleted resource that must be used sustainably. Therefore the framing of the trilemma, where it is implicitly stated that security and sustainability must always conflict, is not necessarily true.

Investigation into primary energy scaling, where the grid efficiency coefficient η_G is used to scale EROI results of renewable energy systems, showed another element to the limits of EROI. As the entire UK's energy systems transition to using more renewable energy sources, the efficiency of the grid increases, meaning that EROI results are scaled less, making them less advantageous in comparison to the grid. However when accounting for reductions in PV EE costs, the EROI of all systems appear to converge to $EROI_{out}$ of 10-20, or $EROI_{used}$ of 5-12: wind-dominant systems drop in EROI, while systems using PV show some improvement.

There are limits to security, and possibly sustainability, imposed by sticking to electricity load only; it was discussed in the literature review that in the future we will likely see the heating and transport systems linked more strongly to our electricity systems, through electric heating and battery electric vehicles or vehicles using hydrogen produced through electrolysis. These will offer more flexibility, which was not successfully expressed through the studies shown here. On the sustainability side, the electricity-only studies ignored the existence of concurrent heating and transport systems that run almost entirely off combustion of fossil fuels. Linking these systems together to use renewable energy sources would reduce the overall primary energy use, and thereby improve EROI values.

If we bring these conclusions back to the initial discussion on whether sustainability can be quantified, or whether there are qualitative aspects that cannot be reduced to simple numbers, the question about limits to sustainability is very different. We can imagine a "perfectly sustainable system", where resources are recycled back into the natural ecosystems at an equal rate of their use, and where pollutants are kept below minimum thresholds etc, but quantifying this idea would require a completely different approach to EROI analysis, and the process of quantification would likely still lose crucial aspects of the ideal. For example, the term "zero-carbon" is sometimes marketed to describe a high level of sustainability, but given that this only looks at greenhouse gases, it is certainly limited in scope.

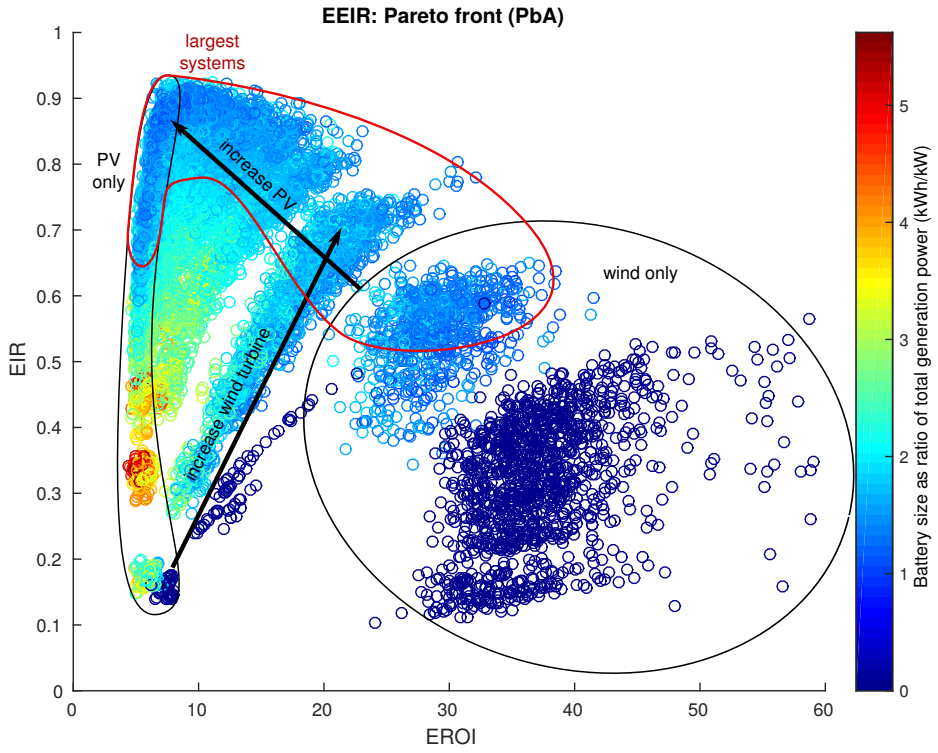

Figure 7.8: The Pareto front created by plotting security against sustainability, using metrics $EROI_{out}$ and EIR. While there is some anti-correlation, mostly for wind-dominant systems, results are more complex and dependent upon the specific technology available. This is a summary of figure 5.44, showing the segmentation of systems that are single-source: wind systems are in the bubble on the right, PV systems are in the thin bubble on the left, and large (delivering at least twice annual demand) systems in the red bubble. If the sensitivity analysis results were included then there would be more points in the top-right section with higher performance.

Finally, it must be remembered that $LOLP$ and EIR don't represent all aspects of security, just as EROI doesn't address all areas of sustainability. $LOLP$ and EIR were designed to measure *adequacy* - how well demand can be met - and do not address network security, while measuring energy flows by EROI can address a number of disparate elements, but does so in a somewhat crude way. Therefore the results for both sustainability and security do not describe the full performance of the systems, meaning that their actual limits are potentially lower than the quantified results.

4. *How can the technology be improved most effectively to surpass such limits?*

   There were a number of tests done into the potential of future technologies and improved manufacturing; these were the sensitivity analysis on embodied energy and storage cycle efficiency, the investigation of hydrogen production and storage, and how demand may be affected by using more electrical heating such as heat pumps.

   There was a dramatic effect when reducing PV embodied energy; this had the implication of making hybrid systems sustainable enough to deploy at full scale, which in turn improves security, and sustainability is improved by having cheaper PV. Improving battery EE was also important, but had a smaller impact and given the natural complementary natures of PV and batteries, it made the most sense to focus on PV first. However improving wind turbine EE was not particularly effective, as it discouraged efforts to improve security, and wind turbines have less potential for improvement as they are a more mature technology. Improving battery cycle efficiency had the least encouraging results, where lower cycle efficiencies returned better performance for exporting systems.

   The investigation into hydrogen production and storage was discouraging, as it showed that its use was only worthwhile for systems that were already low performance: non-exporting systems with at least 80% of demand met by PV production. This is because hydrogen systems have a very high energy cost, the most costly component being the fuel cells, which means that their use is worthwhile only if the energy in the system also has a very high cost. However, this study was too simple, and ignored the most important aspects of hydrogen use, which is its flexibility. Hydrogen's application as an energy vector - more than just energy storage - has the potential to expand electricity systems into the transport and heating systems, in ways that would likely be more user-friendly than battery electric vehicles or electric heating. This is true for hydrogen because it is a physical fuel, and therefore can be stored and transported in ways that electrical energy cannot. A full investigation into the implications of hydrogen is therefore far beyond the scope of this thesis.

   Heat pumps were also investigated, but again their full scope was unable to be realised. The heating load of a typical house was assumed to quadruple the total energy load, which led to system oversizing in summer, and reductions in EROI and security results. This was despite heat pumps' high coefficient of performance, as their constant usage pattern resulted in a high load. However, comparison to the standard electrical system was difficult to make, as previously the heating load was not included in the study at all, and the disconnection between the electric and thermal systems meant that each would have a different level of security. Furthermore, the full potential of improved demand-side management could not be realised in the study, which would likely have had significant implications into the security of the system. This would not remove the problem of generation oversizing alone, but improved thermal insulation would also be a necessary part of any investigation into more sustainable heating, so oversizing could possibly be reduced by this reduction of thermal demand.

These results can be linked to suggestions of how policy could create incentives for better energy systems, not just focus on single technologies. Existing examples are the Renewable Heat Incentive, where households require a minimum level of insulation before qualifying for the financial incentive for heat pumps, or the smart meter roll-out across the UK by 2020, which will facilitate any building of smart-grids. Systems-based policy based on these results could be: reducing energy use in technology manufacturing, for example by shortening supply chains, increasing recycling and minimising shipping; matching regions of high supply or demand with units of storage; and extending the current policy on smart meters to requiring more local grid management, to create real smart-grids.

5. *When the method is applied to a real case study, how do real world limitations affect these results and conclusions?*

   The most obvious change in the Stocksbridge case study was around the availability of certain technologies. Fundamentally, the cheap option of large wind turbines was possibly removed, the option of pumped hydro storage became available when it was not previously, and a minimum capacity of 1.8MW PV was included as a baseline for all the scenarios. Large 1.2MW wind turbines were still included in one of the scenarios, but these were seen as more of a comparison point than a potential solution. This use of different technology had impacts on the quantitative results, as inclusion of PV led to fundamental changes from the earlier generalised model.

   However, a more subtle effect was the fuller realisation of the study. The value of the model was seen differently; rather than just an objective study into performance, it could be considered as a tool for understanding what is possible, and for passing knowledge to others. Therefore while contextualising the systems in terms of their geographical and social implications brought some limitations, the case study brought a new dimension to the research. Relating these results to the generalised model also helped facilitate understanding of those more theoretical results, and built up a picture of how the systems at different sizes related to each other.

Recommendations for further research would include a more thorough look into the behaviour of high resolution energy models, and expand the nature of the models to include further interconnections and applications such as hydrogen production and heating. While all these potentials were touched upon, a more extensive study is necessary to reach definitive conclusions for those systems. Additionally, as this modelling was all done on a local scale, it would be useful to investigate the interaction between these distributed renewable energy systems and the greater electricity network, to see whether the local use of storage can truly reduce the need for reserve capacity on the grid when renewable energy penetration is high, and whether this reduction would be more sustainable than simply using reserve capacity. Such analysis could also include the effects of demand side management, projected renewable energy capacity on the centralised grid such as off-shore wind turbines, and the potential for substantial electricity demand reduction.

Appendix A

Appendix for the Methodology

A.1 Alternative security metrics

When developing security metrics, a number were proposed to replace or supplement metrics that already exist in the literature. Not all were kept for the final results, the main reason being that the additional measurements required did not return strong enough improvements in the analysis to be worth including. Most of the metrics were fairly similar to either $LOLP$ or EIR, but two, $LOEP$ and CC, are worthwhile including here.

A.1.1 Loss of Energy Proportion

The metric $LOEP$ (loss of energy proportion) is the inverse of $LOLP$, measuring the length of time that the system is overproducing and thereby losing energy through exporting or curtailing. Its formulation came about to quantify the security losses in overproduction, however it did not properly address these insecurities and led to results that were not useful. In particular, it is not the length of time of overproduction that is damaging. When considering real life electricity systems, if overproduction is an issue then curtailment is an easy solution, so the impact will truly be on energy losses, which was better measured with the $EROI_{used}$ metric. Calculating the total excess energy, which was done in the main analysis, is then a useful addition for full explanation of the energy flows, but is not useful in the context of optimisation. Combining $LOEP$ with $EROI$ (mirroring the methodology of $ELOLP$ to create $EROI(1 - LOEP)$) led to undersized production that did not satisfy the basic requirements of an energy system, i.e. meeting energy demands.

A.1.2 Correlation Coefficient

In theory, a fully balanced system should have perfect correlation between supply and demand. This proposition formed the basis of the correlation coefficient (CC), which was designed to measure the exact balance of the system through correlation. This was calculated using the Pearson correlation coefficient ρ between electricity demand $D(t)$ and "deployed energy" $E_{dep}(t)$, defined as the available energy at time t (either directly generated or from storage) that is either used directly or exported to the grid. Thus for a system with energy storage capacity n and generation capacity c,

$$CC(n, c) = \rho(D(t)E_{dep}(n, c, t)) \tag{A.1}$$

CC ranges from -1 to 1. However results were found to be erratic and non-intuitive, and added no further information than the more basic metrics of $LOLP$ and EIR. Additionally,

the idea behind using correlation was to combine analysis of overproduction and underproduction into one metric, but this created more problems than solutions, as these are ultimately very different problems and needed to be separated out for fuller investigation, which *CC* was incapable of doing easily.

A.2 Matlab code

The Matlab code for the photovoltaic and wind power simulation was as follows.

```
%Randomly select the prepared input data
% check location, input data only from nearby stations

r  = randi(nstations,1,1); %Select a station randomly
location=loaded_stations(:,r); %initial chosen station
area=find(distances(r,:)<50); %Lists all areas within a diameter of
   100km

%There aren't many PV stations, so increase numbers by including all
    on similar latitude
pvlat=pvstations(1,abs(pvstations(2,:)-location(2))<2); %Guarantees
   at least 2 PV stations
stationsrun=union(pvlat,loaded_stations(1,area));

%Select available wind stations from each year
[a,w11,b]=intersect(midas_windspeed2011(1,:),stationsrun);
[a,w12,b]=intersect(midas_windspeed2012(1,:),stationsrun);
[a,w13,b]=intersect(midas_windspeed2013(1,:),stationsrun);
[a,w14,b]=intersect(midas_windspeed2014(1,:),stationsrun);
[a,s11,b]=intersect(midas_solar2011_loadable(1,:),stationsrun);
[a,s12,b]=intersect(midas_solar2012_loadable(1,:),stationsrun);
[a,s13,b]=intersect(midas_solar2013_loadable(1,:),stationsrun);
[a,s14,b]=intersect(midas_solar2014_loadable(1,:),stationsrun);

%only select wind power if the system has a wind input
if windscale==0
wpowerrun=zeros(l_gen,1);
nwindrun=1;
turbinecap=0;
else

windrun = [midas_windspeed2011(2:end,w11) midas_windspeed2012(2:end,
   w12) midas_windspeed2013(2:end,w13) midas_windspeed2014(2:end,w14
   )];
[a,nwindrun]=size(windrun);

alpha=0.2;
wpowerrun=zeros(size(windrun));
%This code creates wind power output for a 1kW turbine at 10m hub
   height
wpowerrun(windrun<=3.5)=0;
```

```
wpowerrun(windrun>3.5)=-0.000865*windrun(windrun>3.5).^3 + 0.022675*
    windrun(windrun>3.5).^2 - 0.126985*windrun(windrun>3.5)+0.203765;
wpowerrun(windrun>14 )=-windrun(windrun>14)*0.025+0.85;
wpowerrun(windrun>24)=0;

turbinecap=0.2*round(windscale*2.5*sum(sum(demandrun))/mean(sum(
    wpowerrun))); %Picks ideal turbine power capacity (rounded to
    nearest 0.2)
wpowerrun=turbinecap*wpowerrun; %Scales to correct size

end

%Now do solar

if PVscale==0
pvrun=zeros(l_gen,1);
nsolarrun=1;
pvarea=0;
npanels=0;
else

b1=0.02718287;
b2=0.0000201499;
b3=0.00021585;

solarrun= [midas_solar2011_loadable(2:end,s11)
    midas_solar2012_loadable(2:end,s12) midas_solar2013_loadable(2:
    end,s13) midas_solar2014_loadable(2:end,s14)]/3.6; %convert to W
[a,nsolarrun]=size(solarrun);
%Using 13% PV modules
pvrun=real(0.001*0.5*0.9093*((b1+b2*solarrun).*log(solarrun)-b3*
    solarrun).*solarrun)*1.3; %energy output in kWh per 1.3m^2 panel
pvrun(pvrun<0 | isnan(pvrun)==1)=0; %Fix values =0 for very low
    irradiance

npanels=round(PVscale*0.5*sum(sum(demandrun))/(nsol*mean(sum(pvrun))
    )); %Picks ideal round number of panels, each at 1.3m^2
pvarea=npanels*1.3;  %This is array area per house
pvrun=npanels*pvrun;
end
```

The Matlab code for the battery simulation was as follows.

```
%Initialise battery degradation

battage=zeros(nbatt,1); %Shows age of each battery, initially 0, max
    16 (drop below 80% capacity at 17 years)
battdod=dod(batt_type)*ones(nbatt,1); %Shows DOD of each battery,
    initially the nameplate DOD
dodreal=dod(batt_type);
```

```
battlife=ceil(wblrnd(c(batt_type),k(batt_type),nbatt,1)); %Gives
   lifetime of each initial battery, modelled with Weibull
replacedbatts=zeros(lifetime,1);

PR=1.005-0.005*[1:lifetime]; %PV degradation of performance ratio

%% Begin actual simulation of system
for year=1:lifetime

wind=wpowerrun(:,randi(nwindrun,1,1));
pv=nsol*PR(year)*pvrun(:,randi(nsolarrun,1,1));
supply=wind+pv;
demand=demandrun(:,mod(year,2)+1);

%Initialise storages
b(:,1)=c_ind;
b(1,1)=0;

%%Run model
for t=1:l_gen
    %Set initial floating remainder energy
    surplus(:) = supply(t) - demand(t);     %For varying battery,
       fixed supply
    bcon    = max(min( (b(:,t) + (surplus./SB_ind)) ,1),0);

    if surplus<0 %i.e. discharging
        eff=1;
    else  %i.e. charging
        eff      = (1-2*mu(batt_type))*(0.5*(b(:,t)+bcon))+1;
    end


    bless   = max(min( (b(:,t) + (surplus./SB_ind).*eff) ,1),0);
    bmore   = max(min( (b(:,t) + (surplus./SB_ind)./eff) ,1),0);
    %Reduce remainder by amount directed towards battery (charging)
       / amount
    %successfully regained from battery (discharging)
    b(:,t+1)      = min(bless(:),bmore(:));

    used=SB_ind.*max((b(:,t+1)-b(:,t))./eff,(b(:,t+1)-b(:,t)).*eff);
    surplus = surplus - used;
    lost(:,t)       = used + SB_ind.*(b(:,t) - b(:,t+1));

    %Calculate energy imported/exported
    imp(:,t)    = max(0,-surplus(:));
    export(:,t)    = max(0,surplus(:));
end

btminus=b(:,1:l_gen);
```

```
b(:,1)=[];

imp(imp<10^(-10))=0; %Fix rounding errors
export(export<10^(-10))=0;

%%Calculate how much pv is used/stored on site
dem_sat=repmat(demand',lenSB,1)-imp;

%% Battery degradation

battage=battage+1;
battdod=(0.9865+0.0015*randn(nbatt,1)).*battdod; %decrease DOD of
   each battery using normal distribution
deadbatts=find(battage==battlife | battdod<0.8*dod(batt_type)); %
   identifies batteries that die this year or drop below 80%
battage(deadbatts)=0; %Install new batteries to replace them
battdod(deadbatts)=dod(batt_type); %Reset new batteries to starting
   DOD
battlife(deadbatts)=ceil(wblrnd(c(batt_type),k(batt_type),length(
   deadbatts),1)); %Update lifetime of replacement batteries
replacedbatts(year)=length(deadbatts);

dodreal=mean(battdod); %Calculates average DOD of battery network (
   this is the used variable in the model)
```

Appendix B

Appendix for the results

B.1 Optimal results for all battery technologies

Optimal results for all batteries for single household systems were plotted with respect to their PV and wind power capacities. There is a great deal of repetition with the PbA system results and other battery systems, so they were not included in the main body of results but are shown here in full.

B.1.1 Li-ion battery results

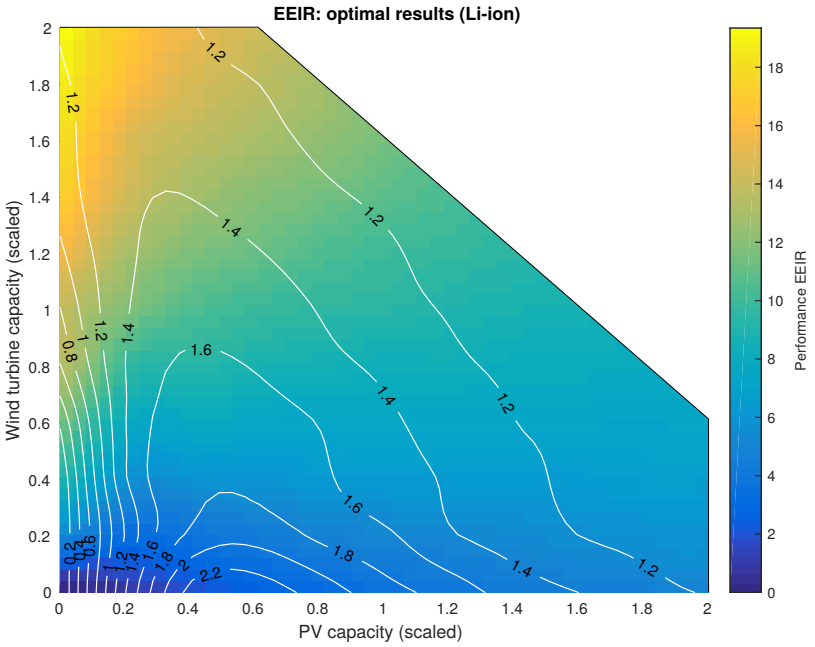

Figure B.1: *EEIR* results showing optimal Li-ion battery capacity for all input capacities.

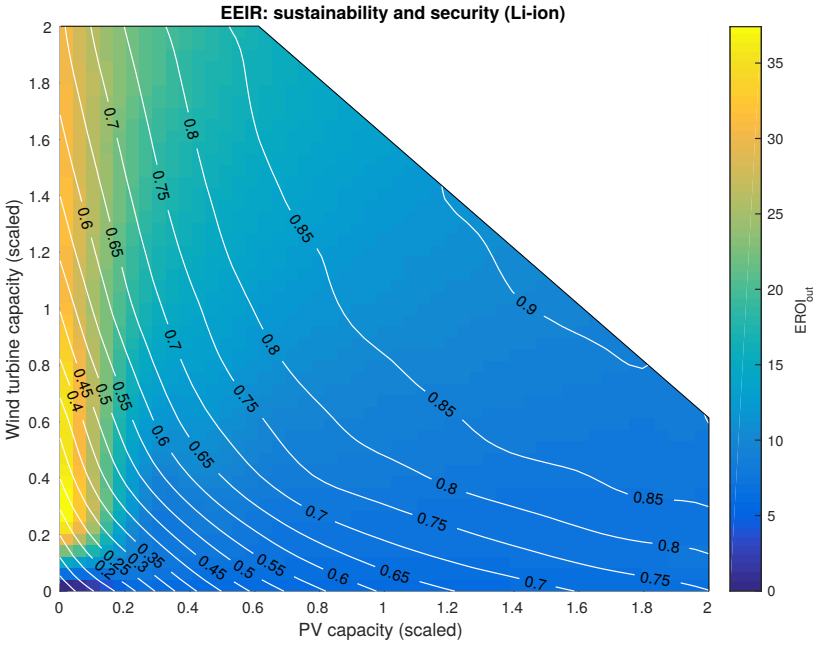

Figure B.2: $EROI_{out}$ and EIR results for optimal Li-ion energy systems.

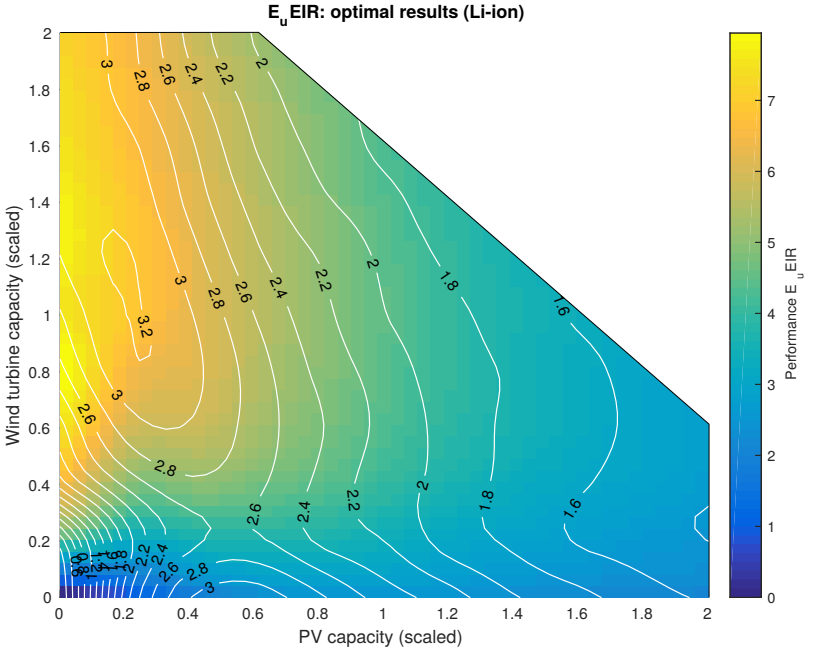

Figure B.3: $E_u EIR$ results showing optimal Li-ion battery capacity for all input capacities.

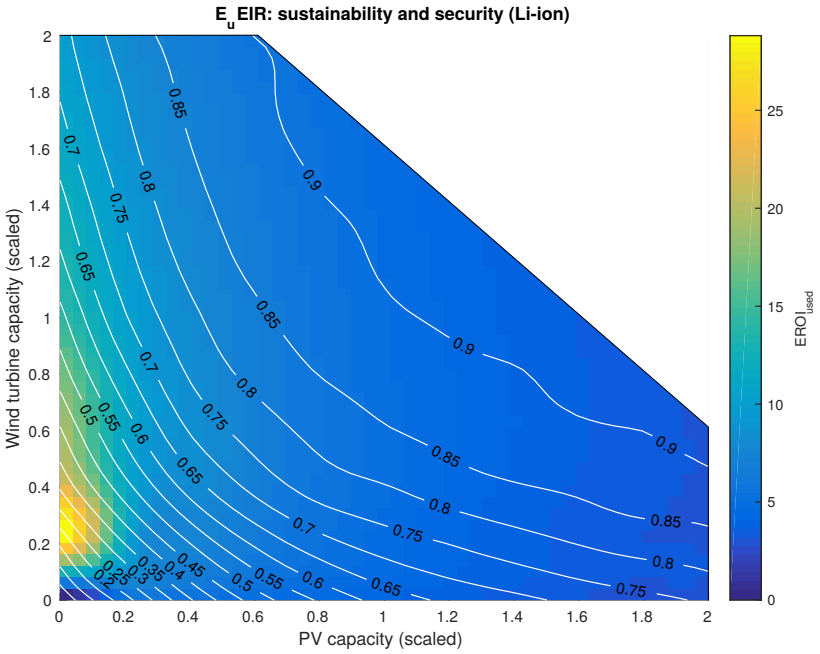

Figure B.4: $EROI_{used}$ and EIR results for optimal Li-ion energy systems.

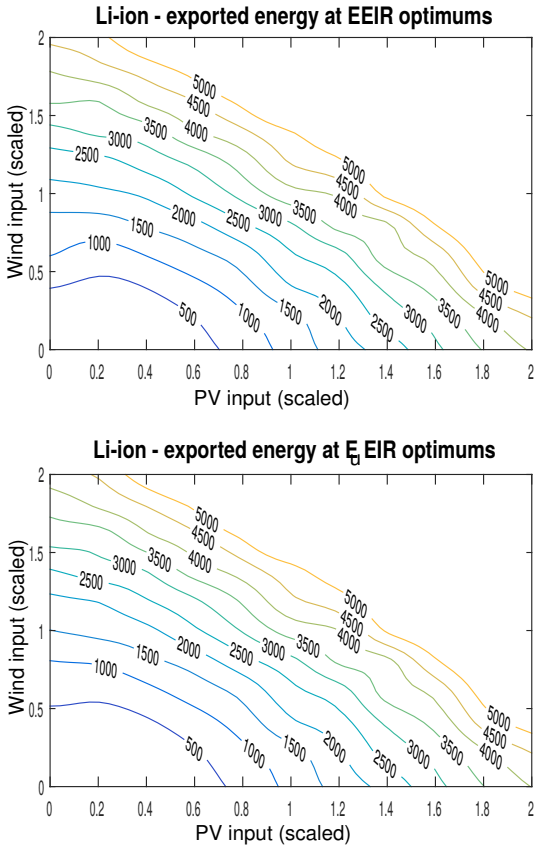

Figure B.5: Optimal $EEIR$ results showing excess energy for Li-ion systems.

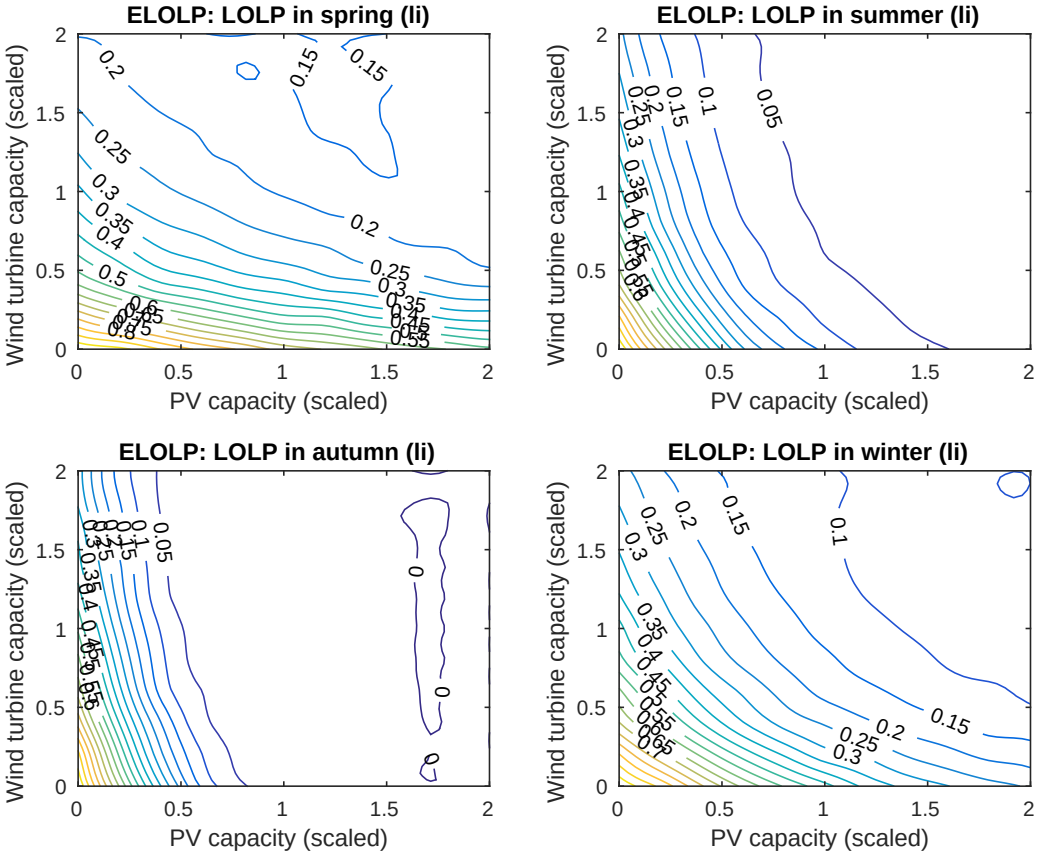
ELOLP: LOLP in spring (li)
ELOLP: LOLP in summer (li)
ELOLP: LOLP in autumn (li)
ELOLP: LOLP in winter (li)
Wind turbine capacity (scaled)
PV capacity (scaled)
0
0.5
1
1.5
2

Figure B.6: Optimal *ELOLP* results split out by season.

B.1.2 NaS battery results

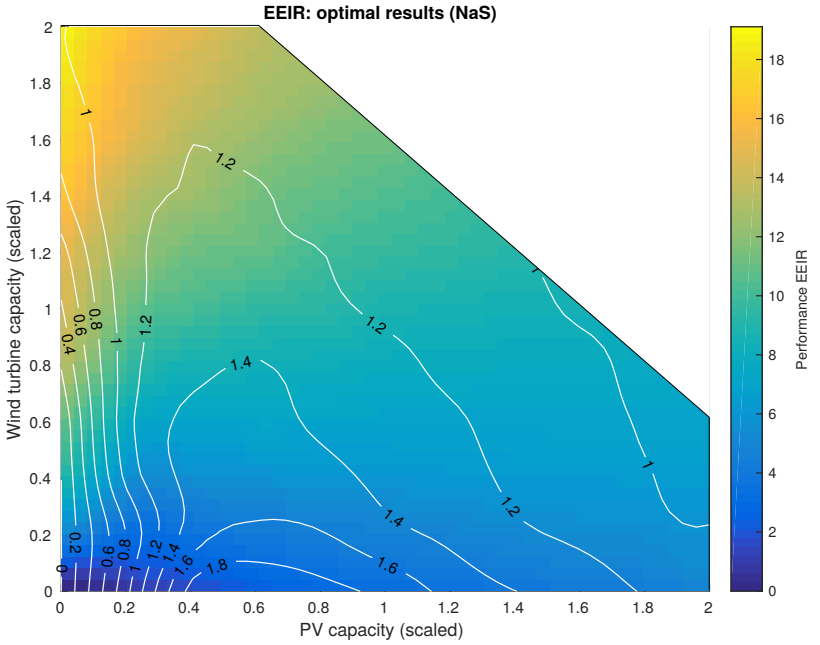

Figure B.7: *EEIR* results showing optimal NaS battery capacity for all input capacities.

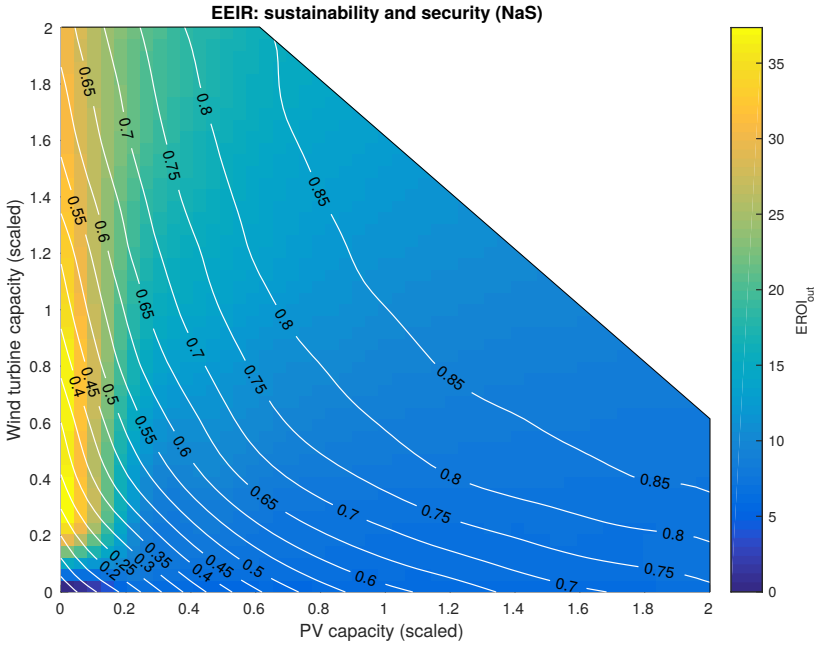

Figure B.8: $EROI_{out}$ and *EIR* results for optimal NaS energy systems.

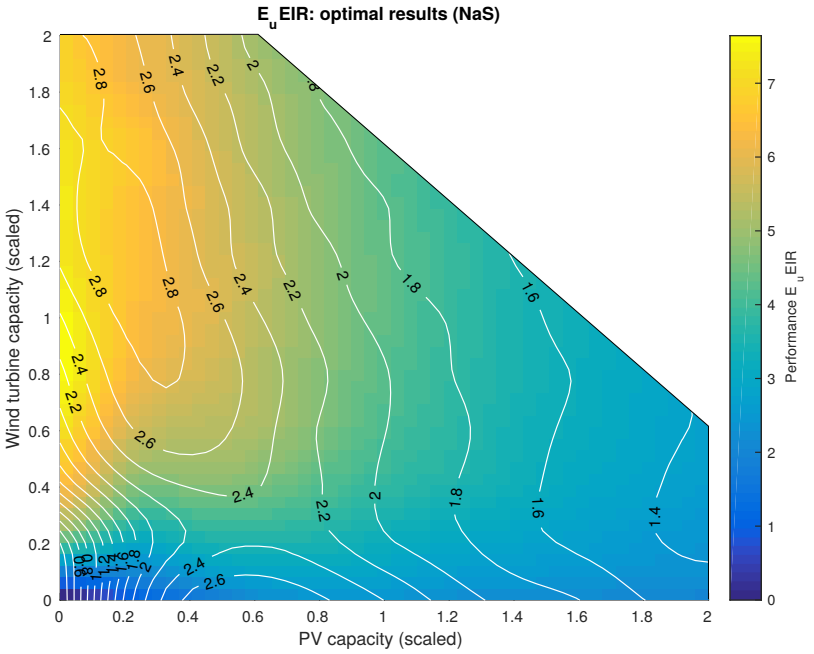

Figure B.9: $E_u EIR$ results showing optimal NaS battery capacity for all input capacities.

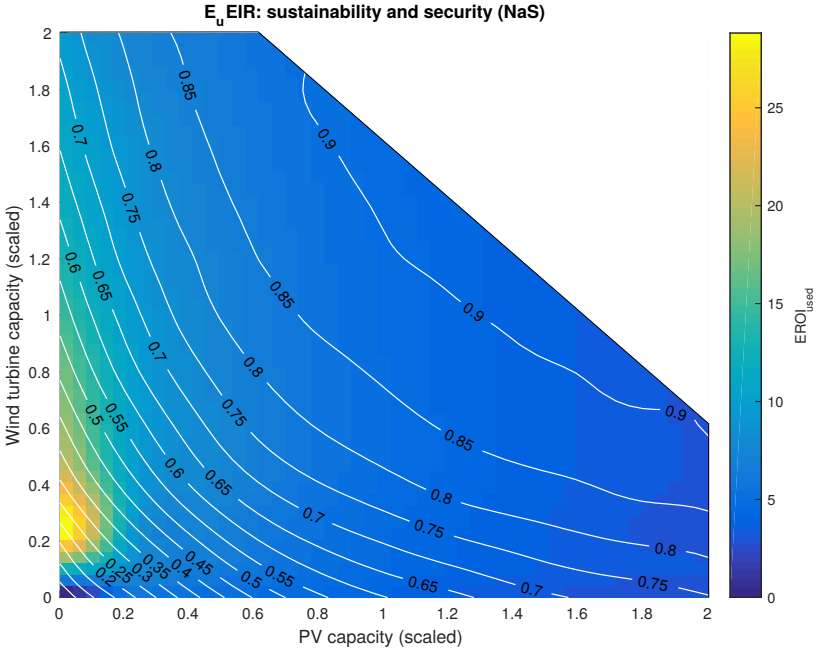

Figure B.10: $EROI_{used}$ and EIR results for optimal NaS energy systems.

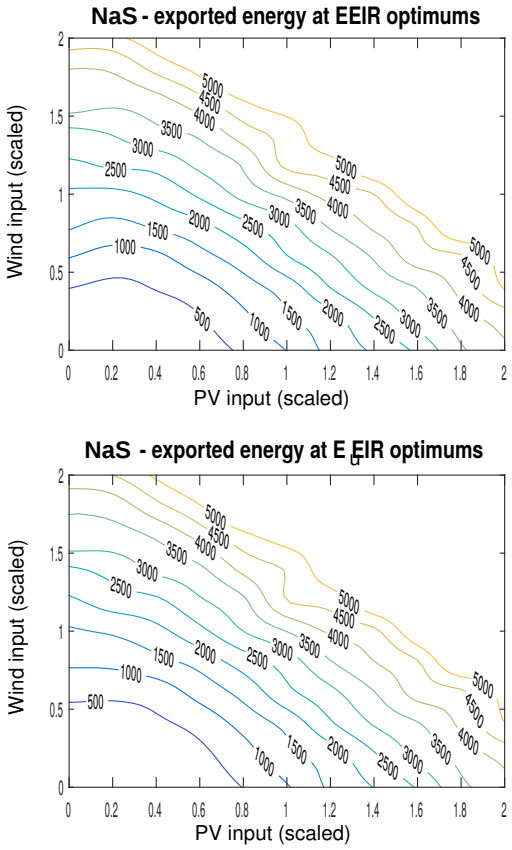

Figure B.11: Optimal $EEIR$ results showing excess energy for NaS systems.

B.1.3 Znbr battery results

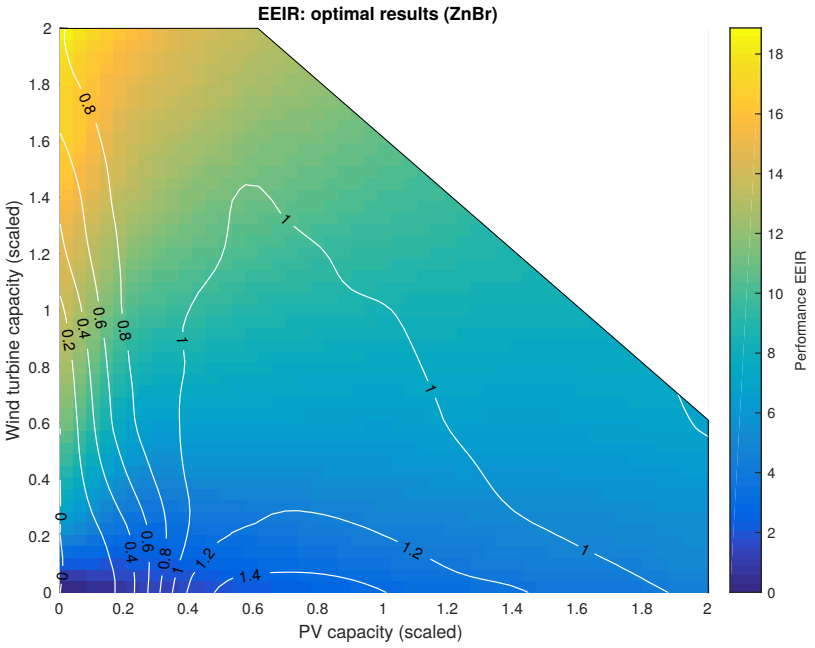

Figure B.12: $EEIR$ results showing optimal ZnBr battery capacity for all input capacities.

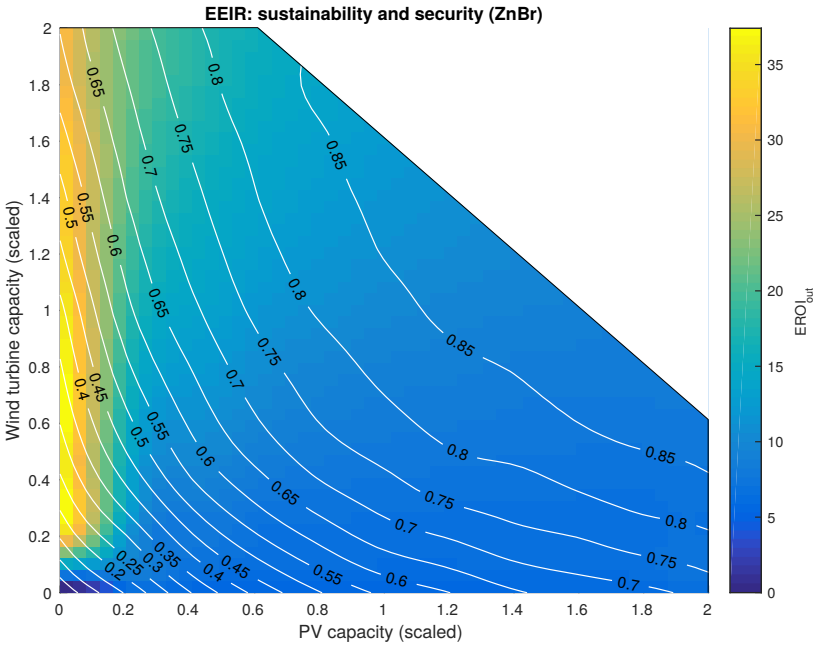

Figure B.13: $EROI_{out}$ and EIR results for optimal ZnBr energy systems.

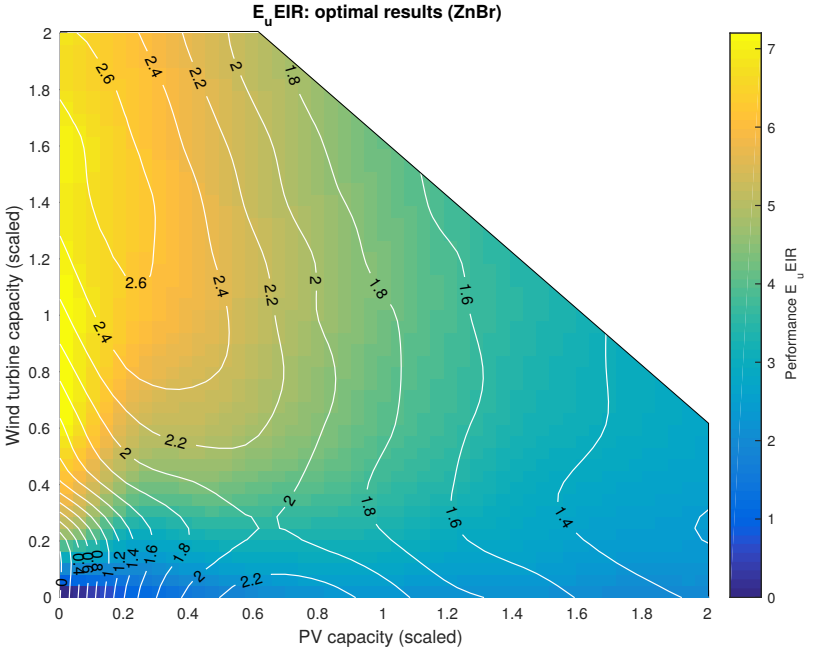

Figure B.14: $E_u EIR$ results showing optimal ZnBr battery capacity for all input capacities.

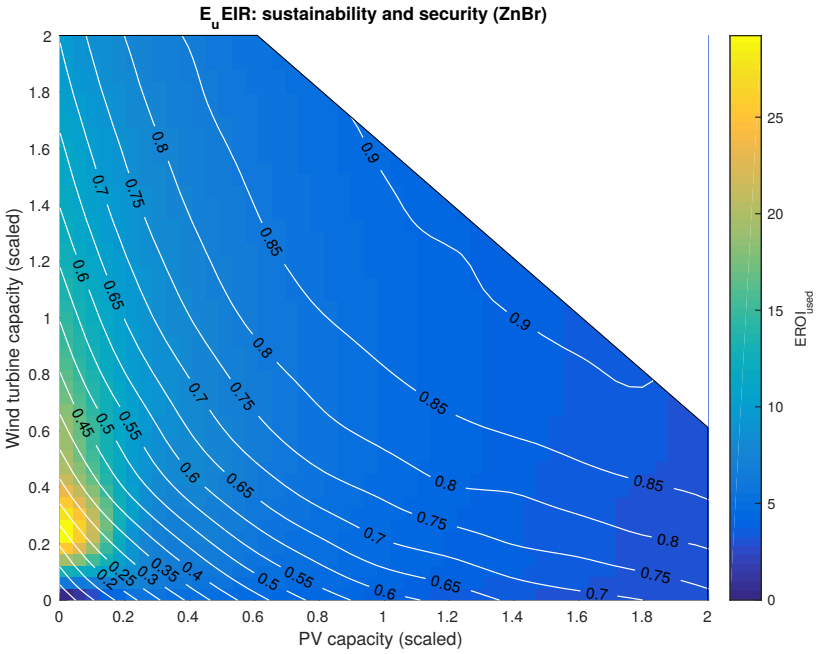

Figure B.15: $EROI_{used}$ and EIR results for optimal ZnBr energy systems.

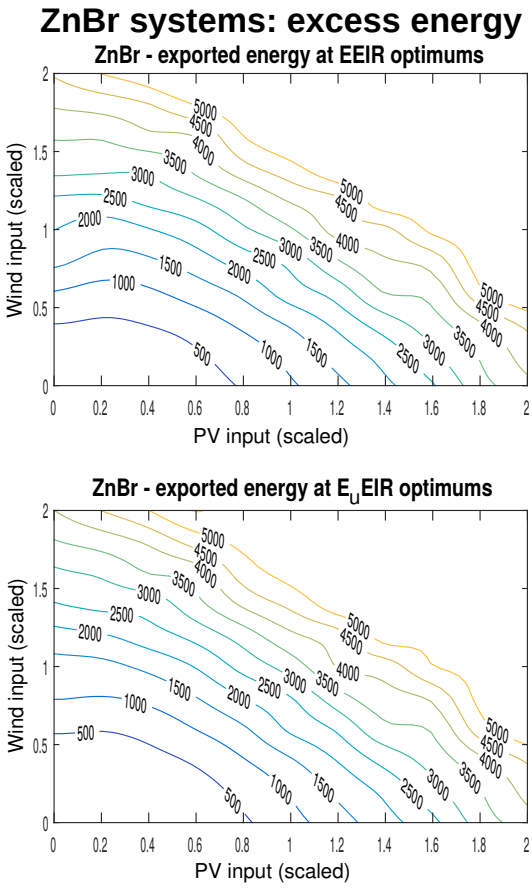

Figure B.16: Optimal $EEIR$ results showing excess energy for ZnBr systems.

B.1.4 VRB battery results

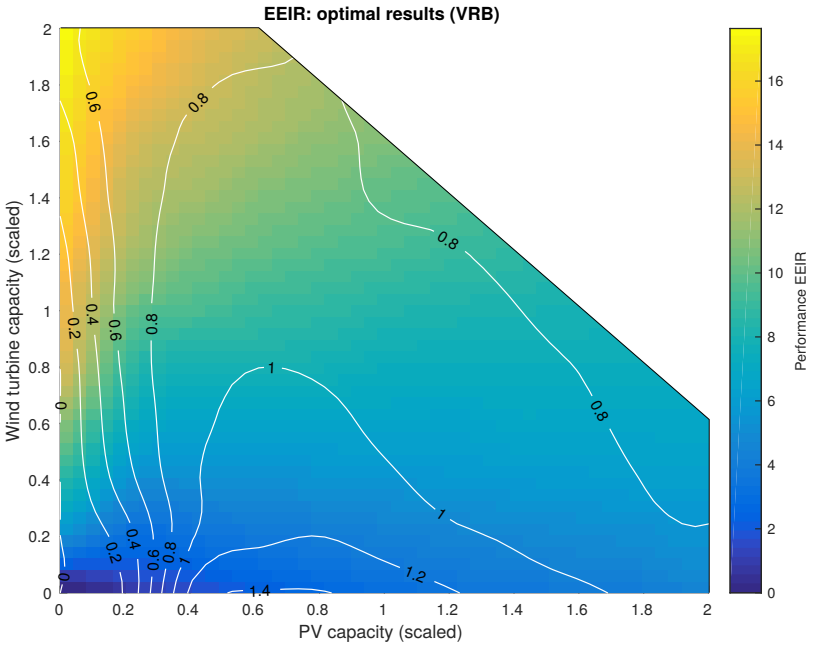

Figure B.17: *EEIR* results showing optimal VRB battery capacity for all input capacities.

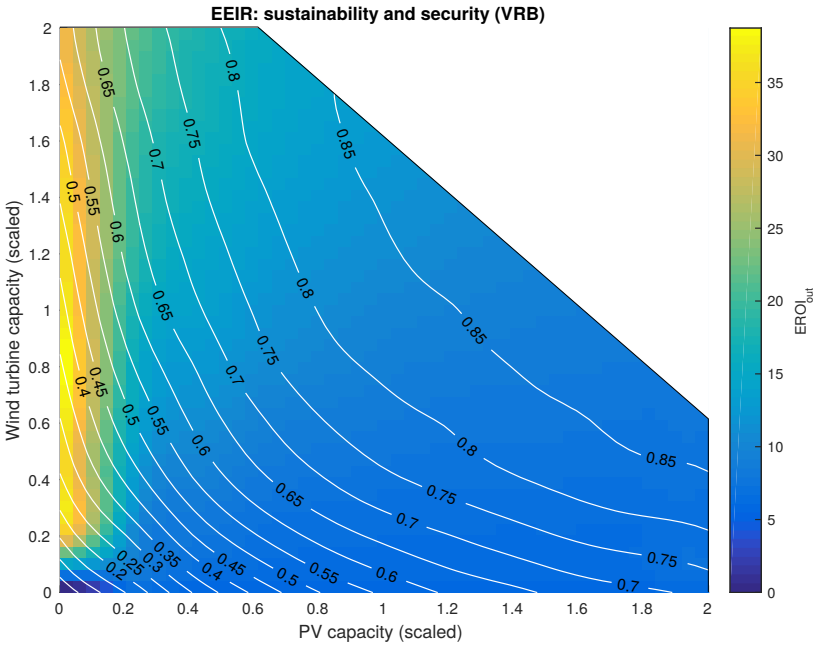

Figure B.18: $EROI_{out}$ and *EIR* results for optimal VRB energy systems.

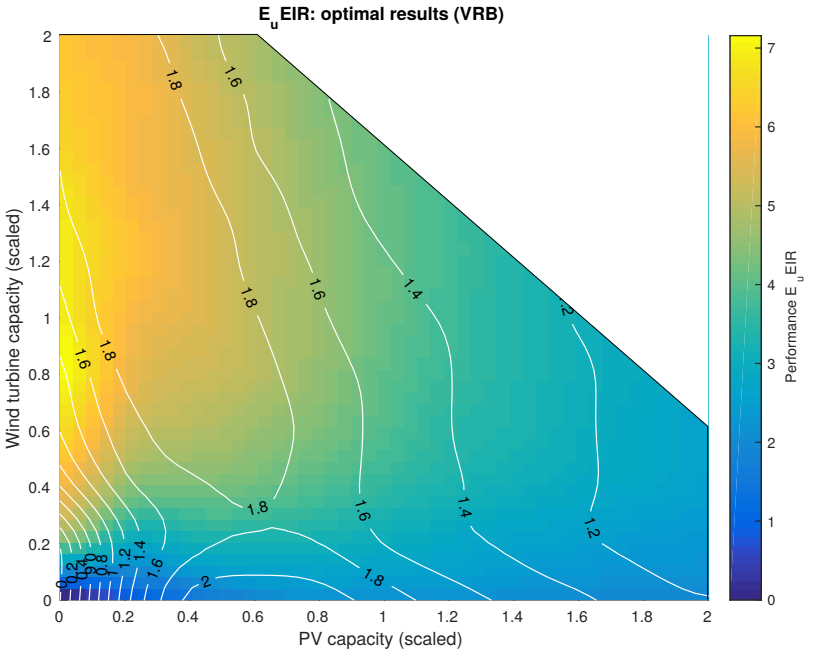

Figure B.19: $E_u EIR$ results showing optimal VRB battery capacity for all input capacities.

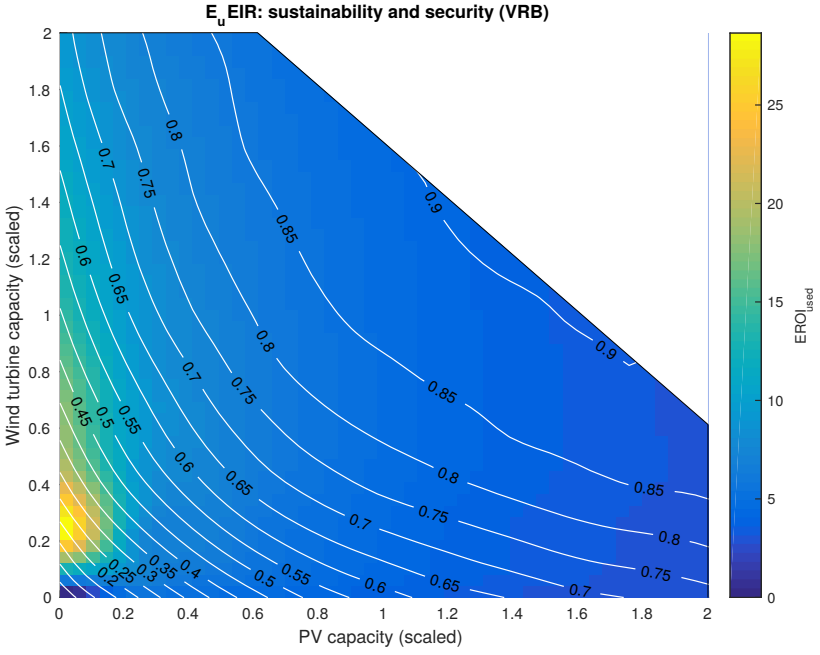

Figure B.20: $EROI_{used}$ and EIR results for optimal VRB energy systems.

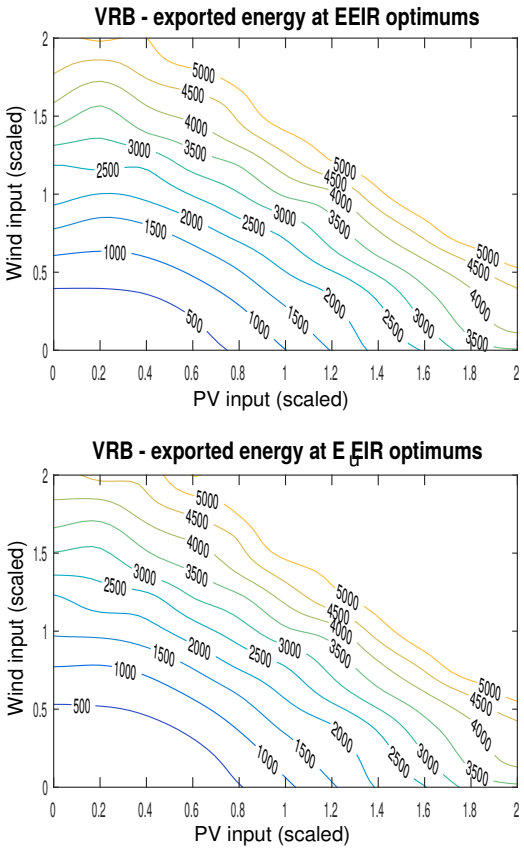

Figure B.21: Optimal $EEIR$ results showing excess energy for VRB systems.

Bibliography

[1] T.F. Stocker, D. Qin, G.-K. Plattner, L.V. Alexander, S.K. Allen, N.L. Bindoff, F.-M. Bréon, J.A. Church, U. Cubasch, S. Emori, P. Forster, P. Friedlingstein, N. Gillett, J.M. Gregory, D.L. Hartmann, E. Jansen, B. Kirtman, R. Knutti, K. Krishna Kumar, P. Lemke, J. Marotzke, V. Masson-Delmotte, G.A. Meehl, I.I. Mokhov, S. Piao, V. Ramaswamy, D. Randall, M. Rhein, M. Rojas, C. Sabine, D. Shindell, L.D. Talley, D.G. Vaughan, and S.-P. Xie. 2013: Technical Summary. In: Climate Change 2013: The Physical Science Basis. Contribution of Working Group I to the Fifth Assessment Report of the Intergovernmental Panel on Climate Change. Technical report, Cambridge University Press, Cambridge, United Kingdom and New York, NY, USA, 2013.

[2] European Union Committee. The EU ' s Target for Renewable Energy : 20 % by 2020 Volume I : Report. Technical Report October, 2008.

[3] National Grid. UK Future Energy Scenarios. Technical Report July, 2014.

[4] Godfrey Boyle, editor. *Renewable electricity and the grid: the challenge of variability.* Earthscan, 2009.

[5] Ahmed F Zobaa and Ramesh C Bansal, editors. *Handbook of Renewable Energy Technologies.*

[6] Abdelhay A Sallam and Om P Malik. Electric Distribution Systems - selected chapters. In *Electric Distribution Systems.* 2011.

[7] Alexandra von Meier. Electric Power Systems - selected chapters. In *Electric Power Systems*, pages 1–88. mar 2006.

[8] Math HJ Bollen. *The Smart Grid: Adapting the Power System to New Challenges.* 2011.

[9] S Chowdhury, S.P. Chowdhury, and P Crossley. *Microgrids and Active Distribution Networks.*

[10] DECC and Ofgem. Government and Ofgem Action Plan : Challenger Businesses (Independent Energy Suppliers). Technical Report August, 2014.

[11] Ofgem. Ofgem Feed-in tariff installation report June 2015, 2015.

[12] Peter Asmus. Microgrids, Virtual Power Plants and Our Distributed Energy Future. *The Electricity Journal*, 23(10):72–82, dec 2010.

[13] Peter Capener. Community Renewable Electricity Generation : Potential Sector Growth to 2020. Technical Report January, 2014.

[14] R M Dell and D A J Rand. Energy storage a key technology for global energy sustainability. *Journal of Power Sources*, 100:2–17, 2001.

[15] Edie.net. http://www.edie.net/news/6/Leading-renewables-firm-to-build-first-UK-energy-storage-project/.

[16] SnowdoniaPumpedHydro.com. http://www.snowdoniapumpedhydro.com/index.php/en/glyn-rhonwy.

[17] UK Power Networks. Demonstrating the benefits of short-term discharge energy storage on an 11kV distribution network. Technical Report June, 2014.

[18] Gill Seyfang, Sabine Hielscher, Tom Hargreaves, Mari Martiskainen, and Adrian Smith. A grassroots sustainable energy niche? Reflections on community energy in the UK. *Environmental Innovation and Societal Transitions*, 13:21–44, dec 2014.

[19] Angel a. Bayod-Rújula. Future development of the electricity systems with distributed generation. *Energy*, 34(3):377–383, mar 2009.

[20] Angus Gillespie, Derek Grieve, and Robert Sorrell. Managing Flexibility Whilst Decarbonising the GB Electricity System: Executive Summary. Technical Report August, 2015.

[21] Morten Boje Blarke and Henrik Lund. Large scale heat pumps in sustainable energy systems: systems and project perspectives. In *Sustainable Development of Energy, Water and Environment Systems, Volume III*, pages 69–78. World Scientific Publishing Co. Pte. Ltd., 2007.

[22] David J C Mackay. *Sustainable Energy without the hot air*. 2008.

[23] Roy Billinton and Ronald N Allan. *Reliability Evaluation of Power Systems*. First edition, 1984.

[24] Hua Chen. *Generating System Reliability Optimization*. PhD thesis, 2000.

[25] Roy Billinton, Rajesh Karki, and Ajit Kumar Verma. *Reliability and Risk Evaluation of Wind Integrated Power Systems*. Springer, 2013.

[26] Gru Brundtland, Mansour Khalid, Susanna Agnelli, Sali Al-Athel, Bernard Chidzero, Lamina Fadika, Volker Hauff, Istvan Lang, Ma Shijun, and Margarita Morino de Botero. *Our Common Future*. Oxford University Press, 1987.

[27] a.F. Sherwani and J.a. Usmani. Life cycle assessment of solar PV based electricity generation systems: A review. *Renewable and Sustainable Energy Reviews*, 14(1):540–544, jan 2010.

[28] Charles a.S. Hall, Jessica G. Lambert, and Stephen B. Balogh. EROI of different fuels and the implications for society. *Energy Policy*, 64:141–152, jan 2014.

[29] Charles a. S. Hall, Stephen Balogh, and David J.R. Murphy. What is the Minimum EROI that a Sustainable Society Must Have? *Energies*, 2(1):25–47, jan 2009.

[30] Fabian Kesicki and Neil Strachan. Marginal abatement cost (MAC) curves: confronting theory and practice. *Environmental Science & Policy*, 14(8):1195–1204, dec 2011.

[31] Peter J. Hall and Euan J. Bain. Energy-storage technologies and electricity generation. *Energy Policy*, 36(12):4352–4355, dec 2008.

[32] José L. Bernal-Agustín and Rodolfo Dufo-López. Simulation and optimization of stand-alone hybrid renewable energy systems. *Renewable and Sustainable Energy Reviews*, 13(8):2111–2118, oct 2009.

[33] M.K. Deshmukh and S.S. Deshmukh. Modeling of hybrid renewable energy systems. *Renewable and Sustainable Energy Reviews*, 12(1):235–249, jan 2008.

[34] Prabodh Bajpai and Vaishalee Dash. Hybrid renewable energy systems for power generation in stand-alone applications: A review. *Renewable and Sustainable Energy Reviews*, 16(5):2926–2939, jun 2012.

[35] Eftichios Koutroulis, Dionissia Kolokotsa, Antonis Potirakis, and Kostas Kalaitzakis. Methodology for optimal sizing of stand-alone photovoltaic/wind-generator systems using genetic algorithms. *Solar Energy*, 80(9):1072–1088, sep 2006.

[36] a.S. Bahaj, L. Myers, and P.a.B. James. Urban energy generation: Influence of micro-wind turbine output on electricity consumption in buildings. *Energy and Buildings*, 39(2):154–165, feb 2007.

[37] G.J. Dalton, D.a. Lockington, and T.E. Baldock. Feasibility analysis of stand-alone renewable energy supply options for a large hotel. *Renewable Energy*, 33(7):1475–1490, jul 2008.

[38] Daniel Quiggin, Sarah Cornell, Michael Tierney, and Richard Buswell. A simulation and optimisation study: Towards a decentralised microgrid, using real world fluctuation data. *Energy*, 41(1):549–559, may 2012.

[39] Y.P. Cai, G.H. Huang, Q. Tan, and Z.F. Yang. Planning of community-scale renewable energy management systems in a mixed stochastic and fuzzy environment. *Renewable Energy*, 34(7):1833–1847, jul 2009.

[40] Y.P. Cai, G.H. Huang, Z.F. Yang, Q.G. Lin, and Q. Tan. Community-scale renewable energy systems planning under uncertaintyAn interval chance-constrained programming approach. *Renewable and Sustainable Energy Reviews*, 13(4):721–735, may 2009.

[41] S.H. Karaki, R.B. Chedid, and R. Ramadan. Probabilistic performance assessment of autonomous solar-wind energy conversion systems. *IEEE Transactions on Energy Conversion*, 14(3):766–772, 1999.

[42] AD Bagul and ZM Salameh. Sizing of a stand-alone hybrid wind-photovoltaic system using a three-event probability density approximation. *Solar Energy*, 56(4):323–335, 1996.

[43] John P Barton and David G Infield. Energy Storage and Its Use With Intermittent Renewable Energy. *Energy*, 19(2):441–448, 2004.

[44] G. Tina, S. Gagliano, and S. Raiti. Hybrid solar/wind power system probabilistic modelling for long-term performance assessment. *Solar Energy*, 80(5):578–588, may 2006.

[45] Jiang Wen, Yan Zheng, and Feng Donghan. A review on reliability assessment for wind power. *Renewable and Sustainable Energy Reviews*, 13:2485–2494, 2009.

[46] José L. Bernal-Agustín, Rodolfo Dufo-López, and David M. Rivas-Ascaso. Design of isolated hybrid systems minimizing costs and pollutant emissions. *Renewable Energy*, 31(14):2227–2244, nov 2006.

[47] W.G.J.H.M. Van Sark. Feasibility of photovoltaic Thermoelectric hybrid modules. *Applied Energy*, 88(8):2785–2790, aug 2011.

[48] Shuhui Li, Donald C. Wunsch, Edgar O'Hair, and Michael G. Giesselmann. Comparative Analysis of Regression and Artificial Neural Network Models for Wind Turbine Power Curve Estimation. *Journal of Solar Energy Engineering*, 123(4):327, 2001.

[49] R. Lanzafame and M. Messina. Power curve control in micro wind turbine design. *Energy*, 35(2):556–561, feb 2010.

[50] Vikrant Sharma and S.S. Chandel. Performance and degradation analysis for long term reliability of solar photovoltaic systems: A review. *Renewable and Sustainable Energy Reviews*, 27:753–767, nov 2013.

[51] Ulrike Jahn and Wolfgang Nasse. Operational performance of grid-connected PV systems on buildings in Germany. *Progress in Photovoltaics: Research and Applications*, 12(6):441–448, sep 2004.

[52] Vasilis Fthenakis, Rolf Frischknecht, Marco Raugei, Hyung Chul Kim, Erik Alsema, Michael Held, and Mariska de Wild-Scholten. Methodology Guidelines on Life Cycle Assessment of Photovoltaic Electricity. Technical report, 2011.

[53] Nils H Reich, Bjoern Mueller, Alfons Armbruster, Wilfried G J H M Van Sark, Klaus Kiefer, and Christian Reise. Performance ratio revisited : is PR $>$ 90 % realistic ? *Progress in Photovoltaics: Research and Applications*, 20(January):717–726, 2012.

[54] DECC. Annual Energy Statement 2012. Technical Report November, 2012.

[55] Tomislav Capuder and Pierluigi Mancarella. Techno-economic and environmental modelling and optimization of flexible distributed multi-generation options. *Energy*, 71:516–533, 2014.

[56] Morten B. Blarke. Towards an intermittency-friendly energy system: Comparing electric boilers and heat pumps in distributed cogeneration. *Applied Energy*, 91(1):349–365, 2012.

[57] Pierluigi Mancarella. Cogeneration systems with electric heat pumps: Energy-shifting properties and equivalent plant modelling. *Energy Conversion and Management*, 50(8):1991–1999, 2009.

[58] A Schafer, P Baumanns, and A Moser. Modeling heat pumps as combined heat and power plants in energy generation planning. *Energytech, 2012 IEEE*, (1):3–8, 2012.

[59] Karsten Hedegaard, Brian Vad Mathiesen, Henrik Lund, and Per Heiselberg. Wind power integration using individual heat pumps - Analysis of different heat storage options. *Energy*, 47(1):284–293, 2012.

[60] Torben Ommen, Wiebke Brix Markussen, and Brian Elmegaard. Heat pumps in combined heat and power systems. *Energy*, 76:989–1000, 2014.

[61] Mikkel Sørensen Torekov, Niels Bahnsen, and Bjørn Qvale. The relative competitive positions of the alternative means for domestic heating. *Energy*, 32(5):627–633, 2007.

[62] Zhi-Ping Song. Total energy system analysis of heating. *Energy*, 25(9):807–822, 2000.

[63] Dominik Saner, Ronnie Juraske, Markus Kubert, Philipp Blum, Stefanie Hellweg, and Peter Bayer. Is it only CO2 that matters? A life cycle perspective on shallow geothermal systems. *Renewable and Sustainable Energy Reviews*, 14(7):1798–1813, 2010.

[64] Henrik Lund. Large-scale integration of wind power into different energy systems. *Energy*, 30(13):2402–2412, 2005.

[65] The Energy Saving Trust. Getting warmer : a field trial of heat pumps. Technical report, 2010.

[66] Viorel Badescu. First and second law analysis of a solar assisted heat pump based heating system. *Energy Conversion and Management*, 43(18):2539–2552, 2002.

[67] H. D. Fu, G. Pei, J. Ji, H. Long, T. Zhang, and T. T. Chow. Experimental study of a photovoltaic solar-assisted heat-pump/heat-pipe system. *Applied Thermal Engineering*, 40:343–350, 2012.

[68] Jeremy Cockroft and Nick Kelly. A comparative assessment of future heat and power sources for the UK domestic sector. *Energy Conversion and Management*, 47(15-16):2349–2360, 2006.

[69] Viktor Dorer and Andreas Weber. Energy and CO2 emissions performance assessment of residential micro-cogeneration systems with dynamic whole-building simulation programs. *Energy Conversion and Management*, 50(3):648–657, 2009.

[70] Juha Kiviluoma and Peter Meibom. Influence of wind power, plug-in electric vehicles, and heat storages on power system investments. *Energy*, 35(3):1244–1255, 2010.

[71] E. Kaplani and S. Kaplanis. A stochastic simulation model for reliable PV system sizing providing for solar radiation fluctuations. *Applied Energy*, dec 2011.

[72] R. Baños, F. Manzano-Agugliaro, F.G. Montoya, C. Gil, A. Alcayde, and J. Gómez. Optimization methods applied to renewable and sustainable energy: A review. *Renewable and Sustainable Energy Reviews*, 15(4):1753–1766, may 2011.

[73] J.K. Kaldellis, P. Koronakis, and K. Kavadias. Energy balance analysis of a stand-alone photovoltaic system, including variable system reliability impact. *Renewable Energy*, 29(7):1161–1180, jun 2004.

[74] Hongxing Yang, Lin Lu, and Wei Zhou. A novel optimization sizing model for hybrid solar-wind power generation system. *Solar Energy*, 81(1):76–84, jan 2007.

[75] Wei Zhou, Chengzhi Lou, Zhongshi Li, Lin Lu, and Hongxing Yang. Current status of research on optimum sizing of stand-alone hybrid solarwind power generation systems. *Applied Energy*, 87(2):380–389, feb 2010.

[76] Pedro S. Moura and Aníbal T. de Almeida. Multi-objective optimization of a mixed renewable system with demand-side management. *Renewable and Sustainable Energy Reviews*, 14(5):1461–1468, jun 2010.

[77] Kalyanmoy Deb and Kaisa Miettinen. *Multiobjective Optimization: Interactive and Evolutionary Approaches*. Springer, 2008.

[78] Dhaker Abbes, André Martinez, and Gérard Champenois. Life cycle cost, embodied energy and loss of power supply probability for the optimal design of hybrid power systems. *Mathematics and Computers in Simulation*, 98:46–62, apr 2014.

[79] Liliana E. Benitez, Pablo C. Benitez, and G. Cornelis van Kooten. The economics of wind power with energy storage. *Energy Economics*, 30(4):1973–1989, jul 2008.

[80] Rodolfo Dufo-López and José L. Bernal-Agustín. Multi-objective design of PVwinddieselhydrogenbattery systems. *Renewable Energy*, 33(12):2559–2572, dec 2008.

[81] Rodolfo Dufo-López, José L. Bernal-Agustín, José M. Yusta-Loyo, José a. Domínguez-Navarro, Ignacio J. Ramírez-Rosado, Juan Lujano, and Ismael Aso. Multi-objective optimization minimizing cost and life cycle emissions of stand-alone PVwinddiesel systems with batteries storage. *Applied Energy*, 88(11):4033–4041, nov 2011.

[82] S. Diaf, D. Diaf, M. Belhamel, M. Haddadi, and A. Louche. A methodology for optimal sizing of autonomous hybrid PV/wind system. *Energy Policy*, 35(11):5708–5718, nov 2007.

[83] Ali Zangeneh, Shahram Jadid, and Ashkan Rahimi-Kian. Promotion strategy of clean technologies in distributed generation expansion planning. *Renewable Energy*, 34(12):2765–2773, dec 2009.

[84] Xavier Pelet, Daniel Favrat, and Geoff Leyland. Multiobjective optimisation of integrated energy systems for remote communities considering economics and CO2 emissions. *International Journal of Thermal Sciences*, 44(12):1180–1189, dec 2005.

[85] Daniel Yergin. Ensuring Energy Security. *Foreign Affairs*, 85(2):69–82, 2012.

[86] Christian Winzer. Conceptualizing energy security. *Energy Policy*, 46:36–48, jul 2012.

[87] Bert Kruyt, D.P. van Vuuren, H.J.M. de Vries, and H. Groenenberg. Indicators for energy security. *Energy Policy*, 37(6):2166–2181, jun 2009.

[88] Benjamin K. Sovacool and Ishani Mukherjee. Conceptualizing and measuring energy security: A synthesized approach. *Energy*, 36(8):5343–5355, aug 2011.

[89] Cristina L. Archer and Mark Z. Jacobson. Supplying baseload power and reducing transmission requirements by interconnecting wind farms. *Journal of Applied Meteorology and Climatology*, 46(11):1701–1717, 2007.

[90] Cory Budischak, DeAnna Sewell, Heather Thomson, Leon Mach, Dana E. Veron, and Willett Kempton. Cost-minimized combinations of wind power, solar power and electrochemical storage, powering the grid up to 99.9% of the time. *Journal of Power Sources*, 225:60–74, mar 2013.

[91] European Wind Energy Association et al. *Large Scale Integration of Wind Energy in the European Power Supply: Analysis, Issues and Recommendations: a Report*. European Wind Energy Association, 2005.

[92] Bert Droste-Franke, Boris Paal, Christian Rehtanz, Dirk Uwe Sauer, Jens-Peter Schneider, Miranda Schreurs, and Thomas Ziesemer. *Balancing Renewable Electricity: Energy Storage, Demand Side Management, and Network Extension from an Interdisciplinary Perspective*. Springer, 2012.

[93] Paul Denholm and Maureen Hand. Grid flexibility and storage required to achieve very high penetration of variable renewable electricity. *Energy Policy*, 39(3):1817–1830, mar 2011.

[94] Paul Denholm and Robert M. Margolis. Evaluating the limits of solar photovoltaics (PV) in traditional electric power systems. *Energy Policy*, 35(5):2852–2861, may 2007.

[95] Arne Faaborg. Impacts of power penetration from photovoltaic power systems in distribution networks. Technical Report February, IEA, Fredericia, Denmark, 2002.

[96] Michael H Coddington, David Baca, Benjamin D Kroposki, and Thomas Basso. DEPLOYING HIGH PENETRATION PHOTOVOLTAIC SYSTEMS A CASE STUDY. *IEEE*, pages 2594–2599, 2011.

[97] P Finn, C Fitzpatrick, M Leahy, and A System Operators. Increased Penetration of Wind Generated Electricity using Real time Pricing & Demand Side Management. In *IEEE International Symposium on Sustainable Systems and Technology*, 2009.

[98] Yun Tiam Tan, Student Member, Daniel S Kirschen, Senior Member, and Nicholas Jenkins. A Model of PV Generation Suitable for Stability Analysis. *IEEE Transactions on Energy Conversion*, 19(4):748–755, 2004.

[99] Jukka V. Paatero and Peter D. Lund. Effects of large-scale photovoltaic power integration on electricity distribution networks. *Renewable Energy*, 32(2):216–234, feb 2007.

[100] Mohamed a. Eltawil and Zhengming Zhao. Grid-connected photovoltaic power systems: Technical and potential problemsA review. *Renewable and Sustainable Energy Reviews*, 14(1):112–129, jan 2010.

[101] N Srisaen and A Sangswang. Effects of PV Grid-Connected System Location on a Distribution System. In *Circuits and Systems*, volume 00, pages 852–855, 2006.

[102] E Wiemken, H G Beyer, W Heydenreich, and K Kiefer. Power Characteristics of PV Ensembles: Experiences From The Combined Power Production of 100 Grid Connected PV Systems Distributed Over The Area of Germany. *Solar Energy*, 70(6):513–518, 2001.

[103] Peter D. Lund, Juuso Lindgren, Jani Mikkola, and Jyri Salpakari. Review of energy system flexibility measures to enable high levels of variable renewable electricity. *Renewable and Sustainable Energy Reviews*, 45:785–807, 2015.

[104] Dirk Van Hertem and Mehrdad Ghandhari. Multi-terminal VSC HVDC for the European supergrid: Obstacles. *Renewable and Sustainable Energy Reviews*, 14(9):3156–3163, dec 2010.

[105] Mary Black and Goran Strbac. Value of Bulk Energy Storage for Managing Wind Power Fluctuations. *IEEE Transactions on Energy Conversion*, 22(1):197–205, 2007.

[106] J.a. Peças Lopes, N. Hatziargyriou, J. Mutale, P. Djapic, and N. Jenkins. Integrating distributed generation into electric power systems: A review of drivers, challenges and opportunities. *Electric Power Systems Research*, 77(9):1189–1203, jul 2007.

[107] Daniel Rech and Andreas Harth. Towards a Decentralised Hierarchical Architecture for Smart Grids. In *2012 Joint EDBT/ICDT Workshops*, 2012.

[108] Antonella Battaglini, Johan Lilliestam, Armin Haas, and Anthony Patt. Development of SuperSmart Grids for a more efficient utilisation of electricity from renewable sources. *Journal of Cleaner Production*, 17(10):911–918, jul 2009.

[109] Dieter Metz, Thorsten Fiedler, Ion Mircea, and Paul-mihai Mircea. Integration of distributed battery storages in modern power grids. *Annals of the University of Craiova, Electrical Engineering series*, 34:137–141, 2010.

[110] EPIA. Connecting the sun - solar photovoltaics on the road to large-scale grid integration. Technical Report September, 2012.

[111] Poul Alberg Østergaard and Henrik Lund. A renewable energy system in Frederikshavn using low-temperature geothermal energy for district heating. *Applied Energy*, 88(2):479–487, feb 2011.

[112] Henrik Lund, Anders N. Andersen, Poul Alberg Østergaard, Brian Vad Mathiesen, and David Connolly. From electricity smart grids to smart energy systems A market operation based approach and understanding. *Energy*, 42(1):96–102, jun 2012.

[113] DTI. Enhancing Security of the UK Electricity System with Energy Storage. Technical report, 2006.

[114] D Rastler. Electricity Energy Storage Technology Options. Technical report, EPRI, 2010.

[115] François Bouffard and Daniel S. Kirschen. Centralised and distributed electricity systems. *Energy Policy*, 36(12):4504–4508, dec 2008.

[116] Elisabeth Lemaire, Jasper Groenewegen, and Nicolas Martin. European White Book on Grid-Connected Storage. Technical report, 2011.

[117] Goran Strbac, Marko Aunedi, Danny Pudjianto, Predrag Djapic, and Fei Teng. Strategic Assessment of the Role and Value of Energy Storage Systems in the UK Low Carbon Energy Future. Technical Report June, 2012.

[118] Alfred J Cavallo. Energy Storage Technologies for Utility Scale Intermittent Renewable Energy Systems. *Journal of Solar Energy Engineering*, 123:387–389, 2001.

[119] Frederik Geth, Johannes Kathan, Lukas Sigrist, and Peter Verboven. Energy Storage Innovation in Europe A mapping exercise. Technical Report October, 2013.

[120] Annette Evans, Vladimir Strezov, and Tim J. Evans. Assessment of utility energy storage options for increased renewable energy penetration. *Renewable and Sustainable Energy Reviews*, 16(6):4141–4147, aug 2012.

[121] K.C. Divya and Jacob Østergaard. Battery energy storage technology for power systemsAn overview. *Electric Power Systems Research*, 79(4):511–520, apr 2009.

[122] Juan Manuel Carrasco, Leopoldo Garcia Franquelo, Jan T Bialasiewicz, Senior Member, Eduardo Galván, Ramón C Portillo Guisado, Student Member, Ma Ángeles, Martín Prats, José Ignacio León, and Narciso Moreno-alfonso. Power-Electronic Systems for the Grid Integration of Renewable Energy Sources : A Survey. *IEEE Transactions on Industrial Electronics*, 53(4):1002–1016, 2006.

[123] Paul Denholm and Gerald L. Kulcinski. Life cycle energy requirements and greenhouse gas emissions from large scale energy storage systems. *Energy Conversion and Management*, 45(13-14):2153–2172, aug 2004.

[124] JR Dahn, GE Ehrlich, and TB Reddy. *Linden's Handbook of Batteries*. McGraw-Hill International, 4 edition, 2011.

[125] Eoghan McKenna, Marcelle McManus, Sam Cooper, and Murray Thomson. Economic and environmental impact of lead-acid batteries in grid-connected domestic PV systems. *Applied Energy*, 104:239–249, apr 2013.

[126] David Parra, Gavin S. Walker, and Mark Gillott. Modeling of PV generation, battery and hydrogen storage to investigate the benefits of energy storage for single dwelling. *Sustainable Cities and Society*, 10(March 2012):1–10, feb 2014.

[127] Carl Johan Rydh. Environmental assessment of vanadium redox and lead-acid batteries for stationary energy storage. *Journal of Power Sources*, 80(1-2):21–29, jul 1999.

[128] J.K. Kaldellis and D. Zafirakis. Optimum energy storage techniques for the improvement of renewable energy sources-based electricity generation economic efficiency. *Energy*, 32(12):2295–2305, dec 2007.

[129] Grietus Mulder, Fjo De Ridder, and Daan Six. Electricity storage for grid-connected household dwellings with PV panels. *Solar Energy*, 84(7):1284–1293, jul 2010.

[130] C. Ponce de León, A. Frías-Ferrer, J. González-García, D.a. Szánto, and F.C. Walsh. Redox flow cells for energy conversion. *Journal of Power Sources*, 160(1):716–732, sep 2006.

[131] rongkepower.net. http://www.rongkepower.com/index.php/article/show/id/140/language/en.

[132] Haisheng Chen, Thang Ngoc, Wei Yang, Chunqing Tan, and Yongliang Li. Progress in electrical energy storage system : A critical review. *Progress in Natural Science*, 19(3):291–312, 2009.

[133] Matthew A Pellow, Christopher J M Emmott, Charles Joseph Barnhart, and Sally Benson. Hydrogen or batteries for grid storage? A net energy analysis. *Energy Environ. Sci.*, 8(7):1938–1952, 2015.

[134] H Ibrahim, A Ilinca, and J Perron. Energy storage systemsCharacteristics and comparisons. *Renewable and Sustainable Energy Reviews*, 12(5):1221–1250, jun 2008.

[135] DTI. STATUS OF ELECTRICAL ENERGY STORAGE. Technical report, 2004.

[136] Michael Carbajales-Dale, Charles J. Barnhart, and Sally M. Benson. Can we afford storage? A dynamic net energy analysis of renewable electricity generation supported by energy storage. *Energy & Environmental Science*, pages 1538–1544, 2014.

[137] Charles J. Barnhart and Sally M. Benson. On the importance of reducing the energetic and material demands of electrical energy storage. *Energy & Environmental Science*, 6(4):1083, 2013.

[138] Marc Beaudin, Hamidreza Zareipour, Anthony Schellenberglabe, and William Rosehart. Energy storage for mitigating the variability of renewable electricity sources: An updated review. *Energy for Sustainable Development*, nov 2010.

[139] J B Copetti. Lead / acid batteries for photovoltaic applications . Test results and modelling. *Journal of Power Sources*, 47:109–118, 1994.

[140] Matthias Dürr, Andrew Cruden, Sinclair Gair, and J.R. McDonald. Dynamic model of a lead acid battery for use in a domestic fuel cell system. *Journal of Power Sources*, 161(2):1400–1411, oct 2006.

[141] Min Chen and Gabriel A Rincon-Mora. Accurate Electrical Battery Model Capable of Predicting Runtime and I V Performance. *IEEE Transactions on Energy Conversion*, 21(2):504–511, 2006.

[142] Rodolfo Dufo-López, Juan M. Lujano-Rojas, and José L. Bernal-Agustín. Comparison of different leadacid battery lifetime prediction models for use in simulation of stand-alone photovoltaic systems. *Applied Energy*, 115:242–253, feb 2014.

[143] John W Stevens and Garth P Corey. A study of lead-acid battery efficiency near top-of-charge and the impact on PV system design. In *Photovoltaic Specialists Conference, 1996., Conference Record of the Twenty Fifth IEEE*, pages 1485–1488. IEEE, 1996.

[144] N. Achaibou, M. Haddadi, and A. Malek. Modeling of Lead Acid Batteries in PV Systems. *Energy Procedia*, 18:538–544, 2012.

[145] AnnMari Jansson. *Investing in Natural Capital: The Ecological Economics Approach To Sustainability*. Island Press, 1994, 1994.

[146] Yi Zhang, Anil Baral, and Bhavik R Bakshi. Accounting for ecosystem services in Life Cycle Assessment, Part II: toward an ecologically based LCA. *Environmental science & technology*, 44(7):2624–31, apr 2010.

[147] Stephen McKenzie. SOCIAL SUSTAINABILITY : TOWARDS SOME DEFINITIONS. 2004.

[148] Christoph Böhringer and Patrick E P Jochem. Measuring the immeasurable A survey of sustainability indices. *Ecological Economics*, 63(1991):1–8, 2007.

[149] Yi Zhang, Shweta Singh, and Bhavik R Bakshi. Accounting for ecosystem services in life cycle assessment, Part I: a critical review. *Environmental science & technology*, 44(7):2232–42, apr 2010.

[150] ecoinvent.

[151] Rush D Robinett, David G Wilson, and Alfred W Reed. Exergy Sustainability for Complex Systems. *InterJournal Complex Systems*, 1616:1–18, 2006.

[152] Ibrahim Dincer. The role of exergy in energy policy making. *Energy Policy*, 30(May 2000):137–149, 2002.

[153] J. Dewulf, H. Van Langenhove, J. Mulder, M. M. D. van den Berg, H. J. van der Kooi, and J. de Swaan Arons. Illustrations towards quantifying the sustainability of technology. *Green Chemistry*, 2(3):108–114, 2000.

[154] Christopher J. Koroneos, Evanthia a. Nanaki, and George a. Xydis. Sustainability Indicators for the Use of ResourcesThe Exergy Approach. *Sustainability*, 4(12):1867–1878, aug 2012.

[155] René L. Cornelissen and Gerard G. Hirs. The value of the exergetic life cycle assessment besides the LCA. *Energy Conversion and Management*, 43(9-12):1417–1424, jun 2002.

[156] Kyrke Gaudreau, Roydon a. Fraser, and Stephen Murphy. The Tenuous Use of Exergy as a Measure of Resource Value or Waste Impact. *Sustainability*, 1(4):1444–1463, dec 2009.

[157] Howard T Odum. Environmental accounting: EMERGY and environmental decision making. 1996.

[158] Jorge L Hau and Bhavik R Bakshi. Promise and problems of emergy analysis. *Ecological Modelling*, 178(1-2):215–225, oct 2004.

[159] S Bastianoni, A Facchini, L Susani, and E Tiezzi. Emergy as a function of exergy. *Energy*, 32(7):1158–1162, jul 2007.

[160] Enrico Sciubba. On the Second-Law inconsistency of Emergy Analysis. *Energy*, 35(9):3696–3706, sep 2010.

[161] R. Kenny, C. Law, and J.M. Pearce. Towards real energy economics: Energy policy driven by life-cycle carbon emission. *Energy Policy*, 38(4):1969–1978, apr 2010.

[162] Michael Common. *Sustainability and Policy: Limits to Economics*. Cambridge University Press, 1995.

[163] K Kaufmann. A biophysical analysis of the energy / real ratio : implications for substitution and technical change. *Ecological Economics*, 6:35–56, 1992.

[164] Cutler J Cleveland, Robert Costanza, Charles AS Hall, and Robert Kaufmann. Energy and the US Economy - A Biophysical Perspective. *Science*, 225:890–897, 1984.

[165] Carey W. King and Charles a.S. Hall. Relating Financial and Energy Return on Investment. *Sustainability*, 3(12):1810–1832, oct 2011.

[166] Marco Raugei, Pere Fullana-i Palmer, and Vasilis Fthenakis. The energy return on energy investment (EROI) of photovoltaics: Methodology and comparisons with fossil fuel life cycles. *Energy Policy*, 45:576–582, jun 2012.

[167] Fred Cottrell. *Energy & Society: The Relation Between Energy, Social Change, and Economic Development*. AuthorHouse, 2009.

[168] Margot J. Hutchins and John W. Sutherland. An exploration of measures of social sustainability and their application to supply chain decisions. *Journal of Cleaner Production*, 16(15):1688–1698, oct 2008.

[169] G. Assefa and B. Frostell. Social sustainability and social acceptance in technology assessment: A case study of energy technologies. *Technology in Society*, 29(1):63–78, jan 2007.

[170] G Rebitzer, T Ekvall, R Frischknecht, D Hunkeler, G Norris, T Rydberg, W-P Schmidt, S Suh, B P Weidema, and D W Pennington. Life cycle assessment part 1: framework, goal and scope definition, inventory analysis, and applications. *Environment international*, 30(5):701–20, jul 2004.

[171] R.H. Crawford. Life cycle energy and greenhouse emissions analysis of wind turbines and the effect of size on energy yield. *Renewable and Sustainable Energy Reviews*, 13(9):2653–2660, dec 2009.

[172] Carey W King and P F Henshaw. DEFINING A STANDARD MEASURE FOR WHOLE SYSTEM EROI. In *Energy Sustainability 2010*, pages 1–10, 2010.

[173] J. Mason Earles and Anthony Halog. Consequential life cycle assessment: a review. *The International Journal of Life Cycle Assessment*, 16(5):445–453, mar 2011.

[174] M Pehnt. Dynamic life cycle assessment (LCA) of renewable energy technologies. *Renewable Energy*, 31(1):55–71, jan 2006.

[175] Scott W White and Gerald L Kulcinski. Birth to death analysis of the energy payback ratio and CO 2 gas emission rates from coal , fission , wind , and DT-fusion electrical power plants. *Fusion Engineering and Design*, 48(248):473–481, 2000.

[176] Marco Raugei. Energy pay-back time : methodological caveats and future scenarios. 2012.

[177] Adam R. Brandt and Michael Dale. A General Mathematical Framework for Calculating Systems-Scale Efficiency of Energy Extraction and Conversion: Energy Return on Investment (EROI) and Other Energy Return Ratios. *Energies*, 4(12):1211–1245, aug 2011.

[178] Adam R. Brandt, Michael Dale, and Charles J. Barnhart. Calculating systems-scale energy efficiency and net energy returns: A bottom-up matrix-based approach. *Energy*, 62:235–247, dec 2013.

[179] Bob Lloyd and Andrew S Forest. The transition to renewables: Can PV provide an answer to the peak oil and climate change challenges? *Energy Policy*, 38(11):7378–7394, nov 2010.

[180] Ajay K. Gupta and Charles a.S. Hall. A Review of the Past and Current State of EROI Data. *Sustainability*, 3(12):1796–1809, oct 2011.

[181] Ida Kubiszewski, Cutler J. Cleveland, and Peter K. Endres. Meta-analysis of net energy return for wind power systems. *Renewable Energy*, 35(1):218–225, jan 2010.

[182] Kenneth Mulder and Nathan John Hagens. Energy Return on Investment : Toward a Consistent Framework. *Ambio*, 37(2):74–79, 2008.

[183] D. Weissbach, G. Ruprecht, A. Huke, K. Czerski, S. Gottlieb, and A. Hussein. Energy intensities, EROIs (energy returned on invested), and energy payback times of electricity generating power plants. *Energy*, 52:210–221, 2013.

[184] Marco Raugei, Michael Carbajales-Dale, Charles J. Barnhart, and Vasilis Fthenakis. Rebuttal: "Comments on 'Energy intensities, EROIs (energy returned on invested), and energy payback times of electricity generating power plants' - Making clear of quite some confusion". *Energy*, 82:1088–1091, 2015.

[185] Carey W King. Matrix method for comparing system and individual energy return ratios when considering an energy transition. *Energy*, 72:254–265, 2014.

[186] Sergio Pacca, Deepak Sivaraman, and Gregory a. Keoleian. Parameters affecting the life cycle performance of PV technologies and systems. *Energy Policy*, 35(6):3316–3326, jun 2007.

[187] Khagendra P. Bhandari, Jennifer M. Collier, Randy J. Ellingson, and Defne S. Apul. Energy payback time (EPBT) and energy return on energy invested (EROI) of solar photovoltaic systems: A systematic review and meta-analysis. *Renewable and Sustainable Energy Reviews*, 47:133–141, jul 2015.

[188] Manfred Lenzen and Ulrike Wachsmann. Wind turbines in Brazil and Germany: an example of geographical variability in life-cycle assessment. *Applied Energy*, 77(2):119–130, feb 2004.

[189] Anders Arvesen and Edgar G. Hertwich. Assessing the life cycle environmental impacts of wind power: A review of present knowledge and research needs. *Renewable and Sustainable Energy Reviews*, 16(8):5994–6006, oct 2012.

[190] V Fthenakis, M Raugei, M Held, J Krones, and H C Kim. Update of PV Energy Payback Times and Life-Cycle Greenhouse Gas Emissions. In *24th European Solar Energy Conference*, number September, 2009.

[191] C Rydh and B Sanden. Energy analysis of batteries in photovoltaic systems. Part I: Performance and energy requirements. *Energy Conversion and Management*, 46(11-12):1957–1979, jul 2005.

[192] I Nawaz and G N Tiwari. Embodied energy analysis of photovoltaic (PV) system based on macro- and micro-level. *Energy Policy*, 34(17):3144–3152, nov 2006.

[193] V.M. Fthenakis and H.C. Kim. Photovoltaics: Life-cycle analyses. *Solar Energy*, 85(8):1609–1628, aug 2011.

[194] Jinqing Peng, Lin Lu, and Hongxing Yang. Review on life cycle assessment of energy payback and greenhouse gas emission of solar photovoltaic systems. *Renewable and Sustainable Energy Reviews*, 19:255–274, mar 2013.

[195] Brice Tremeac and Francis Meunier. Life cycle analysis of 4.5MW and 250W wind turbines. *Renewable and Sustainable Energy Reviews*, 13(8):2104–2110, oct 2009.

[196] S R Allen, G P Hammond, and M C McManus. Energy analysis and environmental life cycle assessment of a micro-wind turbine. *Proceedings of the Institution of Mechanical Engineers, Part A: Journal of Power and Energy*, 222(7):669–684, nov 2008.

[197] S.R. Allen and G.P. Hammond. Thermodynamic and carbon analyses of micro-generators for UK households. *Energy*, 35(5):2223–2234, may 2010.

[198] Fulvio Ardente, Marco Beccali, and Maurizo Cellura. Energy performances and life cycle assessment of an Italian wind farm, 2008.

[199] Brian Fleck and Marc Huot. Comparative life-cycle assessment of a small wind turbine for residential off-grid use. *Renewable Energy*, 34(12):2688–2696, dec 2009.

[200] Begoña Guezuraga, Rudolf Zauner, and Werner Pölz. Life cycle assessment of two different 2 MW class wind turbines. *Renewable Energy*, 37(1):37–44, jan 2012.

[201] Eduardo Martínez, Félix Sanz, Stefano Pellegrini, Emilio Jiménez, and Julio Blanco. Life-cycle assessment of a 2-MW rated power wind turbine: CML method. *The International Journal of Life Cycle Assessment*, 14(1):52–63, oct 2008.

[202] E. Martínez, F. Sanz, S. Pellegrini, E. Jiménez, and J. Blanco. Life cycle assessment of a multi-megawatt wind turbine. *Renewable Energy*, 34(3):667–673, mar 2009.

[203] Nalanie Mithraratne. Roof-top wind turbines for microgeneration in urban houses in New Zealand. *Energy and Buildings*, 41(10):1013–1018, oct 2009.

[204] L Schleisner. Life cycle assessment of a wind farm and related externalities. *Renewable Energy*, 20(3):279–288, jul 2000.

[205] Carl Johan Rydh and Björn a. Sandén. Energy analysis of batteries in photovoltaic systems. Part II: Energy return factors and overall battery efficiencies. *Energy Conversion and Management*, 46(11-12):1980–2000, jul 2005.

[206] E A Alsema. Energy pay-back time and CO2 emissions of PV systems. *Renewable and Sustainable Energy Reviews*, 25(June 1999):17–25, 2000.

[207] Patxi Hernandez and Paul Kenny. Net energy analysis of domestic solar water heating installations in operation. *Renewable and Sustainable Energy Reviews*, 16(1):170–177, 2012.

[208] Charles J. Barnhart, Michael Dale, Adam R. Brandt, and Sally M. Benson. The energetic implications of curtailing versus storing solar- and wind-generated electricity. *Energy & Environmental Science*, 6(10):2804, 2013.

[209] P.F. Lyons, N.S. Wade, T. Jiang, P.C. Taylor, F. Hashiesh, M. Michel, and D. Miller. Design and analysis of electrical energy storage demonstration projects on UK distribution networks. *Applied Energy*, oct 2014.

[210] D C Jordan and S R Kurtz. Photovoltaic Degradation Rates an Analytical Review. *Progress in Photovoltaics: Research and Applications*, 21(October 2011):12–29, 2013.

[211] J. F. Manwell, J. G. McGowan, and A. L. Rogers. *Wind Energy Explained: Theory, Design and Application*. Wiley, 2002.

[212] Ian Richardson. *Integrated High-resolution Modelling of Domestic Electricity Demand and Low Voltage Electricity Distribution Networks*. PhD thesis, 2010.

[213] Lukas G. Swan and V. Ismet Ugursal. Modeling of end-use energy consumption in the residential sector: A review of modeling techniques. *Renewable and Sustainable Energy Reviews*, 13(8):1819–1835, oct 2009.

[214] David J Murphy and Charles A S Hall. Energy return on investment , peak oil , and the end of economic growth. *Ecological Economics Reviews*, 1219(1):52–72, 2011.

[215] Nathan Gagnon, Charles A S Hall, and Lysle Brinker. A Preliminary Investigation of Energy Return on Energy Investment for Global Oil and Gas Production. *Energies*, 2(3):490–503, 2009.

[216] Charles AS Hall, Cutler J Cleveland, and Robert K Kaufmann. *Energy and Resource Quality: the ecology of the economic process*. University Press of Colorado, 1992.

[217] P Zhou Æ B W Ang Æ D Q Zhou. Weighting and Aggregation in Composite Indicator Construction : a Multiplicative Optimization Approach. *Social Indicators Research*, 96:169–181, 2010.

[218] Jukka V. Paatero and Peter D. Lund. Effect of energy storage on variations in wind power. *Wind Energy*, 8(4):421–441, oct 2005.

[219] Sharp Electronics Corporation. Multi-purpose module NT-185U1, 2004.

[220] DECC. Community Energy Strategy : Full Report. Technical Report January, 2014.

[221] ofgem. https://www.ofgem.gov.uk/environmental-programmes/ro/about-ro/ro-closure.

[222] Anna Krzywoszynska, Alastair Buckley, Huw Birch, Matt Watson, Prue Chiles, Jose Mawyin, Helen Holmes, and Nicky Gregson. Co-producing energy futures: impacts of participatory modelling. *Building Research & Information*, 0(0):1–12, 2016.

[223] Boreas. 100kW Air.

[224] Shafiqur Rehman and Naif M. Al-Abbadi. Wind shear coefficients and their effect on energy production. *Energy Conversion and Management*, 46(15-16):2578–2591, sep 2005.

[225] J Taylor, A Everard, A R Buckley, L M H Hall, and J R C Briggs. Investigating Correlation of PV Generation Time Series. Technical report, 2014.

[226] Hebden Bridge Alternative Technology Centre. Upper Don Hydropower study. Technical report, 2011.

[227] DECC/BEIS. https://www.gov.uk/government/collections/electricity-market-reform-capacity-market.